National Library of Canada
Collections Development Branch

Canadian Theses on
Microfiche Service

Bibliothèque nationale du Canada
Direction du développement des collections

Service des thèses canadiennes
sur microfiche

NOTICE

The quality of this microfiche is heavily dependent upon the quality of the original thesis submitted for microfilming. Every effort has been made to ensure the highest quality of reproduction possible.

If pages are missing, contact the university which granted the degree.

Some pages may have indistinct print especially if the original pages were typed with a poor typewriter ribbon or if the university sent us a poor photocopy.

Previously copyrighted materials (journal articles, published tests, etc.) are not filmed.

Reproduction in full or in part of this film is governed by the Canadian Copyright Act, R.S.C. 1970, c. C-30. Please read the authorization forms which accompany this thesis.

THIS DISSERTATION
HAS BEEN MICROFILMED
EXACTLY AS RECEIVED

AVIS

La qualité de cette microfiche dépend grandement de la qualité de la thèse soumise au microfilmage. Nous avons tout fait pour assurer une qualité supérieure de reproduction.

S'il manque des pages, veuillez communiquer avec l'université qui a conféré le grade.

La qualité d'impression de certaines pages peut laisser à désirer, surtout si les pages originales ont été dactylographiées à l'aide d'un ruban usé ou si l'université nous a fait parvenir une photocopie de mauvaise qualité.

Les documents qui font déjà l'objet d'un droit d'auteur (articles de revue, examens publiés, etc.) ne sont pas microfilmés.

La reproduction, même partielle, de ce microfilm est soumise à la Loi canadienne sur le droit d'auteur, SRC 1970, c. C-30. Veuillez prendre connaissance des formules d'autorisation qui accompagnent cette thèse.

LA THÈSE A ÉTÉ
MICROFILMÉE TELLE QUE
NOUS L'AVONS REÇUE

Ottawa, Canada
K1A 0N4

ELECTROCATALYTIC PROPERTIES AND REACTIVITY OF MONOLAYER OXIDE FILMS IN CHLORINE EVOLUTION AND HYDROGEN OXIDATION AT Pt ELECTRODES

by

D. M. NOVAK, Dipl.ing., M.Sc.

A thesis submitted to the School of Graduate Studies
in partial fulfillment of the requirements
for the degree of

Ph.D. in Chemistry

UNIVERSITY OF OTTAWA
OTTAWA, CANADA
March 1979

B.E. CONWAY
Professor of Chemistry
Research Supervisor

D.M. Novak
Ph.D. Candidate

© D.M. NOVAK, University of Ottawa, Ottawa, Ont., 1979.

We dance round in a ring and suppose,
But the Secret sits in the middle and knows.

Robert Frost

To My Nona, and to My

Father and Mother

with Gratitude.

PREFACE

The work in this thesis covers three aspects of the electrocatalytic properties and reactivity of monolayer and sub-monolayer oxide films on Pt anodes with respect to Cl_2 evolution and H_2 oxidation.

Both these reactions have important connections with applied electrochemistry in the chlor-alkali industry, where oxidized noble metal preparations e.g. Pt-Ir or Ru are used as anode coatings, and in the operation of H_2/O_2 fuel cells. However, as will be seen, the work in this thesis is entirely of a fundamental nature.

It will be useful to outline the structure of the thesis since the work is best presented in four distinct sections: three on the original work together with a general introductory review. The experimental details of the three areas of the work are separately described in each of the three respective sections, Chapters II, III and IV, in order to present the results most logically in relation to the experimental procedures. The same applies to previous work more specifically related to each section: this is described as introductory material in each of the Chapters II, III and IV.

Chapter I covers previous work on the state of the surface oxide film at Pt. Chapter II reports new work on the electrocatalytic effect of the oxide film at Pt anodes in relation to the kinetics at an oxide-free surface attainable in a non-aqueous unreactive solvent, trifluoroacetic acid. The kinetics and mechanisms of the Cl_2/Cl^- reaction at electrode interfaces is also discussed. In Chapter III is described an

extension of this work to 100% aqueous solutions with special regard to the effect of Cl^- ion concentration on the kinetics and on the state of oxidation of Pt anodes in the Cl_2 evolution reaction. The effect of the competitive halide ion (especially Cl^-) adsorption is also discussed. Chapter IV describes a study of the reactivity of H_2 at oxidized Pt anode surfaces where an interesting example of oscillatory kinetics of H_2 oxidation was observed and details of this behaviour were investigated.

The three sections of the work described in this thesis have been published or accepted for publication, as follows:

(a) Electrocatalytic Effect of the Oxide Film at Pt Anodes on $Cl^\cdot$ Recombination Kinetics in Chlorine Evolution, by B.E. Conway and D.M. Novak, J.Electroanal.Chem.,(1979).

(b) Chloride Ion Adsorption Effects in the Recombination-controlled Kinetics of Anodic Chlorine Evolution at Pt Electrodes, by B.E. Conway and D.M. Novak, J.Chem.Soc. Faraday Trans.I,(1979).

(c) Oscillatory Kinetics in Electrochemical Oxidation of Hydrogen in an Almost Anhydrous Solvent, by B.E. Conway and D.M. Novak, J.Phys.Chem.,81(1977)1459.

ACKNOWLEDGMENTS

The idea of the theme of this research was first suggested to me by Professor B.E. Conway upon my arrival when Cl_2 evolution chemistry seemed to be an interesting topic with regard to the contraversial accounts provided in the literature. Since then I have been helped by numerous discussions with Professor Conway and the originally proposed theme branched out into the topics covered in this thesis. Therefore I would like to gratefully acknowledge all the help of my supervisor Professor Conway who, with typical generosity, was always prepared to give freely of his time either to deal with experimental research problems or in the discussions that arose during the preparation of the publications and this manuscript. Dr. Conway took the trouble to read this manuscript in detail and to comment on each of the Chapters. He is also responsible for the introduction of all " articles " (indefinite and definite !) and for the " overflow " of commas.

It is also doubtful whether this work would have been completed without the help and enthusiasm of the technical stuff of the Chemistry Department at University of Ottawa to whom I wish to express my grateful thanks:

Mr. Egon Kristof, whose suggestions helped the design and building of special cells and other glass equipment used during the work.

Mr. Joseph Halpern, who was always willing to solve any of the electrical problems which arose during the runs and who also tried to keep my recorder in good working order.

I am also thankful to Dr. Halina Angerstein-Kozlowska for occasional help and discussions, however rare these were.

My thanks are also due to Dr. F.C. Ho, for carrying out the relative reflectance measurements and to Dr. W.B.A. Sharp whose typical potentiodynamic profile of Pt in 0.5 M H_2SO_4 is shown in the Introduction Section of this Thesis.

Grateful acknowledgment is made to Institute "Ruđer Bošković", Division: Centre for Marine Research, for granting me a leave of absence for the period of time needed to complete this project. I would especially like to thank Dr. Marko Branica, director of the Centre for Marine Research and Dr. Božena Ćosović, head of the Laboratory for Physicochemical Separations, for all the help and encouragement they provided.

The Laboratory for Physicochemical Separations, with whose members I worked for three years, I would like to thank too since they all, especially Mgr. Zlatica Kozarac and dipl.ing. Sonja Kozar, unconsciously provided much encouragement during the period of my leave by accepting me unselfishly as one of their number.

I should like to pay special tribute to my family, to whom this thesis is dedicated. All of them constantly provided a reminder of their love and support in all possible ways, making therefore the distance between us less obvious. They shared all my enthusiasm and occasional depression with always the same energetic hope and pride or laughter so characteristic of them all.

Lastly, I would like to express my thanks to the University of Ottawa, Department of Chemistry, for the use of its research facilities.

I would also like gratefully to acknowledge the award of the Joseph W. Richards, Electrochemical Society Summer Research Fellowship for 1978.

TABLE OF CONTENTS

	Page No.
PREFACE	i
ACKNOWLEDGMENTS	iii
TABLE OF CONTENTS	v
LIST OF TABLES and LIST OF SCHEMES	ix
LIST OF FIGURES	x
BRIEF GLOSSARY OF TERMS AND SYMBOLS	xix
ABSTRACT	xxiv

CHAPTER I

GENERAL INTRODUCTION: THE STATES OF OXIDE FILMS ON ANODE SURFACES

1.	INTRODUCTORY REMARKS	1
2.	EQUATIONS FOR THE BEHAVIOUR OF MONOLAYER SURFACE PROCESSES SUCH AS H DEPOSITION OR SURFACE OXIDE FILM FORMATION	3
3.	THE STATE OF THE SURFACE OF ANODES - THICK FILMS AT BASE METALS - THIN FILMS AT PLATINUM	
	(i) General Behaviour	8
	(ii) Thin Oxide Films at Noble Metals (Pd,Ru,Rt,Ir and Au)	10
4.	THE EARLY WORK: USE OF CHARGING CURVES	14
5.	RESULTS FROM THE POTENTIODYNAMIC METHOD	
	(i) Early Work	20
	(ii) Newer Potentiodynamic Work	28
	(iii) Information from the Optical (Reflectivity) Behaviour of Oxidized Pt Surfaces	33
6.	PLATINUM OXIDE FILM GROWTH	38
7.	CHARGE-TRANSFER ACROSS THICK AND THIN FILMS	

Page No.

(i) General 39
(ii) Electron and Ion Transport in Films 40
(iii) Ohmic Resistance 43

8. REACTIONS THAT TAKE PLACE ON AN OXIDE FILM

(i) Types of Effects of Oxide Films 45
(ii) Inhibition Effects in Parallel Reactions 48
(iii) " Demetallization " by Oxide Films 49

CHAPTER II

ELECTROCATALYTIC EFFECTS OF THE OXIDE FILM IN Cl_2 EVOLUTION AT Pt

1. INTRODUCTION

(i) Statement of Objectives 52
(ii) Previous Work on Anodic Cl_2 Evolution 54
(iii) Conclusions 70

2. EXPERIMENTAL

(i) Methods 71
(ii) Solutions and Salts 72
(iii) Rotating Dics Electrode 72
(iv) Oxide Coverage in Cl_2 Evolution Experiments 74
(v) Reference Electrodes 75

3. RESULTS

(i) State of Pt Electrode Surfaces in TFA/H_2O Mixtures with and without Cl^- Ion Present 75
(ii) Kinetic Behaviour in Anhydrous TFA Solutions of RbCl 79
(iii) Kinetic Behaviour in Aqueous and Mixed TFA/H_2O Chloride Solutions 79
(vi) Cl_2/Cl^- Reversible Potentials in TFA and H_2O 81

4. DISCUSSION

(i) Mechanisms 82

Page No.

(ii) Kinetic Analysis for the Recombination Mechanism I, II 83
(iii) Role of the Back Reaction 95
(iv) Simulation of the Tafel Relation for a Recombination-controlled Process 96
(v) Evaluation of k_2 and $\bar{K}_1$ for the Kinetics of Cl_2 Evolution in TFA and Water 98
(vi) Electrocatalysis in Cl· Recombination at Pt: The Presence of the Surface Oxide Film and the Role of Adsorbed Cl^- Ions 99
(vii) Depencence of i_{lim} and k_2 and of $\bar{K}_1$ on Solvent Composition 101
(a) Significance of the Quasi-equilibrium Constant, $\bar{K}_1$ 103
(b) Significance of the Rate Constants, k_1 and k_{-1} 108
(c) Evaluation of K_1 Values 108
(d) Evaluation of k_2 and i_{lim} Values 109
(viii) Coverage by Electrodeposited O Species 111
(ix) Conclusions 116

CHAPTER III

Cl^- ION ADSORPTION AND ITS INFLUENCE ON Cl_2 EVOLUTION KINETICS AND THE STATE OF OXIDIZED Pt ELECTRODES

1. INTRODUCTION
(i) Statement of Objectives 117
(ii) Previous Work on Cl^- Ion Effects on the Cl_2 Evolution Reaction 118
(iii) Relation of Cl^- Ion Adsorption to that of Other Halides at Electrodes: State of Adsorbed Halide Ions:
(a) Introductory Remarks 127
(b) Specific Adsorption of Cl^- and Other Halide Ions 127
(c) Reflectivity and Halide Ion Adsorption 134
(d) Conclusions 137

Page No.

2. EXPERIMENTAL

(i) Methods 138
(ii) Rotating Disc Electrode 139
(iii) Solutions and Salts 140
(iv) Oxide Coverage in Cl_2 Evolution Experiments 140
(v) Reference Electrodes 141

3. RESULTS

(i) The log [current-density] vs. Potential Relations 141
(ii) Surface Oxidation of the Pt Electrode in Cl^- Ion Solutions 146
(iii) Reaction Order 150

4. DISCUSSION

(i) Test for the Recombination Mechanism 155
(ii) Effects of Chloride Ion Adsorption on Extent of Surface Oxidation at Platinum Anodes 161
(iii) Significance of Lateral Interaction Effects at the Pt Surface and the Influence of Adsorbed Cl^- Ion 166
(iv) Significance of Reaction Orders in Relation to Mechanisms 167
(v) Inhibition effects 170
(vi) Conclusions 171

CHAPTER IV

SURFACE OXIDATION IN OSCILLATORY KINETICS OF H_2 OXIDATION AT Pt IN AN ALMOST ANHYDROUS SOLVENT

1. INTRODUCTION 174

(i) Brief Review on the Existence of Periodic Reactions, Especially in Electrode Processes:

(a) General Requirements and Conditions for Oscillatory Behaviour 177
(b) Some Examples of Oscillatory Behaviour in Previous Work:

(1) Metal Oxidation Processes 180

Page No.

(2) Organic Oxidation Processes 181
(3) Oscillations in other Types of Systems 184
(ii) Kinetics of H_2 Oxidation at Pt in Aqueous Solutions 185

2. OBJECTIVES OF THE WORK 191

3. EXPERIMENTAL

(i) Choice of Solvent System 192
(ii) Chemicals and Purification Procedures 193
(iii) Solutions 194
(iv) Glassware and Cleaning Procedures 194
(v) Apparatus 195
(vi) Electrodes and their Purity 195
(vii) Experimental Procedure 195

4. RESULTS AND PRELIMINARY DISCUSSION

(i) The Current-Potential Profiles for Pt in Anhydrous TFA and with Added Traces of Water: 197
(1) Effects of Added Water 197
(2) H Adsorption in Anhydrous and Almost Anhydrous TFA 198
(3) Surface Oxidation of Pt in Almost Anhydrous TFA in Relation to that in Water 200
(ii) Oscillations in H_2-Oxidation under Potentiostatic Conditions 203
(iii) Oscillations in H_2-Oxidation Current under Potentiodynamic Conditions:
(1) Behaviour in almost Dry Solutions 208
(2) Relation to Surface Oxidation of Pt in TFA with Controlled Additions of Water 214

5. GENERAL DISCUSSION

(i) Origins of Oscillatory Behaviour 227
(ii) Kinetic Equations 228
(iii) Role of Inhibition by Anion Adsorption and H_2 Accumulation and Transport in the Diffusion Layer 232

Page No.

(iv) Cycle of Processes in Periodic H_2 Oxidation 234

236

APPENDIX I

238

CONTRIBUTIONS TO ORIGINAL RESEARCH

241

REFERENCES

LIST OF TABLES

Page No.

TABLE 1 Values of k_2 and K_1 from the plots in Figs. 7a and 7b, and from limiting current-densities (T = 298 K). 100

TABLE 2 Charges associated with oscillations in current at constant potential. 206

TABLE 3 Charges associated with successive periodic H_2 oxidation current peaks in potentiodynamic experiments (as in Fig. 35). 224

LIST OF SCHEMES

SCHEME I Cycle of Processes in Pt Oxidation 37

SCHEME II Cycle of Processes in Periodic H_2 Oxidation 235

LIST OF FIGURES

Page No.

Fig. 1 Comparison of galvanostatic and potentiostatic current-potential curves for a Pt electrode (schematic). 19

Fig. 2 Typical potentiodynamic current-potential profile at Pt in 0.5 M H_2SO_4. 21

Fig. 3 Potentiodynamic i-V profiles for a Pt electrode in anhydrous TFA + KTFA as electrolyte with addition of water. 73

Fig. 4 (a) Series of potentiodynamic i-V profiles for a Pt electrode in TFA/H_2O mixtures with 0.5 M Cl^- (as RbCl or KCl) showing development of oxide reduction peak with increasing water content. (b) Charges for surface oxide reduction after holding for 1 min and longer times. 77

Fig. 5 Log current-density vs. overpotential curves for anodic Cl_2 evolution from 0.5 M RbCl solution in TFA and from 0.5 M KCl + 0.05 M HCl in water. 78

Fig. 6 Test of recombination-controlled mechanism for $Cl^\bullet$ according to eqn. (9) for various 0.5 M Cl^- solutions in TFA/H_2O mixtures from 0% to 100% H_2O: a) full range of η . 85

Page No.

b) enlarged scale. 86

Fig. 7 Test of recombination mechanism for $Cl^{\cdot}$ according to eqn. (10) for various 0.5M Cl^- solutions in TFA/H_2O mixtures from 0% H_2O to 100% H_2O : a) full range of η 88
b) enlarged scale . 89

Fig. 8 Computed electrochemical adsorption isotherms according to eqn. (12) for various g values. 91

Fig. 9 Numerical evaluation of the forms of eqn. (13) for values of g = 0, 2, 4, and -2 using eqn. (12) for the quasi-equilibrium chemisorption of $Cl^{\cdot}$ and eqn. (11) for the recombination-controlled current-density. 92
a) enlarged scale. 93

Fig. 10 Simulation of log i vs. V relations for the $Cl^{\cdot}$ recombination kinetics with various g values, using eqns. (11) and (12). 97

Fig. 11 Plot of $i_{2,lim}$ vs. composition (mol% H_2O in TFA) for 0.5M Cl^- solutions (as RbCl or KCl) at 298 K. 102

Fig. 12 Plots of k_2 from $i_{2,lim}$ and from the linear regions of Figs. 6b and 7b together with K_1, against solvent composition (mol% H_2O in TFA) for 0.5M Cl^- solutions (as RbCl or KCl) at 298 K. 104

Page No.

Fig. 13 Surface oxide coverage, as charge, at Pt electrodes in 0.5M Cl^- solutions as a function of anode potential. Comparative data for Cl^-- free solutions of 0.5 M, 0.25 M and 1.5 M H_2SO_4 are also shown. 112

Fig. 14 Plots of k_2 from $i_{2,lim}$ and from Figs. 6b and 7b as a function of Pt surface oxide charge determined after holding the potential for 1 min at various anode potentials. Variation of $\bar{K}_1$ with charge for oxide reduction obtained for the same conditions is also shown. 114

Fig. 15 Log [current-density] vs. overpotential curves for Cl_2 evolution from aq. 0.5 M KCl + 0.05 M HCl (298 K) at a rotating disc Pt electrode at 1600, 3600 and 6400 r.p.m. 142

Fig. 16 Log [current-density] vs. overpotential curves for Cl_2 evolution at Pt from aq. solution of 0.05 M HCl + various concentrations of KCl. 144

Fig. 17 Estimates of i_{lim} and ln i_{lim} as a function of the log of the Cl^- ion concentration for Cl_2 evolution at Pt at 298 K. 145

Fig. 18 Family of cyclic-voltammetry curves for Pt in various aq. solutions of HCl + KCl at 298 K showing blocking of surface oxidation of the Pt anode. 147

Page No.

Fig. 19 Linear relation (Temkin behaviour) between % oxide blocked at Pt by Cl^- ion and log $[Cl^-]$. 148

Fig. 20 Plots of surface oxide reduction charge at Pt as a function of $[Cl^-]$ for surface oxide generated in a potential sweep taken to 1.4V E_H with various times τ_h of holding at 1.4V. 149

Fig. 21 Plots of surface oxide reduction charge at Pt as a function of potential held for τ_h = 60 s at positive end of potential sweep in Cl_2 evolution region, for various Cl^- ion concentrations. Also shown for comparison is the potential dependence of surface oxide reduction charge measured in Cl^--free aq. H_2SO_4 solutions. 151

Fig. 22 Values of limiting surface oxide reduction charge at Pt in Cl^- solutions as a function of log $[Cl^-]$. 152

Fig. 23 Experimental reaction order plots for Cl_2 evolution at Pt at 298 K. Log [i] , i.e. current-densities at various constant η values are plotted against log $[Cl^-]$. 156

Fig. 24 Theoretically based plots for testing a recombination-controlled mechanism for anodic Cl_2 evolution for various Cl^- ion concentrations : a) $(\exp \eta F/RT)/i^{\frac{1}{2}}$ vs. $\exp \eta F/RT$ 159

Page No.

b) $i^{-\frac{1}{2}}$ vs. exp - $\eta F/RT$. 160

Fig. 25 Values of K_1 and k_2 for the Cl_2 evolution mechanism I, II as a function of Cl^- ion concentration. k_2 from i_{lim} is also shown as f[Cl^-]. 162

Fig. 26 Relation between log k_2 for the concentrations indicated : a) 0.1; b) 0.2; c) 0.3; d) 0.4; e) 0.5; f) 0.75; g) 1.0; h) 1.5; i) 2.0; j) 3.0; k) 4.0 and l) 4.8 mol dm^{-3}. 163

Fig. 27 Oscilloscope photos of the inhibition effect in the initial Cl_2 evolution current-potential behaviour in a cyclic-voltammetry experiment at Pt. 172

Fig. 28 Types of current-potential curves arising due to a passivation effect. 179

Fig. 29 Effect of diminishing positive end potential E_a in the anodic sweep at Pt in TFA containing 0.42 mol% H_2O (and in 0.1 and 1.0 M aqueous $HClO_4$ for comparison) on the charge for surface oxide formation and reduction. 201

Fig. 30 Plot of cathodic peak potential V_p for reduction of surface oxide at Pt as a function of the charge for reduction in TFA and aqueous 0.1 and 1.0 M $HClO_4$. 202

Fig. 31 Four examples (a, b, c, d) of potentiostatic (+ 1.24V) oscillations of H_2-oxidation current at the Pt electrode

Page No.

in TFA. e) Record of an apparent simple type oscillation on a faster time base (20 cm s^{-1}) showing " nonsinusoidal " behaviour. 204

Fig. 32 (a) Current-potential profiles for H_2 oxidation in very dry TFA + 0.5 M KTFA solution (stirred and unstirred) (b) Background i-V profile for Pt in the TFA solution in absence of H_2. 209

Fig. 33 Current oscillations in H_2 oxidation on the cathodic sweep in two potentiodynamic experiments on H_2 oxidation at Pt in almost dry TFA + 0.5 M KTFA. Relative reflectance changes ($\Delta R/R$) measured simultaneously with the oscillations are also shown. 210

Fig. 34 Test of relation between current oscillation amplitudes Δi in Fig. 33 and the square-root of the time interval, Δt, between successive oscillations for the two series of oscillations shown in Fig. 33 for separate experiments. 212

Fig. 35 Current oscillations in H_2 oxidation on the cathodic sweep in a potentiodynamic experiment at Pt in TFA + 0.2 mol% added water. 215

Fig. 36 Potentiodynamic i-V profiles for H_2 oxidation at Pt in 0.1M aqueous $HClO_4$ without and with holding at 1.453 V E_H for 2 min;(a) Background curve (without H_2 present) for Pt surface oxidation and reduction over the same potential range at the same sweep rate is shown for comparison in (b). 216

Page No.

Fig. 37 Current difference for H_2 oxidation at Pt in 0.1 M aqueous $HClO_4$ with holding for 2 min (a), and without holding (b), after subtraction of background i-V profile for Pt in absence of H_2. 218

Fig. 38 Transitional case between oscillatory behaviour in Fig. 33 and that in Fig. 35. A small quantity of water is present and corresponding small oxide coverage is generated: (a) background i-V profile for Pt for two additions of trifluoroacetic anhydride, (b) oscillatory behaviour of H_2 current. 220

Fig. 39 Current oscillations in H_2 oxidation at Pt in TFA as in Fig. 35 but with an increased quantity of added water. Lower curve shows background i-V profile for Pt in the TFA solution in absence of H_2. 223

Fig. 40 Oscillations in H_2 oxidation at Pt in TFA containing traces of water on a cathodic sweep initiated just at the potential where surface oxidation commences. 225

Fig. 41 As in Fig. 39 but with further addition of traces of water. Lower curve shows background i-V profile for Pt in the TFA solution in absence of H_2. 226

BRIEF GLOSSARY OF TERMS AND SYMBOLS

Cyclic-voltammetry- The method for studying electrode reactions under controlled-potential conditions when the potential is cycled in the anodic and cathodic directions in a repetitive manner at constant voltage sweep-rate, $\pm dV/dt$; developed by Will and Knorr for the study of surface processes at noble metal electrodes.

" d.l. " or " double-layer " region - the potential range in a cyclic-voltammetry i-V profile over which the currents are predominantly, or only, those for charging of the double-layer capacitance.

" H-region ", " oxide region " - potential ranges for deposition or ionization of H or deposition of OH or O species at Pt in a cyclic-voltammetry experiment.

" Surface oxide " - generic term applied to the monolayer (or thicker) of oxygen species (as OH or O) that can be electrodeposited or reduced at noble metal electrodes.

Potentiostatic - controlled potential procedure

Potentiodynamic - controlled potential procedure used in a dynamic way with a time-variant potential.

Galvanostatic - controlled-current procedure.

" iR " drop - Potential drop near a working electrode due to passage of current (density) i across local resistance R of solution.

Electrosorption - chemisorption of a radical or atom at an electrode surface as a result of a Faradaic charge-transfer process.

" Langmuir conditions " - condition for which the Langmuir isotherm applies (approximately) to the adsorption behaviour of some species.

" Temkin conditions " - conditions for which a Temkin or Temkin-type of isotherm applies to an adsorption process, giving rise to a linear relation between coverage and log concentration (often applied to interaction effects where adsorption effects similar to those due to broad heterogeneity of adsorption sites arise - for such cases, the interaction effects are characterized by a factor g - see below.).

Tafel line - the linear overpotential (η) - log [current-density] , relation found for many activation-controlled processes.

Tafel slope, b - the slope, $d\eta / d \log i$, of such a Tafel line

i_{lim} - limiting current-density due to potential-independent rate of a chemical step at an electrode in an electrochemical reaction sequence.

i - an experimentally measured current-density (A cm^{-2}).

i_o - the exchange current-density (or reversible rate in terms of equal anodic and cathodic current-densities at the reversible potential of a process) .

η - activation overpotential = $V - V_{rev}$

V - an electrode/solution potential difference (p.d.)

V_{rev} - the electrode/solution p.d. when a process is at equilibrium

E or E_{rev} - an electrode potential experimentally measured with respect to some reversible reference electrode

E_H - potential measured with respect to that of a reversible H_2/H^+ electrode in the same solution (" Hydrogen scale ")

β - barrier symmetry factor in an electron-transfer process

α - transfer coefficient in the Tafel slope , $b = RT/\alpha F$

K - an equilibrium constant for a process at an electrode

$\bar{K}$ - an electrochemical equilibrium constant for a process involving charge-transfer and including an " exp VF/RT " term (usually $\bar{K} = K \exp VF/RT$)

k - rate constant for a process at an electrode (normally containing an exp term in electrode potential for charge-transfer processes)

θ - coverage by an adsorbed intermediate or other species

g - parameter defining the extent of variation with coverage θ of that part of free energy of adsorption associated with interaction effects in ad-layer.

Sweep-rate, s , $= dV/dt$ ($V\ s^{-1}$)

C, Capacitance - of double-layer charge distribution at electrode interface or (as a pseudo-capacitance) of an ad-layer where coverage θ is a function of potential V.

Δ - Ellipsometric phase-shift parameter

($\Delta R/R$) - relative reflectivity change for parallel ($\parallel$) or perpendicularly ($\perp$) polarized light

R - reaction order (under some specified conditions)

C_x or $[x]$ - the concentration of a species, X , in solution

a_x - the thermodynamic activity of a species $[x]$

ABSTRACT

This abstract is given in three sections, covering the three respective parts of the work to be described in Chapters II, III and IV as follows:

1. In aqueous medium, Cl_2 evolution on noble metal anodes occurs on a surface oxide film, the properties of which, rather than those of the metal, determine the kinetics of the reaction.

   The kinetics of Cl_2 evolution on an oxidized Pt electrode in aqueous KCl are compared with those for Cl_2 evolution on a demonstrably unoxidized Pt surface in anhydrous trifluoroacetic acid (TFA) as solvent. Hence the effects of development of an oxide film on Pt in aq. medium can be determined in relation to the kinetic behaviour of Cl_2 evolution on the unoxidized Pt metal surface.

   In both TFA and water, and their mixtures, it is shown that Cl_2 evolution kinetics are recombination-controlled and non-diffusion-controlled limiting currents, i_{lim} , are observed. The i_{lim} values in aq. medium, i.e. for the oxide-coverd surface, are some 15 - 45 times larger than on the free Pt surface in TFA; since the mechanism is shown to be same in the two solvents, and their mixtures, this observation indicates a substantial electrocatalytic enhancement of the recombination rate for $Cl^{\cdot}$ on the oxide in comparison with the Pt metal surface. This is presumably due to weaker binding of $Cl^{\cdot}$ on oxidized Pt than on the

" bare " Pt surface. Effects due to specific adsorption of Cl^- ion are also important and give rise to dependence of the recombination catalysis on Cl^- ion concentration.

A method is proposed for analyzing the recombination kinetics by means of linear plots which give both the recombination rate-constant and the quasi-equilibrium constant for the prior Cl^- ion discharge step.

2. The role of chloride ion adsorption in the anodic Cl_2 evolution reaction at Pt electrodes in aqueous chloride solutions is examined for a range of Cl^- ion concentrations. A new method of testing the applicability of a recombination-controlled mechanism is applied, thus enabling both the rate-constant of the prior Cl^- discharge/$Cl^\bullet$ electrosorption step to be evaluated quantitatively as a function of Cl^- concentration.

It is shown that the Cl_2 evolution process at Pt is recombination controlled over a wide range of Cl^- ion concentrations. Despite the approach of the anodic current-potential relation towards limiting-current behaviour, consistent with recombination-controlled kinetics, the limiting current-densities are dependent on Cl^- ion concentration. It is suggested that this is due to (a) effects of specifically adsorbed Cl^- ion on the $Cl^\bullet$ recombination rate constant and (b) changes of state of the Pt anode surface due to competitive effects of Cl^- ion adsorption on the extent of surface oxidation of the Pt surface on which the catalytic recombination of discharged $Cl^\bullet$ takes place in aqueous medium. These two factors

complicate the interpretation of reaction orders in Cl^- for the Cl_2 evolution reaction since both specific adsorption and the competitive effects in surface oxidation have to be taken into account in relating rates to Cl^- ion concentration.

3. In a number of electrochemical (and chemical) reactions, a situation can arise where no stable steady state of the reaction is established. The system then exhibits sustained oscillations around an unstable steady state. The conditions giving rise to this state of affairs often involve diffusion and inhibition of a reaction, leading to a current-potential relation for the process which shows an inversion corresponding to negative resistance or positive feedback. In the present work, the inhibition of oxidation of H_2 at a Pt anode has been studied in trifluoroacetic acid containing controlled traces of water. Under these conditions, only a small fraction of the surface is anodically oxidized and H_2 oxidation occurs in a kinetically periodic way when potentials are reached at which the oxide layer can begin to be reduced and readsorption of trifluoroacetate anion can occur. The oscillations are related to the diffusion-controlled mass trasport of H_2. Sustained, rather than damped oscillations, are observed under potentiostatic conditions since electrical power is provided to the reaction from the external circuit. The participation of the surface oxide and anion adsorption/desorption in the oscillations was deduced indirectly by <u>in situ</u> observation of periodic changes of relative reflectance in-phase with the oscillations. The changing

period, Δt , of oscillation which arises in a cathodic potential sweep can be related to the current pulse amplitudes, Δi . A linear relation to $(\Delta t)^{\frac{1}{2}}$ is demonstrated which provides a key indication that the oscillations arise because of coupling between the kinetics of the electrocatalytic oxidation reaction and diffusion mass transfer of H_2. A cycle of processes that qualitatively gives an account of the oscillatory behaviour is also given.

CHAPTER I

GENERAL INTRODUCTION:

THE STATES OF OXIDE FILMS ON ANODE SURFACES

1. Introductory Remarks

The work described in this thesis involves the study of (i) a reaction of H_2 with the oxide film on Pt anode surfaces; (ii) a reaction of Cl^- to form Cl_2 on Pt anode surfaces and (iii) competitive adsorption of Cl^- ions in (ii) with electrodeposited OH/O species at Pt in anodic oxide film formation. The role of the oxide film at Pt in these processes is a major aspect of the work to be reported here. Therefore, it will be appropriate to begin by a description of previous work in which the states of oxide films formed at Pt and other anodes in aqueous solutions have been characterized under various conditions.

The methods which have been employed are as follows:

(i) Electrochemical: (a) from charging curves for film formation and reduction[1,2]; (b) from integration of cyclic voltammetry current-potential profiles[3]; these methods are based on a microscopic application of Faraday's Laws and can give information on distinguishable states of the film below monolayer coverage.

(ii) Chemical: film stripping by a reagent that reacts with the film, or physical stripping of the film followed by quantitative chemical analysis, if the film is sufficiently thick[4];

(iii) Optical: from ellipsometry; this method, under favourable circumstances, gives the film thickness and the real and imaginary (absorption coefficient) components of the refractive index[5];

(iv) X-ray Photo-electron Spectroscopic (Auger and ESCA): giving information on valence states[6,7] of atoms in the film, elemental analysis and depth profiles of element distribution in complex thick films;

(v) Electrical: giving information on the conductivity behaviour of oxide films[8].

The properties of the surface oxide film at Pt that will be of interest in the present new work are: (i) the oxide film coverage as a function of electrode potential; (ii) the physical state of the film, including the valence states of Pt within it; (iii) its conductivity or electron-transfer properties and (iv) its adsorptive properties with respect to Cl^- ion and $Cl^\bullet$, and its catalytic properties with respect to $Cl^\bullet$- recombination, H_2 oxidation and O_2 evolution.

2. Equations for the Behaviour of Monolayer Surface Processes such as H Deposition or Surface Oxide Film Formation

(i) General Relations: The general kinetic equation for a surface process in which a species, e.g. H, is electrodeposited or desorbed at the level of a monolayer is written

$$i_s = q_1 \frac{d\theta}{dt} = k_1(1-\theta)\, C_{H^+} \exp[-\beta(V - V^{\circ}_{\rightleftarrows H} + \eta)F/RT] - k_{-1}\, \theta_H \exp[(1-\beta)(V - V^{\circ}_{\rightleftarrows H} + \eta)F/RT] \quad \ldots(1)$$

where θ_H is the coverage at a potential $V + \eta$ and is $f(V)$, q_1 is the charge for the formation of a monolayer and η is the overpotential required for net current flow. This equation applies to a surface process such as

$$\underset{1-\theta_H}{Pt} + \underset{C_{H^+}}{H_3O^+} + \underset{V}{e} \underset{k_{-1}}{\overset{k_1}{\rightleftharpoons}} \underset{\theta_H}{PtH_{ads}} + H_2O \qquad (2)$$

over a potential region where H species can be electrochemically deposited or ionized. k_1 and k_{-1} are the rate constants for the surface process, θ_H is the coverage at a given potential. A similar equation to (1) applies to the electrodeposition of OH or O species at higher positive potentials. The coverage θ is thermodynamically related to potential at a given concentration C_{H^+} when $i_s = 0$ for equilibrium conditions, i.e. when $\eta = 0$. Then

$$V - V^{\circ}_{\rightleftarrows H} = \frac{RT}{F} \ln \frac{\theta_H}{1 - \theta_H} \cdot \frac{1}{C_{H^+}} \qquad (3)$$

where $V^{\circ}_{\rightleftarrows H}$ is a standard potential for the surface process defined for $\theta_H = 0.5$ and $C_{H^+} = 1$ (strictly for hypothetical $a_{H^+} = 1$).

Since θ_H requires a corresponding passage of charge q (q_1 for $\theta_H = 1$)* a quantity $dq/d(V - V^{\circ}_{\rightleftarrows H})$ having the nature of a capacitance can be defined

*(as shown in eqn.2)

and follows from eqn.(3) by differentiating $(V-V_{r,H})$ w.r.t. θ_H. $dq/d(V-V_{r,H})$ is not a real capacitance like that of the double-layer and is referred to as the adsorption pseudo-capacitance, denoted by C_ϕ .

For reversible conditions of deposition or removal of an ad-species, C_ϕ is a symmetrical function of θ (or of V) with a maximum at $\theta = 0.5$.

The formation or removal of a mono (or thin)-layer surface film at an electrode can only be examined by non-steady-state techniques since no continuous faradaic process can occur for such a film. Either (a) a constant current pulse is applied ("galvanostatic conditions") and the potential V(t) as a function of time is observed or (b) the potential is varied in a controlled way, e.g. linearly in time (potentiodynamic sweep method), and the resulting current, i(V,t), is observed.

(ii) Galvanostatic Charging : Here a constant controlled current (density) i is applied to the electrode. The potential of the electrode as a function of time, t , is measured and changes because (a) the double-layer capacitance C is charged and (b) species are electrodeposited at the electrode in some kind of a thin film according to eqns.(1),(2). The time-dependence of potential is given by solution of the equation

$$i = \text{constant} = C\left(\frac{dV}{dt}\right) + k_1(1-\theta_H)C_{H^+} \exp -\beta\,(V-V^\circ_{r,H} + \eta)F/RT$$
$$- k_{-1}\,\theta_H \exp(1-\beta\,)(V-V^\circ_{r,H} + \eta)F/RT \qquad \ldots (4)$$

(iii) Potentiodynamic Conditions : Here the equation for the current is

$$i = C\left(\frac{dV}{dt}\right) + C_\phi\left(\frac{dV}{dt}\right) \qquad (5)$$

where C_ϕ is the adsorption pseudo- capacitance defined above for potential-dependence of coverage θ. dV/dt is the sweep rate (s) applied in the experiment.

Equation (2) arises by writing the current for the surface process, $i - C(\frac{dV}{dt})$, as $\frac{dq}{dt}$ where q is the net charge passing which produces (or removes) an electrodeposited species, e.g. H,OH or O, on the electrode surface. $\frac{dq}{dt}$ can be written $\frac{dq}{dV} \cdot \frac{dV}{dt}$. $\frac{dq}{dV}$ has formally the nature of a capacitance like that of the double-layer, so is referred to as an adsorption pseudo-capacitance, C_ϕ.

Under irreversible conditions, or more generally, i must be written as in eqn.(1) with V taken as the independent variable and defined as $V = V_{in} \pm st$, where s is again the sweep rate dV/dt (= constant) and V_{in} is the initial potential in a sweep. Solution of eqn.(1) for these conditions gives the shape of the i-V profile in a potentiodynamic experiment for a species adsorbed in a single state on the surface. Multiple states arise when different V_r^o values apply to the electrodeposited species in the monolayer as θ increases from $0 \rightarrow 1$ or vice versa.

The reason for the normally observed maximum in the i-V profile for a single-state adsorbed species is simply that, at low θ, the deposition current increases in the usual exp manner but, as charge continues to pass, θ increases so that the $1-\theta$ term decreases and eventually inhibits flow of current. Also, in a reversible surface process, the back reaction rate increases with θ.

In evaluations of charges, corresponding to θ values for various

species, allowance must always be made for the current component, $C(\frac{dV}{dt})$, that goes into charging of the double-layer capacitance, C (see p. 4).

(iv) Evaluation of Charges : In the galvanostatic method, the evaluation of charges for a given surface process corresponds simply to the duration of the arrest, Δt , at constant i. Hence the q value is $\Delta t\, i$. In potentiodynamic experiments, the q value for a given process corresponds to the area under the respective i(V,t) peak, viz. $\int_{t_1}^{t_2} i\,dt \equiv \int_{V_1}^{V_2} \frac{i}{s}\,dV$, where the relevant part of the i-V profile extends effectively over a potential interval $V_2 - V_1$. The double-layer charging contribution over the same potential interval must be subtracted out, $q_{d.l.} = \int_{V_1}^{V_2} C\,dV$ (see below).

(v) Double-layer Capacitance : In potentiodynamic work, it is usually assumed that the same double-layer capacitance applies in the oxide region as on a bare metal but this is only an approximation. This matter was considered by Schuldiner and Roe[9] for charging curves, and they took an average value of 40 $\mu F\ cm^{-2}$ up to 1.8 V at Pt. A fall-off of double-layer capacitance may, however, be expected as the oxide film is formed.

In the H and OH/O regions, the double-layer capacitance is masked by the high pseudo-capacitances for the H or OH and O adsorption processes, as pointed out by Breiter et al.[10] The actual value of $C_{d.l.}$ at Pt in the absence of chemisorbed species was considered to be 18-20 $\mu F\ cm^{-2}$ [10-13]. However, Gilman[14] pointed out that this value is certainly too low since the Pt surface is covered with adsorbed species, especially anions such as SO_4^{2-}, from the solution itself. In the region where the Pt surface is covered with adsorbed oxygen , some authors[14,15] have stated that the d.l. capacitance

rises nearly in proportion to the amount of adsorbed oxygen. Gilman[14] and Breiter[10,16] showed that the capacitance rises sharply over the range 0.4V to 0.8V E_H and that when the surface is completely covered with oxide the capacitance drops to a lower value. The rise in capacity in this range was attributed to a change in the structure of the double-layer due to the roughness of the surface. As Gilman[14] stated, above 0.8V in $HClO_4$ or H_2SO_4, the total capacitance at first increases (170 $\mu F\ cm^{-2}$ at 0.9V) and then falls to ca. 100$\mu F\ cm^{-2}$ at ca. 1.5V[16]. This is due to the pseudo-capacitance associated with electrodeposition of oxygen species[16]. The true double-layer capacitance is only accessible in this region by high frequency a.c. measurements.

Gilman[14] considered that the disagreements for the capacitance of Pt in $HClO_4$ may be explained on the basis of varying extents of coverage of the surface with adsorbed impurities. On a clean Pt surface, the capacitance was found to be 33 $\mu F\ cm^{-2}$ at 0.4V E_H. After that it rises to a maximum of 170 $\mu F\ cm^{-2}$ at 1.5V E_H. This behaviour was not attributed to the effect of " adsorbed oxygen " but to a change in the structure of the ionic double-layer with increasing potential. Once the surface is oxidized, the capacitance drops due to thickening of the film. However, for the thin oxide films on Pt and other noble metals, the conductivity is too high[8] for a dielectric capacitance to arise from the film itself as it does with the barrier-layer " valve " metals. Formaro and Trasatti[17] followed up Gilman's work by examining the time-dependence of the differential capacity at Pt measured at 5 kHz in the potential range where the electrode was free from H or O species. The value of $C_{d.l.}$ in this region was ca. 34 $\mu F\ cm^{-2}$. Various reasons, including diffusion of impurities and surface rearrangement were considered, for the time-dependence of double-layer capacitance.

3. The State of the Surface of Anodes - Thick Films at Base Metals - Thin Flims at Platinum

(i) General Behaviour: Metal surfaces can normally undergo or participate in several types of oxidation reactions as anodes in suitable electrolyte solutions[18-20]: (a) oxidation of the metal as free solvated metal ions; (b) oxidation to form an oxide film by electrochemical reaction with the electrolyte; (c) dissolution as solvated ions by passage of ions through the oxide film; (d) O_2 evolution on the oxidized metal surface as a subsequent reaction but often electrochemically coupled with the surface oxidation process and (e) anodic evolution of other species, e.g. Cl_2, on the oxide film at the electrode. Which of these reactions occurs at a given metal depands on several factors: (1) the properties of the metal itself; (2) the experimental conditions, such as choice of electrolyte, current-density and temperature. This means that some metals such as Cu can undergo anodic dissolution in acidic solutions while, in alkaline solutions, their surfaces would become covered with an oxide film.

Most metals, when used as anodes at sufficiently positive electrode potentials, become coated with an oxide film leading to " passivation " of the metal dissolution process. This behaviour occurs in a relatively narrow potential range. The thickness of the resulting film depends on the metal and on the conditions of the growth (interfacial field, temperature, etc.) and can be in the range of a few layers to a few thousand layers. These films can be compact or porous depending on the conditions under which they are grown. They also may be distinguished according to their conductivities, e.g. oxides formed on Pt are known to be fairly thin and conducting, those

at Ni thicker and conducting while those at the "valve" metals (Ti, Ta, Zr, Al) are thick and behave as insulators[18,20a]. Such films are usually highly protective since diffusion of metal cations or O anions through the film is so slow that they almost completely inhibit dissolution of the underlying metal. However, the oxide films on these metals[21] thicken in proportion to the field applied across them by mechanisms involving either cation or anion transport (or both in some cases). Some "leakage currents" do arise through the films and these are ascribed to defects in the film or to the presence of pits[18-20a].

At sufficiently extreme potentials, H_2 or O_2 can be made to evolve upon the protective films if sufficient voltage is applied to overcome the high resistivity of the films. At such oxide films, there are two regions where ion or electron-transport occurs: one at the metal/oxide interface and the other at the oxide/solution interface.

Another type of behaviour can arise at heavily oxide-coated metals where the anodic oxidation process is either partially or completely the anodic dissolution of the metal itself. This process may take place with or without formation of an intermediate reaction film on the electrode surface. In the case of Al or Fe, depending on the type of electrolyte, anodic oxidation is coupled with the anodic dissolution of the metal[21]. Depending on the nature of the electrolyte, Al can develop solid compact films which are virtually insoluble (borate or tartarate buffers, pH ≃ 5-7) or finely porous films which result from slow dissolution of the film itself (acidic solutions: sulphuric, chromic or oxalic acids).

Some metals such as Fe or Ni[18-20a] exhibit a transition between so-called active and passive states. The first is characterized by either

a dissolution of the metal itself or by the formation of a porous salt or hydroxide layer, which becomes transformed into a passive, protective form as the valence state of oxidation of the metal is increased and the oxide film is formed directly or when the lower hydroxide is converted into an higher oxide. The passive film on Fe is in some respects like the oxide film formed on Ta surfaces, although the range of potentials over which the film grows is different.

Less noble metals such as Ag, Cu and Ni tend to form thick oxide layers[9,19]. Depending on the stoichiometry and conditions of formation, oxide films formed at these metals may behave as non-conducting insulators but they are usually semiconducting due to the presence of more than one valence state of the metal.

In the material which follows, attention will be concentrated on the behaviour of very thin oxide films which are formed on the noble metals, especially Pt.

(ii) Thin Oxide Films at Noble Metals (Pd,Ru,Pt,Ir and Au)

In the case of platinum and other noble metals, between the thermodynamic limits for cathodic evolution of H_2 and anodic evolution of O_2, one or two monolayers of oxygen species are electrodeposited (chemisorbed) as the potential is made increasingly positive. At least a full layer of O species (2e passed per substrate metal atom) is usually formed before molecular O_2 evolution proceeds. Since the state of the oxide film required for generation of O_2 at significant (experimentally detectable) rates usually corresponds to potentials well above the reversible potential for O_2

in the given solution, O_2 evolution commences at appreciable overpotentials (0.2~0.3 V) on the oxide film.

The study[18-20] of anodic oxidation of noble metals provides insight into the understanding of the oxidation of metal surfaces in general, as the first stages of metal oxide film growth can be sensitively followed at metals of this group before electrolytic evolution of O_2 occurs. Different noble metal surfaces exhibit a variation in the nature of the anodically formed oxide films[22].

Pt and Rh behave as the noblest metals of the group with respect to the extent of anodic oxide formation that occurs up to moderate potentials (1.8 V). The surface of Pt is normally covered with only a thin (monolayer) oxide layer, which is conducting[8]. Its growth commences[22a] at about + 0.75 V E_H and the electrodeposition of chemisorbed oxygen atoms or ions* into a monolayer is completed already below the O_2 evolution potential[18,19,23]. This growth is rather complex and will be explained in more detail later. Only under special and extreme conditions of anodic polarization[19] can thicker oxide films be formed at Pt.

At Au, initial surface oxidation does not commence until 1.37 V (in 1M H_2SO_4) so this metal appears more noble than all other noble metals. However, it is less noble in the sense that relatively thick oxide films can be formed by continuous anodic polarization for 30-60 min. after the initial monolayer formation[24]. Nevertheless, in short-time experiments

*The charge state of electrodeposited species such as OH, O or H on electrode surfaces is uncertain. It depends on the extent of charge transfer in the electrodeposition process. The so-called " electrosorption valency "[25,26] characterizes the state of electrodeposited species or of chemisorbed ions.

in a time scale[27] of 10 ms to 10 s only monolayer oxide films are formed so that, in this respect, Au behaves much like Pt. At Pt, on the other hand, prolonged anodic polarization will not cause the oxide film to grow beyond about 2 equivalent O monolayers in thickness [28], "PtO_2", although under special extreme conditions, thicker layers can be formed[8,29]. When the monolayer of oxygen is completed, O_2 evolution commences at small but significant rates beyond ca. 1.4 V E_H.

The interpretation of the properties and formation of the oxygen layer on the Pt surface is rather complex since three factors contribute to the difficulty of studying the system:

(i) the state of the bare metal surface itself, as it is important that perfectly clean surfaces be present initially without any other foreign adsorbed species, except inevitably anions from the electrolyte;

(ii) the irreversibility of the film formation and reduction processes, leading to a displacement of current peaks for oxide formation and reduction in comparison to those for reversible H adsorption and ionization processes, and

(iii) the possibility of eventual formation of a multi-layer oxygen film, beyond the initial monolayer, in contrast to that for H where only a monolayer film is formed.

The state of the adsorbed oxygen film on Pt surfaces has been determined variously to be nominally PtOH and/or PtO at potentials below about 1.1 V E_H while, above this potential, a mixture of PtO and PtO_2 is said to appear on the metal surface. The evidence for these states of surface oxidation will be discussed in a following section (p. 28).

When other platinum group metals are anodically polarized, a monolayer of adsorbed oxygen atoms, similar to that at Pt, is initially formed before O_2 evolution occurs. At Pd and Au surfaces, thicker oxide films can easily be produced after longer periods of anodic polarization treatment but sub-monolayer and monolayer films are deposited initially. The oxide films on these metals become visible coatings after prolonged anodic polarization. Various stoichiometric oxides such as PdO, PdO_2, Au_2O_3 are found under these conditions[19]. The stabilities of these oxides greatly depend on the nature of the electrolyte employed, e.g. in alkaline media, the PdO film is stable while the oxide film dissolves significantly in acidic solutions; conversely, with Ru, the oxide film (RuO_2) is stable in acidic solutions but dissolves as the red ruthenate in alkaline solutions (pH > 13).

Rh is similar in behaviour to Pd although, in the case of Rh, even after longer anodic polarization in either acidic or alkaline solutions, the layer of adsorbed oxygen formed prior to O_2 evolution rarely exceeds a monolayer and is a good conductor. The oxide is probably Rh_2O_3 as this is said[19] to be the only existing oxide of Rh. Butler and Drever[30] found that the first film of adsorbed oxygen easily changes to a so-called layer of "peroxidic oxygen" at potentials where O_2 is evolved. Thus, although Rh_2O_3 is present on the surface at higher potentials, the anodic polarization enables oxygen to be dissolved in Rh and a type of alloy "Rh-O" is formed in the outer layers of the metal surface, according to refs. 31 and 32.

When Ir anodes are used in either acidic or alkaline solutions,

a monolayer of adsorbed oxygen can be observed before O_2 evolution takes place. The behaviour of Ir anodes is similar to that of Pt as the oxide film does not tend to grow much beyond a monolayer, except on repetitive cycling [33]. When this behaviour is observed, it is due to the development of a thicker film in which a reversible solid-state redox process can occur[34]. It is believed[19] that a layer of adsorbed O- atoms, Ir-O, is formed on the Ir surface in acidic solutions. When O_2 evolution commences, there is then an increase in the amount of adsorbed oxygen on Ir surfaces[19]. The details of such processes have recently been studied by Arvia et al[34]. The initial monolayer formation process is similar to that at Pt.

4. The Early Work: Use of Charging Curves

The early work on surface oxidation of noble metals was confined to Pt and Au. The constant current charging method (see Section 2) was, of necessity, employed owing to the lack of development of controlled-potential instrumentation of a suitable kind until 1960[22], although a crude potentiostat had been designed by Hickling in 1939.

The first use of the charging current method was by Bowden[35] who evaluated the double-layer capacity, dq/dV, at Hg from cathodic charging curves. Hg behaves almost as an "ideally polarizable" electrode over a potential range of ca. 1.2 V, i.e. no significant transient surface reactions nor continuous Faradaic reactions (H_2 evolution, oxidation of the metal to form HgO or Hg_2Cl_2) occur. The charging curve then gives only the double-layer capacity over the above potential range.

An extension of the technique to Pt revealed that three main regions of anodic charging curves could be distinguished at this metal[2,36]: (i) one for desorption of previously chemisorbed H atoms; (ii) a region of double-layer charging, as at Hg, and (iii) a region of oxidation of the Pt surface prior to onset of a significant rate of anodic O_2 evolution.

In the regions where surface processes of H ionization/deposition or oxide film formation/reduction occur, the apparent capacitance, dq/dV, was much larger than the double-layer capacitance. As explained in Section 2, the dq/dV is, for these conditions, a pseudo-capacitance associated with the electrochemical adsorption reactions. The study of the adsorption behaviour of H and oxygen species at platinized Pt was pursued in more detail in several important papers by Frumkin and Slygin[2,36].

Solution impurity problems were recognized in the early work and, in particular, the role of reduction of dissolved O_2 either from the atmosphere or generated at the most positive potentials of an anodic current pulse gave rise to complications in the early work. By using "rapid" charging techniques[35], i.e. with high current pulses, these difficulties were minimized but the role of reduction processes involving diffusing O_2 was not initially well understood. Butler and Armstrong[37,38] used the rapid charging method at Pt in solutions containing O_2. They measured a value of 1×10^{-3} C cm^{-2} as the charge required to establish a constant potential at which O_2 is evolved. This is the charge for surface oxidation of Pt up to ca. 1.8 V, but the real area of their electrode is uncertain. The above quantity of charge, it was noted, is sufficient to form at least two monolayers of O species at the Pt electrode.

These early experiments provided the first quantitative evidence

that the formation of an oxide "monolayer" occurs at Pt (and also at Au[39]) and is followed by evolution of O_2. The weakest point in this early work was the estimation of real areas of the electrodes as the use of the " H-charge " (for Pt) as an "internal" real area measurement was not, at that time, used for this purpose.

An important conclusion arose from work in which a cathodic current was applied, following fast anodic polarization. It was realized[35] that in the course of passage of cathodic current, the previously electrodeposited oxide film will become reduced. However, Armstrong, Himsworth and Butler[40] offered a somewhat different explanation based on experiments made in solutions containing dissolved O_2. They observed that the cathodic reduction curve was dependent on stirring and also on concentration of impurities in the solution. They concluded therefore that the cathodic process consists not only of the reduction of adsorbed oxygen but also of molecular oxygen present in the solution.

Some of the behaviour observed in this early work referred to above was unnecessarily complicated by the presence of residual O_2 in the solutions, and/or of O_2 generated in a previous constant current pulse. Then, in the cathodic current pulse, some diffusion-controlled reduction of dissolved O_2 occurs. These complications can be easily diminished by using solutions outgassed by N_2 bubbling, and are not involved in more modern experiments where the surface oxide formation and reduction behaviour is well defined in the absence of molecular O_2 processes.

Pearson and Butler[39] used large current-densities at Pt electrodes in dilute H_2SO_4 solutions to study the effects of impurities on the shape of the anodic charging curve. When a fresh electrode was used, which was

previously cathodically polarized, a so-called " inactive " type of charging curve was obtained. The electrode became " active " after anodic polarization and then the typical curve consisting of a region over which H is adsorbed, followed by a longer region evidently due to the deposition of a monoatomic layer of adsorbed oxygen on the clean surface, was obtained. Between these two regions, the usual process of charging the double-layer at Pt was observed. Activation of a Pt electrode by anodic/cathodic cycling was later investigated in some detail by Breiter[41].

It is also to be noted that this seems to be the first* work in which anodic activation of Pt electrodes for removal of adsorbed impurities was reported: it is a very important matter with regard to obtaining reliable results for clean surfaces.

In the important work of Frumkin and Slygin[2,36], impurity effects were minimized by use of platinized Pt and the slow charging method could be reliably applied. Three main regions of the charging curve were identified, as mentioned earlier. In H_2SO_4 and KOH, two states of H adsorption were distinguished. This work was the first in which the behaviour of halide ion solutions was studied[42,43]. The main difference noted at that time was the current for anodic halogen evolution instead of O_2.

Impurity effects were virtually eliminated in work by Ershler et al.[44-47] by use of large electrode surface-to-solution-volume ratios. However, the charging curves were less reversible than those at platinized Pt electrodes referred to above. Possible contamination effects were considered and led to the study of the effects of poisons such as sodium arsenate on the surface processes at Pt[46].

---

*Faraday noted, however, that Pt could be made catalytically active for $H_2 + O_2$ combination if it had just been used as an anode; a recently cathodized surface was not active.

For smooth Pt electrodes, activated by anodic-cathodic pulsing, it was found that the ratio of $q_O/2q_H$ was close to 1 in solutions of H_2SO_4, H_3PO_4 or NaOH at room temperature [37-40,42]. Similar ratios were observed for anodically pretreated platinized platinum[43]. This indicates that, in those experiments, a state of oxidation of Pt of 1 O-atom to each Pt-atom was attained. However, it is clear that the O : Pt ratio, or the number of electrons per Pt-atom passed in surface oxidation of Pt electrodes, must depend on the potential attained; it also depends on the duration of the current pulse.

In conclusion, it should be noted that the early work on oxidation of Pt surfaces provided the first information about the range of potentials over which oxidation of the surface proceeds. From this work, it was obvious that oxidation of Pt surfaces occurs before evolution of O_2 commences. The oxide film was considered to be a monolayer of PtO which at higher potentials becomes converted to PtO_2. This was deduced from slow rate charging curves[48]. The cathodic reduction of the surface oxide was well resolved as a single process corresponding to one plateau in the (cathodic) charging curve.

This observation, however, did not lead to any speculations on the different steps in the oxidation or reduction processes which are now known to be involved in the film on the surface.

The effect of impurities on the oxide film formation behaviour was well appreciated in the early work and led to some contraversial reports about the state of the oxide film on Pt.

The later work, to be described below, especially that conducted by means of cyclic-voltammetry or by controlled-current charging[49-53], upholds the general conclusions reached in the early work described above,

but adds much more qualitative and quantitative detail about the stages of formation and reduction of thin oxide films on Pt, and about the role of impurities and effects of anion adsorption.

An important point, to which little attention was given in the early work, was the marked hysteresis between the anodic charging curve for oxide film formation and the cathodic one for reduction at Pt or Au. Similar hysteresis is observed in the potentiodynamic curves for oxide film formation and reduction at these and other metals, to be discussed below; see Fig. 1 where the various types of curves for Pt are compared.

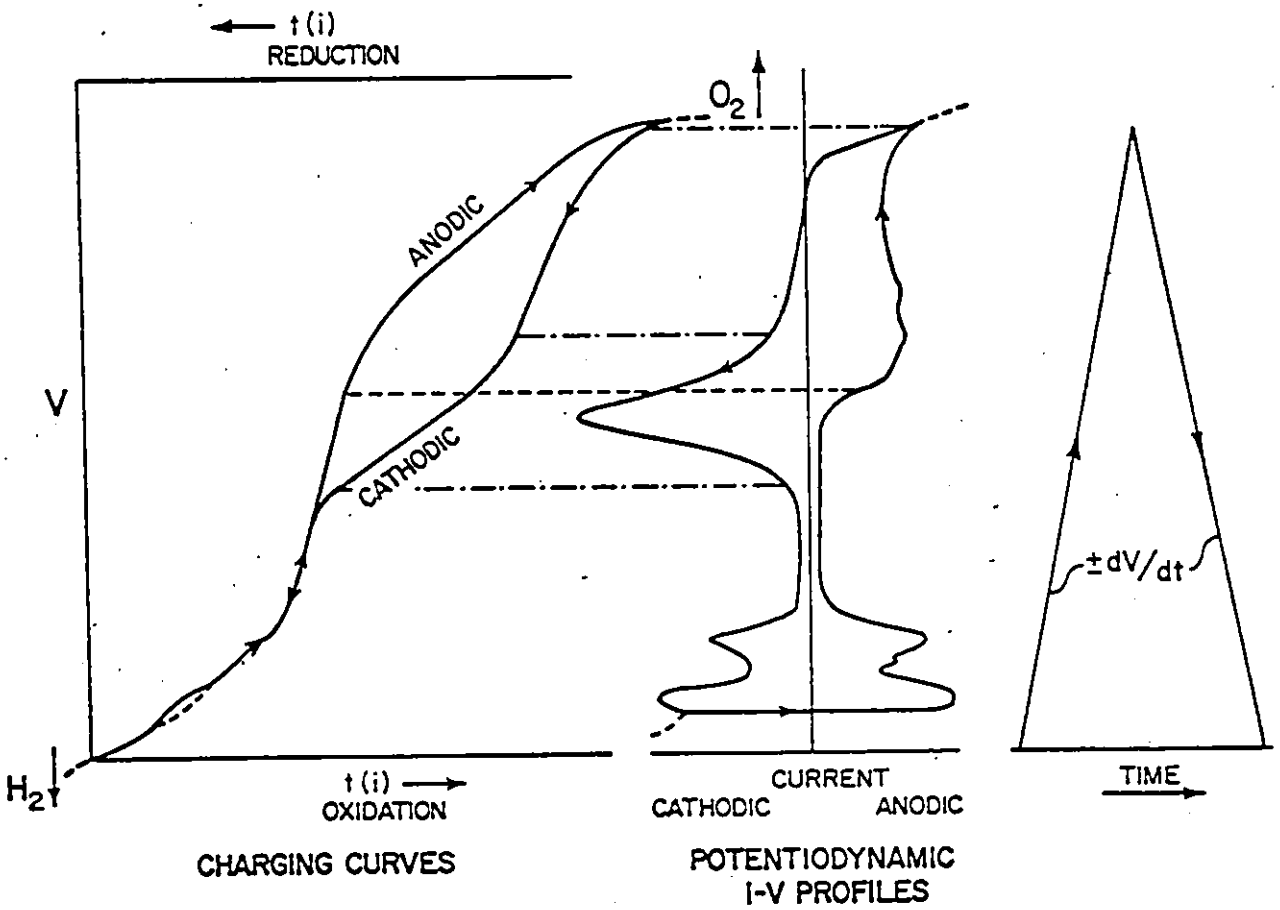

Fig. 1 · Schematic comparison of current-potential relations for surface oxide formation and reduction, and for H desorption and ionization at a Pt electrode as generated by galvanostatic charging and potentiodynamic sweep methods.

5. Results from the Potentiodynamic Method

(i) Early Work: A different and very important, type of approach was developed by Breiter, Knorr and coworkers[54,55] and especially by Will and Knorr[22]; it involves the observation of the potential-(and hence time-) -dependent charging currents which result when a repetitive or a single potential sweep, linear in time ($V_t = V_{in} \pm st$), is applied to an electrode by means of a potentiostat at a rate $s = dV/dt$, programmed by means of a function generator. The change of potential V with time t is referred to as a " potentiodynamic sweep "; in the repetitive mode, when potential is cycled " anodically " and " cathodically " over some set potential range, the method is called cyclic- voltammetry.

As the potential is gradually changed, the current at the electrode passes through a series of maxima in the cathodic as well as in the anodic directions corresponding to surface reactions that can take place over various ranges of potential. At a given electrode, e.g. Pt, H and oxygen (OH and O) species become adsorbed in one direction of the sweep or desorbed in the other, as in anodic and cathodic charging curves. Eventually, at sufficiently large positive potentials in the anodic sweep, the aqueous electrolyte will decompose giving a continuous, potential-dependent Faradaic current for O_2 evolution while at sufficiently negative potentials in the cathodic sweep, H_2 evolution current arises. A typical potentiodynamic i-V profile for a Pt electrode in 0.5 M H_2SO_4, obtained in the cyclic-voltammetry mode is shown in Fig.2 .

As the potential is changed from ca. 0.0 V to ca. 1.5 V E_H, the following processes occur, e.g. at a Pt electrode:

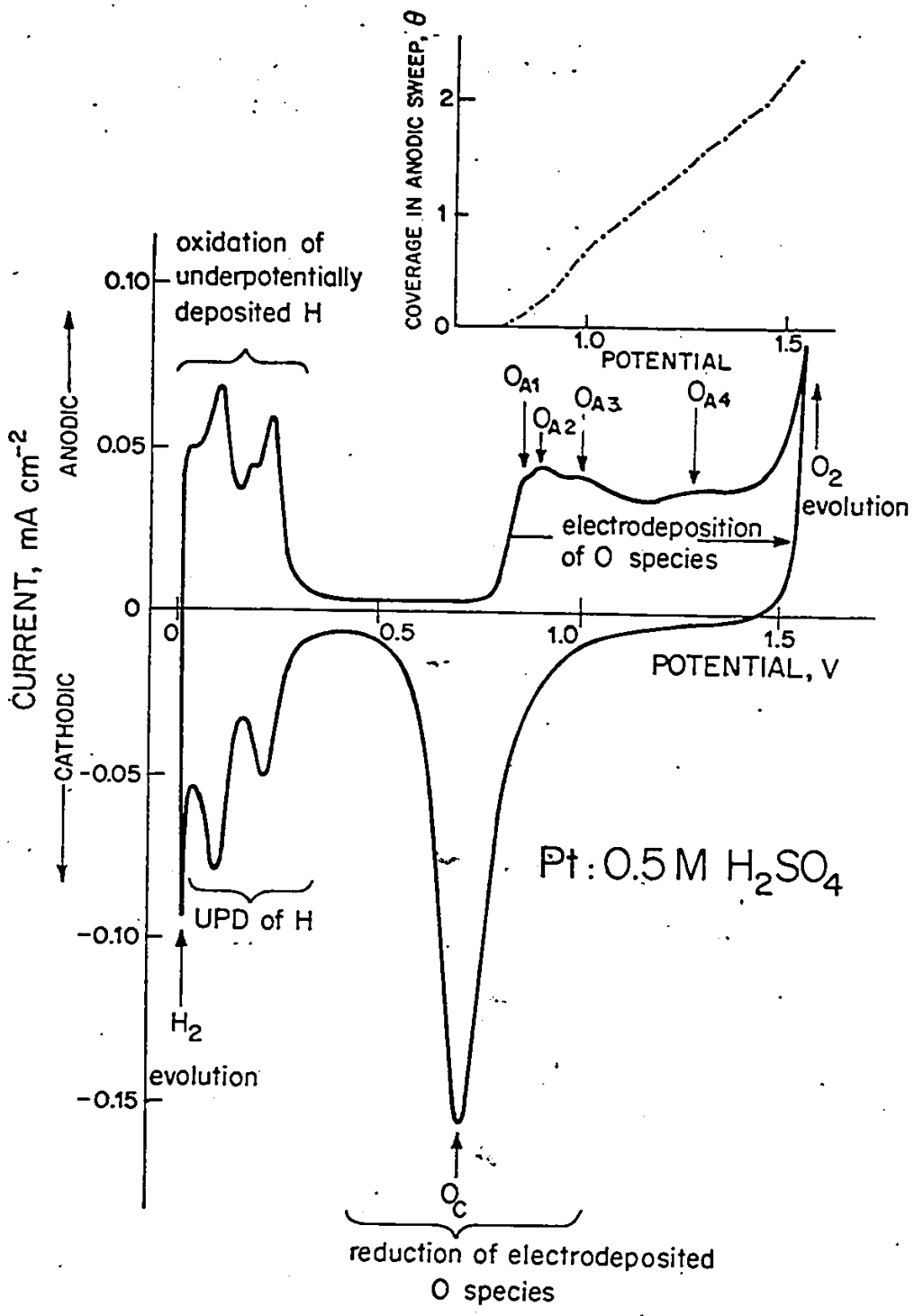

Fig. 2 Typical potentiodynamic current-potential profile at Pt in 0.5 M H_2SO_4. O_{A1}, O_{A2}, etc. refer to distinguishable stages of Pt surface oxide formation.

(a) Ionization of previously adsorbed H in 3-4 distinguishable states over the potential range of 0.0 V to 0.35 V E_H, depending on electrolyte composition and concentration;

(b) Between 0.35 V and ca. 0.78 V E_H in acid solutions, a region of double layer charging;

(c) From 0.78 V to ca. 1.1 V E_H, formation of a monolayer of OH species in three distinguishable but overlapping states;

(d) From 1.1 V onward, a broad range of current for further oxidation of the surface in an unstructured i-V profile;

(e) Beyond ca. 1.4 V, depending on electrolyte composition, pH and temperature, O_2 evolution in parallel with further oxidation.

In the reverse direction of the sweep:

(a) The oxide film is reduced in an apparently* single peak over the potential range 1.05 V to 0.5 V E_H, depending on previous film-formation conditions;

(b) A short, ill-defined double-layer charging region 0.5~0.35 V E_H;

(c) A region (0.35~0.0 V E_H) over which H atoms are redeposited on the surface in 3-4 distinguishable states, depending on electrolyte composition and concentration.

(d) Below ca. 0.05 V E_H, depending on pH and temperature, H_2 evolution in parallel with probable further increase in coverage of the electrode by adsorbed H species.

An important feature of the behaviour of most noble metals is the hysteresis which is observed between the processes of (anodic) formation and (cathodic) reduction of the film, and correspond to that

*In special experiments at fast sweeps or low temperatures, this peak can be resolved into 3 components, as at Au. Will and Knorr[22a] also noted two reduction stages under certain conditions.

found in the anodic and cathodic charging current behaviour. The two types of behaviour are, of course, related, as shown qualitatively in Fig.1 . This hysteresis is a fundamental feature of monolayer film formation and reduction at Pt, Pd, Rh, Ru and Au, as will be discussed later, and corresponds to an irreversible change of state of the film. In the H region, by contrast, the anodic and cathodic processes are almost reversible with respect to one another. Reversible behaviour is also found in the initial stages of oxidation of Ru and Ir, and at Pt at alkaline pH.

Will and Knorr[22a] measured the charges q associated with the oxide and hydrogen regions by the cyclic-voltammetry method at a sweep rate of 1 V sec^{-1} and found that the ratio of $q_O/2q_H$ is close to 1 when measurements were made in acid solutions. The value of q_O was not entirely constant with current-density or sweep rate, and decreased gradually as the sweep rate was increased from 1 to 100 V sec^{-1}. This is due to time-dependent growth processes in the oxide film. On the other hand, q_H was found to be constant over the entire range of sweep rates. Böld and Breiter[56] found 1-2% agreement between the oxygen film charges measured from the areas of the i-V profiles in the anodic and cathodic sweeps if the potential was kept below 1.6 V, i.e. if no significant O_2 evolution was allowed to occur. Cyclic-voltammetry i-V profiles were obtained for H_2SO_4 and NaOH solutions at various pH's and different temperatures. From the pH-dependence of the potential for onset of surface oxidation (low coverages of oxide), it was observed that the cathodic back reaction currents remained significant in comparison with the anodic currents for oxide formation up to 1.0 V E_H. The anodic currents were found to be pH-dependent and,

as there were two obviously distinguishable peaks; they suggested that the oxidation of the surface proceeds through two consecutive discharge reactions. The currents for these steps during surface oxidation were assumed to be equal and lead to the formation of a chemisorbed layer of PtO . Thus:

$$Pt + H_2O \longrightarrow PtOH + H^+ + e^- \qquad (1)$$

$$PtOH \longrightarrow PtO + H^+ + e^- \qquad (2)$$

The back-reactions in the steps (1) and (2) at low oxide coverages were assumed to be responsible for the pH dependencies of the anodic and cathodic sweep behaviour. Laitinen and Enke[15], using the galvanostatic charging method in the anodic and cathodic directions, also found that the formation of the Pt surface oxide is highly irreversible. They studied the shapes of the anodic and cathodic charging curves and, from the charges associated with the arrests for oxide film formation and reduction, concluded that more electricity was required to form the oxide than to reduce it. They concluded that the formation of the oxide is energetically possible at potentials less positive than the potential of O_2 evolution, but it was assumed (incorrectly) that the oxide is not formed at an appreciable rate except when supposed intermediates of the O_2 evolution reaction were present. In order to reduce the surface oxide, it is necessary to reach the potential at which the oxide on the electrode surface is unstable. At such a potential, the instantaneous rate of oxide reduction would be proportional to the instantaneous quantity of oxide on the surface, as confirmed experimentally by following the hysteresis of oxide formation and reduction.

Similar behaviour had been found in controlled current experiments by Vetter and Berndt[57] who observed ratios of anodic to cathodic charge for formation and reduction of oxide at Pt, of about 2. It was suggested that this arose because (a) some anodic charge goes to form evolved O_2 on the anodic pulse and this charge is not recovered on the cathodic pulse on account of diffusion of O_2 away from the electrode; and (b) the oxidized Pt surface may be reduced to Pt + H_2O_2 rather than H_2O.

Feldberg, Enke and Bricker[11], in controlled potential and controlled current experiments, observed similar discrepancies between the oxide formation (q_A) and reduction (q_C) charge at Pt and found q_A/q_C varied from ca. 2.0 to ca. 1.4~1.0 depending on electrochemical pretreatment of the electrode. They suggested that an half-reduced state $Pt(OH)_x$ could be formed on reduction from a state $Pt(O)_x$ produced on oxidation, giving $q_A/q_C \simeq 2$. These results from various workers[11,15,57] gave rise to much confusion in the early '60's concerning the state of oxide films on Pt. This matter will not be considered further here since, in later work, there is no question that any disbalance of anodic/cathodic charge exists: the cathodic charge for oxide reduction is consistently and reproducibly within 2% of the anodic charge for film formation. The earlier discrepancies may have originated from some O_2 evolution in anodic current pulses and/or from the presence of organic impurities which give an extra anodic oxidation charge not recovered in the cathodic sweep, but the origin of these effects is still obscure.

In these early papers on Pt oxide formation, it was common to regard the various species supposedly adsorbed on the Pt surface (PtOH,

PtO, PtO_2, PtOOH)* as intermediates in the O_2 evolution reaction. However, it must be stressed that whatever species are discharged at Pt below 1.23 V, and probably below 1.4 V, are strongly bound surface compounds produced independently of the subsequent O_2 evolution reaction that arises at higher potentials. Indeed, current thinking discounts the strongly bound OH or O species as kinetically significant intermediates in O_2 evolution. Probably such intermediates as are involved are more weakly bound species deposited on top of the oxide film. Equivalent ideas apply to H_2 evolution.

Gilman[14] reexamined the question of surface oxidation of Pt, in particular the range of potentials over which oxidation occurs. He employed the potential-step method in aq. $HClO_4$ to avoid not only effects of impurities but also to minimize anion specific adsorption on the metal surface. He also objected to the controversial conclusions of the previous works[11,15] in which the charge ratio q_A/q_H was found to be ca. 2 . Gilman[14] determined values of the ratio q_A/q_C for various potentials between 0.8 V - 1.6 V and various oxidation times. These charges were determined by direct integration of (anodic) current-time curves. For potentials higher than 1.6 V, the charge q_O was determined by means of the film reduction procedure.

Unlike the behaviour found by Vetter and Berndt[57] or by Laitinen and Enke[15], it was found that good cathodic/anodic charge balance ($q_A/q_C \simeq 1$) could be demonstrated at 0.95 V up to 1.6 V E_H. However, the oxidation charge, $q_O/2q_H$, relative to that for H deposition (assuming 1 H per Pt-atom of the surface) depends upon the anode potential and the

*These formulae represent only the formal degrees of oxidation of Pt surface atoms, i.e. the number of electrons passed, per Pt-atom, to achieve a given state of surface oxidation. They do not represent well-defined bulk chemical compounds since only monolayers, or less, of the species are formed.

time-scale of the experiment, i.e. the charging current; thus, longer times for the surface oxidation arise at lower anodic charging currents and generate relatively more oxide due to the slow kinetics of film growth.

The question is what sort of oxide species are adsorbed on Pt surfaces below O_2 evolution remained to be answered. The structure was examined through the ratios of $q_O/2q_H$. If this ratio was 0.5 then the surface structure could consist of:

(a) one monolayer of PtOH (or of adsorbed OH-radicals)*

(b) 0.5 monolayer of PtO (or of atomic oxygen species)*

and (c) 0.25 monolayer of PtO_2*. However, from Gilman's charge/potential data[14], it was only possible to conclude that below 1.2 V, the charge corresponds to less than that equivalent to one layer of chemisorbed O species on Pt. At higher potentials, the charge for film formation as O was found to increase progressively. Between 1.6 - 1.8 V, it corresponds to a PtO_2* monolayer, but at higher potentials multilayer formation was considered to occur.

The valence states in these oxide films were determined[58] by dissolving the oxide layers in boiling HCl solution which gave $Pt(II)Cl_4^{2-}$ and $Pt(IV)Cl_6^{2-}$ in a 6:1 ratio, from which it was concluded that the ratio of PtO : PtO_2 states in the film was 6:1. Breiter and Weininger[59] objected to this conclusion on the basis that some metallic Pt may also have been dissolved under the conditions of the experiment. In modern work, valence states of metal atoms in oxide films can be deduced from X-ray photo-electron spectroscopy[6, 60].

---

*See footnote on previous page.

(ii) Newer Potentiodynamic Work: The cyclic-voltammetry method can provide more detailed and quantitative information on the initial stages of oxide film formation if the proper resolution of i-V profiles is obtained. One of the most important conditions for the satisfactory study of surface oxidation processes is ultra-purity of the solutions, and of the cell and electrodes used. The anodic peak currents must be independent of solution stirring; observation of this behaviour confirms the absence of impurities that may be oxidized in a diffusion-controlled process at the Pt surface.

The i-V profiles obtained under such conditions provide more details about the development of successive stages of formation of Pt. oxide surfaces than do constant current charging curves. Each of the current peaks is related to a distinguishable state of the oxide film on the Pt surface or to the properties of the successively occupied adsorption sites. Considering the fact that the adsorbed oxide layer is reduced over a different potential range from that over which the film is formed, and that the i-V profiles differ substantially in shape in the anodic and cathodic directions, shows not only that the kinetics of these processes are different but that the mechanism of the reduction is different from that for film formation.

Conway et al.[61] examined time and anodic end-potential effects at Pt, Rh, Ir and platinized Pt by using single and multiple sweep voltammetry. The surface oxide was allowed to grow at potentiostatically controlled positive potentials in $HClO_4$ solutions for known times in the range 0 to 600 s, and then the film was reduced in successive transients at a fixed sweep rate. It was found that with increasing potential for the electrode oxidation process there would be a shift in cathodic oxide reduction current peak potential, E_p, to progressivelly less positive

potentials. It was necessary to determine whether this effect was caused only because higher potentials for polarization were used or whether this effect was associated with greater extents of oxidation that could occur at higher potentials: the latter was the case. The charges q_c for the oxide reduction vary in a linear manner with E_p (potential of oxide reduction) up to a monolayer of OH (1 e per Pt-atom) but between a state of oxidation " PtOH " and " PtO ", E_p is independent of q_c. This is probably because further oxidation of PtOH to PtO can occur without further addition of O-atoms to the surface. Distinguishable stages of oxidation as " PtOH " and " PtO " were recognized in the works of Will and Knorr[22], Gilroy and Conway[62] and Tikhomirova et al.[63]; for example, the electrochemical adsorption isotherm, q_0 *vs.* potential, shows a break at the PtOH (1 e per Pt-atom) stage, as does the reflectivity *vs.* q_0 relation[64].

Quantitative evaluation of the oxidation charge as a function of potential shows that a nominal monolayer of OH species (220 μC cm^{-2}) is formed at 1.1 V E_H[65,66] with further oxidation to a PtO monolayer at 1.4 V. Beyond this potential, further oxidation in the film occurs, giving eventually an apparent limiting[28] state of oxidation of PtO_2 (880 μC cm^{-2}). However, under extreme conditions of anodic polarization at higher temperatures, thicker films may be observed[8,62,67,68].

While there are three broad and overlapping peaks up to 1.1 V[69], the overall anodic sweep i-V profile really corresponds to a progressive and continuously increasing state of oxidation of the surface with eventual thickening[70,71].

The nature of this " progressive " oxidation was considered in detail by Kozlowska, Conway and Sharp[69] and by Tilak, Kozlowska and Conway[72].

They identified[50,67,121,141] three anodic current peaks up to monolayer OH coverage (1.1 V E_H) at Pt (1 e per Pt-atom). This resolution can only be achieved with very clean solutions, e.g. made up with pyro-distilled water[73]. It was therefore difficult to account for two different chemical species, PtOH and PtO, as suggested by Böld and Breiter[56], up to this potential where only 1 e per Pt-atom has been passed, although it is possible that some PtOH is oxidized to PtO in a parallel reaction with PtOH formation, before the PtOH monolayer is completed.

Conway et al.[69] concluded that the resolution of the i-V profile into three, well-defined peaks below OH monolayer coverage should be attributed to successive stages of occupation of the surface lattice of Pt in three significantly different overlay lattices of OH on Pt. Each sub-lattice has a different structure identified as "Pt_4OH ", " Pt_2OH " or " PtOH ". The " Pt_4OH " sub-lattice corresponds to the first peak in the i-V profile (O_{A1}) (see Fig. 2) in which only one OH group is electrosorbed per four Pt-atoms. The maximum adsorption charge in that stage is q_0 = 55 $\mu C\ cm^{-2}$. The second peak (O_{A2}) requires an additional 55 $\mu C\ cm^{-2}$ to fill the "Pt_2OH" sub-lattice. To obtain the third lattice, a total charge q_0 = 220 $\mu C\ cm^{-2}$ is required, and " PtOH " is formed on the surface. In the broad region beyond 1.1 V E_H, " PtO " species arise after further oxidation.

The stages of the Pt oxidation were written as:

$$Pt + H_2O \longrightarrow Pt_4OH + H^+ + e^-$$

$$Pt_4OH + H_2O \longrightarrow Pt_2OH + H^+ + e^-$$

$$Pt_2OH + H_2O \longrightarrow PtOH + H^+ + e^-$$

(The formulae here do not represent stoichiometric compounds, but simply the states of occupation of the Pt lattice as Pt/OH ratios.) The

further oxidation (1 e per Pt-atom) must proceed as[22,28,56,64]

$$PtOH \longrightarrow PtO + H^+ + e^-$$

or by thickening of the existing PtOH layer[61].

The existence of regular overlay lattice structures of adsorbed oxygen or of iodine atoms from the gas phase on to various metal surfaces is well known from LEED studies on chemisorption[74,75] and surface restructuring at metal-"vacuum" interfaces.

In the plateau beyond ca. 1.2 V structural details are not expected to be observed as the surface is then always fully covered in a geometrical sense, although further changes of state from OH to O have to occur.

The above scheme suggests that PtO states formed at higher potentials cannot begin to be formed until at least some PtOH or rearranged PtOH (" OHPt " - see below) is already covering the surface.

The important fact that all species adsorbed in the anodic sweep are reduced apparently in one cathodic peak, no matter how slow the sweep rate, can be rationalized in terms of formation of an irreversibly formed rearranged surface phase of lower free energy than that of species progressively deposited in the anodic sweep.

Such a rearranged, so-called " phase oxide " film can be more stable than a two-dimensional chemisorbed layer of OH or O species on the Pt surface since (a) lateral repulsions are relieved and (b) in the rearranged state, a two-dimensional surface lattice of Pt OH Pt OH , or Pt O Pt O ... is formed, which can be thermodynamically more stable. This would account for the less positive potential for the cathodic peak of oxide reduction when oxidation occurs beyond ca. 0.95 V E_H. The idea that a chemisorbed film of oxygen species on a metal can become rearranged into a two-dimensional phase oxide lattice by a so-called "place-exchange" mechanism:

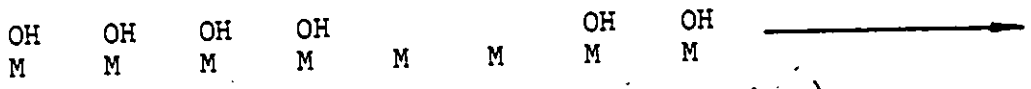

(or with corresponding MO species)

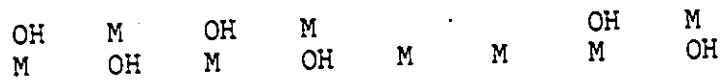

originated in interpretation of growth of oxide films on Fe in work by Sato and Cohen[76] and in the treatment of chemisorption of oxygen on metals in work by Trapnell[77]. It is also indicated from LEED and XPS work on oxygen adsorption at metals where extensive two-dimensional restructuring of the metal surface has been demonstrated[7,60,74,78] upon adsorption of oxygen.

The idea of place-exchange was first applied to the Pt surface oxidation problem by Reddy, Genshaw and Bockris[79,80] who observed (see below) a difference in ellipsometric behaviour of the first 10-15% of oxide coverage from that at higher coverages where significant optical effects could be observed. They also wrote kinetic equations for the place-exchange process as did Sato and Cohen[76] for the oxidation of Fe.

It must be mentioned that the germ of the idea of surface oxide rearrangement originated in the work by Schuldiner and coworkers[50,81,82] who, for some years in the '60's, had proposed in an ill-defined way that anodically electrodeposited oxygen species were in some kind of " dermasorbed " state, i.e. in the skin (≡ derma) of the metal surface. Thacker and Hoare[68,83] took this view further and sought to prove that O became physically dissolved deeper in the Pt lattice and could even diffuse through Pt but this behaviour was never substantiated. The first adsorbed oxygen is detected[78], as also found in work of Schuldiner and Roe[9,84], between 0.8~0.9 V E_H but " dermasorbed " O-species are not detected until potentials

>1.0 V E_H are attained. This is consistent with other evidence that the turn-over mechanism sets in appreciably only after some small initial degree of surface oxidation has been attained.

Conway, Kozlowska and Sharp[69] showed clearly by fast cathodic sweep measurements at low temperatures (213 K) in H_2SO_4 that an initial stage of Pt surface oxidation could be resolved which was formed and reduced reversibly but that, with increasing positive potential, a further irreversibly reduced species developed and eventually dominated the i-V reduction profile. The two states of the film could be well resolved at the low temperatures. Even at room temperature, but in alkaline medium, similar behaviour can be demonstrated. These results showed clearly for the first time in an electrochemical experiment that a reversible and irreversible stage in oxidation of Pt can be distinguished. For extensive oxidation the reversible component is obscured by the much larger irreversible one, so that the reduction i-V profile appears as an apparently single peak.

The presence of the initial reversible component, also indicated optically[28,64] (see Section 5(iii)), is very important in considering (a) the mechanism of oxidation of organic substances and of H_2 at Pt and (b) the competitive adsorption of anions in the same potential region, of interest in the present work.

(iii) Information from the Optical (Reflectivity) Behaviour of Oxidized Pt Surfaces: From the ellipsometric parameters (the phase shift Δ and ψ the amplitude change of polarized light), Reddy et al.[79,80] were unable to detect any changes in Δ or ψ until a sudden change of optical properties became detectable at ca. 1.0 V E_H. Thus, the Δ and ψ did not initially correlate with the measurable charge passed for oxide

film formation which commences at ca. 0.8 V. Beyond 1.0 V the optically detectable film grows linearly with increasing potential up to 1.6 V with continuously changing Δ and ψ . Above ca. 1.0 V the optical constants of the film differ sufficiently from those for the surrounding bulk medium for the film formation to be detected optically. In later work by Greef[85] and by Conway et al.[64,86], using more sensitive instrumentation, it was, however, shown that the very initial stages of film formation, down to the lowest oxide formation charges, can be detected optically and the Δ , ψ and relative reflectivity change does correlate with the oxide formation charge. The optical behaviour in this region is reversible with respect to increasing or decreasing coverage, but above 15% coverage irreversibility sets in, as is also observed in the cyclic-voltammetry curves[69]. However, when a monolayer of OH species is formed at 1.1 V, a discontinuity was observed by Greef[85] between q and Δ. Hence, although more recent ellipsometric measurements indicate[71,87,88] that the initial film can be detected as well as the rearranged " phase oxide " film, the conclusions of Reddy et al.[79,80] on properties of the oxide film above 1.0 V E_H are probably essentially correct.

The average thickness of the oxide film at 1.0 V E_H, when its optical behaviour became detectable in the experiments of Reddy et al.[79,80], was estimated to be 0.02 nm and the platinum " oxide" film was regarded as a " monolayer film " partially covering the metal surface. The potential at which the oxide film starts to grow was also found to depend on the method of surface preparation of the electrode. Reddy et al.[80] used a mechanically polished Pt electrode. When sputtered platinum was used as the electrode[89], a definite oxide film phase was developed at 1.1 V E_H. The values of the

optical constants of the films are consistent with those reported[64] for bulk $PtO \cdot H_2O$ but comparison with bulk materials is unrealiable for surface phases. The optically measured thickness of this film increases with increase of the polarization potential.

Parsons and Visscher[87] suggested that the reflectivity properties of the oxide film are constant, as no change in composition of the film is observed at high potentials and therefore the optical behaviour can be represented by a single refractive index. This conclusion differs from that of Ord and Ho[90] who found a change in film properties at 1.1 V E_H (1 e/ Pt). However, this difference may be due to the different techniques employed to form the films. Assuming that the film is PtO and that the density is 14.9 g cm^{-3}, they[87] calculated the film thickness from coulometric data[67] and compared it with that derived from ellipsometric data. The oxide formed above 2 V corresponded to a layer over 0.8 nm thick. The average thickness of the PtO monolayer would be 0.42 nm if it were assumed that only the first layer of Pt-atoms have modified optical properties as a result of adsorption. This value is not very much modified if it is assumed that the surface is completely ionic and that ionic radii of Pt^{2+} and O^{2-} are 0.052 and 0.135 nm, respectively. In fact, Moore and Pauling[91] report for the Pt-O distance in PtO, 0.202 nm, so the thickness of a plane of O atoms on top of a plane of Pt atoms when a monolayer is reached would be close to 0.4 nm. Such a structure is oversimplified but the real dimensions of the film cannot differ largely from the figures given above.

The oxidation of Pt surfaces below 1.1 V vs. E_H has been also characterized by means of electric modulated reflectance measurements and the behaviour compared with that found from impedance studies[64]. In the

modulated reflectance measurements, the change in the in-phase and out- of- phase components of $\rho(V)$ ($=d(\Delta R/R)/dV$) is found to increase sharply in the range of 0.72 - 0.90 V. Then, as the potential reaches 0.9 V, $\rho(V)$ drops and as the potential reaches 1.4 V and then remains almost constant. Also, above 0.9 V, the cathodic branch of $\rho(V)$ is found to be different from the anodic one to an extent depending on the potential of the reversal of the anodic sweep. Similar types of curves were obtained from differential capacity measurements[16,64].

As the oxide film starts to be formed on the Pt surface, the (parallel) capacity (C_p) shows an increase from the $C_{d.l.}$ value in the range of potentials 0.75 V to 0.90 V E_H. At the same time, the reflectivity of the surface decreases as a result of the formation of the light absorbing oxide film on the electrode surface. The drop in reflectivity at Pt surfaces which occurs when about 10 ~ 15% of the PtOH monolayer is formed must mean that the continuing formation of OH on the surface beyond 0.9 V E_H occurs by a different mechanism from that for 0.9 V and involves the formation of the place-exchanged surface phase[61,69,76] which is only reducible at less positive potentials. Formaro and Trasatti[17] reached a related conclusion based on pseudo-capacitance measurements. They regarded the change in the state of Pt surfaces with potential as due to " strengthening " of the Pt surface - oxygen bond in the course of oxidation.

(iv) Conclusion: It will be useful to end this Section with a summary of the conclusions from electrochemical and optical measurements on surface oxide film formation at Pt. This is conveniently done by means of a scheme I (see below) of states in, and progression of, surface oxidation. The hysteresis which arises between the oxide formation and reduction processes,

found in all the work since the earliest contributions in the '30's, is due to an irreversible transformation of the electrodeposited OH and/or O species beyond ca. 15% coverage as further increase of electrode potential and coverage takes place. This transformation is associated with a place-exchange or reconstruction of the Pt surface as OH or O species are deposited, as shown in the scheme below. Accompanying the formation of the initial PtOH stages, and continuing with more extensive surface oxidation, are important anion desorption processes[92,93,94] in electrolytes other than OH^- solutions. These effects are important in the new work to be described later.

SCHEME I : CYCLE OF PROCESSES IN Pt OXIDATION

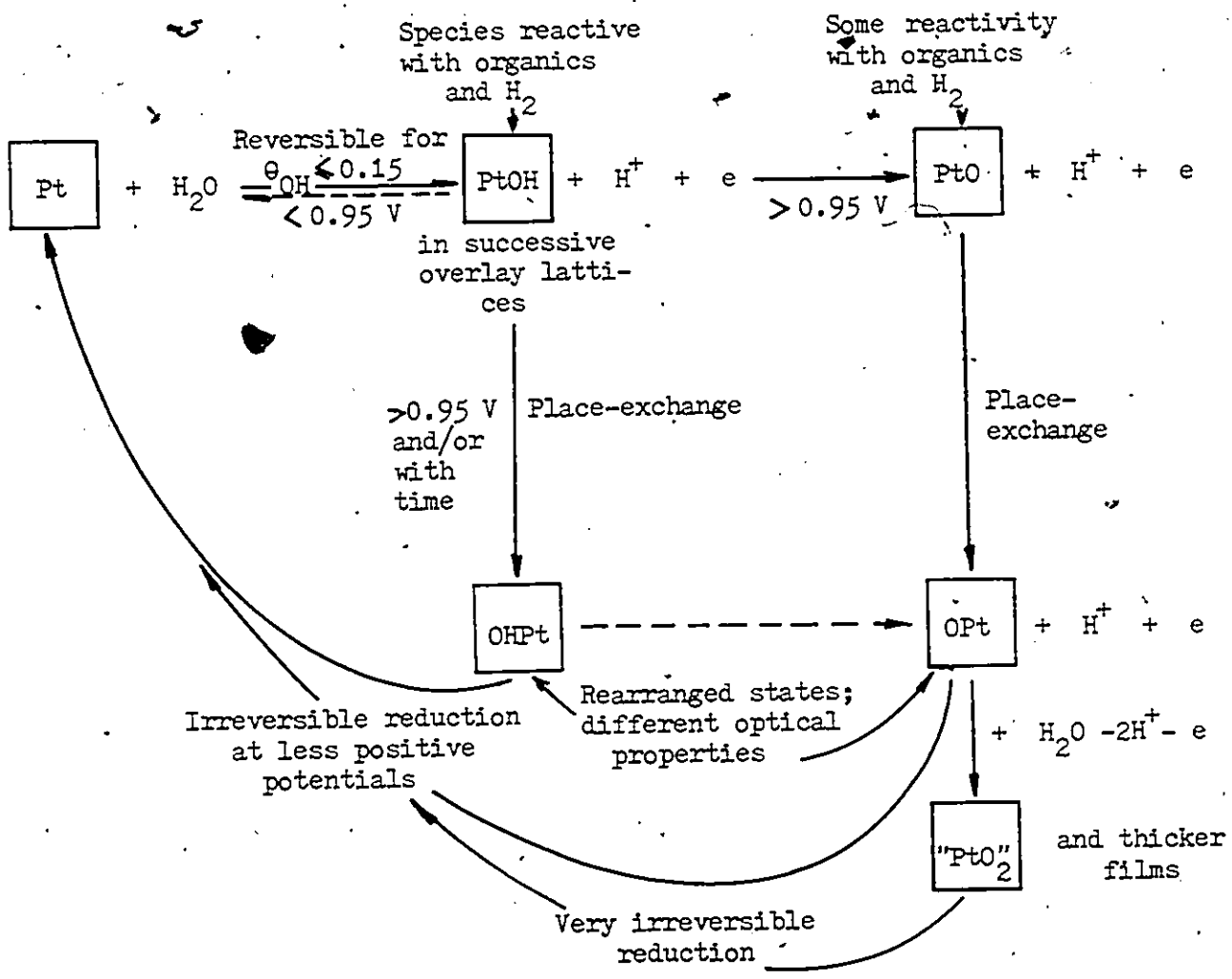

6. Platinum Oxide Film Growth

While the extent and coverage of Pt anodes by an oxide film increases with potential, as described earlier, extension of the film or thickening will always occur in time at a given constant potential. This is because a given coverage of O species at Pt is not a thermodynamically well defined quantity at any potential as is the coverage by H. Such behaviour arises on account of the progressive place-exchange process which is kinetically controlled and allows more oxygen species to be deposited at a given potential with increasing time than would correspond to the equilibrium adsorption isotherm for that potential. Experimentally, the extent of growth of the Pt oxide film is logarithmic in time[70,71] as is also observed for oxide film growth processes at metals where thicker films are formed (Al, Ti, Zr, Ta). This type of behaviour was observed by Gilroy and Conway[62] and later extended by Gilroy[96,97]. The log growth law applies over $4 \sim 5$ decades of time [96].

Ord and Ho[90] considered that the Mott-Cabrera model for growth of thick oxide films on base metals also applied to Pt. Similar views have been published by Damjanović et al.[98,99] but it is difficult to see how the Mott and Cabrera high-field ion transport model for film growth can apply to the very thin (monolayer) films that are initially present on Pt anodes. However, there appears to be no discontinuity in the film growth kinetics between growth at monolayer levels and growth in thicker films at Pt[71] (but still very thin in comparison with the oxide films at base metals). Possibly a succession of place-exchange events is involved, as discussed by Sato and Cohen[76] for Fe, rather than high-field transport

of ions across an oxide barrier layer film.

A number of theories of oxide growth on Pt have been presented, e.g. by Ord and Ho[90], Reddy, Genshaw and Bockris[79,80], Vetter and Schultze[100,101], Gilroy and Conway[62], Gilroy[96,97] and in several papers by Damjanovic et al[70,71,98,99]. We shall not examine these treatments here as they are beyond the scope of the present work but it should be mentioned that in anodic evolution of Cl_2 or O_2 at Pt there will initially be two current components: a small anodic current for oxide film growth and a much larger one for the main Faradaic reaction of Cl_2 or O_2 evolution. The film-growth current will rapidly fall in a log manner with time to a very small fraction of the total current and is normally negligible. However, the electrocatalytic properties of the developing film and its blocking effects for anion adsorption, may have important effects on the kinetics of the main reaction which is occurring on the oxide film. This is one of the topics considered in the new work reported in a following Chapter of this thesis.

7. Charge-Transfer Across Thick and Thin Films

(i) General: When an oxide film is formed at a metal surface, transfer of electrons and ions is usually necessary: (a) for the film to continue growing and (b) to sustain any parallel faradaic process such as Cl_2 or O_2 evolution that may be occurring on its surface, depending on electrode potential and solution composition. The conductance of the film is therefore important for either of these processes so that the Ohmic and non-Ohmic behaviour of oxide films, determined by their properties

as semi-conductors, is often a significant, if not dominant, factor in anodic processes in the aqueous medium.

(ii) Electron and Ion Transport in Films: Charge transfer across oxide films is determined by three important factors:

(a) whether the oxide film is thick or thin;

(b) whether the film is homogenous and compact, or the structure varies across it; and

(c) the electronic and/or ionic conductivity of the film[20].

During the oxide formation process on a metal surface, if no other parallel reaction occurs, both electrons and ions are transported through the growing oxide film. At the metal-film interface, cations are formed in an interfacial electron transfer process and if the resulting cation migrates through the film and becomes further oxidized at the outer surface of the oxide film, the balance of the electrons has then to be transported back through the oxide film from the oxide/solution interface to the metal surface. This behaviour is observed e.g. on Fe electrodes[99,102]. The so-called low-valence oxide covers the electrode surface in the initial stages of the oxide growth up to 2 nm. This film gradually becomes converted into an oxide containing Fe^{3+} ions and if anodization persists, finally a ferric oxide layer is formed. This means that for the oxide film to be formed there must be transfer of cations or anions (or both) through the film itself and in certain cases, electrons. The overall rate of oxide growth depends on the rate at which charge flows through the film rather than on the rate of ion transport[99]. Very thick films usually have high resistances and are regarded as a barrier to electron charge transfer. Also a potential-difference normally exists across the oxide film

and gives rise to an iR drop*. The overall potential difference, ΔV, is the sum of the potential difference across the oxide film (ΔV_0) and that across the double-layer ($\Delta V_{d.l.}$)[98]:

$$\Delta V = \Delta V_0 + \Delta V_{d.l.} \qquad (5).$$

With small applied currents the thickness, δ, of the oxide film remains almost constant and small and thus ΔV_0 would be small. As the film continues to grow in time, however, ΔV_0 changes. Normally for constant current growth, the field $\Delta V_0/\delta$ must remain approximately constant. In the case of poorly conducting oxide films such as on Fe, where an oxidation from ferrous to ferric states is required, the oxide growth depends on the rate at which electrons rather than ions are transported through the film. Damjanović[99] states that this can arise in one of the following ways: (a) electrons on the adsorbed ions could be thermally injected into the conduction band of the oxide phase from where they can migrate to the metal surface; (b) electrons tunnel through the oxide film and (c) holes are injected from the metal into the valence band of the oxide and migrate in the field to the oxide/solution interface where they combine with electrons from adsorbed ions, e.g. OH^- ‡. In the case of thin oxide films on metals grown in atmospheric O_2, the original Mott-Cabrera[103] theory is usually considered, in which an electric field arises across the film by electrons which leave the metal

*In the case of thin films, i.e. for sufficiently high fields across the film, the resistance in the film, associated with ion transport is non-Ohmic. That is, the transport rate in the film is an exp rather than a linear function of ΔV_0. Ohm's law follows as particular low-field case.

‡This statement does not seem altogether correct unless O_2 were to be evolved as a parallel process at the oxide-solution interface, consuming OH^-.

surface. In an anodic prosess, this field is provided by the externally applied potential difference. The rate-determining step was assumed to be the movement of ions through the metal-oxide interface under the influence of the external field but Cabrera[104] pointed out later that when thin films are considered transfer of electrons through the film should be also taken into account.

In the case of passive Zr in acid solutions of Na_2SO_4, the film involved is ZrO_2[105]. In the study of reduction of O_2 at ZrO_2, so-called dual barrier charge-transfer through the film is assumed to play a predominant role. The thin oxide layer, forming a barrier to charge transfer, is in series with the double-layer electron charge-transfer barrier. Whether ion transfer or electron transfer would be favourable depends greatly on whether the reaction is proceeding at low or high current densities. When the film is established at low current densities, it is assumed[105] that the rate-determining step is the transfer of electrons <u>through</u> the film to adsorbed oxygen species at the surface. Charge-transfer through the surface would cause formation of OH^- species, so at low current-densities there would be an equilibrium $OH^-_{ads.} + H_3O^+ \rightleftharpoons 2H_2O$, while this reaction would be polarized in the case of high current densities.

The precise mechanism of charge transfer through films is sometimes difficult to identify. If tunneling of electrons occurs, it will be extremely dependent on the thickness of the oxide film and its rate becomes negligible beyond 5 nm thickness[106]. As the oxide layer continues to grow, there must be a transition between electron-tunneling to ion migration as the rate-controlling process[107,108]. Fromhold and Cook[108] calculated that oxide growth is controlled by formation or migration of ions in the initial stages of the oxide formation. As the oxide film

continues to grow, tunneling becomes rate-controlling. Such behaviour could be applied to Pt since the initial oxide growth on Pt was found to follow an inverse log law[109] until a thickness of 0.6~0.7 nm is reached. After that the oxide proceeds to grow according to the direct logarithmic law[88,99].

Formation of oxide films on metal surfaces is sometimes accompanied by a parallel reaction which occurs on the oxidized metal surface, e.g. O_2 or Cl_2 evolution. Then the total external current is divided between that associated with the film growth and that required for the parallel reaction. The ratio between these currents normally changes with time as the oxide film grows and eventually attains a steady thickness; then the total current is close to that for the parallel reaction. In the case of some films, there is a change of valence state in the film which makes the film a degenerate semi-conductor so that there is no barrier to electronic conduction across the film for the parallel reaction.

(iii) Ohmic Resistance: It has been mentioned earlier that the growth of the oxide film on a Pt anode is not limited to a monolayer but at higher potentials (above 1.1 V E_H) the quantity of deposited oxygen not only exceeds a monolayer but an increase in thickness of the film occurs with increasing potential[3,11,14,61,67,79,95]. It has been found that under severe conditions of anodic polarization, two types of oxide films are generated[74,110]:

(a) an oxide, α , e.g. PtO reducible over a broad potential range, is formed only to a limiting amount[67,111,112]; and

(b) an oxide, β , e.g. PtO_2 which is reduced over a narrow

potential range, extending into the H deposition region, i.e. much more negative than that for oxide α , and which grows at much slower rate, forming a multilayer[113].

These two types of oxide layers were shown by Shibata[8] to have different conductivity properties. Naturally the conductivity behaviour of the oxide film is of interest in regard to processes such as anodic Cl_2 or O_2 evolution which take place on the oxidized anode surface. Normally the oxide film at Pt is thin enough (1∼2 monolayers) that conductivity (tunneling of electrons through the film) is not a limiting factor in anodic process at this metal. Shibata[8] formed various states of the surface oxide at Pt electrochemically and determined their conductivities in a dry state, ex situ , in a sandwich-like cell between Hg contact electrodes. The oxide films were formed for various periods of time, 10 s to 210 min, at 318 K with a current density of 0.2 A cm^{-2}. The state of the oxide films formed under these conditions was evaluated by a galvanostatic cathodic current pulse or by a linear potential sweep.

Only the PtO oxide α was formed when $t \leq 4$ min. This oxide had virtually the same conductivity as Pt until a film corresponding to a reduction charge > 2100 μC cm^{-2} (ca. 5 PtO layers) was formed. Ord and Ho[90] estimated, from ellipsometry, the thickness of the PtO monolayer to be in the range 0.08∼0.16 nm; the conductivity of this layer is equal to that of metallic Pt. Beyond the 2100μC cm^{-2} extent of oxidation, the resistance of the film increases, an effect that was ascribed to development of the β type oxide. The thicker layer β oxide, " PtO_2 ", was found to exhibit a conductivity of 0.67×10^{5} Ω^{-1} cm^{-2} area per monolayer thickness in the direction normal to the Pt surface. The specific conductance of the

β oxide could not be exactly evaluated as the precise thickness of the β oxide was unknown. The factor which might be assumed as correct is that the monolayer thickness of PtO_2 is larger than that of PtO. If it could be assumed that the PtO_2 layer is at least twice the size of the PtO layer, then the calculated value of specific conductance of β oxide is about $1.1 - 2.1 \times 10^{-3}\ \Omega^{-1}\ cm^{-1}$.

Except at very high anodic current densities for Cl_2 or O_2 evolution, the less conducting thicker β oxide film will not normally be formed. Hence conduction problems in the Pt surface oxide film will not be significant in the kinetics of these processes under ordinary conditions, as they are at metals such as Ti, Zr, Ta, where thick insulating films are normally present on these metals when they are used as anodes. Significant ohmic resistance of the Pt oxide film would also distort the i-V profile for Pt oxide reduction in cyclic-voltammetry as shown by Stonehart, Kozlowska and Conway[61]; such effects are not observed experimentally.

8. Reactions that Take Place on an Oxide Film

(i) Types of Effects of Oxide Films: Oxide film surfaces at anodes play a role in a number of continuous Faradaic electrochemical reactions either directly, by modifying the energy of adsorption of reactants or intermediates on the surface or indirectly, by changing the catalytic activity of the surface. A number of reactions occur under conditions where the electrode surface may have either an electrodeposited layer of oxide, which may be very thin or exists in patches, or when an adsorbed layer of oxygen is present. Such films can have an important effect on the reaction kinetics of other parallel processes occurring at

the electrode surface. For example, O_2 evolution or reduction of oxygen and oxidation of hydrogen (as H_2) exhibit different kinetics and mechanism on oxide-free and oxide-covered surfaces[114,115,116,117].

In the case of Pt electrodes, there is only a narrow range of potentials over which the electrode is free from either adsorbed H atoms or oxygen species, dependent in magnitude on whether the electrode is in an acidic or alkaline electrolyte. Other metals such as Ru or Ir have narrower ranges for existence of the " free " metal surface, depending on ion adsorption. Therefore, it is common to find that anodically formed oxide films play an important role in influencing parallel reactions[118,119], such as O_2 or Cl_2 evolution, or oxidation of organic compounds[120,121,122,123], that begin to occur at certain potentials in particular electrolytes.

The anodic oxide film can have three principal effects on a parallel reaction at an electrode surface:

(a) It blocks the initially free metal surface on which the parallel reaction may have previously been occurring (. passivation or inhibition effect), e.g. see refs. 95,123.

(b) When the oxide film has been formed, it has usually different electrocatalytic properties for the parallel reaction than the free metal surface so that the reaction's mechanism can be changed, e.g. see refs. 109,124,125.

(c) The " blocking " oxide film may be relatively non-conducting and lead to a so-called[20] " demetallization " of the surface. This effect usually occurs only on baser metals that form thick films or poorly semi-conducting films, as on the valve metals.

Several common " parallel " reactions that occur in aqueous solutions, e.g. O_2 or Cl_2 evolution, or the Kolbe reaction, proceed only on an oxide-or partially oxide-covered surface since the potentials for their onset arise above those for the initial stages of surface oxidation of the substrate electrode metal. Then, with increasing anode potential, the changing state of the oxide film is reflected in changing kinetics of the parallel reaction that proceeds on its surface.

Bockris and Huq[124] showed that the catalytic activity for the O_2 evolution reaction at Pt decreases significantly with time of polarization, e.g. at a given constant current density, the extent of surface oxidation of Pt electrodes increases logarithmically with time of polarization, so that the decrease in catalytic activity with time is a consequence of the continuous increase in the extent of formation of the anodic oxide film. A similar effect was observed at Au electrodes[126]. Also the rates of O_2 reduction at oxide-free Pt, Au and Rh electrode surfaces are found to be about two orders of magnitude higher than the rates for the same type of reaction on oxide-covered surfaces[127].

For reactions such as anodic O_2 or Cl_2 evolution, which necessarily go on, in aqueous solutions, on an oxide film, the catalytic properties of this film can be indirectly controlled by use of alloy metals as the substrates. This can lead to mixed oxide films having advantageous catalytic properties for the parallel reaction occurring on the films[119,125,128].

The catalytic properties of transition metal anodes and their affinities for O-species are related (e.g. refs. 129,130) to the electronic band structure of the metal, e.g. the " d-character "[131] of the " dsp " hybrid bonding in the metal lattice or the number of " d-holes "

per atom, viz. the number of unpaired d-electrons.

(ii) Inhibition Effects in Parallel Reactions: With increasing potential, the developing oxide film at anodes usually first inhibits any parallel (continuous) Faradaic process that may initially be occurring on the surface. Virtually complete inhibition is called " passivation " and arises not only in the familiar case of anodic metal dissolution but also with other anodic reactions. Inhibition arises for two reasons:

(a) blocking of the original substrate surface on which the reaction was proceeding; and

(b) change in the nature or activity of the surface by the blocking oxide film.

Rates of reaction can decrease markedly as an oxide film is formed on a metal surface, as is found in the study of the oxidation of H_2[116,117] or hydrocarbons[123,132] at catalytic noble metals; this is a passivation effect. In this case, the oxidation current is initially diffusion-controlled over a range of anodic potentials < 0.8 V E_H at Pt but becomes activation-controlled after formation of the initial stage of the oxide film. With some organic substances, e.g. CH_3OH at Pt[133-135], the initially deposited oxide species ($\theta_{OH} < 15\%$) is reactive with the organic residues derived from dissociative chemisorption of the organic subst[redacted], but the more developed oxide film is not.

In a number of cases, as the oxide film is completed or becomes somewhat thicker, the parallel reaction can continue but at a different rate and over a different potential range than it did previously on the " bare " metal. Usually the adsorptive and electrocatalytic properties of an oxide-modified surface of a metal are quite different from those of

the free metal itself, and the mechanism of the parallel reaction may even be changed. The variation of rate of the parallel process with increasing potential then often takes the form of an " S-shaped " relation with the current first increasing exponentially with potential on the bare metal surface, then decreasing with potential after an inflection. This is usually followed by a further increase with potential but with the kinetics and mechanism are characterized by different i_o (exchange current) and Tafel slope values from those for the same (overall) process on the bare metal. In certain cases, the anodic process on the oxide film may be not only kinetically but chemically different from that on the metal, e.g. in some organic or inorganic oxidation reactions.

These aspects of the effects of oxide film formation on other continuous Faradaic reactions that may be occurring on the anode surface are of special interest in the new work reported in this thesis.

(iii) " Demetallization " by Oxide Films: In the case of valve metals, a thick almost non-conducting oxide film is normally formed upon anodization. This means that all other reactions which might otherwise occur on the unoxidized surface e.g. a redox reaction[136,137] or H_2[116,117]*, O_2[115,124] or Cl_2[119] evolution tend to be inhibited by the oxide film. This arises for two main reasons: (i) the original metal surface sites are completely blocked by the oxide film and (ii) the oxide film provides a barrier to electron-transport required for a continuing electrochemical reaction to occur. The conductivity of the film depends on the band-gap, E_g, or on the presence of impurities.

An attempt was made by Vijh[138] to generalize the forgoing behaviour in terms of the solid-state properties of the oxide films at

*H_2 can be evolved on valve metal oxide surfaces without their reduction due to the high thermodynamic stabilities of these oxides.

various metals. Most metal oxides of the valve-metal group have exothermic heats of formation, ΔH_e, greater than 46 kcal (~ 2 eV). A general relation seems to exist[139] where the band-gap E_g of the film increases in proportion to ΔH_e ($E_g \simeq 2 \Delta H_e$). This means that oxide films grown on the valve metals are highly insulating since the band-gap values are high. Such high band-gap values result in low electronic conductivity and hence low rates of parallel reactions on these metal surfaces. Therefore, upon anodization, ionic currents result and lead to oxide film thickening. However, with a sufficient field across the oxide barrier, parallel reactions can be made to occur.

The electrochemical behaviour at the semoconductor oxide/solution interface is largely determined by the effective band-gap of the oxide, while chemical factors are involved mostly with the formation of defects during anodization.

The change of properties of a metal surface when a high band-gap film is formed upon it was referred to by Vijh[20,139] as " demetallization ". When demetallizing barrier-layer films are formed on base metals they usually give rise[105,140] to abnormally high Tafel slopes for any "parallel" reaction going on on the film due to the involvement of the " film barrier " for electron transport in series with the regular activation barrier for the electron transfer process across the double-layer at the oxide film/solution interface. This effect arises because the potential drop (eqn. 5) across the double-layer, $\Delta V_{d.l.}$, where the electron transfer process in the reaction occurs, is only some fraction γ of the overall metal-film-solution potential drop, ΔV. Hence the apparent barrier symmetry factor is $\beta V_{d.l.} = \beta \gamma \Delta V$, so that the slope of ΔV vs.

log i plots is $RT/\beta\gamma F$ for a 1-electron transfer process.

With Pt and other noble metals, the oxide films normally developed during processes such as Cl_2 and O_2 evolution do <u>not</u> " demetallize " the surface so that electron transfer across the film is not usually a limiting factor in the kinetics of such " parallel " reactions. From an electrical charge-transfer point of view, reactions such as O_2 or Cl_2 evolution occur easily but not without some major influence of the oxide film on their kinetics for non-electrical reasons, as will be shown in the present work.

Similar conclusions apply to certain base metals such as Ag, Cu, Co and Ni which form relatively thick (30 - 40 layers) films of the metal oxide. In these cases, however, mixed-valency oxide films are formed which have appreciable electronic conductivity. These films are also more porous and hydrated than those on the valve metals.

CHAPTER II

ELECTROCATALYTIC EFFECTS OF THE OXIDE FILM IN Cl_2 EVOLUTION AT Pt

1. INTRODUCTION

(i) Statement of the Objectives: The production of Cl_2 as a major " heavy chemical " has continuously expanded during the last three decades. The two commonly used processes for its generation[142] are: (a) the chemical conversion of HCl into Cl_2 via the Deacon process and (b) far more competitively, the electrolytic production of Cl_2.

With regard to the latter process, the use of carbon anodes has been common for many years. However, more recently, in order to diminish Cl_2 overvoltage and associated power losses and increase anode lifetimes, much attention has been given to the study of the behaviour of various noble metal and noble metal oxide surfaces which are currently being used as improved electrocatalyst surfaces for commercial electrochemical Cl_2 production[143-148]. These are:

(i) titanium electrodes coated with noble metals of the platinum group (e.g. Pt, Pd, Ir, Rh)[142,143] and

(ii) titanium electrodes coated with oxides of Ru and Ir[144-148].

Although Pt is considered one of the best catalysts, it is not commercially used since it is expensive and it is also known that Pt electrodes undergo strong passivation and some corrosion when used as anodes for Cl_2 production[142,143]. However, Ti-supported Pt-Ir alloy anodes have shown

much better performance since Ir contents as low as 0.5% were found sufficient to eliminate almost completely the passivation effects[143].

Special attention has been given to the study of the electrochemical behaviour of metal oxide films, particularly RuO_2, on a passive metal support such as Ti/TiO_2 in the so-called dimensionally stable anodes ("DSA" electrodes)[146,148,149]. Such oxide films have been found not only to be good conductors but it is likely that they play an important role in the kinetics and mechanism of anodic Cl_2 evolution. It may be expected that the electrocatalytic properties of noble metal surfaces will also be considerably changed when oxide film formation occurs during their use as anodes (Chapter I).

From the general electrochemical properties of the noble metals reviewed in Chapter I , it would appear that, in aqueous media, Cl_2 evolution should proceed on an <u>oxidized</u> or <u>partially oxidized</u> surface of the anode metal since most metal surfaces are already oxidized at potentials below, or close to, the Cl_2 reversible potential (standard value = 1.358 V E_H)[150]. This would suggest that it is the properties of the surface oxide film on the metal anode that are of greater importance for the Cl_2 evolution reaction than the properties of the bare metal surface itself.

The first of the new work described in this thesis deals with this question and reports a comparative study of the electrocatalytic behaviour of an <u>unoxidized</u> Pt anode surface, which can be obtained in anhydrous trifluoroacetic acid (TFA) with RbCl as electrolyte, with that of an <u>oxidized</u> Pt electrode surface in regular aqueous KCl solutions. Hence the effects of development of an oxide film on Pt anode surfaces in aqueous

medium can be determined in relation to the kinetic behaviour of Cl_2 evolution on an unoxidized Pt metal surface. Other factors also enter into this comparison and will be examined in detail later.

In aqueous medium, the probability that most anode surfaces involved in Cl_2 evolution will be covered to some degree with an oxide film, and the potential-dependence of the extent of formation of such a film, are important factors in the study of anodic Cl_2 evolution kinetics. In the early work, the role of the oxide film was not well understood but later workers recognized this matter as one of importance. It is also related to the question of anodic O_2 evolution as a parallel anodic process.

(ii) Previous Work on Anodic Cl_2 Evolution: The Cl_2 evolution reaction occurs at 1.358 V E_H at the standard Cl^- concentration and thus, in aqueous solutions, the reaction normally proceeds in parallel with oxide film formation and theoretically with O_2 evolution (standard potential 1.230 V E_H [150]). Oxide species at the electrode surface are said to have an inhibiting effect on both the formation[120,151] and reduction[151] of Cl_2. Early studies on the Cl_2 evolution reaction were made by Chang and Wick[152] on Pt and Ir electrodes in 1M HCl electrolyte, using steady-state polarization techniques in both the anodic and cathodic directions. They found that the η vs. log i relations were curved so that the currents at higher overpotentials were smaller than expected from a linear Tafel relation.

Such behaviour was already mentioned by Glasstone and Hickling[153] who made the same type of measurements and found that the Cl_2 evolution reaction occurring at the anodes causes a change in the anodic behaviour of the electrode. At higher overpotentials[153,154], after Cl_2 evolution

commences, a subsequent determination of the potential-time plot gave a sudden rise of potential of a few hundred millivolts as the reaction proceeded for some time. This has been interpreted as due to passivation of the electrode by the formation of surface oxide[153-155] or to depletion of Cl^- ion concentration at the electrode surface[154]. The i-V curves exhibit the same type of the behaviour that was attributed to adsorbed oxygen[155]. This has generally not been found in subsequent work.

One of the main concerns in the early work on Cl_2 evolution kinetics was to determine the extent to which co-evolution of O_2 occurs at anodes as a parallel process to Cl_2 evolution. Hickling[156] found that addition of NaCl to a solution in which O_2 had been evolved anodically at Pt electrodes resulted in a rapid decrease in the potential and that the predominant process then became Cl_2 evolution.

Frumkin and Tedoradze[157] studied the kinetics of the Cl_2 reduction reaction by using a rotating Pt disc electrode in solutions of $HClO_4$ and H_2SO_4 as supporting electrolytes containing small concentrations of Cl^- ions (less than 6.3×10^{-2} M Cl^-). They found that the Tafel relationship for the plots V vs. log i was linear and proposed the following mechanism for the reduction reaction:

$$M + Cl_2 + e^- \rightleftharpoons M\text{-}Cl_{ads} + Cl^-$$

$$M\text{-}Cl_{ads} + e^- \rightleftharpoons Cl^- + M$$

in which the two steps are comparable in rate and both back reactions are negligibly slow at moderate overpotentials.

Tedoradze[155] studied the trend in anodic potential/time curves and confirmed that no significant O_2 evolution occurs before oxidation of Cl^- ions commences on Pt surfaces. He pointed out that the anodic behaviour of Pt in chlorine solutions is a complex one since the nature of the anode

surface changes with increasing anodic polarization (due to changes of surface oxidation - cf. Chapter I). He suggested that the mechanism of the Cl_2 evolution process involves two steps: one being the discharge of Cl^- ions on Pt surface oxide which occurs at low current-densities and low overpotentials and also low Cl^- ion concentrations, and the other, the so-called recombination step which was assumed to take place at higher overpotentials and higher current-densities, viz.

$$M + Cl^-_{aq.} \longrightarrow M\text{-}Cl_{ads.} + e^-$$

$$2M\text{-}Cl_{ads.} \rightleftharpoons Cl_{2(aq.)} + 2M$$

It was considered that the rate-determining step in the oxidation of Cl^- ions involves one electron. The discontinuity in the V-log i curves at relatively high overpotentials and high current-densities was ascribed to the O_2 evolution reaction. At low overpotentials, however, the O_2 evolution reaction does not take place significantly before oxidation of Cl^- ion, although the formation of Pt surface oxides may take place under these conditions[155].

Llopis and Sancho[158] considered the competitive adsorption of Cl^- ions and oxide species on Pt surfaces and suggested that only at the potential of 1.6 V E_H, with a corresponding current-density of 63 mA cm^{-2} in 2M NaCl solution, is the inhibition of oxide formation or oxygen adsorption overcome. In 0.5M NaCl solution the required current-density at 1.6 V E_H needed to reduce inhibition effects was found to be 8 mA cm^{-2}. As the oxidation of the Pt surface takes place, there was assumed to be a change in the kinetics of the reaction

$$M\text{-}Cl_{ads.} + Cl^- \longrightarrow Cl_2 + e^-$$

leading to a reduced rate of the Cl_2 evolution reaction.

Ershler[159] observed that, for a given potential, the current diminishes exponentially in Cl^- ion solutions as the fraction of the surface covered with the oxide film increases. Littauer and Shreir[160] studied the behaviour of Pt anodes in NaCl solutions and found that the " potential jump " occurs at 1.6 V E_H for a range of current-densities from 2-100 mA cm^{-2} corresponding to various concentrations and pH's. They also observed that the nature of the electrode is altered and the same type of i-V curve as initially observed[160] could be obtained only after the electrode surface was rigorously cleaned. The explanation of that behaviour was given by taking into consideration the formation of an oxide film and/or discharge of O_2 molecules at the anode surface. They noted that thermodynamically the potential for Cl_2 evolution, according to the process

$$Cl_2 + 2e^- \longrightarrow 2Cl^-,$$

is determined by

$$E = 1.359 + 0.0295 \log p_{Cl_2} - 0.059 \log a_{Cl^-}$$

while that for O_2 evolution according to the process

$$O_2 + 4H^+ + 4e^- \longrightarrow 2H_2O,$$

is given by

$$E = 1.230 - 0.059\ pH + 0.015 \log p_{O_2}$$

This implies that the oxidation of OH^- ion or H_2O should occur in preference to the oxidation of Cl^- ion. Hence the observed evolution of Cl_2 as the predominant anodic reaction arises for kinetic rather than thermodynamic reasons. The " potential jump " in the V vs. log i relations arises when Cl_2 evolution reaches a limiting rate so that, at sufficiently high

potentials, a new V vs.log i relation for O_2 evolution dominates the electrode kinetic behaviour[160]; then the extent of surface oxidation is increased[152,155]. Thus Littauer and Shreir[161] observed two linear Tafel relationships for the current-density range from 2-100 mA cm^{-2}. At low current-densities, the oxidation of the Pt surface was considered as only a minor process leading thus to Cl_2 evolution either on a free Pt surface or on " patches " of a film of chemisorbed Pt-O or Pt-Cl. At high current-densities ($\sim$150 mA cm^{-2}) the discharge of Cl^- ions occurs on an oxidized Pt-surface, since the electrode was considered to be covered with a stable oxide or perhaps chloride film[160].

As the Pt surface changes supposedly from an " oxide-free " surface to an " oxide-contaminated " surface, a rapid increase in potential can be observed[160]; the current-density at which it occurs was found to be dependent on the solution composition. On the other hand the rate-controlling step of the reaction was considered by Tedoradze[155] to be the discharge of Cl^- ions. However, it was stressed by Littauer and Shreir[160] that the kinetics of the reaction must be much more complex since it was recognized that the coverage of the surface with oxide should be also taken into consideration. Measurements of the extent of surface oxidation were not, however, attempted in that work.

Dickinson, Greef and Wynne-Jones[151] made an attempt to study the formation and reduction of Cl_2 at Pt electrodes; they supposed that both these processes would be inhibited by the oxide film formed on the electrode surface. It was assumed that oxide formation would be a rather slow process in concentrated Cl^- ion solutions, such as 1M HCl, but it was found that the extent of oxidation of the electrode varied markedly with increasing potential and therefore they were unable to obtain i-V

curves at constant oxide coverages in the anodic direction of the reaction. However, in the cathodic direction (Cl_2 reduction) it is easier to obtain constant oxide coverages above 0.9 V, and therefore they were able to obtain a series of i-V curves for the Cl_2 reduction process at Pt, at different Cl^- ion concentrations and different oxide coverages. They took into account the results of Balashova[161], and of Breiter[162] and Gilman[163], who indicated that the extent of Cl^- adsorption on oxidized electrode surfaces is determined by the degree of oxidation of the electrode. Dickinson et al.[151] noted that, most probably, oxide coverages of the surface and thus the quantity of Cl^- ions adsorbed, depend on the pre-treatment of the electrode. They indicated that as the quantity of oxide increases on the Pt surface the rate of Cl_2 reduction would decrease at constant potential. The oxide-covered sites were assumed to be unavailable for the reaction to occur and thus, as the available surface is decreased, the standard free energy of adsorption of intermediates[95] would rise, tending to cause an inhibition[117,164] of the Cl_2 reduction reaction.

Since non-linear V-log i relations were obtained, Dickinson et al.[151] proposed the following simple mechanism for Cl_2 reduction :

$$Cl_{2(aq.)} + M + e^- \rightleftharpoons Cl\text{-}M + Cl^-_{(aq.)}$$

$$Cl\text{-}M + e^- \longrightarrow M + Cl^-_{(aq.)}$$

in which the desorption step was supposed to be rate-determining, but comparable in rate with that of the back reaction of the first step. With increased oxide coverage, the rate of the reduction process decreases but there was no evidence that the mechanism of the reduction changed.

Further studies on the role of oxide surfaces in the Cl_2 evolution reaction was provided from the impedance studies of Pt electrodes in

Cl_2/Cl^- solutions as obtained by Llopis and Vazquez[165]. They observed that blocking of the surface due to the surface oxide formation leads to a passivation of the electrode, by forming so-called inactive areas where electron-transfer is strongly inhibited. In the case of the Cl_2/Cl^- couple, the potentials at which oxidation of Cl_2 occurs are high enough to allow oxidation of the electrode. The oxidation of the Pt surface would cause a decrease in the exchange current of the overall process. In the case of Br_2 evolution, the potentials at which reaction commences are less positive than that of O_2 evolution and therefore the fraction of the oxide-blocked surface is small and most probably does not affect the Br_2 reaction. In the case of I_2 evolution the reactants have great tendency to be adsorbed on the electrode surface so that the surface oxide has only a minor influence on the reaction.

Further information on the role of the oxide surface in Cl_2 evolution reaction was reported in the papers of Faita et al[143,144,166]. They obtained mixed oxide coated electrodes by thermal deposition of Pt and Pt-Ir alloys, as well as RuO_2 on titanium matrices. The procedure was based on knowledge of the rather irreversible oxide formation and reduction on Pt surfaces compared with the relatively reversible oxide formation and reduction in the case of Ir electrodes[167]. They also took into account Breiter's[162] observation that the formation of the oxide film on Pt surfaces starts to develop at more positive potentials in solutions containing halide ions than in their absence. The amount of adsorbed oxide species was found to decrease with increasing halide ion concentration. The formation of the oxide film on Pt was considered[142-144] to cause a passivation effect[143,144,166] on the Cl_2 evolution reaction, dependent on Cl^- mass-transfer. The presence of Ir on Pt (e.g. at Pt-Ir alloy surfaces

with even only a very low Ir content of 0.5%) was found to minimize passivation effects. When 30% Ir is present, no passivation effect was observed for the same experimental conditions for Cl_2 evolution[166]. Faita et al.[143,144,166] considered also Breiter's statement[162] that oxide formation disappears almost completely when the Cl^- ion concentration is higher than 10^{-2}M. They assumed that it is more likely that oxide formation is slowed down considerably so that Cl^- ions are discharged at a Pt electrode surface at low potentials only when the surface is free from electrodeposited oxide. The rate of oxide formation is inversely proportional to Cl^- ion concentration and increases with increasing electrode potential. In the case of Ir, a more reversibly formed oxide is deposited already at low anodic potentials so that the Cl_2 evolution reaction must occur on an oxidized surface in that case. In the case of RuO_2, the electrochemical properties are similar to those of Pt and Pt-Ir alloy electrodes; linear V-log i relationships were obtained, giving rather low Tafel slopes of 30-40 mV. Such low values can be explained through the following mechanism:

$$Cl^- \rightleftharpoons Cl_{ads.} + e^- \qquad (1)$$

$$2Cl_{ads.} \longrightarrow Cl_2 \qquad (2)$$

in which step (2) was considered to be rate-determining.

Yokoyama and Enyo[168] made a detailed study of the i-V and reaction order behaviour for Cl_2 evolution and reduction at Pt, Ir and Rh electrodes in 1M H_2SO_4 solution with various Cl^- ion concentrations. They concluded that Cl^- ion discharge was rate-controlling in the anodic direction followed by Cl' recombination. Their conclusions will be discussed in more detail later in relation to the results of the present work.

Kuhn and Wright[169] also studied the Cl_2 evolution reaction on Pt, Ir and RuO_2 electrodes in relation to (a) the different amounts of oxides which could be formed on these surfaces and (b) the different electrocatalytic properties of these surfaces. They did not find in the case of Pt any evidence for oxide formation below the Cl_2 evolution potential in cyclic-voltammetry experiments. As the sweep moves towards more anodic potentials the Cl^- ions effectively block the tendency for the electrode surface to develop a surface oxide film as found by Breiter[162] and also in the present work. In the case of Ir, it was found that the oxide film formed on the surface is not easily reduced above the Cl_2 evolution potential. In strong Cl^- ion solutions, there was no evidence found for the specific adsorption of Cl^- ions at Ir. Ruthenium electrodes[170,171] easily form an higher oxide at high anodic potentials in 0.5M H_2SO_4[172]. This oxide was characterized as RuO_4 and was found to dissolve partially as H_2RuO_5. In strong Cl^- ion solutions, such behaviour occurs more readily but the surface could be modified easily by continuous oxidation and reduction procedures.

A thick film of coherent oxide was also found on the electrodes at potentials where Cl_2 is evolved, by Kuhn and Mortimer[148]. The non-linear V-log i polarization behaviour of RuO_2 and IrO_2 seems to be the same since both of the metals produce fairly thick oxide films. These oxides were classified as n-type semiconductors[145].

Arikado et al.[173] used the thermal decomposition method to prepare RuO_2 electrodes which they characterized later electrochemically. They found that, upon longer anodization, the Ru electrodes became modified. This was ascribed to oxygen permeation into the electrode bulk but it may simply have been due to thickening of the oxide film [see Chapter I,

Section 3.(iii)] .

Krishtalik et al.[174,175] studied Cl_2 evolution and ionization at RuO_2-TiO_2 electrodes. In their first paper[174], they showed that the Cl_2 evolution reaction proceeded through a complex mechanism in two parallel stages: recombination of adsorbed Cl· and electrochemical desorption ($M\text{-}Cl_{ads.} + Cl^- \longrightarrow Cl_2 + e^-$). It was concluded that the recombination step is faster than desorption so that at high anodic polarizations, the principal transfer from Cl· to Cl_2 is via the catalytic recombination pathway. However, later they[175] reexamined their results and proposed a new mechanism which proceeded first through fast discharge of Cl^- ion on the surface with the formation of adsorbed atomic chlorine:

$$Cl^-_{aq.} \rightleftharpoons Cl_{ads.} + e^-$$

The next step involved the further oxidation of chlorine atoms to the chloronium intermediate, Cl^+, viz.

$$Cl_{ads.} \longrightarrow Cl^+ + e^-$$

which, in a fast third stage, reacts with Cl^- from the solution to form the Cl_2 molecule:

$$Cl^+ + Cl^- \rightleftharpoons Cl_2 .$$

Since the proposed mechanisms and also the values of the experimentally obtained Tafel slopes differ in various works, the mechanism of the Cl_2 evolution reaction on RuO_2/TiO_2 electrodes, as well as on the RuO_2 electrode itself, was reexamined by Janssen et al[176]. They recorded potentiodynamic current-density / potential curves as a function of time of anodic pre-polarization, composition of solution and temperature. They also measured potential decay curves and gave simulated (theoretical) V-log $\frac{i}{}$ curves for both the Tafel ($2Cl_{ads} \longrightarrow Cl_2$)' and the Heyrovsky

type reactions (Cl^- + $Cl_{ads.} \longrightarrow Cl_2$) as possible rate-determining steps in the formation of Cl_2. These results were compared with the experimentally obtained ones and it was found that for the electrodes in question, Cl_2 is formed via the Volmer-Heyrovsky mechanism, where the Heyrovsky reaction is the rate-determining step regardless of the technique employed. The theoretical Tafel slope is 40 mV at 298 K, with which the experimental results were in good agreement. The reason for slopes higher than 40 mV being observed was said to be due to the temperature effects while lower slopes (~ 30 mV) could be due to the different compositions of the electrodes used in various works[143,144,166,177].

Arikado et al.[178,119] also studied the mechanism of Cl_2 evolution on a series of electrocatalysts aiming to find the relation between the Cl_2 evolution mechanism and the catalytic activities of the oxide electrodes by taking into account the characteristics of their oxides (e.g. RuO_2, IrO_2, WO_3, Ti/PtO_2 etc.) In the case of RuO_2 electrodes used for Cl_2 evolution, they supposed that that the active site on the electrode is a Ru(III) centre and Cl^- ion adsorbs at an " Ru-OH " site, completing the coordination shell there. The coverage of Cl^- ions on the electrode surface was found to depend on concentration of the electrolyte and on pH. The mechanism was determined by the interaction between the electrode surface and the adsorbed Cl atoms. If the electrode contains a transition metal cation with partially filled t_{2g} levels and empty e_g levels, as is the case with RuO_2 or IrO_2, the Volmer-Heyrovsky mechanism applies. However, if the electrode surface contains a transition metal cation with half or just filled t_{2g} and partially filled e_g levels, as is the case with TiO_2/"PtO_2", the Volmer-Tafel mechanism could be proposed. They[178]

further related log current-densities at various potentials to the d-band vacancies and associated " oxide coverages " at Pt and Pt alloys. The d-band vacancies of the alloy electrodes were assigned by proportional allotment of the values for each metal component, based on the composition of the alloy. A linear relationship between oxide coverage at the electrode, determined by reduction coulometry at potentials where Cl_2 is evolved, and the d-band vacancy of each of the alloys was found for constant potential, Cl^- concentration and pH. It is unclear, however, how these authors determined reliably the oxide coverage in the presence of Cl_2 by means of a reduction pulse. The log i_o values were further related to the dissociation energy of the metal-to-Cl bond and it was suggested that the dissociation energy of this bond plays an important role in Cl_2 evolution reaction.

It was concluded that the state of adsorbed Cl-atoms at Ru cation sites in two types of electrode surface preparation determines whether the " Volmer-Tafel " or the " Volmer Heyrovsky " types of mechanisms determine the kinetics.

In a recent paper, Augustynski et al.[179] examined RuO_2 and mixed RuO_2-TiO_2 electrode surfaces by means of X-ray photoelectron spectroscopy in order to obtain information about RuO_2-based electrodes especially with regard to their low overpotential for the Cl_2 evolution reaction and excellent corrosion resistance at anodic potentials. Spectra were obtained for freshly prepared RuO_2 and RuO_2-TiO_2 electrodes as well as for electrodes used as anodes in the electrolysis of 4M NaCl solution. By comparing these results, distinct changes in the composition of the outermost 2-3 nm of the electrode surface layer were observed.

Since the XPS analysis is performed under high vacuum conditions, an RuO_3 defect structure is found on the surface of RuO_2 and RuO_2-TiO_2 electrodes. Spectra of the surfaces of RuO_2 and RuO_2-TiO_2 electrodes used as anodes for Cl_2 evolution reaction showed also the existence of two distinguishable chlorine species: one identified as adsorbed Cl^- ions and the other as adsorbed atomic chlorine. The surface coverage of adsorbed chloride species was estimated to be roughly equal to unity ($\theta \approx 1$), assuming that there was one Cl atom per Ru and/or Ti atom. Such a high degree of chloride ion adsorption was regarded as preventing surface oxidation of the electrode. Thus, although further experimental information is needed to understand more fully the behaviour of RuO_2 electrodes in Cl_2 evolution, the work of Augustinsky et al.[179] demonstrated that both adsorbed chloride as well as Ru(IV) species could play an important role in the Cl_2 evolution reaction when RuO_2 or mixed RuO_2-TiO_2 electrodes are employed.

The Cl_2 evolution process on graphite anodes has been studied in molten salts[180,181] as well as in aqueous solutions[144,182-184]. Bockris et al.[180] used the galvanostatic transient method to study Cl_2 evolution in molten KCl at graphite electrodes at different temperatures using various kinds of graphite (spectroscopic and porous). The experimental data follow satisfactorily a straight Tafel line with a slope $b = 2.3 \frac{RT}{\alpha F}$ with α approximately equal to 2. Such a low value of the slope is consistent with fast discharge of chloride ions followed by rate-determining recombination of chlorine atoms on a surface sparsely covered by $Cl^\cdot$ atoms or more appreciably covered under Temkin conditions.

Krishtalik et al.[181,182] used non-porous graphite electrodes in melts of $PbCl_2$ and AgCl to study the kinetics of the Cl_2 evolution reaction.

They found polarization curves which consisted of two straight-line regions, one at lower overpotentials with a slope of 60-90 mV and the other with a slope of 120-160 mV at higher potentials. These experimental data were explained by " barrierless " discharge* of Cl^- ion on the graphite surface which would go over normal discharge at increased current-densities. In interpreting activation energies for Cl_2 evolution on graphite[181], it was necessary to consider the surface to be oxidized in order to account for discrepancies in data for heats of dissociation of carbon-to-Cl bonds formed with the surface of the carbon electrodes used.

Cl_2 evolution on graphite electrodes exhibits also complex behaviour[182-184] in aqueous Cl^- ion solutions, since the overall reaction is complicated by the formation of an oxide layer, so that the electrolysis of Cl^- ion solutions at higher potentials consists of the discharge of Cl_2 as well as formation of "oxide" species or oxidation of the carbon interface in other ways.

Janssen and Hoogland[183,184] critisized Kristalik's paper[182] and stated that the mechanism of Cl_2 evolution on graphite anodes in acid chloride solution consists of a discharge reaction

$$Cl^- \longrightarrow Cl_{ads.} + e^- \text{ (Volmer reaction)}$$

followed by molecular Cl_2 formation by discharge of Cl^- ion on adsorbed chlorine atoms according to the Heyrovsky reaction

$$Cl^- + Cl_{ads.} \longrightarrow Cl_2 + e^-$$

---

*" Barrierless-discharge " is a term used by Krishtalik[185] to refer to the hypothetically possible situation where the activation energy is identical with the endothermicity of a discharge step. This situation can only arise at low overpotentials over a limited potential range and corresponds to a symmetry factor $\beta = 1$. The complementary situation of " activationless discharge " ($\beta = 0$) can occur at very high overpotentials. Generally speaking, these limiting conditions are not often encountered experimentally.

Which of these two reactions is rate-determining depends on the history of the electrode and the concentration of the electrolyte. These authors[184] also found that during electrolysis of acid chloride solutions, atomic chlorine diffuses into graphite anodes, so the rate of the Cl_2 evolution reaction would be influenced by the rate of diffusion of atomic chlorine out of the graphite in relation to the coupled rate of the Heyrovsky reaction.

Since the behaviour of graphite electrodes used for Cl_2 evolution from aqueous Cl^- ion solutions was found to differ so much from that of Pt or Pt-Ir electrodes, Hine and Yasuda[186,187] suggested that the " carbon oxide " layer should be considered to have an effect on the Cl_2 evolution reaction. They found that there are actually two states of oxidation of the graphite surface[186]: a so-called " lower oxide ", which begins to form at about 0.78 V E_H. Upon further anodization the " higher oxide " tends to form. In the potential range of 1.26 - 1.56 V E_H both types of oxides coexist on the graphite surface. However, at even higher anodic potentials (> 1.56 V E_H) the " lower oxide " is found to be fully converted into the " higher oxide ". The " lower oxide " was found to be easily removed form the graphite surface as either O_2, CO or CO_2. The displacement of the " higher oxide " is more difficult and it could occur only above 2.24 V E_H, when it is removed as CO and/or CO_2. Hine et al.[187] also found that the specific adsorption of Cl^- ions takes place on graphite surfaces only when the electrode surface is free from either type of oxide. Thus, under normal conditions for Cl_2 generation, graphite electrodes would be initially covered with the " lower oxide " if polarization is done in the potential region

0.76~1.56 V E_H; then Cl_2 evolution would take place at significant rates. At higher potentials than 1.56 V E_H, Hine et al.[186] assumed that " higher oxide " formation becomes a major electrochemical process at graphite anodes. This oxide would cause an increase in the Cl_2 overpotential due to occupation of the active sites on the electrode surface. Exchange between oxide and chlorine atoms was considered to be irreversible and was found to depend on potential and the concentration of electrolyte.

The reduction behaviour of Cl_2 in alkaline solutions in which Cl_2 gas was bubbled was studied[188] on glassy-carbon disc electrodes and compared with the results obtained at Pt electrodes. In both cases it was found that the electrochemical reaction is irreversible and proceeds through the possible mechanism:

$$Cl_2 + H_2O \longrightarrow 2H^+ + OCl^- + Cl^-$$

$$OCl^- + H_2O + e^- \xrightarrow{\text{slow}} Cl_{ads.} + 2OH^-$$

$$Cl_{ads.} + e^- \xrightarrow{\text{fast}} Cl^-$$

An oxide film was found to form in both cases in parallel with the OCl^- reduction. It was found that the oxide on Pt inhibits the reduction of OCl^- in the early stages of the growth of the film but, with further growth of the oxide, the inhibition effect disappears. It was suggested that a " relaxation " in the oxide structure takes place, relieving the inhibition effect.

(iii) Conclusions: In aqueous media, Cl_2 evolution necessarily proceeds on an oxidized or partially oxidized surface of the anode metal since most metal surfaces are oxidized at potentials below or close to the Cl_2 reversible potential, or well below the potentials required for Cl_2 evolution at practical rates (> 100 mA cm^{-2}). For practical Cl_2 evolution, it is therefore the properties of the oxide films of the anode metal (with co-adsorbed Cl^- anions) that are of interest for this reaction rather than the properties of the free metal surface itself. Therefore it is of interest to study the kinetics of anodic Cl_2 evolution at Pt firstly on a Pt surface free of surface oxide. This can be achieved in an anhydrous non-aqueous medium, and then, for comparison, in aqueous solutions where the metal oxide film is developed.

Cl_2 evolution on an oxide-free Pt surface can be achieved by conducting experiments in trifluoroacetic acid (TFA)* as solvent with RbCl as electrolyte. TFA is electrochemically inactive in an anodic direction up to ca. 2.1 V E_H when it undergoes the Kolbe reaction, giving at higher potentials C_2F_6[189]. It can also be prepared in an extremely dry state[189b,190]. Hence an interesting comparison of the kinetics of Cl_2 evolution on a " bare " Pt surface in TFA and on an oxidized surface in water can be made.

If the same kinetics of anodic Cl_2 evolution at Pt apply for both solvents and their mixtures, e.g. recombination- controlled kinetics, then any differences in the rates of Cl_2 evolution at a given overpotential, which may arise as water is added to TFA solution of Cl^- salt, could be

---

*Some work has been published on Cl_2 evolution from Cl^- solutions in other non-aqueous solvents, viz. CH_3COOH [191] and CH_3NO_2 [192a,b], but not for the purposes desired in the present work.

treated on terms of (a) the different catalytic effectiveness for Cl· recombination of oxide free and oxide-covered Pt surfaces; and (b) interaction effects due to specifically adsorbed Cl^- ions.

2. EXPERIMENTAL

(i) Methods: In order to characterize the electrocatalytic behaviour of the Pt electrode surfaces, steady-state current-potential relations were obtained potentiostatically at a rotating-disc Pt electrode. Measurements were made in both ascending and descending directions of potential change. Currents were recorded on a Sensitive Research micro-milliammeter and potentials were read from a digital millivoltmeter previously calibrated by means of a Weston cadmium cell. Currents were measured 30 sec. after each adjustment of potential; this procedure ensures very reproducible curves.

The log current-potential curves all exhibited an approach towards limiting currents at elevated potentials (cf. 169,193) so that it was important to conduct a series of runs at various rotation speeds in order to evaluate the role, if any, of mass transfer control at high current-densities. For similar reasons, " iR " corrections were made to the data by obtaining the iR drop values, ΔV, by the current interruption technique*, using a vacuum relay and recording ΔV on an oscilloscope with a fast time-base setting. Small but significant values of ΔV arose at high current-densities.

That the approaches to limiting current behaviour were not due to an artefact arising from limited current output from the potentiostat, was demonstrated by conducting some experiments with a galvanostatic

*A useful review on " iR " correction methods has been given recently by Britz[194].

power source: similar limiting current behaviour was exhibited.

Cyclic voltammetry experiments were conducted in the usual way[22,61] in order to evaluate oxide film coverages and demonstrate the absence of an oxide film in the anhydrous TFA experiments. Previous experiments[189,190] in TFA containing traces of water, but without Cl^- present, showed that the water content could be related to the extent of surface oxidation of Pt observed in potentiodynamic sweeps up to ca. 1.6 - 2.0 V E_H. A really dry solution gave no detectable currents for formation or reduction of surface oxide at Pt as shown in Fig. 3.

After each run at ascending and descending anodic currents, the electrode potential was returned to a value (0.05 V E_H) at which the oxide film formed on the Pt in the aq. solutions would have been reduced. This procedure was adopted prior to each evaluation of the current-potential relationship for Cl_2 evolution, in order to achieve reproducible initial Pt surfaces.

(ii) Solutions and Salts: Trifluoroacetic acid was prepared by drying and multiple distillation by the method described previously[190]. The anhydride used[190] for " gettering " any remaining traces of water was similarly purified. RbCl used for the work in TFA was recrystallized twice and dried at 150° C in vacuo. KCl used in water solutions was similarly purified. Water used in the aqueous solution work and in the preparation of TFA/water mixtures was pyrodistilled according to the procedure described previously[73] and developed in this Laboratory.

(iii) Rotating Pt Disc Electrode: The electrode (Pine Instrument Co. Pa.), mounted in Teflon, was exhaustively cleaned in cold Aristar 98% H_2SO_4, washed repeatedly in the pyrodistilled water and then left to

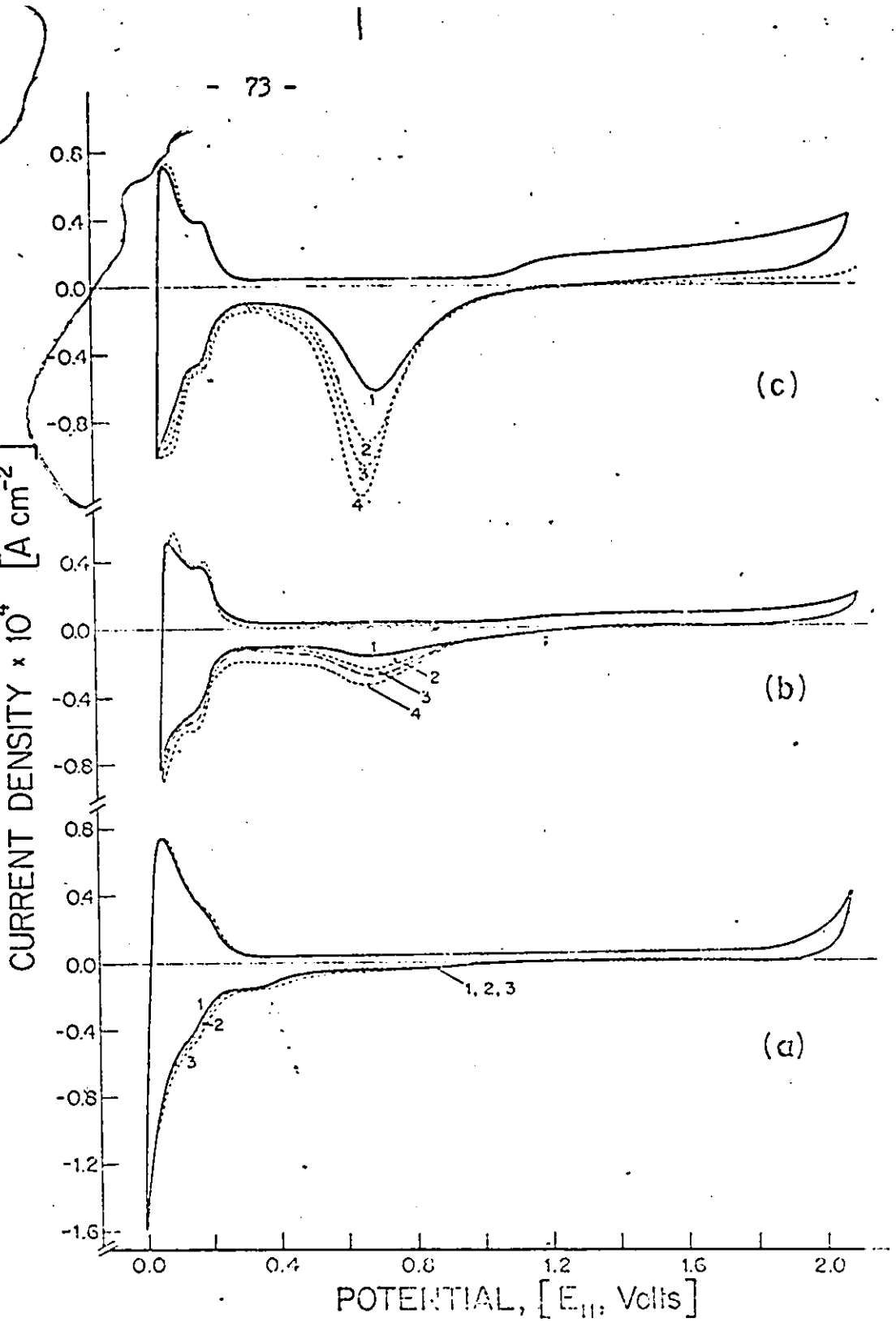

Fig. 3 Potentiodynamic i-V profiles for a Pt electrode in anhydrous TFA + KTFA as electrolyte with addition of traces of water. (a) Anhydrous TFA gettered by a trace of trifluoroacetic anhydride: (1) multisweep; (2,3) holding at 2.164 V for 120 and 300 s. (b) TFA with water added: (1) multisweep;(2,3,4) holding at 2.164 V for 30, 60 and 120 s, respectively. Water concentration = 0.19 mol %. (c) TFA with water added: (1) multisweep;(2,3,4) holding at 2.09 V for 30, 60 and 120 s. Water concentration = 0.42 mol %. Sweep rate = 8.2×10^{-2}. T = 298 K.

stand in this water for 12 h. It was then electrochemically cleaned by cyclic-voltammetry between + 0.05 V and + 1.4 V E_H. The current-potential profile for the surface processes at a clean Pt surface (cf. 73) was attained after ca. 20 sweeps at 20 mV s^{-1}. After this initial cleaning procedure, a " clean " surface could usually be regenerated after 5 sweeps. The Pt disc electrode was usually more difficult to clean than a Pt wire electrode sealed in glass that can be subjected to initial hot acid treatment. Hot acid cannot be used with a Teflon mounted disc.

(iv) Oxide coverage in Cl_2 evolution experiments: The coverages or quantities of electrodeposited O species generated just up to Cl_2 evolution were evaluated in various solutions from the cathodic i-V profile in a cyclic-voltammetry curve obtained at the Pt disc electrode rotated at a nominal slow rate (400 r.p.m.). As Cl^- ion concentration is increased in water solutions, the oxide coverage attained just prior to Cl_2 evolution decreases due to competitive adsorption by Cl^- ion. Oxide coverages within the range of potentials used for studies of Cl_2 evolution could also be measured by rotating the electrode at much higher angular velocities in a sufficiently large volume of the electrolyte solution, so that evolved Cl_2 is spun away.

In one experiment, a known degree of surface oxidation was established in aq. 0.5 M H_2SO_4; the electrode was then transferred to the 100% TFA solution after a brief wash with TFA. This procedure did not diminish the oxide coverage (as measured by the reduction charge per cm^2) by more than 2%. Cl_2 evolution on this pre-oxidized electrode was then studied.

(v) Reference Electrodes: Both the H_2 (1 atm)/Pt and the $\alpha + \beta$ PdH electrodes[195] were used as calibrating reference electrodes. Both were satisfactorily reversible and gave stable potentials in TFA and in aq. solutions. During runs, a Ag/AgCl electrode, formed on a Ag wire mounted within a thin-walled capillary tube acting as a Luggin probe, was used.

3. RESULTS

(i) The State of Pt Electrode Surfaces in TFA/H_2O Mixtures with and without Cl^- Ion Present: The extent of dryness of the TFA solutions is conveniently indicated from cyclic-voltammetry curves at the Pt electrode taken to ca. + 2.0 V E_H. In a really dry solution, the i-V profile shows no current plateau for surface oxide formation in the anodic sweep nor then any peak for surface oxide reduction in the cathodic sweep. Also, upon holding the potential at 2.0 V, no cathodic peak develops if the solution is dry. Only an almost straight and parallel pair of current-potential lines results (Fig. 3a), corresponding to the double-layer charging currents, $C_{d.l.}$ dV/dt. At the negative end of the sweep (Fig. 3a) a current profile arises for underpotential H deposition and desorption, as at Pt in H_2O, but here the proton source is the carboxyl group of CF_3COOH. The results shown in Figs. 3a,b,c were obtained in TFA containing 0.5 M CF_3 COOK as electrolyte.

In this solution, added traces (0.19 and 0.42 mol %) of water give measurable currents for surface oxide formation and reduction. The peak on the cathodic sweep increases (a) with water content (Figs 3b, 3c) and (b) with potential holding at the positive end of the anodic sweep due to increased surface oxidation by reaction from water (cf. 61).

Attempts to detect any underpotential deposition of Cl· before the reversible potential of Cl^-/Cl_2 is attained in anodic/cathodic potentiodynamic sweeps in TFA/RbCl solution gave negative results. This means that $\theta_{Cl\cdot} <$ ca. 0.05~0.1 at the reversible Cl^-/Cl_2 potential in TFA but the observed kinetics (see later Figures) require that $\theta_{Cl\cdot}$ becomes rapidly larger as $\eta > 0$ and Cl_2 is evolved. In TFA, a small amount of Pt dissolution occurs upon cycling which could interfere with evaluation of Cl· coverage, but the extent is quite small.

In solutions of Cl^- ion (as RbCl) in TFA, the H underpotential region is displaced to less positive potentials, so that it is not resolved from the H_2 evolution current; also virtually no surface oxide film is developed at the Pt electrode until the water content in TFA/H_2O mixtures exceeds ca. 60% (Fig 4). These results illustrate the strong competitive role of Cl^- ion adsorption in relation to surface oxidation and H deposition processes (well known in aq. solutions[162]) in comparison with the situation with TFA$^-$ as the electrolyte anion (Figs 3a,b,c).

In the presence of an appreciable concentration of water (> ca. 60%), the initial Cl_2 evolution currents show a small inflection with increasing potential in the cyclic-voltammetry curves; similar behaviour is seen on the cathodic sweep i-V profiles (Fig. 4). The fact that this type of behaviour is not observed on the steady-state i vs. V profiles (Fig. 5) suggests that it is associated with a transitory state of the oxide film at the Pt electrode before growth and rearrangement processes (cf. refs. 61,69) have become established. The significance of this initial inhibition effect will be treated in more detail in the following Chapter of this thesis.

Fig. 4 - see following page

Fig. 4 (a) Series of potentiodynamic i-V profiles for a Pt electrode in TFA/H_2O mixtures with 0.5 M Cl^- (as RbCl or KCl) showing development of oxide reduction peak with increasing H_2O content. Sweep rate 5×10^{-2} V s^{-1}. T = 298 K. Electrode rotation rate 1600 r.p.m. (b) Curves below show charges for surface oxide reduction after holding for 1 min and longer times.

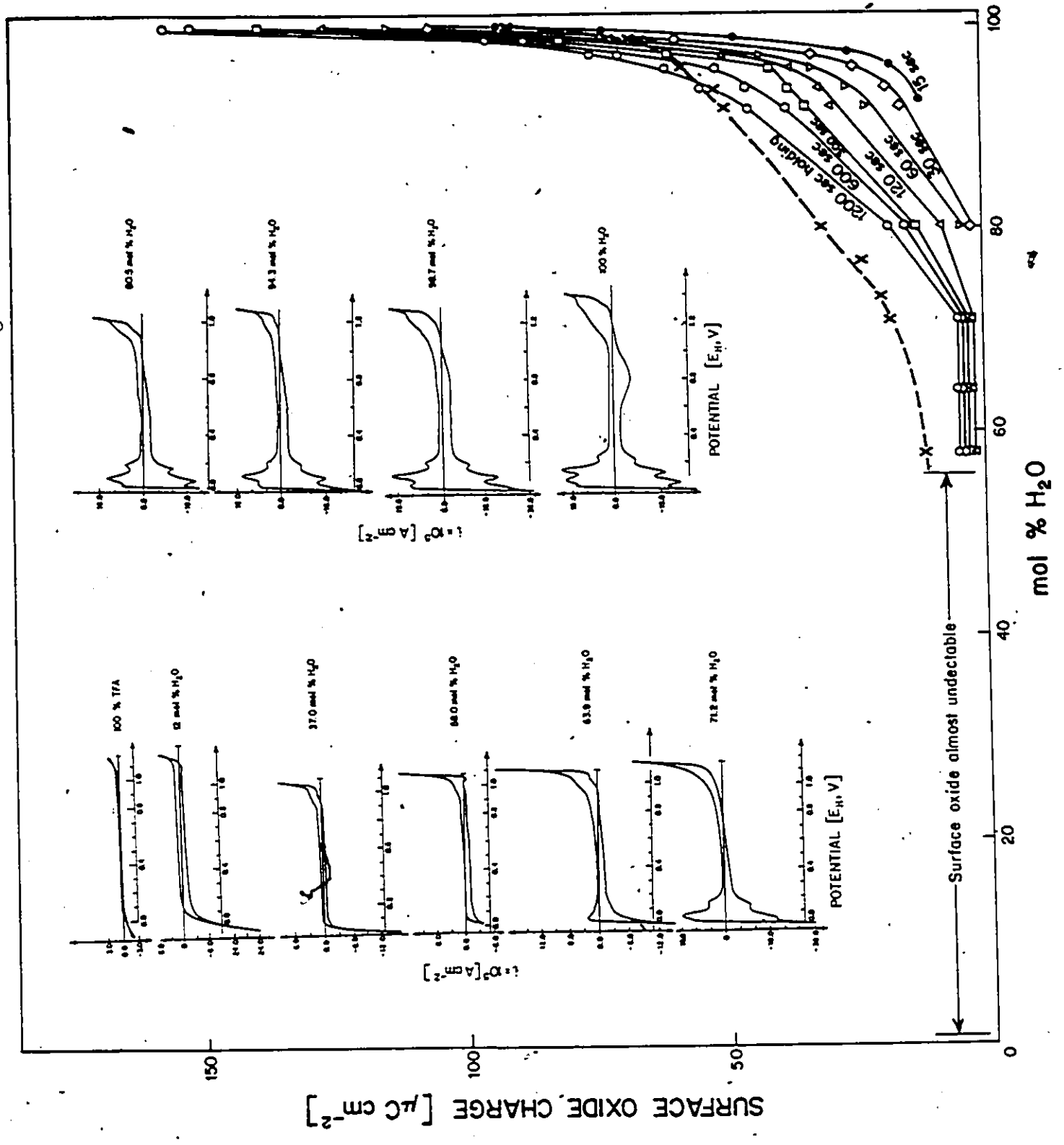
SURFACE OXIDE CHARGE [μC cm⁻²]
mol % H2O
Surface oxide almost undetectable
15 sec
30 sec
60 sec
120 sec
600 sec
1200 sec
600 sec Holding
POTENTIAL [EH, V]
i = 10⁵ [A cm⁻²]
100 % TFA
12 mol % H2O
37.0 mol % H2O
66.0 mol % H2O
83.9 mol % H2O
71.2 mol % H2O
80.3 mol % H2O
94.3 mol % H2O
96.7 mol % H2O
100 % H2O

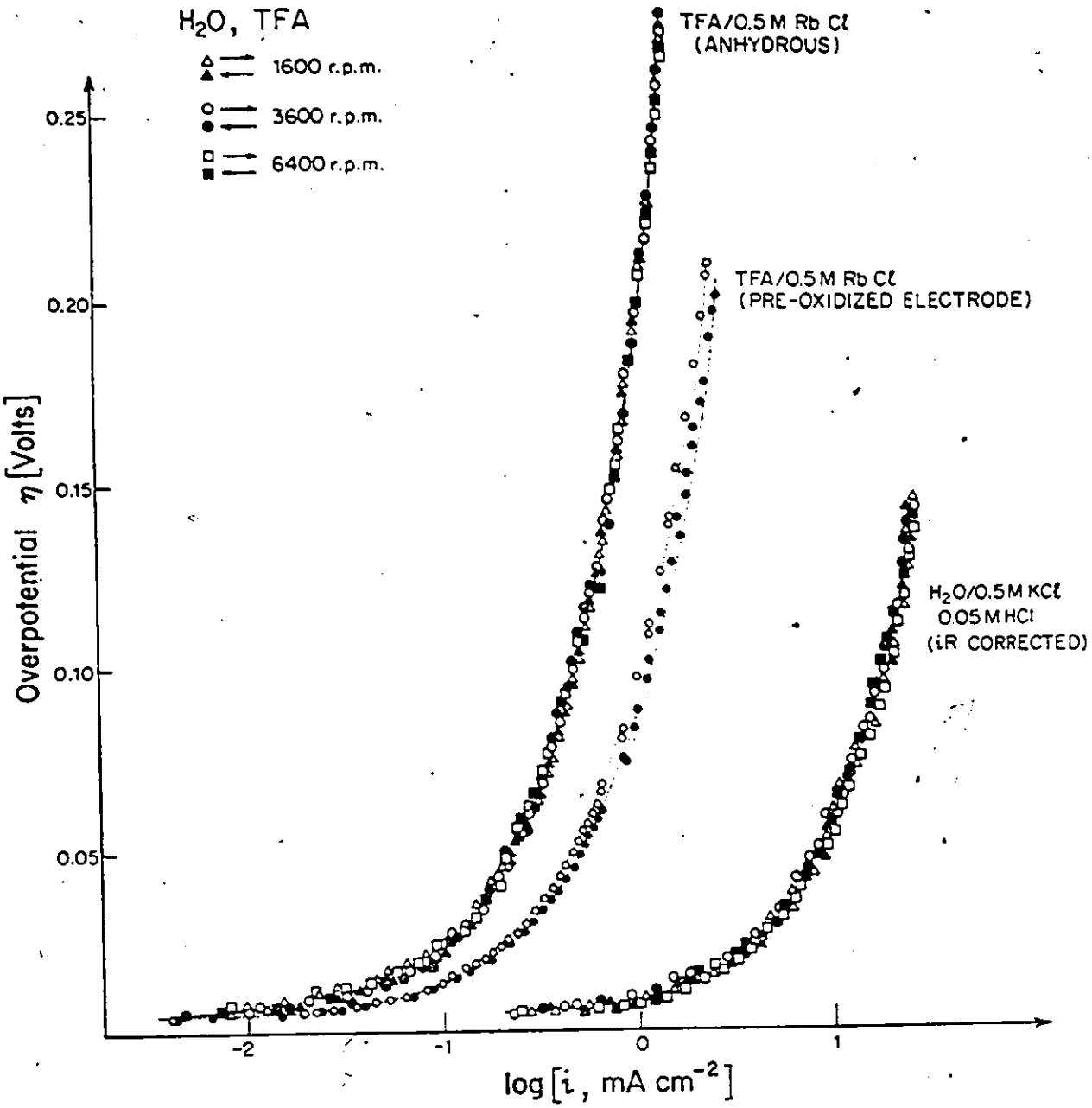

Fig. 5 Log current-density vs. overpotential curves for anodic Cl_2 evolution from 0.5 M RbCl solution in TFA and from 0.5 M KCl + 0.05 M HCl in water (T = 298 K). Data are shown for various rotation speeds at a rotating Pt-disc electrode. Two curves are also shown for Cl_2 evolution from 0.5 M RbCl in TFA at the same Pt electrode, but pre-oxidized in 0.5 M aq. H_2SO_4, bearing a surface oxide charge of 520 $\mu C\ cm^{-2}$ and 340 $\mu C\ cm^{-2}$.

(ii) Kinetic Behaviour in Anhydrous TFA Solutions of RbCl: In Cl^- (as RbCl) solution in TFA, currents (i) for anodic Cl_2 formation become significant at ca. 1.1 V E_H and the current- (over)potential (η) behaviour can be followed accurately by point-by-point measurements up to quite high current densities. In the plot of η vs. log i, a " parabolic " curve results (Fig. 5) with an obvious approach to a limiting value of log i at the higher η values.

Since the significance of i_{lim} is important with regard to $Cl^\cdot$ recombination control in the kinetics, two types of experiments were performed to identify it as a kinetically-limited current:

(a) Ohmic polarization (" iR ") was checked over a wide current range by the galvanostatic interruption technique; iR drops were, however, negligible in the anhydrous TFA experiments.

(b) Current-potential relations were established at the rotating Pt disc electrode at various rotation speeds, ω , and were found to be independent of ω, using a range of ω from 0 to 6400 r.p.m. (Fig. 5). Thus, the log i vs. overpotential curves and, in particular, the limiting currents observed are kinetically controlled.

(iii) Kinetic Behaviour in Aqueous and Mixed TFA/H_2O Chloride Solutions: In aq. Cl^- (0.5M KCl + 0.05M HCl) solution, similar " parabolic " log [current] -potential curves are found with a trend to well-defined limiting values (Fig. 5 , curves at r.h.s.). The current profile is displaced at all potentials to values some 45 times larger than in TFA, including i_{lim} at high η . Because of the higher current-densities attained in the aqueous solutions, iR corrections on the raw data are more important.* (They were up to 60 mV at the highest currents

*Resistance effects due to the Pt surface oxide film which is present in aq. solutions at Cl_2 anodes are negligible (cf. ref. 8)

and linear in i). The curves in Fig. 5 are drawn from the iR-corrected data. Also, because of the larger currents, mass-transfer effects could have become significant, but they are evidently still small, as seen in Fig. 5 where results are plotted for several ω values at the rotating Pt disc electrode. It can be concluded that the i_{lim} value attained in aq. solutions is still kinetically-controlled as it is in the TFA solution.

The important conclusion from these experiments is therefore that the i vs. η profile for Cl_2 evolution, over the same range of over-potentials, arises at much larger currents (by factor of 15~45) in aq. Cl^- than in TFA solutions of Cl^- ion . In both types of solutions, kinetically-controlled limiting currents are observed. In the aq. medium, the Pt electrode surface is partially oxidized (see below and Fig. 4).

Similar kinetic behaviour was found for all compositions studied in the series of TFA/H_2O solvent mixtures, and also for the Pt electrode pre-oxidized in aq. H_2SO_4 and then studied in 100% TFA/RbCl solution (see central curves in Fig. 5). The limiting currents for the pre-oxidized electrode lie between those for the 100% TFA solution and 100% H_2O solution and probably correspond to part of a volcano relation with respect to extents of oxide coverage and Cl^- ion adsorption.

In order to compare the kinetics of Cl_2 evolution in TFA and H_2O quantitatively, it is necessary to place the data for the current-potential relations on a common overpotential (η) scale. This was done by evaluating the reversible potentials for the Cl_2/Cl^- process vs. Ag,AgCl, H_2/H^+ or $\alpha + \beta$ $PdH/H^{(195)}$ electrode in the same solution, as will be described below.

(iv) Cl_2/Cl^- Reversible Potentials in TFA and H_2O: Comparison of the kinetics of Cl_2 evolution from TFA, water and their binary mixtures requires that all the current-potential relations be compared on a common overpotential scale. This was achieved by referring all measured potentials to the observable reversible potential for Cl_2/Cl^- in the same solution. For TFA, water and the solvent mixtures, the reversible potentials were easily identified in all experiments by the asymptotic approach of the i vs. V profiles to the log [current-density] axis.

While the above procedure is sufficient to provide a basis for comparison of the kinetic behaviour in the various solvents or solvent mixtures, it will be of interest to quote several results for the actual measurements of reversible potentials.

The cyclic-voltammetry experiments show that Cl_2 evolution currents become significant at Pt in Cl^--containing TFA solutions at less positive potentials (vs. the Ag, AgCl electrode in the same solution) than in aq. Cl^-. Cl_2-reversible potentials were measured at Pt in TFA (0.5M RbCl) and in water (0.5M KCl + 0.05M HCl) vs. the Ag/AgCl electrode and also vs. the H_2 (1 atm)/H^+ electrode in the same respective solutions. The following values for the potentials vs. Ag/AgCl were obtained at 298 K: 1.020 V (Cl_2 in the TFA solution); 1.130 V (Cl_2 in the aq. solution). Against the H_2/H^+ electrode, the values were 0.960 V and 1.454 V, respectively.

Cl_2 is therefore reversibly evolved from solvated Cl^- in TFA at a potential 0.494 V less positive than from Cl^- in water, referred to the H_2/H^+ electrode in the respective solutions. These results enable the experimental current-potential relations in the two solvents to be placed on a common overpotential scale as in Fig. 5 . For the solvent mixtures, the reversible potentials were easily identified in all experiments by the

asymptotic approach of the i-V profiles to the log [current-density] axis as mentioned earlier.

4. DISCUSSION

(i) Mechanisms: An obvious mechanism (cf. refs 168,174,175,193,196) that has frequently been discussed for Cl_2 evolution is

$$Cl^- + S \underset{k_{-1}}{\overset{k_1}{\rightleftharpoons}} S\,Cl^{\cdot} + e^- \qquad \text{I}$$

$$2S\,Cl^{\cdot} \xrightarrow{k_2} Cl_2 \qquad \text{II}$$

where S is the surface of the electrode on which a $Cl^{\cdot}$ radical is discharged into a presumably chemisorbed state. In anhydrous TFA, S is the oxide-free metal surface, probably with some coverage by adsorbed anions and of course solvent. In aq. medium, S is an oxidized or partially oxidized (Fig. 4) Pt electrode surface. The degree of oxidation of the surface at the reversible potential for Cl_2 evolution in H_2O is ca. 2e per surface Pt atom in the absence of adsorbed Cl^-, i.e. nominally " PtO "; but due to competitive Cl^- adsorption, Cl_2 evolution occurs on an only partially oxide-covered surface (see below and Fig. 4).

The form of the kinetic behaviour in Fig. 5 is similar to that expected (cf. the case of H_2 evolution[196]) for a mechanism in which the rate is limited by the recombination step II proceeding at a surface on which $Cl^{\cdot}$ atom coverage, $\theta_{Cl^{\cdot}}$, is between ca. 0.2 and 1 since a region of linear Tafel behaviour is expected only for $\theta_{Cl^{\cdot}} <$ ca. 0.15. Yokoyama and Enyo[168,193] considered the scheme I, II for cathodic and anodic reactions of Cl_2 from aq. Cl^- solutions but concluded from reaction order and stoichiometric number data that the current-potential relation for appreciable anodic polarization was determined by the rate constant of step

I with step II in quasi-equilibrium.

Krishtalik and co-workers[174], using ruthenium oxide electrodes, concluded that the recombination step II was rate-controlling for the anodic direction of the Cl_2 electrode reaction. However, in later work[175], a chloronium ion pathway was also proposed but would not lead to the limiting current or Tafel slope features of the experimental behaviour at Pt.

(ii) Kinetic Analysis for the Recombination Mechanism I, II:

Since the form of the i-V profiles of Fig. 5 appears characteristic of a kinetically limited rate (cf. 196) yet, in the work of Yokoyama and Enyo[168,193] and of Krishtalik[174,175], $Cl^{\cdot}$ recombination was not proposed as the rate-limiting step, it is necessary to examine the form of the i-V profiles quantitatively in a way in which such a mechanism can be more exactly tested. In order that such a treatment could be reliably pursued, the i-η curves for TFA and H_2O solutions, and their mixtures, have been defined, by many experimental points (Fig. 5).

The following method enables the kinetic behaviour associated with pathways I, II to be represented over the whole range of $\theta_{Cl^{\cdot}}$ and corresponding currents up to i_{lim}, i.e. without restriction to special conditions (cf. 197,198) that may lead limitingly to a Tafel slope of RT/2F, RT/F or$^{\infty}$ (limiting current), or some intermediate values.

The current-density for II is written as

$$i_2 = 2Fk_2\theta_{Cl^{\cdot}}^2 \qquad (6)$$

in the absence of interaction or heterogeneity effects (see refs. 197, 198 and below). If II is rate-determining, $\theta_{Cl^{\cdot}}$ may be represented as $f(\eta)$ in the usual way (employing the quasi-equilibrium hypothesis) approxi-

mately by the electrochemical (Langmuir) adsorption isotherm as a first approach to the discussion of current-potential behaviour:

$$\theta_{Cl\cdot} = \frac{\bar{K}_1 \, C_{Cl^-} \exp [\eta F/RT]}{1 + \bar{K}_1 \, C_{Cl^-} \exp[\eta \, F/RT \,]} \qquad (7)$$

where $\bar{K}_1 = k_1/k_{-1}$, is the quasi-equilibrium constant* for step I and C_{Cl^-} is the chloride ion concentration. Then the i_2 vs. η relation over any range of anodic overpotentials is

$$i_2 = 2Fk_2 \left[\frac{\bar{K}_1 \, C_{Cl^-} \exp[\eta \, F/RT]}{1 + \bar{K}_1 \, C_{Cl^-} \exp[\, \eta \, F/RT]} \right]^2 \qquad (8)$$

It is convenient to rearrange eqn. (8) to the form

$$\frac{\exp[\eta \, F/RT]}{i_2^{\frac{1}{2}}} = \frac{1}{(2Fk_2)^{\frac{1}{2}} \, \bar{K}_1 \, C_{Cl^-}} + \frac{\exp[\eta \, F/RT \,]}{(2Fk_2)^{\frac{1}{2}}} \qquad (9)$$

Hence, a plot of $\exp[\eta \, F/RT \,] / i_2^{\frac{1}{2}}$ vs. $\exp[\eta \, F/RT \,]$ should give a straight line of slope $(2Fk_2)^{-\frac{1}{2}}$ and an intercept $(2Fk_2)^{-\frac{1}{2}}/\bar{K}_1 \, C_{Cl^-}$.

Application of eqn. (9) to the experimental results of Fig. 5 and to similar curves obtained for TFA/H_2O mixtures gives the plots shown in Figs. 6a and 6b. Good linearity evidently obtains over almost the whole range of η (except, for understandable reasons, as $\eta \to 0$; see below) indicating applicability of the recombination-controlled mechanism.

*$\bar{K}_1$ is really an electrochemical equilibrium constant containing an exp term in potential - see p. 103 - 106 .

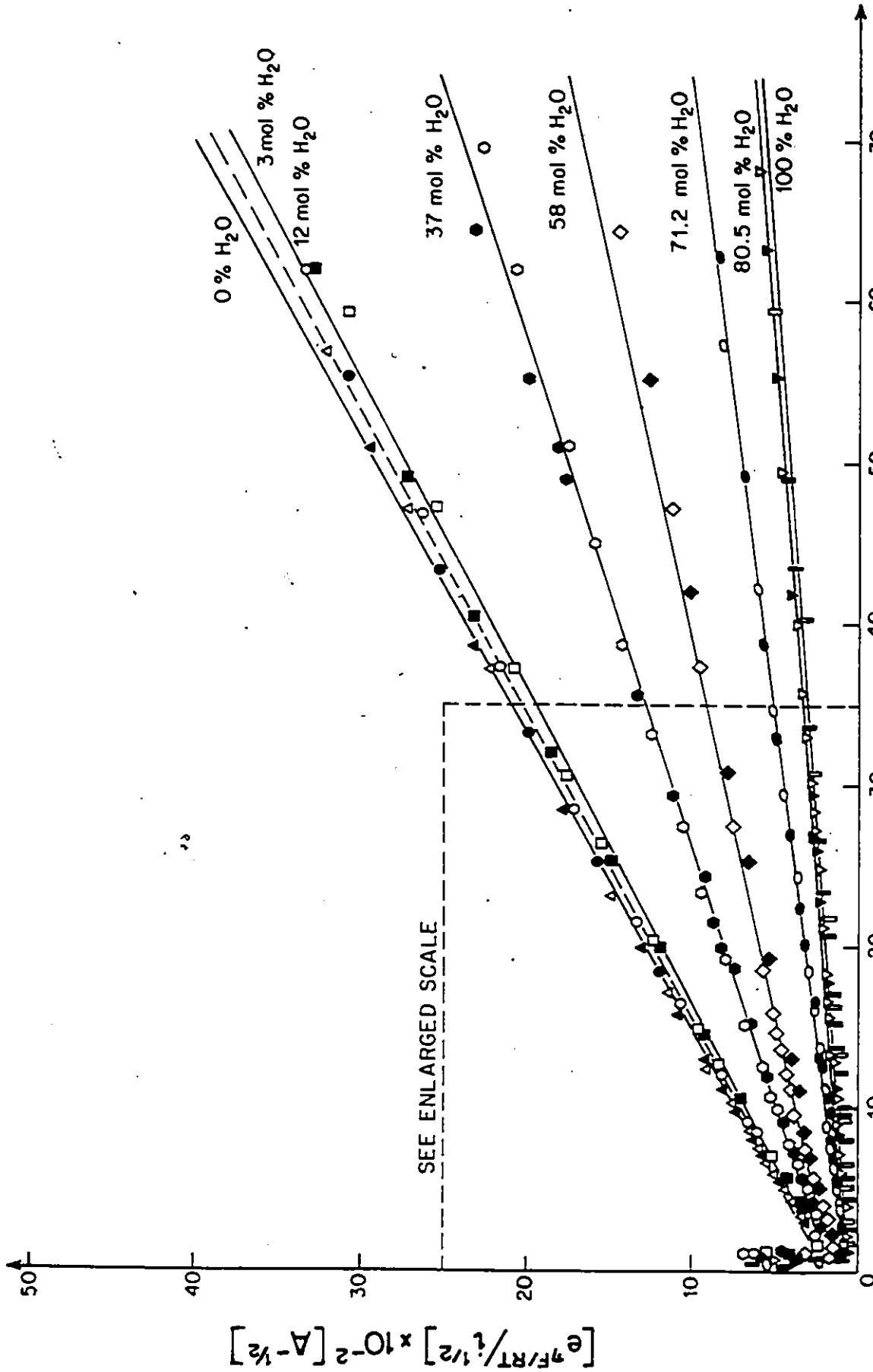

Fig. 6 Test recombination mechanism for Cl^- according to eqn. (9) for various 0.5M Cl^- solutions in TFA/H_2O mixtures from 0% to 100% H_2O, T = 298 K. a) full range of η.

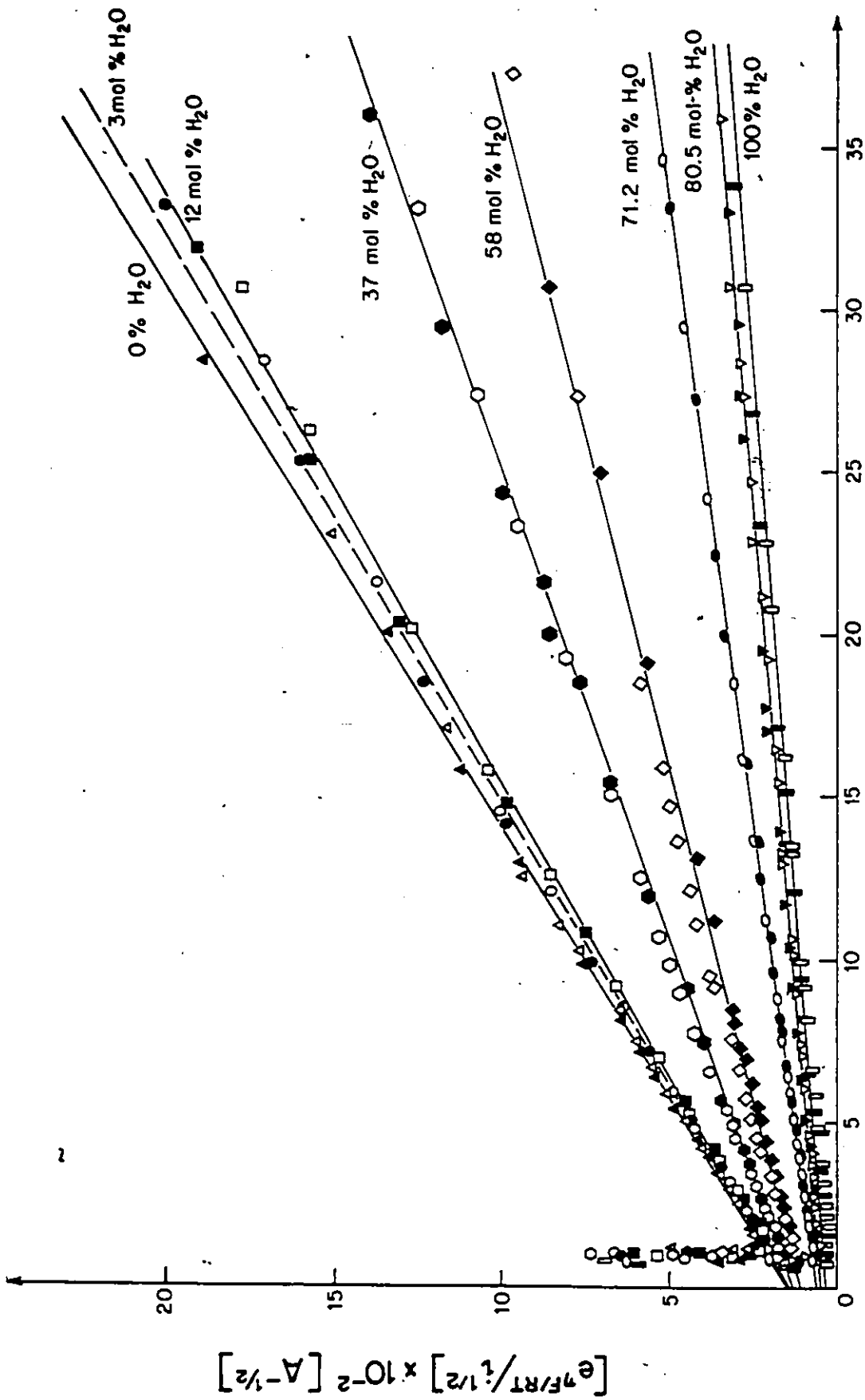

Fig. 6 Test of recombination mechanism for $Cl^{\cdot}$ according to eqn. (9) for various 0.5M Cl^- solutions in TFA/H_2O mixtures from 0% H_2O to 100% H_2O, T = 298 K. b) Enlarged scale.

It is of interest that the results of Yokoyama and Enyo[168,193], obtained from an enlarged photo of their published η vs. log i curves, plot out in a similar way (based on eqn. 9) and thus indicate recombination-controlled kinetics.

From an estimate of i_{lim} based on the true electrode area determined from the H monolayer charge (210 μC cm^{-2}), the rate constant k_2 for $\theta_{Cl\cdot} \to 1$ can be found in addition to its evaluation from eqns. (9) or (10) (see below) for $\theta_{Cl\cdot} < 1$. With k_2 evaluated for a known Cl^- concentration, the intercept of the plot based on eqn. (9) will give $\bar{K}_1$ for quasi-equilibrium in step I. Thus, the principal features of the reaction scheme are both qualitatively and quantitatively evaluated. Values of k_2 and $\bar{K}_1$ derived in this way are tabulated in Section (vi), p. 100.

An alternative way of plotting the results, which provides a more sensitive basis for analysing the kinetic behaviour at high $\theta_{Cl\cdot}$, follows by rearranging eqn. (8). Thus,

$$i_2^{-\frac{1}{2}} = (2Fk_2)^{-\frac{1}{2}} + (2Fk_2)^{-\frac{1}{2}}(\bar{K}_1 C_{Cl^-})^{-1} \exp[-\eta F/RT] \qquad (10)$$

which enables both k_2 and $\bar{K}_1$ to be evaluated from the slope and intercept of a plot of $i_2^{-\frac{1}{2}}$ vs. $\exp[-\eta F/RT]$. Such plots are shown in Figs. 7a and 7b. Were the log [current-density] vs. potential relations simple Tafel lines having constant slopes, the results would not plot out according to eqns. (9) or (10) with intercepts related to $\bar{K}_1$ and k_2.

There is some significant curvature* in the lines of Figs 6a and 6b at the higher currents where $\theta_{Cl\cdot} \to 1$. Under these conditions, it is likely that lateral interactions between adsorbed Cl· become significant and give rise to this deviation from the behaviour expected according to

*The curvature at the low current ends of the lines in Figs. 7a and 7b is due to the participation of the back reaction, as in Figs. 6a and 6b at the lower ends of the lines. See Section (iii), p. 95.

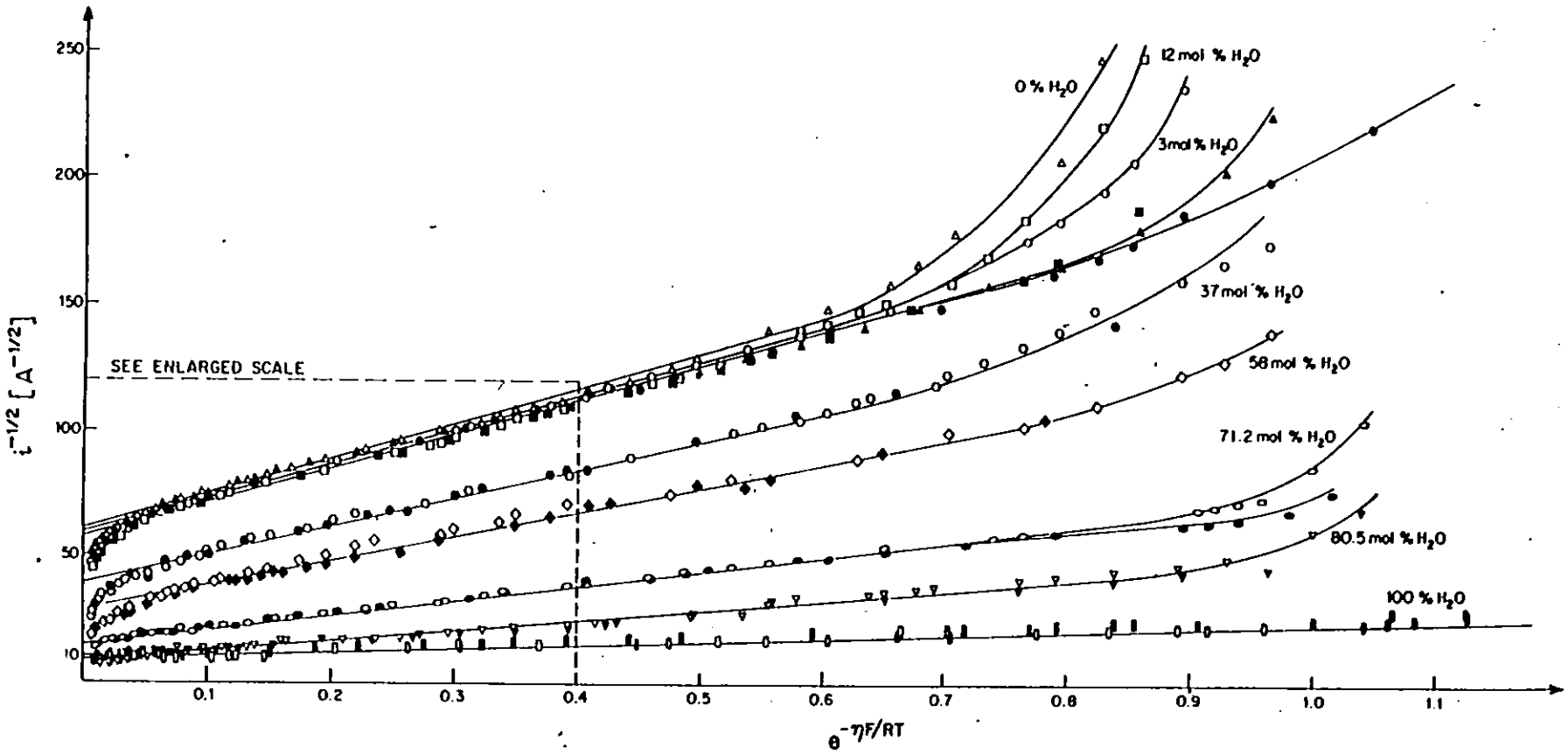

Fig. 7 Test of recombination mechanism for Cl˙ according to eqn. (10) for various 0.5M Cl^- solutions in TFA/H_2O mixtures from 0% H_2O to 100% H_2O, T = 298 K. (These plots are best for analysis of the kinetics at high coverages by Cl˙).

a) Full range of η .

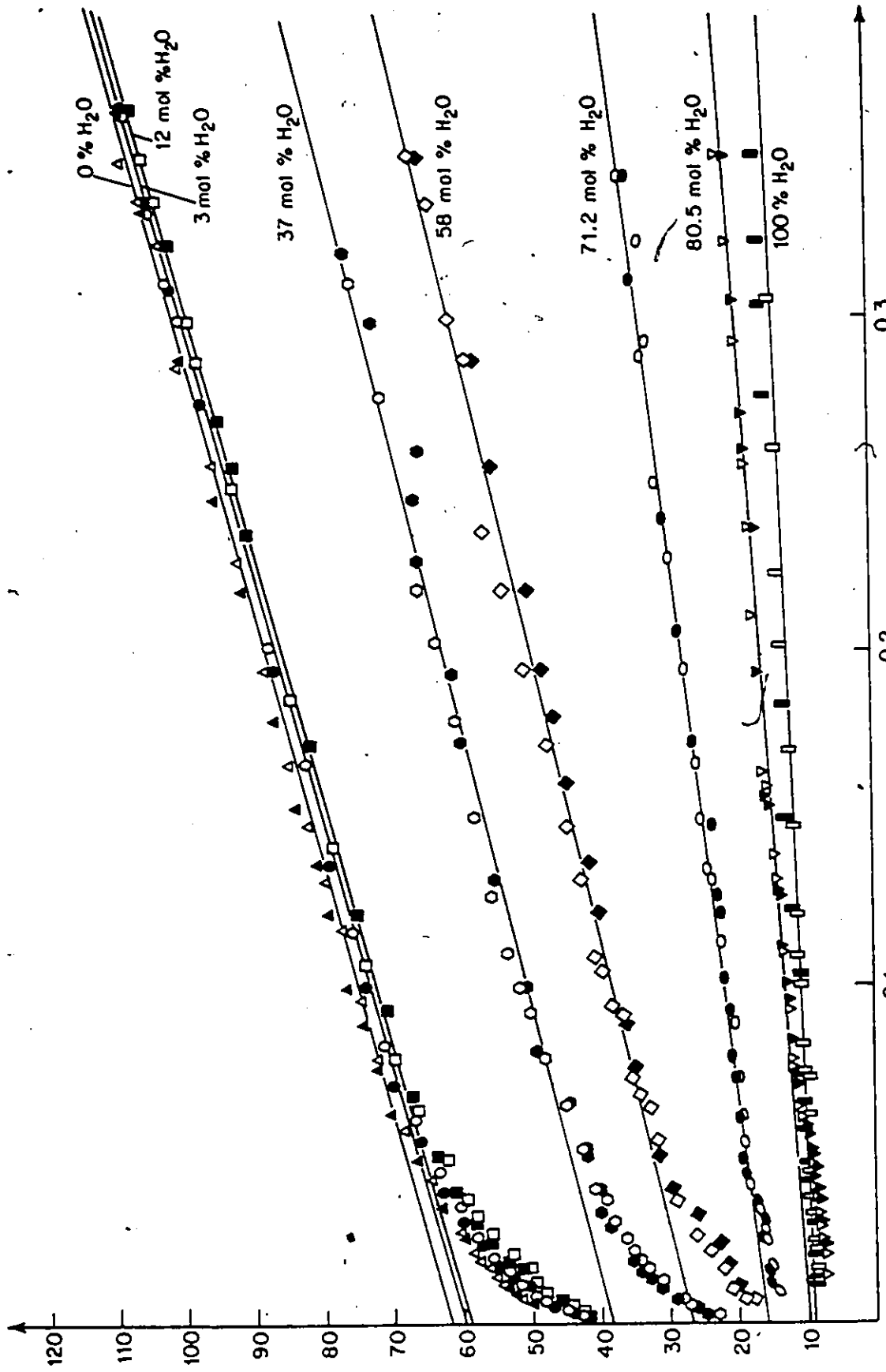

Fig. 7 Test of recombination mechanism for $Cl^{\cdot}$ according to eqn. (10) for various 0.5 M Cl^{-} solutions in TFA/H_2O mixtures from 0% H_2O to 100% H_2O, T = 298 K. (These plots are best for analysis of the kinetics at high coverages by $Cl^{\cdot}$) b) Enlarged scale.

eqn. (10). The recombination rate equation should then be written (cf. 198, 199) in the form:

$$i_2 = 2Fk_2\theta_{Cl\cdot}^2 \cdot \exp[2g\theta_{Cl\cdot}] \qquad (11)$$

for " non-activated " adsorption(198), where g is a lateral interaction parameter(199) *. The corresponding isotherm for adsorption of Cl· is of the form:

$$\frac{\theta_{Cl\cdot}}{1 - \theta_{Cl\cdot}} = \bar{K}_1 \exp[-g\theta_{Cl\cdot}] \cdot c_{Cl^-} \exp[\eta F/RT] \qquad (12)$$

Proceeding as in eqns. (8) and (9) by substituting for $\theta_{Cl\cdot}$ from eqn. (12) into eqn. (11) and rearranging, gives

$$i_2^{-\frac{1}{2}} = (2Fk_2)^{-\frac{1}{2}} \exp[-g\theta_{Cl\cdot}] + (2Fk_2)^{-\frac{1}{2}}(\bar{K}_1 c_{Cl^-})^{-1} \exp[-\eta F/RT] \qquad (13)$$

Thus, for $g \neq 0$, $i^{-\frac{1}{2}}$ is no longer proportional simply to $\exp[-\eta F/RT]$ as in eqn.(10) since $\theta_{Cl\cdot}$ in eqn.(13) is a function of potential by eqn.(12) involving g. Then the variation of $\theta_{Cl\cdot}$ with η is changed in comparison with the Langmuir case, depending on the magnitude and sign of g, as shown in Fig. 8 . This Figure shows the variation of θ with relative potential in RT/F units calculated for an interaction term in $\exp -g\theta_{Cl\cdot}$ (solid lines) and in $\exp - g\theta_{Cl\cdot}^{3/2}$ (dashed lines), the latter case for surface-Cl dipole-dipole interaction.

Numerical evaluation of the <u>form</u> of eqn. (13) for various g values may be made as shown in Fig. 9 for various values of g (= 0, 2, 4, and -2 units of RT) so that the <u>form</u> of the variation of $i_2^{\frac{1}{2}}$ with $\theta_{Cl\cdot}$ and hence η may be derived. Arbitrary values of $k_2 = 1$, $K_1 = 1$ and $C_{Cl^-} = 1$ are

* g is defined as the ratio of the change of adsorption energy, $\delta\Delta G_{ads}$, to RT, assumed to be linear with coverage θ, as θ increases from 0 to 1. $\delta\Delta G_{ads}$ arises, in this model, from lateral interactions.

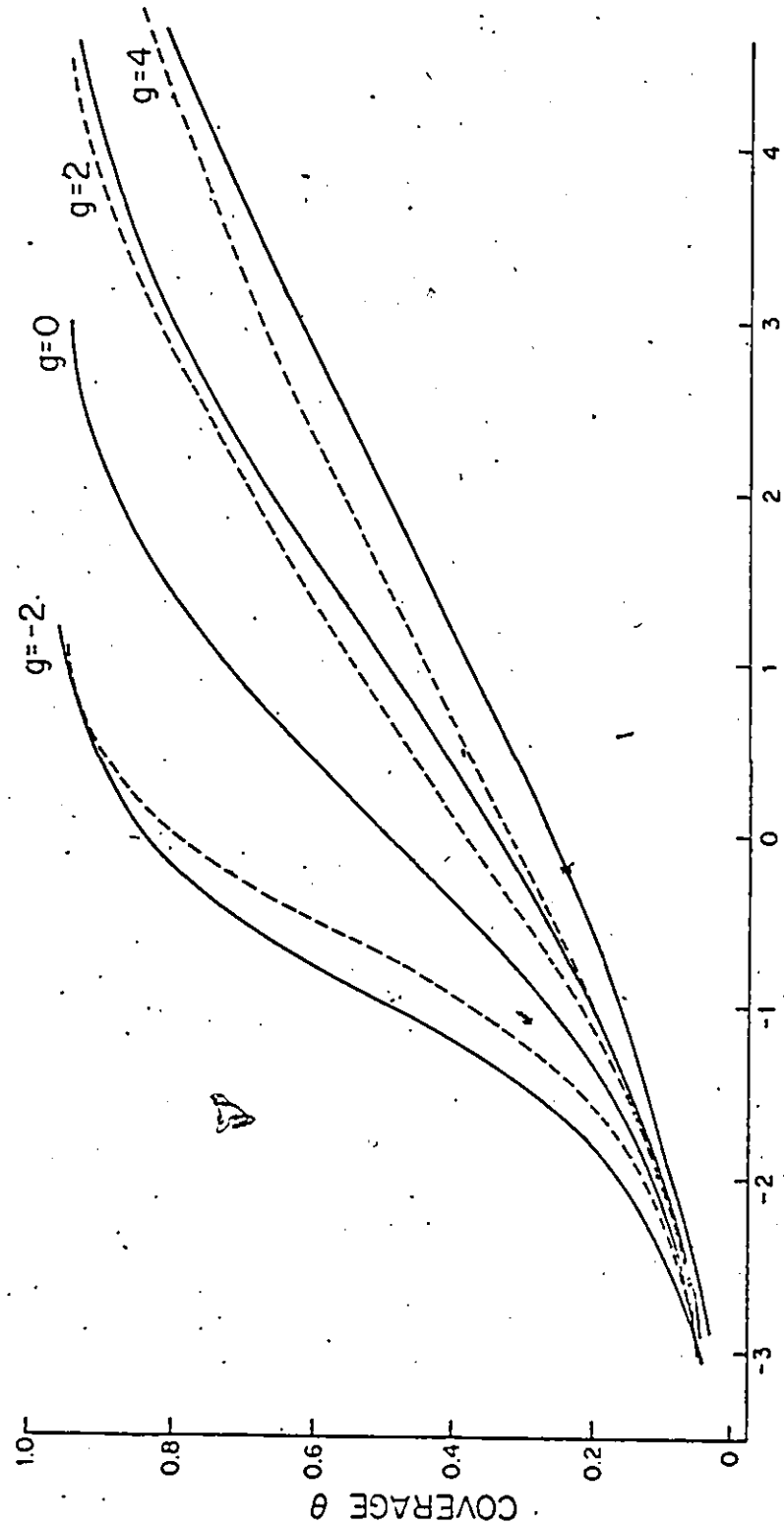

Fig. 8 Computed electrochemical adsorption isotherms according to eqn. (12) for various g values. Solid line for $\exp -g\theta_{Cl}$, and dashed line for $\exp -g\theta_{Cl}^{3/2}$. interaction term. Langmuir case for g = 0.

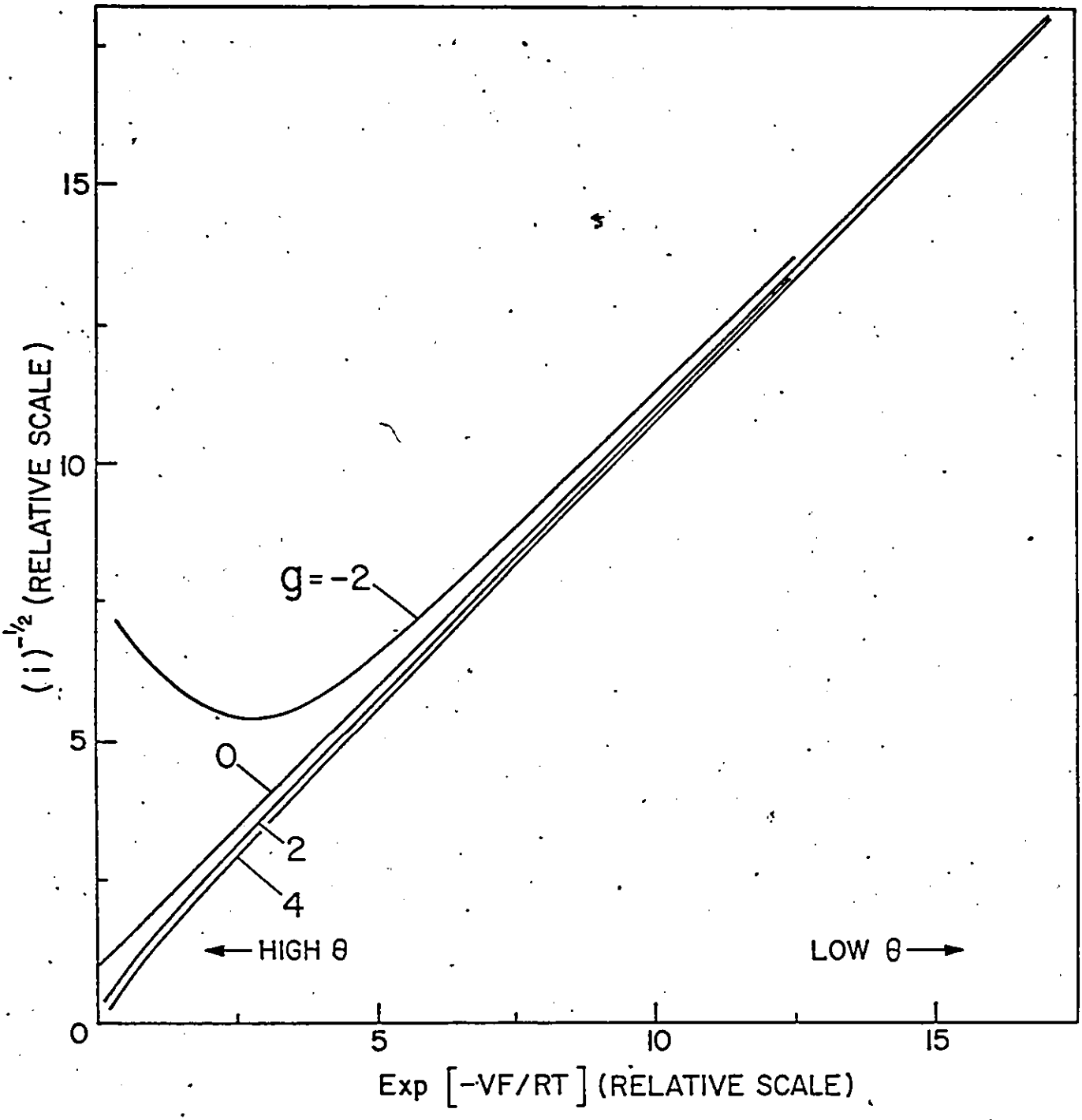

Fig. 9 Numerical evaluation of the forms of eqn. (13) for values of g = 0, 2, 4 and -2 using eqn. (12) for the quasi-equilibrium chemisorption of Cl• and eqn. (11) for the recombination-controlled current-density. Parameters as mentioned in text.

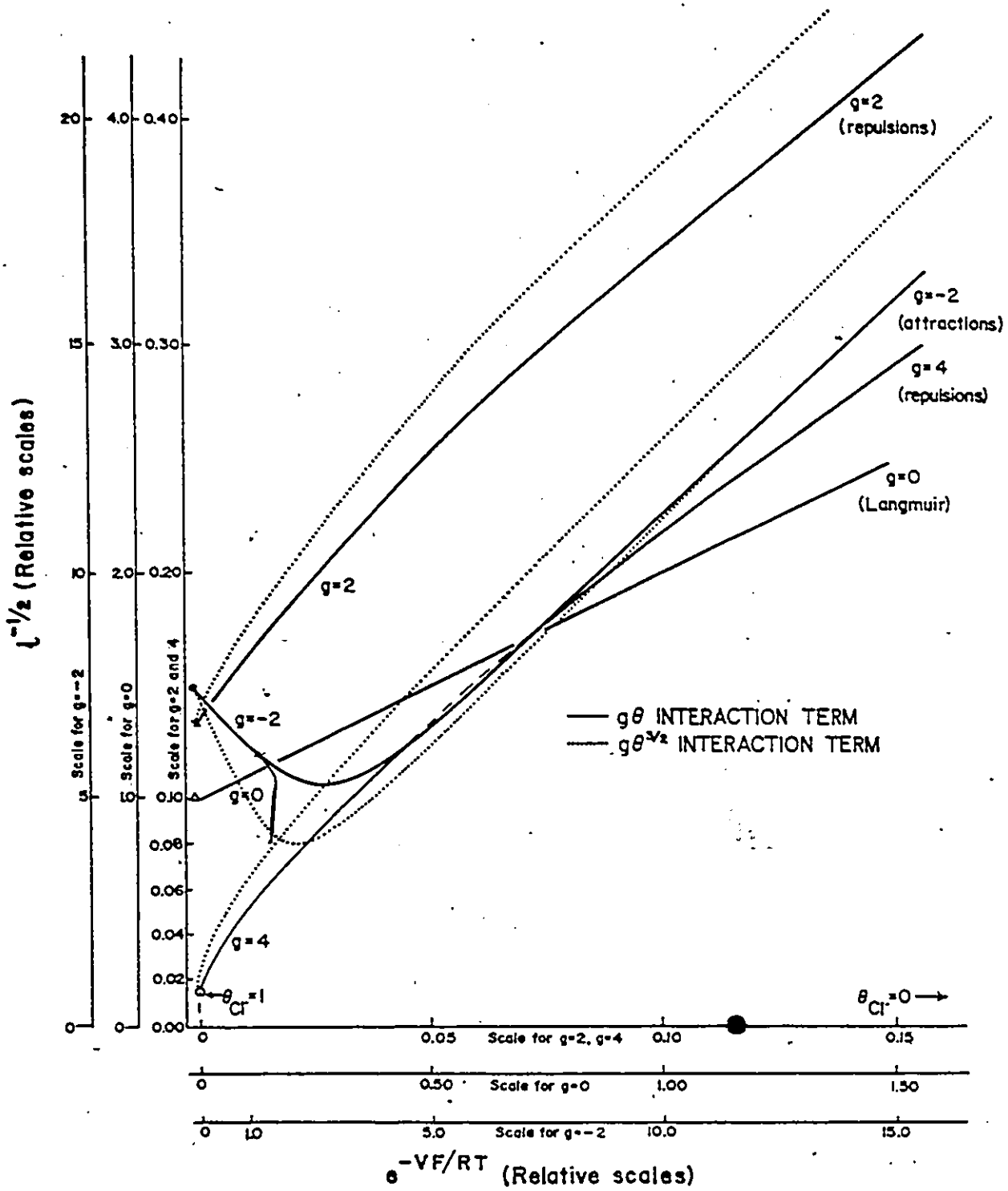

Fig. 9 Numerical evaluation of the forms of eqn. (13) for values of $g = 0$, 2, 4, and -2 using eqn. (12) for the quasi-equilibrium chemisorption of Cl· and eqn. (11) for the recombination-controlled current-density. Parameters as mentioned in the text. Different scales are required since current-density ranges vary according to values of exp $2g\theta$ for

taken for convenience, so that the scales of the plots are relative ones; the potential scale in exp [- ηF/RT] is an overpotential scale relative to a reversible potential, E_r, taken as zero, corresponding to $\bar{K}_1 = 1 \cdot \exp[E_r F/RT] = 1$.

It is seen that the calculated plots for values of $g > 0$ have similar directions of curvature to those of the experimental data in Figs. 7a and 7b, as $\theta_{Cl\cdot} \rightarrow 1$ (i.e., as $i^{-\frac{1}{2}} \rightarrow 0$). The Langmuir case ($g = 0$) gives, of course, a linear plot as for eqn. (10). The steepness of the curvature as $\theta_{Cl\cdot} \rightarrow 1$ arising from an isotherm such as (12) is, however, smaller than that in Figs. 7a and 7b as $i^{-\frac{1}{2}} \rightarrow 0$. This suggests that eqn. (12) should probably be written with an $\exp[-g\theta_{Cl\cdot}^{3/2}]$ term instead of the linear argument in $\theta_{Cl\cdot}$; such a function of $\theta_{Cl\cdot}$ would arise[200] from surface dipole repulsion in the nearest neighbour approximation.

It is to be noted that the i_{lim} will depend on g and differ from that for Langmuir conditions [eqns. (6) and (7)] by a factor of exp[2g] , whatever is the sign and magnitude of g. These limiting values (as $i_{lim}^{-\frac{1}{2}}$) are shown, in a relative way, on the l.h. axis of Fig. 9a. This factor is of significance in the dependence of recombination-controlled limiting currents on Cl^- concentration through Cl^- adsorption effects to be considered later.

Also, when $g \neq 0$, the apparent rate constant k_2' obtained from the limiting current with $i_{lim} = 2Fk_2\theta_{Cl\cdot}^2$, i.e. $k_2' = k_2 \exp 2g\theta$, will differ from the value obtained from analysis of the $i = f(\eta)$ data at lower potentials where $\theta_{Cl\cdot} \ll 1$ since the $\exp 2g\theta_{Cl\cdot}$ factor will then be smaller or negligible.

(iii) Role of the Back Reaction: Figs. 6a and 6b and all tests that were made of eqn. (9), show a bend-up of the line at low values of η. This can be accounted for simply by the increasing participation of the back-reaction as the condition $\eta = 0$ is approached. The kinetics, which are tested by eqn. (9), pertain to the rate of the forward (anodic) direction of the current. Near the reversible potential, however, this is not measured by the net recorded current-density, but rather by $i_2 + i_c$, since $i_2 = i_a - i_c$, where i_a and i_c are the anodic and cathodic partial currents, respectively. The i_c component can be readily calculated in terms of Cl' coverages and overpotentials as shown in the Appendix I. The true i_a component current is found to be

$$i_a = i_2 / [\, 1 - \exp(-2\eta F/RT)] \qquad (14)$$

and it is this current that has be tested as $f(\eta)$ near the reversible potential rather than the net measured i_2. Thus, $\exp \eta F/RT$ must be divided by $\left\{ i_2 / [\, 1 - \exp(-2\eta F/RT)] \right\}^{\frac{1}{2}}$ rather than by $i_2^{\frac{1}{2}}$. It is seen that when η is sufficiently large, $\exp(-2\eta F/RT) \to 0$ [eqn. (14)], so that $i_a \to i_2$. Thus, most of the curve can be treated in terms of the directly measured i_2 values.

The above correction lowers all the points near $\eta = 0$ in Figs. 6a and 6b so that a continuous, almost straight line results without the hook at the lower end. This, incidentally, shows that the mechanism which applies at high η, giving a limiting current, persists essentially down to the reversible potential without change. Similar corrections extend the linearity of plots based on eqn. (10) at low η (Figs. 7a and 7b).

(iv) Simulation of the Tafel Relation for a Recombination-controlled Process: In order to examine further the detailed form of a recombination-controlled current-potential curve, a calculation of the Tafel relation for this case was performed. The purpose was to simulate the current-potential relation over a wide range of coverages, $\theta <$ 0.1 up to $\theta \to 1$, for various values of g.

The current-density of the recombination controlled step II is given by eqn. (11) for any value of g. Since $\theta_{Cl\cdot}$ is the coverage of the surface with adsorbed Cl·, it can be expressed by eqn. (12). By evaluation of $\theta_{Cl\cdot}$ as f (η) and insertion in eqn. (11), ln i_2 as f (η) may be evaluated numerically.

The overall forms of the ln i vs. η relations for various g values, assuming eqn. (12), were simulated using the same values of k_2, $\bar{K}_1$ and $C_{Cl^-} = 1$ as those taken above for the simulations of the behaviour of eqn. (13). Curves for g = -2, 0, 2 and 4 are shown in Fig. 10 and illustrate the dependence of the approach to the limiting current on the interactions in the ad-layer of Cl· characterized by the g value. It is interesting that the log i vs. η relation for negative g values (g = -2 in Fig. 10) shows a maximum without any other inhibiting substance being codeposited (cf. 95,164) on the surface. When g > 0, the range of potentials over which i_2 approaches its limiting value is, of course, extended, since $\theta_{Cl\cdot}$ goes from 0 to 1 over a proportionately wider, g-dependent range of potentials[198]. A g value of ca. 2 is required to account for the form of the ascent of η with current-density, on the log scale, in Fig. 5 with increasing overpotential.

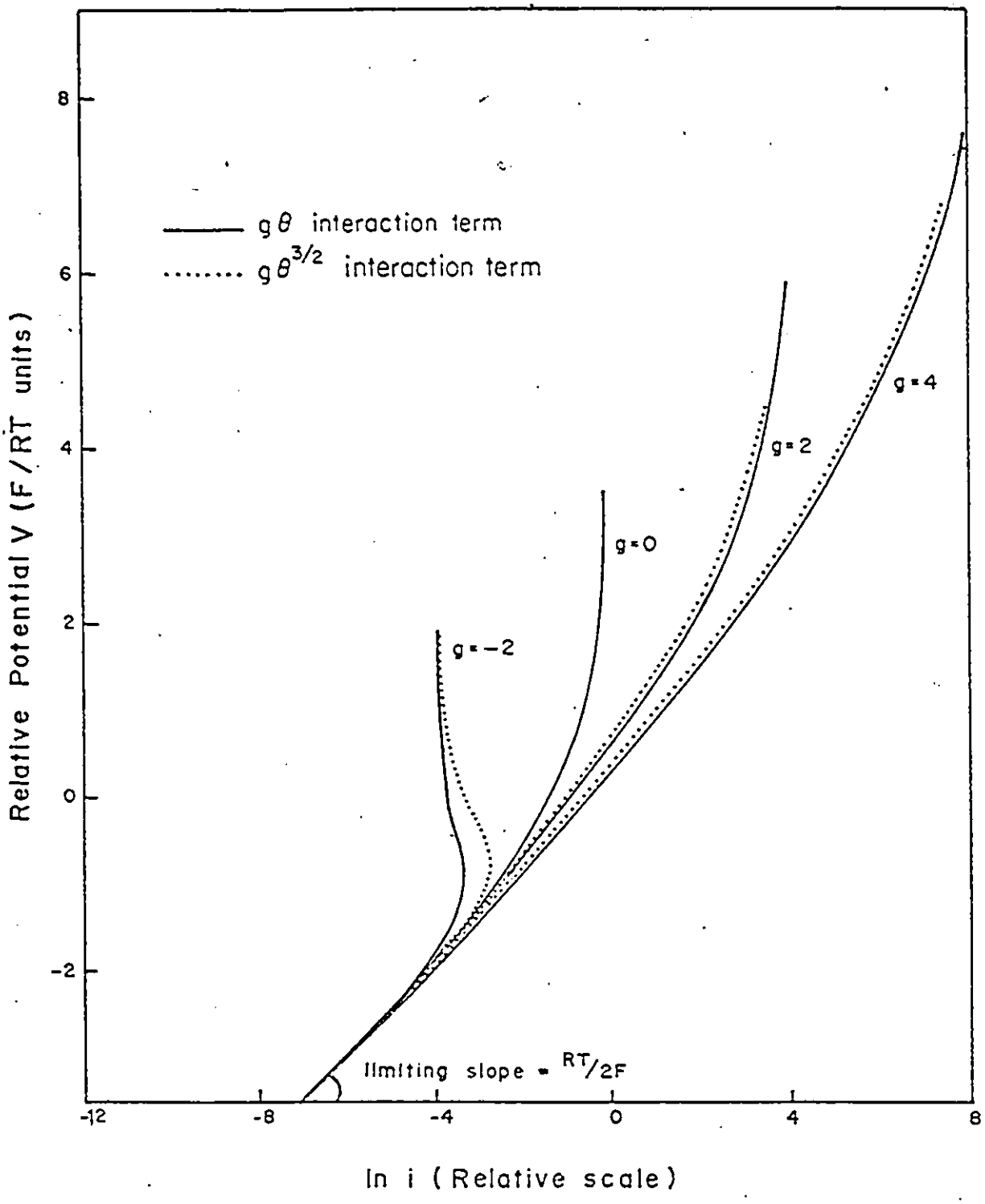

Fig. 10 Simulation of log i vs. V relations for the $Cl^{\cdot}$ recombination kinetics with various g values, using eqns. (11) and (12).

Linear ln i *vs.* η behaviour must arise in all cases at sufficiently low $\theta_{Cl\cdot}$, dependent on the g value. For sufficiently small or zero g values, a Tafel relation with slope near to RT/2F will be observed below $\theta_{Cl\cdot} \simeq 0.15$ or a corresponding overpotential. This is seen in the lower regions of the curves of Fig. 10 where each of them approaches a common line with the recombination slope RT/2F, independent of the g value.

Experimentally (Fig. 5), in the presence of Cl_2 at 1 atm., the log i *vs.* η relation does not show any linear region of slope 2.3 RT/2F. This means that $\theta_{Cl\cdot}$ is already >*ca.* 0.15 near the reversible potential where the back reaction is important in the presence of 1 atm. Cl_2 . When N_2 is bubbled, the Cl_2-reversible potential is made less positive so that a linear Tafel relation (with slope *ca.* 0.03 V) can be observed before i_{lim} is approached. However, this behaviour is difficult to define in an experimentally satisfactory way, since an uncontrolled local partial pressure of Cl_2 arises from the Cl_2 anodically evolved in the experiment to extents dependent on the increasing current-density.

(v) Evaluation of k_2 and $\bar{K}_1$ for the Kinetics of Cl_2 Evolution in TFA and Water: Using the plots in Figs. 6a,b and 7a,b and an experimental value for the " H-area " of the Pt electrode determined by cyclic-voltammetry in 0.1M aq. H_2SO_4, together with estimates of the limiting currents in Fig. 5, enables k_2 and $\bar{K}_1$ to be evaluated giving the results shown in Table 1.

Both k_2 , being a chemical rate-constant, and $\bar{K}_1$, an electrochemical quasi-equilibrium constant, are not influenced by electrostatic double-layer effects dependent on ionic concentration. However, k_2 , the recombination rate-constant, can be dependent for chemical reasons on

specific adsorption of anions, solvent adsorption in the two solvents or their mixtures and oxide-film coverage, as will be discussed below.

It is found (Table 1) that k_2 evaluated from the plots of Figs. 7a and 7b is appreciably smaller than k_2 evaluated from i_{lim} with eqn. (6). This is probably due to the fact that k_2 evaluated from i_{lim} corresponds to a condition $\theta_{Cl\cdot} \rightarrow 1$ while k_2 evaluated from the linear parts of the plots of Figs. 7a and 7b corresponds to lower values; thus if interaction effects in the ad-layer are important as $\theta_{Cl\cdot} \rightarrow 1$, as expressed by eqn. (11) , k_2 values from i_{lim} will differ from those for lower $\theta_{Cl\cdot}$ approximately by the factor exp 2g. A g value of only α 1 RT unit is required to account for the difference of k_2 on this basis and is consistent with the small value of g required to account for the curvature of the plots of Figs. 7a,b at large i values as $\theta_{Cl\cdot} \rightarrow 1$ (see also simulations in Fig. 10).

(vi) Electrocatalysis in Cl$^{\cdot}$ Recombination at Pt: the Presence of the Surface Oxide Film and the Role of Adsorbed Cl^- :

Comparison of the log i- η curves of Fig 5. and the data in Table 1 for k_2 indicates that there is a substantial electrocatalytic effect of the presence of the surface oxide film at Pt in aq. solutions on $i_{2,lim}$ or k_2 in comparison with the behaviour in TFA (no oxide film detectable) where Figs. 6a,b and 7a,b indicate that the same recombination-controlled mechanism applies. The ratio $k_2(H_2O)/ k_2 (TFA)$ is between 15 and 45, depending on potential or $\theta_{Cl\cdot}$.

Presumably this is the result of weaker binding of Cl$^{\cdot}$ radicals and consequent better catalysis (lower activation energy) for their recombination at the oxidized Pt interface in water than at the Pt metal

TABLE 1

VALUES OF k_2 AND $\bar{K}_1$ FROM THE PLOTS IN Figs. 7a and 7b AND FROM THE LIMITING CURRENT-DENSITIES (T = 298 K)

Solution (mol % H_2O)	k_2 [from Figs. 7a, 7b with eqn.(11)] $\times 10^9$		k_2 from $i_{2,lim}$ $\times 10^9$		$\bar{K}_1$ [from Figs. 7a, 7b with eqn.(11)] $\times 10^{-2}$	
TFA	1.95	± ca. 10%	7.77		7.64	± ca. 10%
TFA/H_2O, 3%	2.05		10.4		7.45	
TFA/H_2O, 12%	2.11		10.4		7.33	
TFA/H_2O, 30%	4.97		28.5		5.38	
TFA/H_2O, 58%	10.1		82.9		3.94	
TFA/H_2O, 71.2%	28.8		103.8		4.13	
TFA/H_2O, 80.5%	76.6		110.9		5.48	
H_2O, 100%	90.8		113.9		10.07	

Units of k_2 are mol cm^{-2} sec^{-1} with surface concentration expressed as fractional coverages θ . In terms of surface concentrations in mol cm^{-2}, the units would be mol^{-1} cm^2 sec^{-1}. $\bar{K}_1$ is derived for Cl^- concentration expressed in mol cm^{-3} and surface concentration in the isotherm in terms of fractional coverages, θ . The $\bar{K}_1$ quantities in this Table are electrochemical equilibrium constants for step I and contain the exp term, $\exp \Delta V_{rev,Cl_2} F/RT$, as explained on p. 103-106 .

surface in TFA. While weaker $Cl^{\cdot}$ binding will also affect the kinetics and quasi-equilibrium in step I, and consequently the coverage when $\theta_{Cl^{\cdot}} \ll 1$, the conclusion concerning the effect of weaker binding on k_2 is unambiguous so far as the interpretation of the limiting currents goes since then $\theta_{Cl^{\cdot}} \to 1$. Generally speaking, the effects of binding energy of the $Cl^{\cdot}$ intermediate will follow those previously treated for the case of the H_2 evolution reaction where, for all mechanisms, a volcano-type relation is predicted[200] between rate constants and free-energies of adsorption.

Specific adsorption of Cl^- ion is the second factor: it is likely that this will depend on the state of solvation of the Cl^- ion and of the Pt surface, so that the surface coverage by coadsorbed Cl^- ions and the resultant competition[201-203] with surface oxidation processes, will be solvent-dependent. Certainly, Cl^- ion adsorption has significant effects on the recombination kinetics in " 100% H_2O " solutions since, in the concentration range 0.1 - 4.8M Cl^-, it is found (see Chapter III) that i_{lim} increases substantially with increasing Cl^- ion concentration, as may also be seen from the log i vs.η results of refs. 168,192. This effect probably arises on account of a repulsive energy contribution in the $2g\theta$ term of eqn. (11) due to $Cl^{\cdot}/Cl^-$ interactions in the surface layer at the electrode as well as to $Cl^{\cdot}/Cl^{\cdot}$ repulsion.

(vii) Dependence of i_{lim} and k_2 and of $\bar{K}_1$ on Solvent Composition:

The experimental values of i_{lim} at Pt (298 K) are shown in Fig. 11 as a function of mol% H_2O in TFA/H_2O mixtures. There is a sigmoidal dependence, roughly symmetrical about the 50% composition level. The corresponding plots for k_2 (from both i_{lim} at $\theta_{Cl^{\cdot}} \to 1$ and from the linear regions of the plots of Figs. 6a,b and 7a,b which apply to lower coverages,

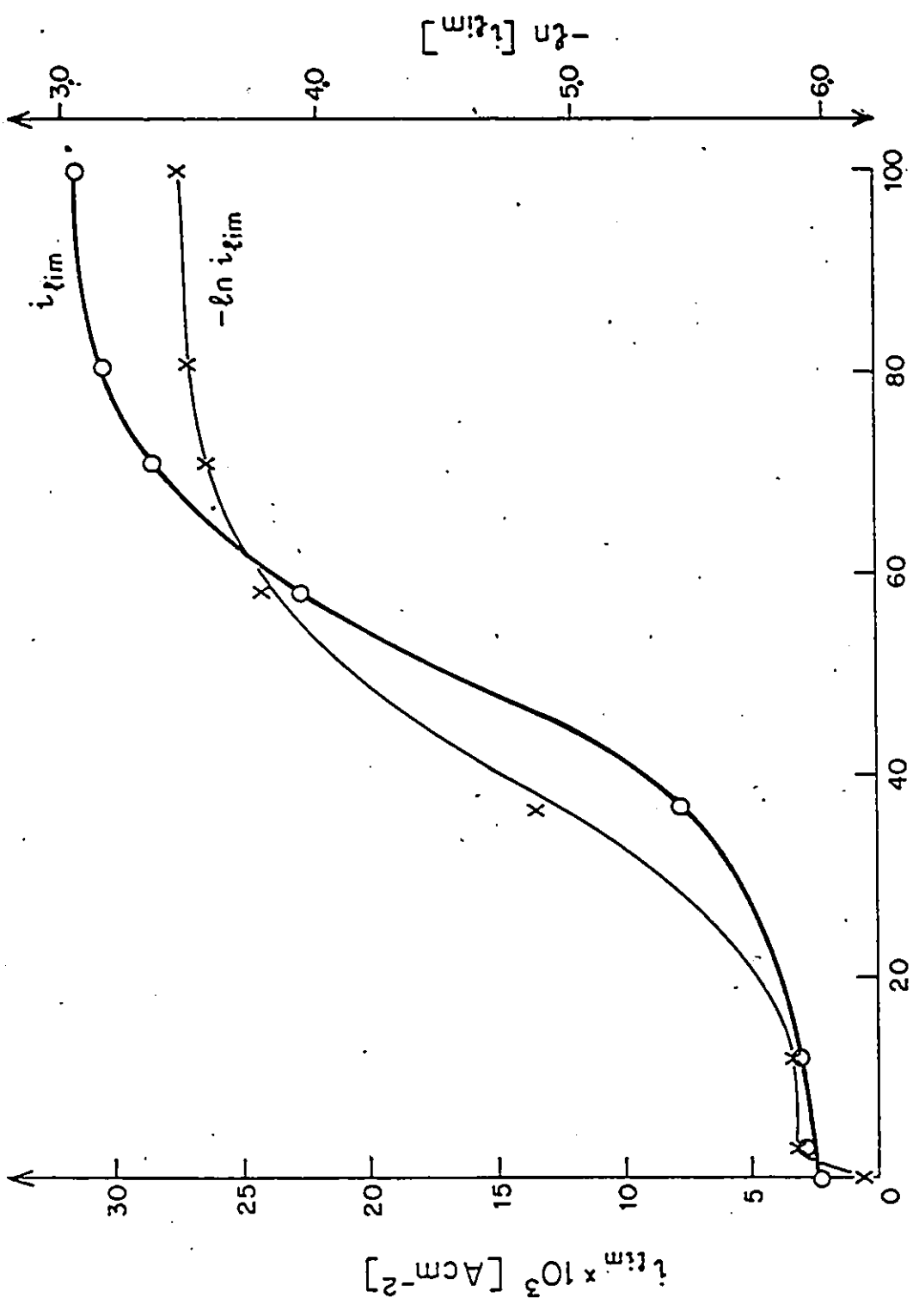

Fig. 11 Plot of $i_{2,lim}$ vs. composition (mol % H_2O in TFA) for 0.5 M Cl^- solutions (as RbCl or KCl) at 298 K. Dashed curve shows same data plotted as ln i_{lim} .

$\theta_{Cl} < 1$) are shown in Fig. 12 .

The values of k_2 derived from i_{lim} and those from the plots of Figs. 7a,b are shown in Fig 12 and differ for the reason discussed in Section (v) .

(a) Significance of the Quasi-equilibrium Constant, $\bar{K}_1$: The kinetics of the Cl_2 evolution reaction were treated in terms of quasi-equilibrium in the discharge step I, i.e.

$$\underset{(a_{Cl^-})}{Cl^-} + \underset{(1-\theta)}{Pt} \underset{k_{-1}}{\overset{k_1}{\rightleftharpoons}} \underset{(\theta)}{Pt\text{-}Cl_{ads}} + e^- \qquad \text{I}$$

prior to rate-determining recombination of adsorbed $Cl^{\cdot}$ species. The quasi-equilibrium in step I is treated in terms of an equilibrium constant $\bar{K}_1 = k_1 / k_{-1}$.

The significance of this equilibrium constant requires some special discussion before its dependence on (a) solvent composition and (b) Cl^- ion concentration or hypothetical activity, a_{Cl^-} , can be interpreted.

First, it is to be noted that the quasi-equilibrium constant for I is an electrochemical equilibrium constant dependent on the metal/solution p.d., ΔV, prevailing at the electrode interface as in any electrochemical charge-transfer process at equilibrium. Thus, the quasi-equilibrium in step I rearly must be written in terms of the electrochemical equilibrium constant, $\bar{K}_1$, as

$$\bar{K}_1 = K_1 \exp \Delta VF/RT = k_1 / k_{-1} \qquad (16)$$

where K_1 is the value of the equilibrium constant for process I at hypothetical zero value of the p.d. ΔV, and k_1 and k_{-1} are standard electro-

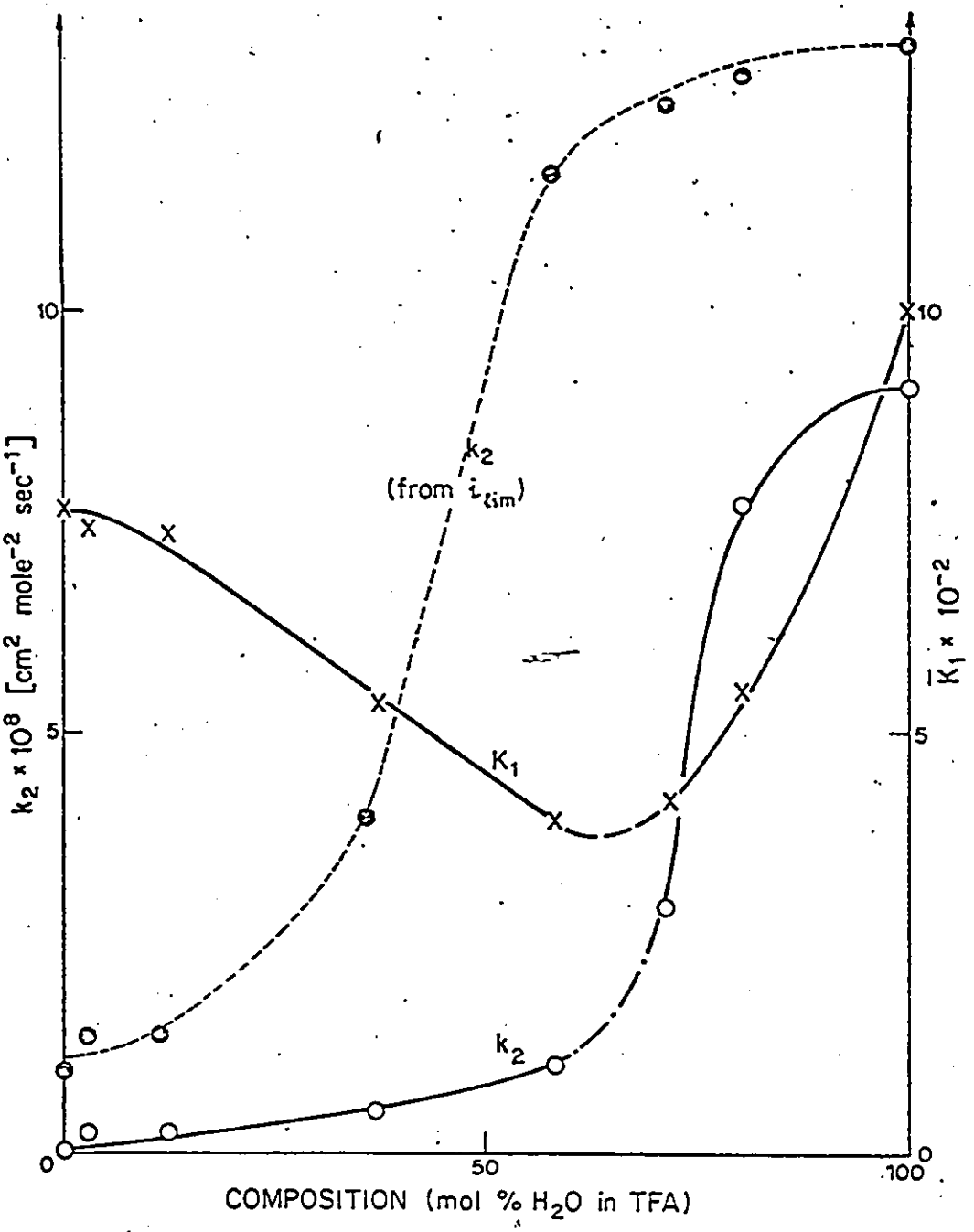

Fig. 12 Plots of k_2 from $i_{2,lim}$ and from the linear regions of Figs. 6b and 7b, together with $\bar{K}_1$, against solvent composition (mol % H_2O in TFA) for 0.5 M Cl^- solutions (as RbCl or KCl) at 298 K.

chemical rate constants.

Secondly, unlike the situation for an electrochemical equilibrium involving a charge-transfer process between an ion in solution and a pure bulk phase which has an invariant and unique activity (at a given standard temperature and pressure), the equilibrium in step I involves a coverage-dependent activity term $\frac{\theta}{1-\theta}$ for the discharge deposited species, $Cl^{\cdot}$, on the electrode surface. Thus the thermodynamic condition for equilibrium in step I is

$$\overline{K}_1 = \frac{\theta}{1-\theta} \frac{1}{a_{Cl^-}} = K_1 \exp[\Delta VF/RT] \qquad (17)$$

or, in the usual way

$$\frac{\theta}{1-\theta} = K_1 \exp[\Delta VF/RT] a_{Cl^-} \qquad (17a)$$

Thus, for a given a_{Cl^-} , θ is dependent on ΔV, or vice-versa.

A standard value of ΔV (ΔV°) is given, in the usual way, by considering standard state conditions as follows: hypothetical $a_{Cl^-} = 1$ and $\theta = 0.5$ for the surface " monolayer " film of adsorbed $Cl^{\cdot}$ discharged in step I.

Since, for a given a_{Cl^-} , θ is determined only by ΔV (and K_1), the relevant ΔV values in the test of the recombination reaction on a Cl_2- overpotential scale are those corresponding to the overpotential values for Cl_2 evolution. By definition of η , these values of ΔV in eqn. (17a), applying to the analysis for the Cl_2 reaction, are therefore

$$\Delta V = \eta + \Delta V_{rev,Cl_2} \qquad (18)$$

where $\Delta V_{rev,Cl_2}$ is the <u>reversible</u> metal-solution p.d. for the Cl_2/Cl^- reaction (<u>not</u> any hypothetical reversible potential for step I). Hence the $\bar{K}_1$ values evaluated contain, in particular, an exp term " $\exp \Delta V_{rev,Cl_2} F/RT$ ". Then eqn. (17) can be written

$$\theta = \frac{K_1 \exp [\Delta V_{rev,Cl_2}] \; a_{Cl^-} \; \exp \eta F/RT}{1 + K_1 \exp [\Delta V_{rev,Cl_2}] \; a_{Cl^-} \exp \eta F/RT} \qquad (19)$$

Thus the θ values which are involved in the kinetics of Cl· recombination ($i = 2Fk_2 \theta^2$) were expressed in terms of overpotentials, η , for the overall Cl_2 reaction through the relation which follows from eqn. (19) with eqns. (15) and (16):

$$\theta = \frac{\bar{K}_1 a_{Cl^-} \exp \eta F/RT}{1 + \bar{K}_1 a_{Cl^-} \exp \eta F/RT} \qquad (20)$$

or the corresponding relation for finite g (eqn. 12).

The $\bar{K}_1$ values derived from the test plots thus have the particular significance:

$$\bar{K}_1 = K_1 \exp [\Delta V_{rev,Cl_2} F/RT] \qquad (21)$$

and the θ involved in reaction I or in eqn. (17a) at the <u>Cl_2</u>- reversible potential is that ($\theta_{\eta = 0}$) determined by eqn. (17a) when ΔV in that eqn. is equal to $\Delta V_{rev,Cl_2}$, i.e., when the experimentally measurable η is taken = 0 . Thus, in eqn. (17), $\bar{K}_1$ is given by eqn. (21) above, and includes the exp term in $\Delta V_{rev,Cl_2} F/RT$.

We are now in a position to make further comment on the two matters mentioned earlier: (1) the dependence of $\bar{K}_1$ on solvent composition

and (2) on Cl^- concentration (activity).

(1) The equilibrium in step I will depend on solvent composition on account of (a) the changing free-energy of solvation of the Cl^- ion on the l.h.s. of eqn. I; (b) on the possibly solvent-dependent free-energy of adsorption of $Cl^\cdot$, since $Cl^\cdot$ is electrosorbed competitively with TFA + H_2O at the Pt electrode surface. Also (c) the absolute metal-solution p.d. of the Pt electrode will probably also depend on solvent composition in the standard state of $\theta = 0.5$ and $a_{Cl^-} = 1$, due to composition-dependent solvent-dipole orientation (surface-potential effect). Finally (d), the equilibrium in step I will be determined also by the effect of oxide-film coverage on the free-energy of adsorption of discharged $Cl^\cdot$, especially at relatively high H_2O contents in TFA/H_2O mixtures.

(2) In the case where varying KCl concentrations are involved, the quantity, $\bar{K}_1$, evaluated from the intercept/slope values of the test plots involves the term $\exp \Delta V_{rev,Cl_2} F/RT$ for all concentrations. However, the $\Delta V_{rev,Cl_2}$ term in $\bar{K}_1$ is concentration (activity)-dependent according to a Nernst equation:

$$\Delta V_{rev,Cl_2} = \Delta V^{o}_{rev,Cl_2} - \frac{RT}{F} \ln a_{Cl^-} \qquad (22)$$

Note: $a_{Cl^-} = a_{\pm,KCl} = (a_{K^+} a_{Cl^-})^{\frac{1}{2}}$. Thus,

$$\bar{K}_1 = K_1 \exp[\Delta V_{rev,Cl_2} F/RT] = K_1 \exp [\Delta V^{o}_{rev,Cl_2} F/RT] \frac{1}{a_{Cl^-}} \qquad \ldots.(23)$$

Hence, the $\bar{K}_1$ evaluated from the test plots for various Cl^- concentrations includes a factor in $(a_{Cl^-})^{-1}$ as indicated from eqn. (19). For this reason, the values of $\bar{K}_1$ calculated from the results for various

Cl^- concentrations decrease in an hyperbolic way with increasing Cl^-, as will be shown in Chapter III.

(b) Significance of the Rate Constants, k_1 and k_{-1}: As in the case of $\bar{K}_1$, the rate constants k_1 and k_{-1} are " electrochemical " rate constants. In the usual way, they contain therefore the terms $\exp \beta \Delta V_{rev,Cl_2} F/RT$ and $\exp -(1-\beta) \Delta V_{rev,Cl_2} F/RT$, respectively since ΔV in the exponential terms is related to V_{rev,Cl_2} and η by the eqn. (19) given earlier. The quotient k_1/k_{-1} gives, in the usual way, $\bar{K}_1$ as expressed by eqn. (16) for the Cl_2/Cl^- reversible potential.

(c) Evaluation of $\bar{K}_1$ Values: $\bar{K}_1$ is determined in part by the solvation energy of Cl^- ion which is involved in the backward or forward directions of the ion discharge step I. Table 1 shows that $\bar{K}_1$ is dependent, as expected, on solvent (through step I) as is the overall Cl_2/Cl^- equilibrium demonstrated by the electrode potentials (relative to H_2/H^+) measured in the two pure solvents. However, for well-known thermodynamic reasons, it is not possible to separate out the individual ionic effect due to Cl^- solvation at all reliably.

Since $\bar{K}_1$ is solvent-dependent, the coverages $\theta_{Cl\cdot}$ for $\theta_{Cl\cdot} < 1$, will tend to be different at various overpotentials in TFA and in water solutions of Cl^- ion according to eqn. (7).

$\bar{K}_1$ shows an ineresting minimum at the composition where k_2 (From Fig. 12) begins to ascend rapidly with increasing H_2O content. This behaviour suggests that there are competing factors determining $\bar{K}_1$: (i) changing solvation of the Cl^- ion; (ii) changing energy of adsorption of electrodeposited $Cl\cdot$ due to (a) onset of significant oxide film formation see Section (viii) ; (b) changing specific adsorption of Cl^- ion and (c) changing solvent adsorption; a third factor (iii) is changing surface dipole p.d. at the electrode interface due to solvent

composition change and to appearance of the oxide film at high H_2O contents.

(d) Evaluation of k_2 and i_{lim} Values: Figs. 6a,b and 7a,b indicate that recombination control applies to the Cl_2 evolution reaction at Pt in both TFA and H_2O, and their mixtures at all compositions. Hence the dependence of k_2 and i_{lim} on various factors related to changing solvent composition can be examined in terms of a common mechanism. Because a chemical recombination mechanism evidently applies at all compositions, k_2 or i_{lim} cannot directly depend on the state of solvation of the Cl^- ion, as does $\bar{K}_1$. Therefore the observed dependence of k_2 on solvent composition must arise from a dependence on changing surface properties of the Pt electrode with solvent composition due to (a) development of a Pt surface oxide film; (b) composition-dependent specific adsorption of Cl^- ion which may influence the activation energy for recombination through the $\exp 2g\theta_{Cl}$. factor of eqn. (11); and (c) composition-dependent solvation of the electrode interface by TFA and H_2O which may determine, in part, the adsorbability of Cl^- which itself will be preferentially solvated by TFA or H_2O, depending on bulk solvent composition. A possible effect of adsorbed TFA solvent molecules (electrostatically at the O-atoms, since there is no evidence of dissociative chemisorption at the CF_3-group) in interfering with the $Cl^\cdot$ recombination by impeding surface diffusion must be recognised but no information is available concerning such behaviour. However, water itself is also known to be strongly adsorbed at Pt.

The symmetrical shape of i_{lim} vs. mol% H_2O in Fig. 11 is an interesting feature of the results with regard to the solvent effect in the kinetics of Cl_2 evolution. It is suggestive of a selective replacement

of one solvent component by the other in the electrode interphase (analogous to a titration curve) with a corresponding influence on the free energy of activation for the Cl˙ recombination step.

This effect may arise from (a) dependence of specific adsorption of Cl^- ion on local solvent composition in the double-layer and (b) from the composition-dependent oxide film coverage [see Section (viii)] .

In TFA/H_2O mixtures with Cl^- present, it is not possible to detect (cf. Fig. 4) any oxide film coverage (i.e. $\theta_{Ox} \gtrsim 5\%$) at Pt, even with 1 min holding time at potentials above the Cl_2 evolution potential, until ca. 58 mol% H_2O is reached. This corresponds to the composition in Fig. 11 where $\overline{K}_1$ changes its direction with solvent composition and k_2 begins to increase rapidly.

Nevertheless, in the composition range 0 to 50 mol% H_2O, k_2 is increasing substantially (Fig. 12). Hence it seems necessary to attribute the initial increase of k_2 to changing specific adsorption of Cl^- and/or to changing composition of the interphase layer of solvent at the electrode surface. Both the selective solvation of the surface and that of the Cl^- ion will determine the specific adsorption characteristics of the Cl^- ion at Pt under the conditions of the present work.

Above ca. 58 mol% H_2O, surface oxide coverage begins to become significant and will tend to influence the kinetics of Cl˙ recombination due to change in the nature of the Pt surface, as will be discussed in Section (viii).

(viii) Coverage by Electrodeposited O Species: The kinetic behaviour of the Cl_2 evolution reaction in TFA/H_2O mixtures does not approach that characteristic of 100% aq. solutions of Cl^- ion until quite high (~0.5 - 0.6) mol fractions of water are present. This seemed at first unexpected, since (a) it is found (Fig. 3) that in TFA (without Cl^- present) the Pt oxide film becomes easily detectable already with 0.2~0.5 mol% H_2O present; and (b) recombination kinetics are found to apply in all the solvent mixtures studied, so that only the surface state of the Pt electrode, e.g. as determined by oxide film coverages, would be expected to determine the kinetics, as noted by Littauer and Shreir[160].

Measurements of the extents of Pt surface oxidation in 0.5M KCl + 0.05M HCl over the Cl_2 evolution potential region were made at the rotating Pt disc electrode by means of a cathodic sweep from various positive potentials held constant for periods of 60 s at each potential. Provided that sufficient ω (> 2000 r.p.m.) is maintained with a large volume of solution, the Pt surface oxide reduction peak can be well resolved from currents for reduction of previously evolved Cl_2 (N_2 is bubbled in such solutions). These experiments (cf. Fig. 4) gave the interesting results shown in Fig. 13. From 1.3 to 1.6 V E_H, the extent of surface oxidation remains quite constant at ca. 90 μC cm^{-2}, viz. ca. 40% of a monolayer counted in terms of OH species. For comparison, the potential-dependent oxide coverage observed (cf. refs. 61,69) in 0.25M K_2SO_4 + 0.025M H_2SO_4 at Pt is also shown in Fig. 13.

Thus, even at potentials where Cl_2 is evolved at relatively rapid rates (e.g. 20~30 mA cm^{-2}), the coverage of the Pt electrode by oxide* is less than 50% and remains almost constant with varying anode potential

*In dilute aq. H_2SO_4 or $HClO_4$, free of Cl^-, a monolayer of OH species appears to be formed at the Pt electrode at 298 K when the potential has reached + 1.10 ± 0.03 V E_H[69].

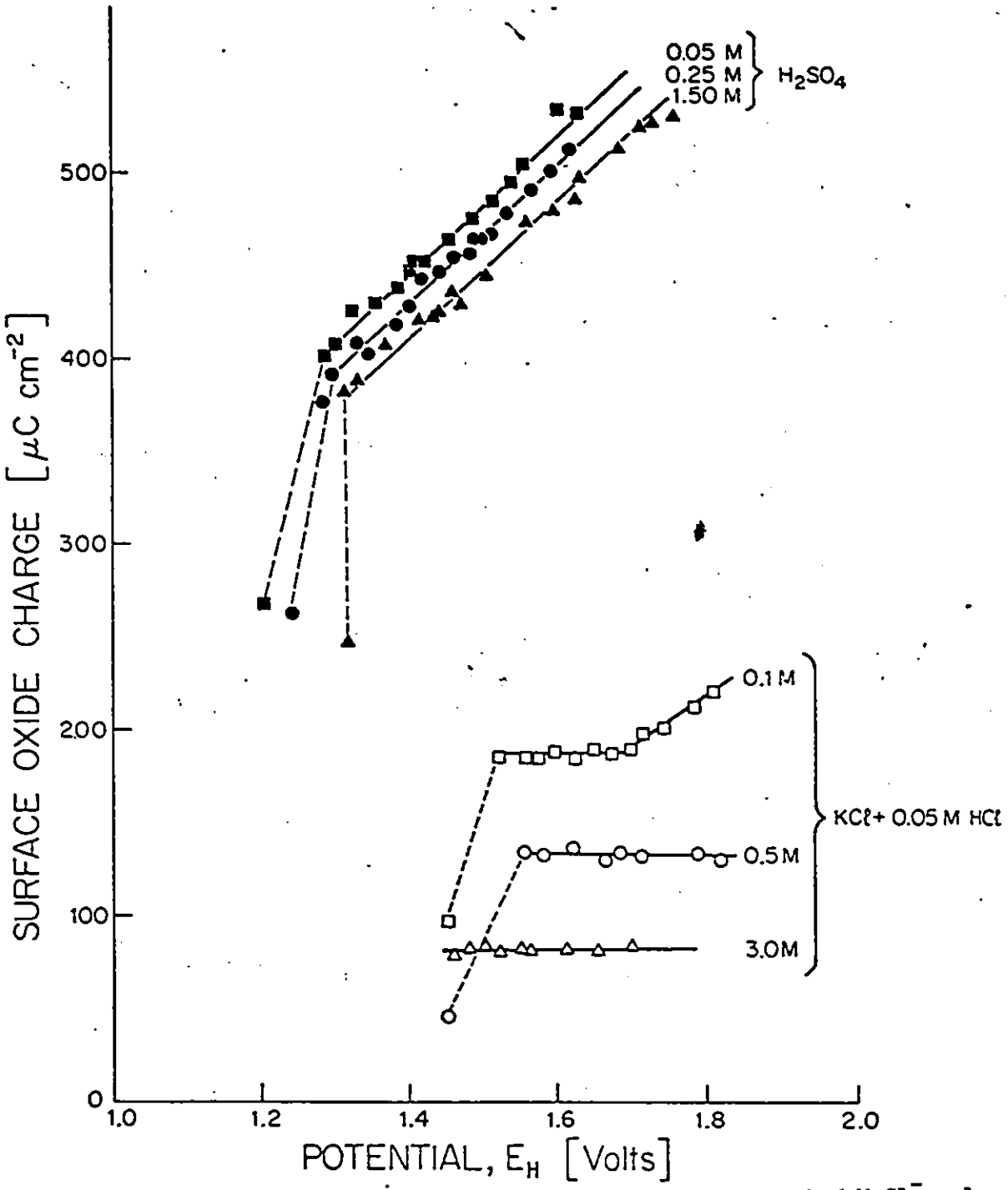

Fig. 13 Surface oxide coverage, as charge, at Pt electrode in 0.5 M Cl^- solutions as a function of anode potential for τ_h = 60 s at positive end of potential sweep. (Rotated Pt electrode 1600 r.p.m. , sweep-rate = 25 mV s^{-1}, T = 298 K). Comparative data for a Cl^- - free solutions of 0.05 M, 0.25 M and 1.5 M H_2SO_4 solutions are also shown. Initial points marked are for τ_h = 0 in multiple sweep at the lowest potential.

over most of the experimental range of potentials for Cl_2 evolution.

This result explains why the plots in Figs. 6a,b and 7a,b are (a) linear over an appreciable range of potentials, giving a constant k_2 value except as $\theta_{Cl\cdot} \rightarrow 1$, i.e. as $i_2 \rightarrow i_{2,lim}$; and (b) exhibit very little hysteresis (cf. Fig. 5) w.r.t. the η factor for ascending and descending current densities (contrast the case for O_2 evolution where there is a substantial hysteresis in the kinetic behaviour related to hysteresis in the curve for degree of oxidation of Pt electrode surfaces as a function of ascending and descending potentials).

The results in Fig. 13 for oxide coverage as a function of potential in the presence of Cl^- ion in comparison with the more familiar behaviour in its absence (e.g. in aq. H_2SO_4 or $HClO_4$), implies that the normal potential-dependence of oxide coverage is almost completely cancelled by that of Cl^- and/or $Cl^\cdot$ coverage, when Cl^- ion is present. Thus " θ_{Ox} " and θ_{Cl^-} or $\theta_{Cl\cdot}$ are both probably determined by competing exp factors in VF/RT together with similar exp " $g\theta$ " factors (cf. refs. 196,197).

Fig. 14 shows how values of k_2 and $\bar{K}_1$ depend on the oxide coverage (as charge measured in cathodic sweeps, after 1 min. holding at various positive potentials). k_2 from $i_{2,lim}$ and from the plots of Figs. 6a,b and 7a,b differ in their dependence on oxide coverage for the reasons mentioned earlier (p. 99.). Three of the values of k_2 in Fig. 12 for low H_2O contents are not shown in Fig. 14 since they correspond to zero observable oxide coverage.

It may be suggested that the origin of the rather continuous

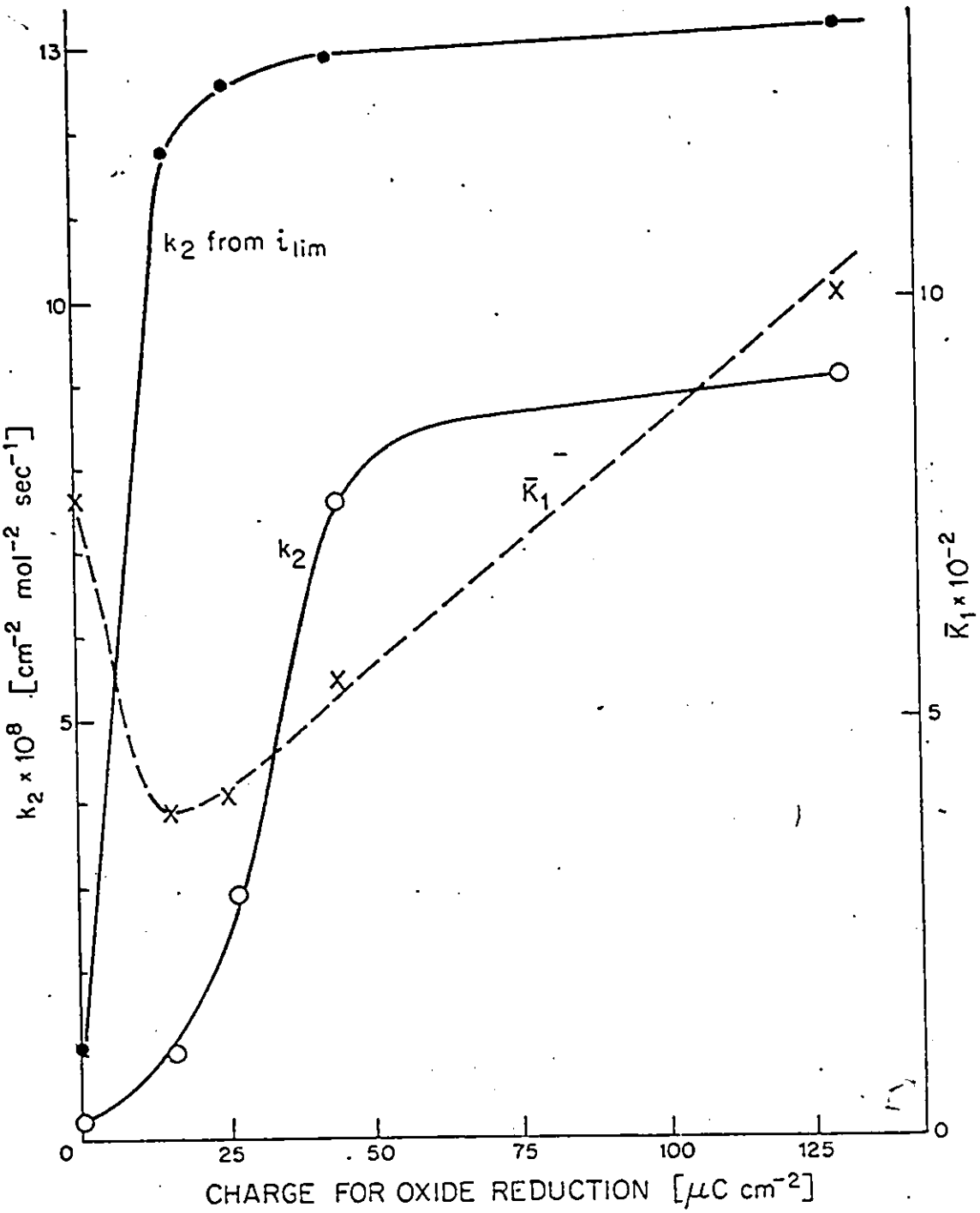

Fig. 14 Plots of k_2 form $i_{2,lim}$ and from Figs. 6b anf 7b as a function of Pt surface oxide charge determined after holding the potential for 1 min at various anode potentials. (Based on experiments of the kind that gave the results shown in Fig. 4). Variation of $\bar{K}_1$ with Pt surface oxide charge is also shown.

dependence of k_2 on solvent composition (Fig. 12), all the way from small H_2O contents in TFA up to 100% aq. solution of Cl^-, is as follows: Up to ca. 58 mol% H_2O, the variation of k_2 appears to be due principally to Cl^- ion, as suggested earlier. Beyond 58 mol% H_2O, the Pt surface begins to become increasingly oxidized but the well known[162,204] competition between Cl^- adsorption and OH/O[201,202] is still important. Thus, even in fully aq. solution, surface coverage by OH + O species is substantially less than 100% at the Cl_2 evolution potential ($\geq$ 1.35 V E_H) while in aq. Cl^- - free H_2SO_4 the degree of surface oxidation of Pt would normally correspond to ca. 2e/Pt atom at these potentials. Eventually the Pt surface is appreciably oxidized as the 100% H_2O composition is reached and k_2 then approaches a new constant value characteristic of a Pt surface partially covered by oxygen and Cl^- species, as well as the intermediate $Cl^\cdot$ of the reaction mechanism. The ratio of oxygen to Cl^- species adsorbed at the electrode appears to attain a constant value with increasing potential beyond ca. 1.1 V E_H.

The experiment conducted in 100% TFA but with a pre-oxidized electrode (central curve in Fig. 5) shows that when there is no free Pt surface on which Cl^- can be specifically adsorbed, the i_{lim} values are between those for the 100% anhydrous and the 100% aq. solutions. This result confirms that the best conditions for catalysis of the $Cl^\cdot$ recombination process are those where some partial degree of surface oxidation of Pt exists but some free metal surface remains on which Cl^- ion can be co-adsorbed.

(ix) Conclusions: Some general conclusions arise from this work. It is found that Cl_2 evolution occurs with greater facility on an electrode which is partially covered by an oxide film than on either the " free " metal surface or a " fully oxidized " Pt surface. The substantially greater values of k_2 for partially oxide-covered than for the free-metal surface indicate that the $Cl^{\cdot}$ intermediate is more weakly bound at the oxide than at Pt metal sites. This seems reasonable, since the surface orbitals are already involved in interaction with chemisorbed OH and O species in the former case. However, co-adsorbed Cl^- ion appears also to have an important influence on the recombination kinetics. The fact that recombination-controlled kinetics apply under all conditions investigated means that $k_1 \gg k_2$, i.e., the coupled desolvation of Cl^- and electron discharge are facile for this ion. It is to be noted that recombination-controlled kinetics are also observed in molten salt systems[179].

Similar conclusions apply to O_2 evolution: e.g., on Au and Pt, it is found that a certain anion-dependent state of the oxide film must be attained before O_2 can be evolved at appreciable rates. Also, it is found that the efficiency of the Kolbe evolution of hydrocarbons at Pt from carboxylic acids depends on the state of the oxide film at Pt. This approach may possibly also apply to cathodic H_2 evolution: this reaction occurs with the highest exchange currents on those metals on which a strongly-bound film of adsorbed H is already present at at or below the reversible potential.

CHAPTER III

Cl^- ION ADSORPTION AND ITS INFLUENCE ON Cl_2 EVOLUTION KINETICS AND THE STATE OF OXIDIZED Pt ELECTRODES

1. INTRODUCTION

(i) Statement of Objectives: The results discussed in Chapter II demonstrated the important catalytic role of Pt surface oxide in Cl_2 evolution at Pt-anodes; this was shown by comparing the kinetics of the reaction at Pt in aqueous solutions with those in an anhydrous non-aqueous solvent, trifluoroacetic acid (TFA) : in both TFA and H_2O as solvents, and in their mixtures, the reaction was shown to be recombination controlled but the rate constant was substantially larger on the oxidized Pt surface in aqueous medium than on the free metal surface in the anhydrous medium where complete absence of an oxide film was demonstrated.

The study also indicated the possible importance of solvent-dependent specific adsorption of Cl^- ion on the recombination kinetics through a competitive effect of Cl^- ion on the extent of surface oxidation attained at various anodic potentials in TFA/H_2O solvent mixtures. The latter effect, in water, is qualitatively well known from earlier studies[162,202,203], as will be discussed in Section 1, (iii).

Thus, the work on Cl_2 evolution kinetics at Pt anodes in TFA/H_2O mixtures was extended to a study of its dependence on $[Cl^-]$ in aqueous medium in relation to (a) the state of the oxidized Pt anode surface and (b) the dependence of that state on Cl^- ion adsorption. This is important since the state of oxidation of the Pt surface, which is modified by Cl^-

ion adsorption[162,201], can determine the catalytic properties of the surface for Cl· recombination.

There are therefore two main aspects of the work to be decribed in this Chapter: (a) a demonstration that Cl· recombination controls the kinetics of the overall reaction at all Cl^- concentrations and (b) that the properties of the electrode surface, influenced jointly by Cl^--dependent extent of surface oxidation and by co-adsorbed Cl^- ions, determine the rate constant for the surface-catalyzed Cl· recombination step.

(ii) Previous Work on Cl^- Ion Effects on the Cl_2 Evolution Reaction:

The mechanism of the reaction was previously often discussed on the basis of the Tafel slope[119,143,166,176]. An important further criterion is the reaction order[205,206] - here the dependence of rates on Cl^- concentration[168]. For simple charge-transfer redox processes, there is little interaction between the reacting species and the electrode surface, and the rate-determining step is simply a quasi-homogeneous charge-transfer. Vetter[205] formulated a general method for evaluating reaction orders for simple charge-transfer controlled reactions of this kind.

Many electrode processes are, however, heterogenous and thus much more complex. There is usually then (a) an enhanced surface concentration of reactants due to adsorption; (b) a surface concentration of adsorbed intermediates when the reaction is a multi-step one; (c) specific adsorption of ions (usually anions) which influences the surface properties of the electrode and the interfacial electrode/solution potential-profile and (d) surface-specific electrocatalytic effects.

The Cl_2 evolution reaction at Pt is complicated by specific adsorption of Cl^- ions and their influence on the surface oxide film at

Pt which exists at potentials where Cl_2 evolution occurs at appreciable rates.

In H_2O, the Cl_2 evolution reaction can only be studied over a range of potentials where the Pt surface is covered significantly with an oxide film which, according to some authors (cf. refs. 144,151,160), causes inhibition of the overall reaction. Since the amount of adsorbed oxide species varies with the potential, the interpretation of the kinetics of Cl_2 evolution must take into account the potential-dependent coverage of the electrode by oxide species. Also, the influence of the Cl^- ion itself should be taken into account since it has been found experimentally that Cl^- ion species are strongly adsorbed on Pt electrode surfaces[162] [see below Section 1. (iii)(b)] . This factor was rarely taken into consideration in early studies on Cl_2 evolution reaction kinetics.

However, Frumkin and Tedoradze[157] made detailed investigations of the reduction of Cl_2 and showed the reaction order of that process with respect to $[Cl_2]$ to be unity and with respect to $[Cl^-]$ to be zero at low $[Cl^-]$ where the plots of V vs. log i are linear and independent of $[Cl^-]$.

In order to determine the reaction order for the Cl_2 evolution reaction at a Pt electrode, Frumkin and Tedoradze[157] used a simple method based on extrapolation of the linear region of the Tafel lines to zero overpotential which gives the concentration-dependent exchange-current. As the Tafel line observed at high cathodic overpotentials consisted of two regions, it was assumed that the reaction is composed of two consecutive charge-transfer steps with exchange-current densities of comparable magnitudes. Frumkin[207] demonstrated for the case of a

reaction composed of two consecutive charge-transfer steps that the extrapolation of current-densities to zero overpotential of the linear part of the Tafel line would lead to the stoichiometric number of the reaction twice as large as the true value if the exchange current-densities were comparable in magnitude. This would then lead to an apparent value of 2 instead of the true value in the mechanism, which is unity. Thus, the stoichiometric number ν could be obtained from the following relation

$$i = i_+ - i_- = i_+(1 - i_-/i_+) = i_+ [1 - \exp(-n\eta F/\nu RT)] \quad (24)$$

and hence, near equilibrium,

$$\nu = i_o(nF/RT)(d\eta/di)_{\eta=0} \quad (25)$$

Parsons[208] doubted the applicability of this equation since i_o values were obtained by extrapolation to $\eta = 0$ when the reversible potential was near the potential zero charge. According to theoretical equations derived by Parsons[208], the apparent i_o evaluated by such a procedure would change with potential in the potential region where V_{rev} is near the potential of zero charge.

Dickinson et al.[151] studied the mechanism of the Cl_2/Cl^- reaction in some detail. In this work it was realized that, in the anodic direction, the potential-dependent degree of Pt surface oxidation complicates elucidation of the kinetics of the electrochemical Cl_2 reaction. However, by pre-conditioning the electrode surface with respect to oxide film formation, they showed that the Cl_2 reduction reaction could more satisfactorily be studied.

A rotating disc electrode was employed[151] in 1M HCl electrolyte solution. The order of the cathodic Cl_2 reduction reaction

was determined using two methods, one in which the bulk concentration of reactant was varied and the other in which the current at constant potential was related to the rotation speed of the electrode and hence to the local concentration at the electrode surface determined by the forced flow mass-transfer rate. Thus, at potentials sufficiently negative to the reversible potential, the current-density would be determined by

$$i = k\,[Cl_2]_s^R \qquad (26)$$

where k is a rate constant at constant electrode potential and R is the order of reaction. The concentration of Cl_2 at the electrode surface is given by the quantity $[Cl_2]_s$. By using different rotation speeds, the concentration of Cl_2 at the surface could be expressed through the diffusion current ratio:

$$[Cl_2]_s = \frac{i_d - i}{i_d}\,[Cl_2] \qquad (27)$$

At constant potential, the extent of oxide formation at the surface during Cl_2 reduction could be kept constant so that, for a constant rotation speed, a plot of log i *vs.* $\log[Cl_2]_s$ would give a slope equal to the order of the reaction. Dickinson et al.[151] used a range of rotation speeds up to 4000 r.p.m. at different potentials and found that the reaction order was unity at low Cl_2 concentrations but decreased to 0.8~0.6 at higher concentrations. By plotting current *vs.* potential relations, they concluded that the simplest reduction mechanism in accord with these results would be:

$$Cl_{2(aq)} + M + e^- \rightleftharpoons M\text{-}Cl + Cl^-_{(aq)}$$

$$Cl\text{-}M + e^- \longrightarrow M + Cl^-_{(aq)}$$

in which the last step was considered to be rate-determining, but comparable in rate to the reverse of the first step.

In order to investigate more satisfactorily the mechanism of the Cl_2 evolution reaction, Enyo and Yokoyama[209] extended Vetter's method to make it applicable not only to charge-transfer controlled processes but also to more complex reactions involving an heterogeneous chemical step. They derived the reaction order for the anodic Cl_2 evolution process, taking into account the variation of rate with Cl^- concentration and Cl_2 pressure in the usual way. The derived reaction order was found to depend on the concentration of Cl^- ions, and varied from 1 to 0 at Pt in 1M H_2SO_4 solution at 25° C for p_{Cl_2} varying from 1 to 0.089 atm, C_{Cl^-} from 0.2 to 0.006 M for overpotentials up to 300 mV. Although they reported curved η - log i plots, reminiscent of a recombination-controlled i-η relation, they concluded that the Cl^- ion discharge step was rate-determining rather than the discharged Cl· recombination. It should be mentioned, however, that it was concluded that the influence of oxide formation was almost invariant in the experiments since the current vs. potential behaviour was observed to be the same with increasing and decreasing current-densities. They assumed (incorrectly) that the formation and reduction of Pt surface oxide is a slow process and thus the state of the surface was assumed to be unchanged during the short time current transients of about 10 ms that were used in these experiments.

The kinetics of both the Cl_2 evolution and Cl_2 reduction processes on Ti-supported metals[143] and metal oxides[144,166] such as Ti/Pt-Ir (in different ratios) or Ti/IrO_2 and RuO_2 were studied by Faita et al.[143,144] in solutions of NaCl in the concentration range 0.1 to 1M and 1.0 to 4.0 M,

respectively. These authors[145] also studied Pt in 1M NaCl at pH 2. They defined the E_{rev} for Cl_2/Cl^- as $E^\circ + RT/F \ln \frac{(a_{Cl_2})^{1/2}_{soln.}}{a_{Cl^-}}$ in the usual way while the potential values of the electrode at different current-densities were defined as:

$$E = E_{rev} + \eta_1 + \eta_2 \qquad (28)$$

where η_1 is the concentration polarization defined as

$$RT/2F \ln \frac{(a_{Cl_2})_{surface}}{(a_{Cl_2})_{solution}} \qquad (28a)$$

and η_2 is the activation polarization. The total overpotential is $\eta_1 + \eta_2$.

They observed that $(a_{Cl_2})_{surface}$ increased as the anodic current-density increased, until a limit was reached (at rotating disc electrodes with a current-density of 10 mA cm^{-2} [144]) after which $(a_{Cl_2})_{surface}$ became constant. At high anodic current-densities, the potential should be decreased to an extent determined by the ratio

$$\frac{(a_{Cl_2})_{surface}}{(a_{Cl_2})_{solution}}.$$

They concluded that the potentials were independent of the Cl_2 concentration in the solution. Thus the Tafel plots exhibited a steady slope of 32 mV* above 10 mA cm^{-2} in 4M NaCl solutions. This indicated that the recombination-controlled mechanism applied.

Krishtalik et al.[175] revised his own earlier proposal that the recombination-controlled mechanism applied at RuO_2/Ti-supported electrodes on the basis that the observed dependence of the overpotential on Cl^- ion concentration gave a reaction order for the anodic reaction equal to 1.

*These authors bubbled N_2 in their experiments and were thus able to detect the linear Tafel region below the standard (1 atm Cl_2) reversible potential (see p. 98).

Therefore a so-called " chloronium ion " pathway was proposed:

$$M + Cl^- \rightleftharpoons M\text{-}Cl_{ads} + e^-$$

$$M\text{-}Cl_{ads} \longrightarrow Cl^+ + e^- + M$$

$$Cl^+ + Cl^- \rightleftharpoons Cl_2 \quad \text{(fast)}$$

The reaction mechanism on RuO_2 electrodes seems to be more complex possibly due to the relatively thick oxide film on the surface which should be taken into account. The adsorption of Cl^- ions on the electrode surface depends not only on Cl^- concentration but also on the pH of the solution[210]. This is because the state of the oxide is pH dependent.

Arikado et al.[119] obtained information on the reaction order at RuO_2 with respect to Cl^- ion concentration indirectly from the slopes of plots of log i_o vs. E_{rev} , according to the method discussed by Yokoyama and Enyo[168,209]. It was found, rather inexplicably, that E_{rev} did not obey Nernst's equation when the " a_{Cl^-} " of the bulk solution was used. Therefore, they stated that the information on the reaction order with respect to Cl^- ion cannot be successfully obtained from the plots of the log i_o vs. E_{rev}. A value of 2.3 was obtained but it was considered that this figure indicated that the reaction order was 2. Since the observed Tafel slope was 40 mV, it was concluded that the most probable mechanism was the Volmer-Heyrovsky one with the Heyrovsky step ($Cl^{\cdot}_{ads} + Cl^- \longrightarrow Cl_2 + e^-$) rate-determining at low overpotentials.

In the case of graphite anodes used for Cl_2 evolution, the electrode process is more complex due to the porosity of the graphite electrodes normally employed and to the oxidation of the surface of the carbon, as well as to Cl^- ion adsorption. In the early work, possible mechanisms were deduced on the basis of Tafel slope evaluations [180-184]. Hine et al.[186] took into

account the surface roughness of the graphite electrodes they used, the surface oxidation and the Cl^- ion dependence of the currents in a study of the mechanism of Cl_2 evolution. The Tafel slope for potentials < 1.56 V E_H, when the Cl_2 evolution reaction proceeds on the " lower oxide ;" was found to be 120-130 mV but at higher potentials the slope rises. The reaction order* was obtained by following the dependence of current-density on Cl^- ion concentration in the anodic process, and

$$R = \left(\frac{\partial \log i}{\partial \log C_{Cl^-}} \right)_{E, C_{Cl_2}} \simeq 0.6 \qquad (29)$$

was found. The reaction order for cathodic Cl_2 reduction at graphite was found to be 1 with respect to Cl^- concentration. The difference‡ between these two values was ascribed to disturbance of the oxide layer on the working electrode. In a later paper(187) on studies of the anodic Cl_2 evolution reaction on carbon at potentials up to 1.56 V E_H, evidence was presented that the Volmer-Heyrovsky pathway applies with the desorption step $Cl^{\bullet}_{ads} + Cl^- \longrightarrow Cl_2 + e^-$ rate-determining. At high anodic potentials, the formation of carbon oxide species complicates the kinetics.

Kim and Jorne(211) studied the kinetics of the cathodic and anodic processes in the Cl_2/Cl^- reaction on graphite electrodes in concentrated $ZnCl_2$ solutions, in order to understand the behaviour of the Cl_2

---

*The significance of reaction orders for electrochemical reactions will be discussed in more detail in a later Section, p 150.

‡At the equilibrium potential, E_{rev}, the reaction orders must be the same for both directions of the reaction since the same rate-controlling step applies. However, at considerable overpotentials in either direction, this is not necessarily the case as the rate-limiting mechanism can then be changed in some cases.

electrode in zinc-chlorine batteries. During anodization, Cl_2 is evolved and it accumulates within the porous graphite structure. In the cathodic direction, the reaction $Cl_2 + 2e^- \longrightarrow 2Cl^-$ is mass-transfer limited by the Cl_2 dissolved in the $ZnCl_2$ solution and through Cl_2 accumulated in the graphite electrode. The reaction order for the cathodic reaction was obtained by the conventional method of varying the bulk concentration of Cl_2; a value $R_{Cl_2} = 0.74$ was obtained. It was assumed that the real reaction order was 1, the smaller value being obtained on account of slow diffusion of Cl_2 from within the graphite electrode to its surface.

Tafel polarization relations for both the anodic and cathodic directions of the reaction consisted of two regions with different slopes. For the cathodic direction, the slope was ca. 40 mV at low overpotentials ($E < 1.0$ V E_H) and ~120 mV at higher overpotentials ($E > 1.06$ V E_H). In the region of low Tafel slope, the fractional coverage by $Cl^\cdot$ was assumed to be small, $\theta_{Cl^\cdot} \simeq 0$ but, increasing to $\theta_{Cl^\cdot} \simeq 1$ at high current-densities. The mechanism proposed for the cathodic reaction followed that suggested by other workers, viz. the reverse of the Volmer-Heyrovsky pathway:

$$Cl_2 + e^- \rightleftharpoons Cl^\cdot_{ads} + Cl^-$$

followed by a rate-determining step

$$Cl^\cdot_{ads} + e^- \longrightarrow Cl^-$$

(iii) Relation of Cl^- Ion Adsorption to that of Other Halides at Electrodes: State of Adsorbed Halide Ions

(a) Introductory Remarks: The state and strength of Cl^- ion adsorption at Pt and other electrodes is relevant to the interpretation of the kinetics of anodic Cl_2 evolution, especially with regard to (1) effects dependent on Cl^- concentration and (2) changes of state of anode surfaces due to chemisorption of Cl^- ion. Before presenting the new work on the dependence of Cl_2 evolution kinetics on Cl^- concentration and on the state of oxidation of Pt electrodes, it will be useful to review briefly the present state of knowledge on adsorption of Cl^- and other halide ions at noble metal electrodes.

The methods that have been used to study halide adsorption at Pt are (1) cyclic-voltammetry, from changes in H and surface oxidation due to halide coverage; (2) relative reflectivity and (3) the direct method, using radioactively labelled ions.

(b) Specific Adsorption of Cl^- and Other Halide Ions: It has been demonstrated by various techniques that halide ions other than F^- are specifically adsorbed on Pt surfaces[2,36,42,43,162,212,213]. The adsorption of halide anions was found[2,36,212,213] to " compress " the hydrogen region in charging curvesor cyclic-voltammetry measurements, and tends to shift the H region of the charging curve to less positive potentials. It was also observed that adsorbed anions block the initial stage of Pt surface oxidation[43,46,162,164]. It has been found that the adsorption of halides at Pt increases in the order $F^- \ll Cl^- < Br^- < I^-$ at the same electrode potential and for a given bulk concentration. Most studies were done at halide concentrations $> 10^{-3}$M.

Gilman[214] studied the effect of adsorbed Cl^- ions on anodic

charging curves obtained in 1M $HClO_4$. When 10^{-3}M HCl was present, a substantial modification of the anodic charging curve was observed, caused by the " compression " of the oxide region due to adsorption of Cl^- ions.

Breiter[162] used a periodic potentiostatic technique and impedance measurements in a systematic study of the adsorption of halide ions with different additions of HCl, HBr and HI (10^{-6} - 10^{-2}M) at smooth Pt in 1M $HClO_4$ solution. From previous work[2,36,212,213] on halide ion adsorption, it was found that over the potential range between H_2 evolution and O_2 evolution, halide ions exhibit competitive adsorption with H-atoms[2,36,212,213] in the H-region as well as with oxygen species in the oxide region[43,215]. Thus, by following changes in the shape of the voltammograms resulting from increasing concentration of halide ions in the solution, it is possible to obtain information on the adsorption of these ions. Since the three halide ions, Cl^-, Br^- and I^-, are discharged to form the respective elements at potentials less positive than that for O_2 evolution (at a detectable rate) it was considered that halogen evolution will always occur prior to O_2 evolution. This means that the range of potentials for surface oxidation of Pt is diminished in the presence of halide ions in comparison with that for halide-free solutions, apart from the initial blocking effects referred to earlier. The kinetics of evolution of the respective halogen elements were studied in a number of papers, e.g. Cl_2 evolution[144,149,152,155,168], Br_2 evolution[152,165] and I_2 evolution[216].

In the case of Cl^- and Br^- ions, Breiter[162] found (a) that the adsorption at Pt is noticable already at low concentrations, 10^{-4} and 10^{-6}M, respectively; (b) that the adsorption also occurs over the H region and (c) when a potential of 0.8 V E_H is reached, adsorbed halide ions

cause blocking of surface oxide formation. Breiter[162] suggested that adsorbed halide ions partially replace electrodeposited oxide species. In the cathodic direction of the sweep, adsorbed halogen ions can be desorbed in the H region if their concentration is not too high. Since Br_2 evolution occurs at less positive potentials than Cl_2 evolution, Breiter also concluded[162] that Cl_2 evolution most probably occurs in parallel with oxide formation processes while, in the case of Br_2 evolution, it proceeds on the Pt surface which is not as yet covered by oxide species.

I^- ions exhibit much stronger adsorption than Cl^- and Br^- ions[217] and they are more strongly adsorbed than H-atoms[218], causing a diminution in the accessibly measurable H coverage at Pt. The adsorption of I^- is more complex since already at a concentration 10^{-6}M I^-, the formation of I_3^- species occurs in parallel with oxide formation and the I_2 evolution reaction. Oxide formation in this case is strongly hindered by competitive and strong I^- adsorption. Another type of reaction might also be mentioned; it occurs at high concentrations of halide ion solutions. Under such conditions, Pt electrode surfaces can undergo significant anodic dissolution by forming complexes of the type PtX_4^{2-}. However, as pointed out by Breiter[162], this reaction does not occur in the studies on competitive adsorption of halide ions since the concentrations are usually kept very low in comparison with the concentration of the supporting electrolyte ($HClO_4$ or H_2SO_4).

Adsorption of Br^- ions on platinized Pt electrodes in 0.5M H_2SO_4 has been studied by tracer methods by Bagotskii et al[161,219]. The aim of this work was to investigate the effects of Br^- ion adsorption on both H and oxide coverages at Pt electrodes. In order to determine surface coverages of the electrode upon adsorption of Br^- ion, they used three parallel techniques: (a) measurement of decreases in oxygen adsorption;

(b) observation of redistribution of adsorbed hydrogen amongst the multiple states of adsorption and (c) measurement of decrease in methanol adsorption. The first technique, if used above 1.1 V E_H, leads to oxidation of adsorbed Br^- and thus could be employed only for the potential range 0.5 V to 1.1 V E_H. In the second method, the amount of H strongly bound to the Pt surface decreases as a result of Br^- adsorption but the amount of weakly bound H apparently increases. The third method is based on the fact that when a Pt electrode covered with adsorbed Br^- ions is placed in a solution of MeOH of such a concentration that, in the absence of adsorbed Br^- ions, a monolayer of MeOH would cover the surface, the MeOH will be found to adsorb only on that fraction of the surface not occupied by Br^- ions. The coverages in all three methods can be determined by fast anodic or cathodic pulse methods in which the decrease in total charge for either oxide or hydrogen adsorption is measured. A limiting coverage by Br^- ions was reached at concentrations of $Br^- \geq 10^{-6}$M in the potential range 0.3 - 1.0 V E_H on smooth Pt electrodes. When the limiting coverage of Br^- ions was attained, there could be 0.4 monolayer of oxide co-adsorbed on the surface. At potentials higher than 1.0 V E_H, a decrease in surface coverage by Br^- ions occurs due to oxidation of Br^- ion to Br_2.

An interesting difference between the state of adsorbed Cl^- ion at Pt and that of Br^- or I^- was determined by Sobkowski and Wieckowski[220] in studies of competitive adsorption with MeOH. The rate of adsorption of MeOH at 0.5 E_H was decreased in the presence of halide ions when simultaneous adsorption of a given ion and the molecule was taking place. However, the effect of Cl^- ion in decreasing the rate of MeOH chemisorption (MeOH is dissociatively chemisorbed at Pt as $Pt_3C\text{-}OH + 3PtH$) was found to be greater than that of I^-. If MeOH was <u>previously</u> adsorbed on the electrode and

halide ions then added, the organic species were competitively desorbed only by Cl^- ions. The differences in behaviour of the halide ions were attributed (a) to the greater electrostatic interaction of the Cl^- ion with Pt and (b) in the case of Br^- and I^-, to some reactions of these ions with the species derived from chemisorption of MeOH.

Since experiments at Pt are usually performed in H_2SO_4 solutions, it is of interest to know the degree of adsorption of HSO_4^- ions at Pt surfaces. Such experiments were performed by means of the potentiodynamic triangular sweep technique as well as by radioactive tracer measurements by Bagotskii et al.[93] and Balashova and Kazarinov[92]. The maximum value of surface coverage of HSO_4^- ions was found to be 18%[92] and it is concentration-dependent; in more concentrated H_2SO_4 solutions Bagotskii et al.[93], found it reaches 21% coverage of the surface. The specific adsorption of HSO_4^- ions is thus much weaker than that of Cl^-, Br^- or I^- ions.

Hubbard et al.[221] used the cyclic-voltammetry method to define the properties of chemisorbed layers of F^-, Cl^-, Br^- and I^- on Pt electrodes. They found that each of the chemisorbed halide species had an influence on the H and O adsorption regions of the i-V curves but the most dramatic changes occurred with I^-. When the surface is exposed to 1 mM aqueous solution of NaI, the I^- adsorption completely prevents H and O electrodeposition over the normal ranges of potential characteristic of the clean Pt surface[162]. The changes in the i-V profiles are not so drastic in the case of Br^- and Cl^- and are least for F^-, although the compression of H and O electrodeposition/desorption peaks is obvious. As Breiter[162] showed, halide ion adsorption has the effect of decreasing the amount of H deposited at a given electrode potential so that the current peaks are shifted to less positive potentials. Hubbard et al.[221] pointed out that the chemisorption of halides on Pt surfaces is an irreversible process, e.g. the chemisorbed

halide ion is not removed from the surface until the surface is cleaned at high negative electrode potentials. Chemisorbed layers of Cl^-, Br^- or I^- were found to be less reactive with respect to oxidation than the corresponding free ions in solution.

Aqueous I^- anion was shown to react with the Pt surface to form uncharged adsorbed species. On the other hand, F^-, Cl^- and Br^- are adsorbed in the anionic form. Thus F^-, Cl^- and Br^- cause the electrode surface to be less positively charged. The I^- causes an opposite effect. This was deduced on the basis of the negative shift in " rest " potential of a Pt electrode when I^- anions are adsorbed. The reason for this behaviour was given (a) by Bagotskii et al.[201] who proposed that the shift in potential is due to the specific adsorption of I^- in anionic form and (b) by Hubbard et al.[222,223] who showed that chemisorbed I^- is converted to a neutral species which displaces (or replaces) adsorbed anions and thus shifts the outer Helmholtz layer potential. These measurements were done using thin-layer electrodes[221,224] consisting of a specially pretreated Pt rod electrode positioned concentrically within a close-fitting precision capillary. The electrode surface in a " clean " state was obtained by heating the electrode in an oxygen flame after which it was cycled in 1M $HClO_4$ solution to remove any remaining traces of organics from the surface. Prior to the adsorption experiment, the electrode was reduced at 0.0V E_H to remove the surface oxide and then it was exposed to the halide solution for 180 s at open-circuit in order to obtain a reproducible surface coverage by the adsorbed ion. " Thin-layer " coulometry was used to determine the charge associated with adsorbed halide ions on the Pt surface by comparing the experimental values of ion coverages with theoretically calculated charges.

The electrochemical investigation of adsorption of anions on Pt surfaces shows that anions such as Cl^- and Br^- lead to a redistribution of H adsorbed over the H region, but cause only a small change in the total H coverage. These anions also block the formation of surface oxide at more positive potentials (≥ 0.8 V E_H). The I^- anion, however, exhibits quite different behaviour since its adsorption reduces the amount of H which can be adsorbed as well as the oxide. Adsorption of halide ions was also studied on Ir electrodes by Bagotskii et al.(225).

The surface properties of Pt, Rh and Ir electrodes in solutions containing F^- anions were studied by Frumkin et al.(226,227). Measurements were made(226,227) from galvanostatic and potentiodynamic charging curves, and the so-called isoelectric potential shifts(228) were also determined. The absorbability of F^- ions on Pt, Rh and Ir was found to be substantially less than that of SO_4^{2-} or ClO_4^- which previously(92,93,201) were considered to be the least specifically adsorbed at platinum metals. On the basis of isoelectric potential shifts (potential shift due to adsorption of surface-active ions at constant electrode charge) coupled with the charging curve measurements, it(225) was possible to characterize quantitatively the dependence of F^- adsorption on potential at the above electrodes. In the range of potentials 0.5 - 0.8 V E_H , F^- ion was markedly less adsorbed than SO_4^{2-} ion. As the potential is shifted to more positive values, the amount of adsorbed F^- and SO_4^{2-} ions on Pt, Rh and Ir surfaces decreases due to their displacement with adsorbed oxide species. It was found that the amount of adsorbed F^- ion is greater at Rh and Ir than on Pt in the H and " double-layer " regions. This was ascribed to the fact that oxide adsorption at Rh and Ir occurs at less positive potentials than on Pt (< 0.4 V E_H). The displacement of H region peaks in potentiodynamic sweeps shows the

shift in the ionization region of adsorbed hydrogen towards more anodic potentials at Rh and Ir electrodes in 0.14M HF solutions, while in the case of Pt only a decrease in the $H_{2,C}$ peak (see Fig. 2) was observed. This type of experiment also confirmed that at Pt hydrogen is much more strongly bound than the F^- ion, while at Pt, Rh and Ir, F^- is the most weakly adsorbed anion .

Since the effects of specifically adsorbed Cl^-, Br^- and I^- ions are found to be detectable already at very low concentrations, it is useful to mention that some standard concentrated reagents normally used for preparation of supporting electrolyte solutions contain significant traces of halide ions, e.g. conc. H_2SO_4, conc. H_3PO_4 and conc. $HClO_4$ contain 0.00005%, 0.0003% and 0.003% of Cl^- ions, respectively. Horanyi et al.(203) employed the radiotracer technique(202) to determine the effects such low concentrations of Cl^- ions could have on other adsorption processes at Pt surfaces. They concluded that even slight contamination of standard mineral acids with Cl^- ions would result in a sharp change in the adsorption behaviour of these acids on Pt.

(c) Reflectivity and Halide Ion Adsorption: An interesting study of halide ion adsorption on Au was performed by Yeager et al.(229) using the specular reflectance technique. It was found that the reflectivity vs. potential curves depend on the halide ion concentration at potentials where halide ions are adsorbed. As the halide ion concentration is increased, the reflectivity decreases and approaches a limiting value at higher ion concentrations (up to 10^{-4}M). At that point it was stated that the diffusion of halide ions to and from the electrode becomes the rate-controlling process. From the reflectivity and voltammetry data, the so-called " adsorption potentials " (the potential for maximum rate of change of reflectivity

with potential) were estimated for I^-, Br^- and Cl^- anions, and were linearly dependent on the third power of ionic radius; this indicates that the principal factor responsible for adsorption of these three ions is their polarizability, but lone-pair donicity may be an equally significant and more ion-specific factor that was not considered.

Halide adsorption on Pt electrodes was also studied by ellipsometry by Chiu and Genshaw[230], where the main effect is a diminution of the ellipsometric parameter, Δ. They found, however, that ellipsometry is not as sensitive as voltammetric techniques[162,201] since Br^- adsorption was detectable from 10^{-6}M solutions by the latter method but only at concentrations > 10^{-3}M in ellipsometry.

Barrett and Parsons[231] measured the relative reflectance changes, $\Delta R/R_{\parallel}$, caused by Cl^- and Br^- ion adsorption on Pt and showed that lowering of the reflectance was detectable even with 10^{-5}M solutions of bromide. They stated that the increase in coverage of adsorbed Br^- ions with increasing anodic potential could be determined from the lowering of $\Delta R/R_{\parallel}$ caused by the presence of Br^- ions in the solution.

Gottesfeld and Conway[232] showed, in reflectance measurements, that the transition between electrostatic adsorption and chemisorption of halide ions could be distinguished during the anodic polarization of a mercury electrode in halide ion solutions. A reversal of sign in the plot of $(\Delta R/R)_{\parallel}$ vs. V, detected at ca. -200 mV vs. the Hg/Hg_2Cl_2 reversible potential, could be explained only by an absorbing surface film formed due to partial covalent bonding between the specifically adsorbed anions and Hg atoms.

Gottesfeld and Reichman[233] used combined ellipsometric-reflectometric measurements to follow halide anion adsorption at very low concentrations at Pt. Two effects are involved: the change of optical constants with anion coverage and their change with potential. As the coverage of adsorbed

halide anion increases (viz. θ_{Br^-}) at a constant potential, this causes an increases in the refractive index on the solution layer adjacent to the electrode[230] and also causes a modulation of the complex dielectric constant of the surface metal atom layer due to the increase in excess positive charge. These two contributions were estimated as $(\partial\Delta / \partial\theta_{Br^-})_V$ for constant potential. The change of electric field across the film of adsorbed bromide ions at constant coverage may also result in a modulation of the optical constants of both the metal surface layer and the layer of the specifically adsorbed ions themselves (polarization effect). These effects were considered in terms of $(\partial\Delta / \partial V)_{\theta_{Br^-}}$ for constant Br^- adsorption; this derivative was found to have a negative sign due to anionic coverage. The explanation was given in terms of a field-induced charge-transfer model in which the field-induced charge-transfer from the adsorbed layer to the metallic substrate results in a decrease of the effective film thickness and its refractive index, as well as its extinction coefficient.

A concentration of 8×10^{-4}M Br^- is known[162] to cause considerable adsorption of Br^- ion at Pt resulting in a decrease of Δ with increasing potential in the " double-layer " region. The decrease in Δ due to oxide formation was found to be shifted to higher anodic potentials in the presence of Br^- ion; this is consistent with the cyclic-voltammetry behaviour. Also the lowering of $(\Delta R/R)_{\parallel}$ with anodic polarization in the " double-layer " region was stronger in the presence of 8×10^{-4}M Br^- ion. When 8×10^{-4}M Cl^- was used, ellipsometric measurement of cathodic desorption of Cl^- showed that the changes in the " double-layer " region are larger than with Br^- ion.

Yeager et al.[234] studied the specific adsorption of Br^- ions on gold in the presence of a large excess of non-specifically adsorbed

supporting electrolyte, NaF, by the specular reflectance technique accompanied by cyclic-voltammetry studies. The change in relative reflectance, $(\Delta R/R)_{\parallel}$, produced by the addition of Br^- at a given potential could be correlated with the change in charge obtained from cyclic-voltammetry curves for the same concentration of Br^- ion at a given potential. This led to the conclusion that the reflectance changes are directly proportional to the coverage by the specifically adsorbed halide ion. The change in optical properties of the surface due to the adsorbed layer was due to the replacement of solvent molecules by the halide ions. Since the reflectivity changes with Br^- were less pronounced than those produced by adsorption of I^- on Au, where localized orbital interactions were assumed[235], the bonding of Br^- to the surface was assumed to have much less covalent character.

(iv) Conclusions: From the above review of previous work on the kinetics and mechanism of anodic Cl_2 evolution, and on adsorption of Cl^- and other halide ions, it is concluded that the role of coverage of Pt anodes by the surface oxide film in the kinetics of Cl_2 evolution is poorly understood. The situation is evidently complicated by the dependence of this coverage on Cl^- ion adsorption, as found in various previous works. Also, the potential dependence of oxide film coverage and Cl^- ion adsorption has not been well defined. These are clearly matters which are likely to be of importance in the interpretation of anodic Cl_2 evolution kinetics; for example, they complicate the significance and interpretation of reaction orders in $[Cl^-]$.

The work described in Chapter II gave information on the role of the oxide film in the kinetics of Cl_2 evolution in TFA/H_2O mixtures. In the new work to be described below in this Chapter, an attempt has been made to examine the effects of Cl^- concentrations on the kinetics up to high Cl^- concentrations and relate it to (a) the mechanism applying; (b) the reaction order and (c) the Cl^--dependent state of the oxidized Pt surface which (d) determines the catalytic properties of the electrode for discharged Cl· recombination.

2. EXPERIMENTAL

(i) Methods: In order to characterize the electrocatalytic behaviour of the Pt electrode surfaces in Cl^- solutions at various concentrations, steady-state current-potential relations were obtained potentiostatically at a rotating-disc Pt electrode. Measurements were made in both ascending and descending directions of potential change. Currents were recorded on a Sensitive Research micro-milliammeter and potentials were read from a previously calibrated digital millivoltmeter. Currents were measured 30 s after each adjustment of potential; this procedure enabled very reproducible curves to be obtained. In all the steady-state measurements, Cl_2 gas (1 atm) was bubbled through the solutions, the whole apparatus being maintained in a fume hood.

The log [current-density] vs. potential curves all exhibited (see below) an approach towards limiting currents at elevated potentials (cf. 168) so that it was important to conduct a series of runs at

various rotation speeds in order to evaluate the role, if any, of mass-transfer control at high current-densities. For similar reasons, " iR " corrections were made to the data by obtaining the iR drop values, ΔV, by the current interruption technique, using a vacuum relay and recording ΔV on an oscilloscope with a fast time-base setting. Small but significant values of ΔV arose at high current-densities and were linear in i.

Cyclic-voltammetry experiments were conducted in the usual way[22a,69] in order to evaluate oxide film coverages or the degrees of surface oxidation of the Pt electrode in terms of e per Pt atom in the surface, based on[66] a charge for deposition of an H monolayer of 210 $\mu C\ cm^{-2}$. The observed charge for monolayer H desorption (anodic sweep) gave the real area of the electrode and hence the real current-densities corresponding to the Cl_2 evolution current measurements, based on the above figure of 210 $\mu C\ cm^{-2}$ (real area).

After each run at ascending and descending anodic currents, the electrode potential was returned to a value (0.05 V E_H) at which the oxide film formed on the Pt electrode surface in aqueous solutions would have been reduced. This procedure was adopted prior to each evaluation of the current-potential relationship for Cl_2 evolution, in order to achieve reproducible initial Pt surfaces, as in the work in TFA (Chapter II).

(ii) Rotating Pt Disc Electrode: The electrode (Pine Instrument Co., Pa.) mounted in Teflon was used for all experimental runs. The same rigorous cleaning procedure was employed as already described in Chapter II, Experimental Section (iii), page 72.

(iii) Solutions and Salts: A.C.S. analytical grade KCl used in this work was recrystallized twice and dried at 150°C in vacuo. The KCl solutions at various concentrations were made up with analytical grade aq. HCl to give solutions 0.05M in the acid. Water used as solvent was pyrodistilled, following two regular distillations, according to the procedure described previously[73].

(iv) Oxide Coverage in Cl_2 Evolution Experiments: The coverages or quantities of electrodeposited O species generated just up to Cl_2 evolution were evaluated in various solutions from the cathodic current vs. potential profile in a cyclic-voltammetry curve obtained at the Pt disc electrode rotated at a nominal slow rate (400 r.p.m.), in the same way as described previously in Chapter II, Experimental Section (iv), page 74.

Another technique was also used to estimate the actual percentage of the surface blocked by Cl^- ions. This procedure was based on the fact that adsorbed Cl^- ions block the formation of surface oxide on Pt, as well as modify both the cathodic and anodic H regions (see Chapter I and refs. 162,201). Since the charges corresponding to the oxide coverages could be accurately obtained in the case of Cl^--ion-free solution and for solutions containing Cl^- ions at various concentrations by following the procedure already described (Chapter II), it was of interest to evaluate the percentage of the surface oxide blocked in terms of the change of oxide formation charge at the Pt electrode surface as a function of Cl^- ion concentration. This type of experiment was carried out by means of a precise "micro-titration" procedure; thus the initial solution of 0.05M H_2SO_4 in the

cell was titrated with HCl solution which was added incrementally (10^{-3} cm ^{3}) from a precise micrometer syringe. As the addition of Cl^- ion progresses the " compression " in the oxide formation region and the diminution of the charge for the oxide reduction peak can be easily observed.

(v) Reference Electrodes: Both the H_2 (1 atm)/Pt and (α + β) PdH/H^+ electrodes[195] were used as calibrating reference electrodes. Both were satisfactorily reversible and gave stable potentials. During runs, a Ag/AgCl electrode, formed on a Ag wire mounted within a thin-walled capillary tube acting as a Luggin probe, was used. Cl_2 overpotentials (η) were calculated from the potentials measured vs. the Ag/AgCl electrode, knowing the published standard potential data and information on activity coefficients[195].

3. RESULTS

(i) The log [current-density] vs. Potential Relations: Fig. 15 shows the log [current-density, i] vs. overpotential, η , relation for Cl_2 evolution from 0.5M aq. KCl + 0.05M HCl at the Pt rotating-disc electrode for ascending and descending changes of potential and at a number of electrode rotation speeds up to 6400 r.p.m. The curves show an ascent towards a limiting value of the log of the current-density, characteristic of recombination-control (cf. refs. 180,196) in the kinetics. The data presented in Fig. 15 demonstrate that the currents are not significantly influenced by the mass-transfer rate, so

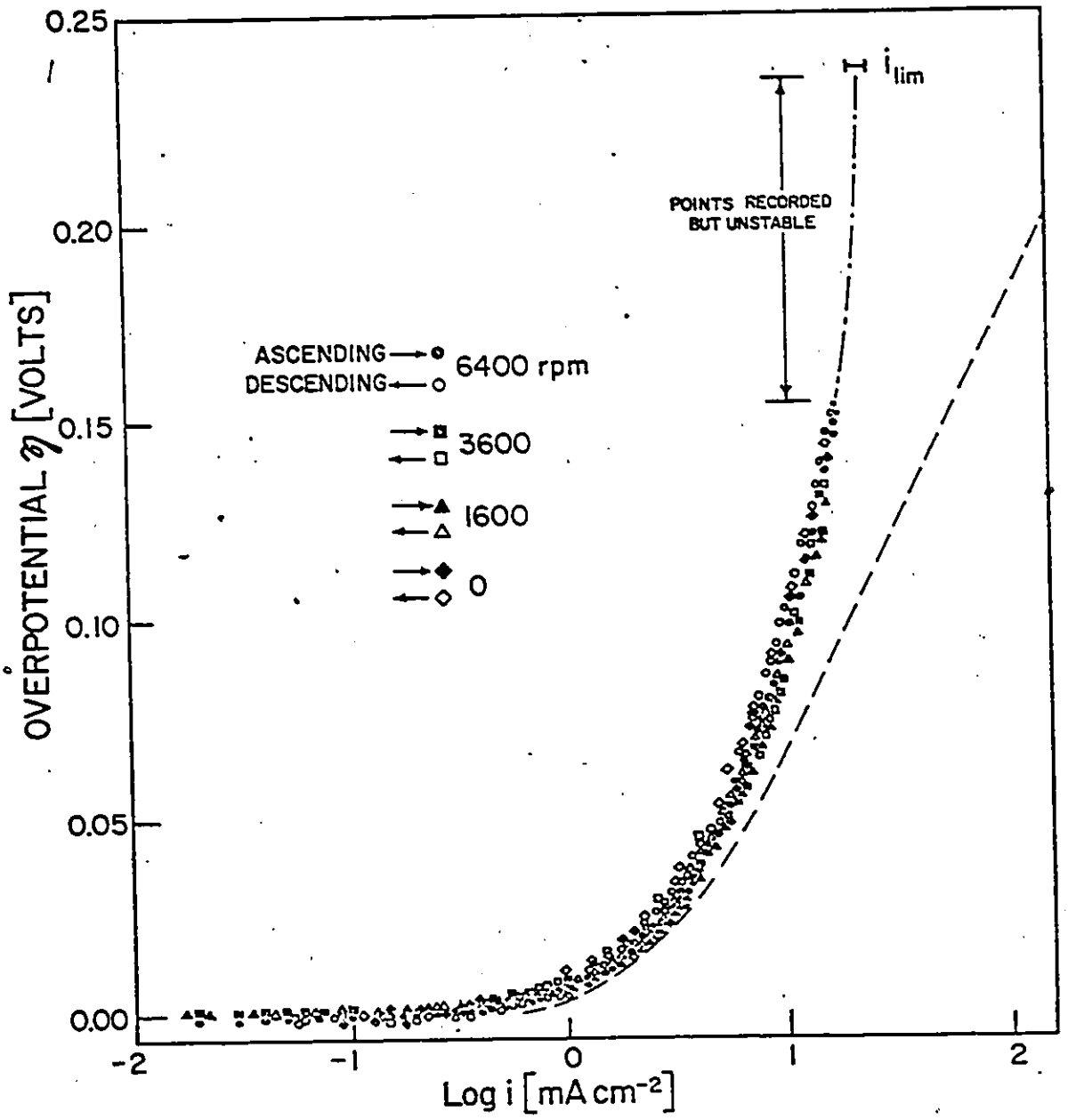

Fig. 15 Log [current-density] against overpotential curves for Cl_2 evolution from aq. 0.5M KCl + 0.05M HCl (298 K) at a rotating-disc Pt electrode at 1600, 3600 and 6400 r.p.m. (—•— ascending change of overpotential; ←— descending changes of overpotential). Separate dashed line is Tafel relation for hypothetical charge-transfer control reaction, with $\beta = 0.5$.

that the approach to the limiting current is kinetically controlled, as was found in previous work in TFA/H_2O mixtures (see Chapter II). It is to be noted that the log i *vs.* η data shown in Fig. 15 have already been corrected for iR drop as mentioned in Chapter II under " Results ", so that this is not the reason for the approach towards apparent limiting current behaviour. It was also shown, by using a " galvanostatic " current generator rather than a potentiostat, that the approach to a limiting current was not an artifact arising from limited current output from the potentiostat.

In subsequent experiments at eleven other concentrations, the log i *vs.* η relations were also recorded at rotation rates of 1600, 3600 and 6400 r.p.m. and iR drop corrections were made to all data points. The results of seven of these experiments are shown in Fig 16. where data taken at 6400 r.p.m. for ascending and descending changes of η are plotted. Mass-transfer control was not significant at any of the concentrations studied. The highest currents recorded in Fig. 16 are those just before a rapid ascent to the respective limiting currents occurs. When the latter behaviour arises, the potentials cease to be steady due to the high slope of the current-voltage characteristics. These effects are observed in both the aqueous and non-aqueous solution work (see Chapter II).

Estimates of the limiting current-densities, i_{lim} , and of ln i_{lim} are shown as a function of Cl^- ion concentration in Fig. 17. There is evidently a clear approach to almost concentration-independent values of i_{lim} at concentrations above *ca.* 0.8 ~ 1.0 M which is probably connected with saturation specific adsorption of the Cl^- ion (see below).

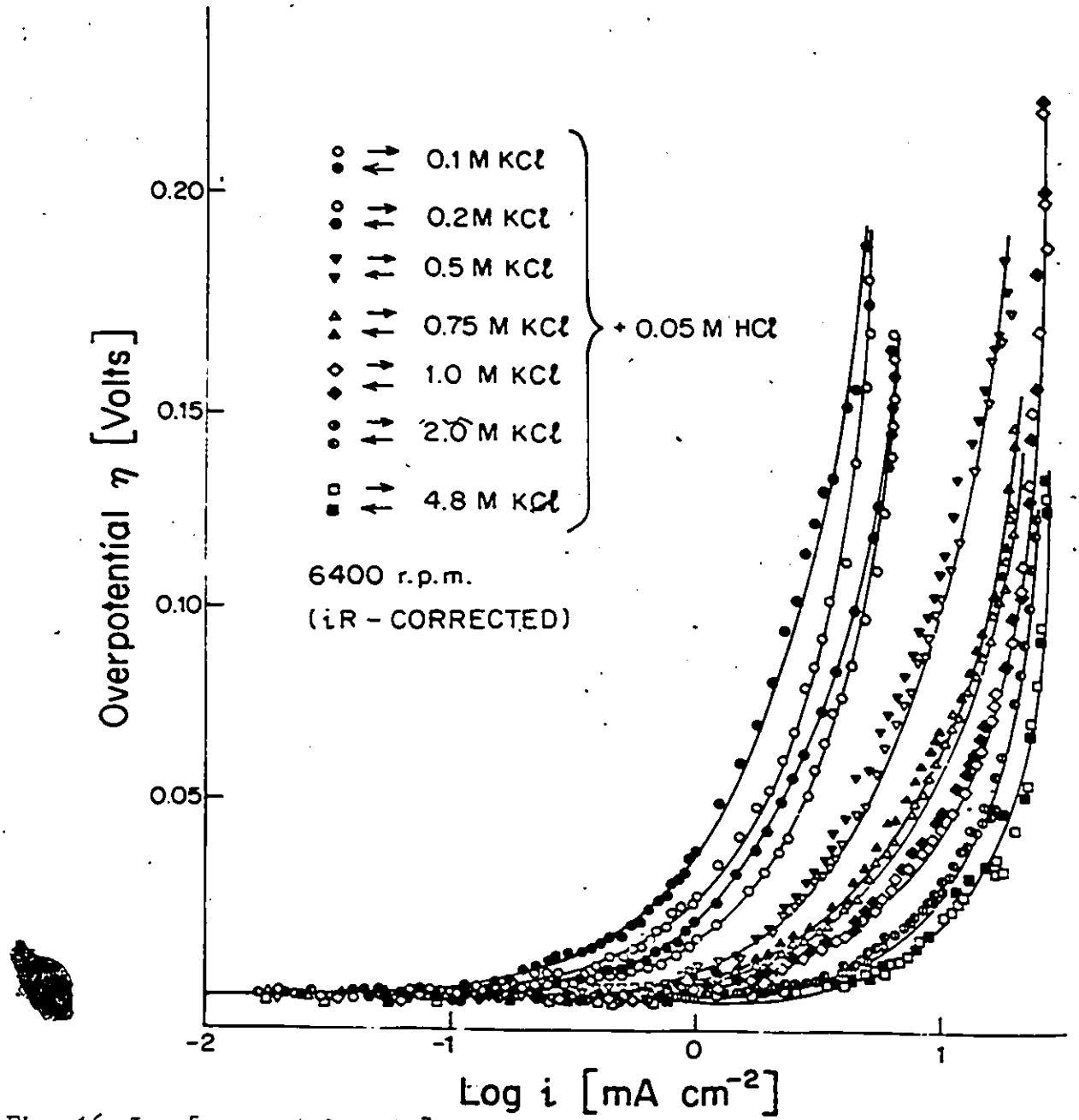

Fig. 16 Log [current-density] vs. overpotential curves for Cl_2 evolution at Pt from aq. solution of 0.05M HCl + various concentrations of KCl. Rotation rate 6400 r.p.m.; T = 298 K. (12 concentrations were studied; the data for only 7 can be conveniently shown on this graph.).

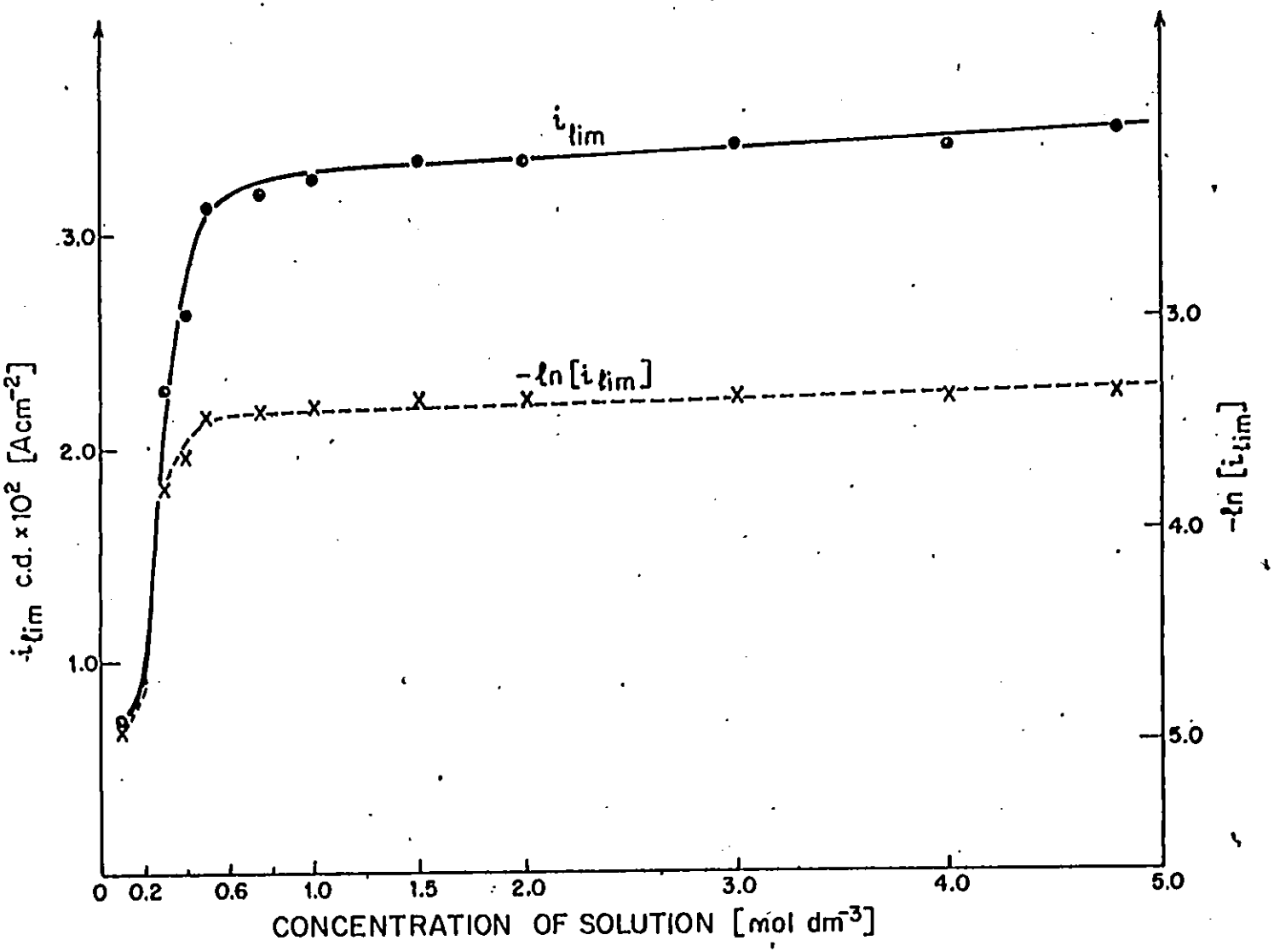

Fig. 17 Estimates of i_{lim} and $\ln i_{lim}$ as a function of the log of the Cl^- ion concentration for Cl_2 evolution at Pt at 298 K.

(ii) Surface Oxidation of the Pt Electrode in Cl^- Ion Solutions: From the cathodic sweep of cyclic-voltammetry curves (examples shown in Fig. 18), the surface oxide generated as a function of potential attained at the positive end of the anodic sweep can easily be measured without (in 0.05M aq. H_2SO_4) and with Cl^- ion present; results of this kind, which serve to characterize the state of the Pt electrode surface in Cl^--containing solutions prior to Cl_2 evolution are shown in Fig. 19 as a function of log Cl^- (as HCl).

These results are obtained by the " micro-titration " procedure described already in the Experimental section (iv), page 140 . The results show clearly that the competitive electrochemical adsorption of Cl^- ions vs. electrodeposition of OH/O species at Pt follows a Temkin type isotherm due to electrostatic interaction effects. That the " Temkin " behaviour with Cl^- is not due to broad heterogeneity of adsorption sites on the Pt surface was indicated in other work in our Laboratory with Br^- and I^- ions which showed that with these ions the competitive adsorption behaviour is not a linear log relation in halide ion concentration. Were heterogeneity the main factor in the Cl^- ion behaviour, the same effect should apply to the other halide ions.

The competitive adsorption effect of Cl^- on surface oxide formation at Pt up to $[\ Cl^-\ ] = 4.8M$ is shown in Fig. 20 for various times, τ_h, of holding the potential at the positive end of the sweep. By making similar measurements, but into the potential region where Cl_2 is evolved at significant rates, the extents of surface oxidation of the Pt electrode during Cl_2 evolution at various overpotentials, can also be determined, as shown in Fig. 20 . These measurements require electrode rotation at

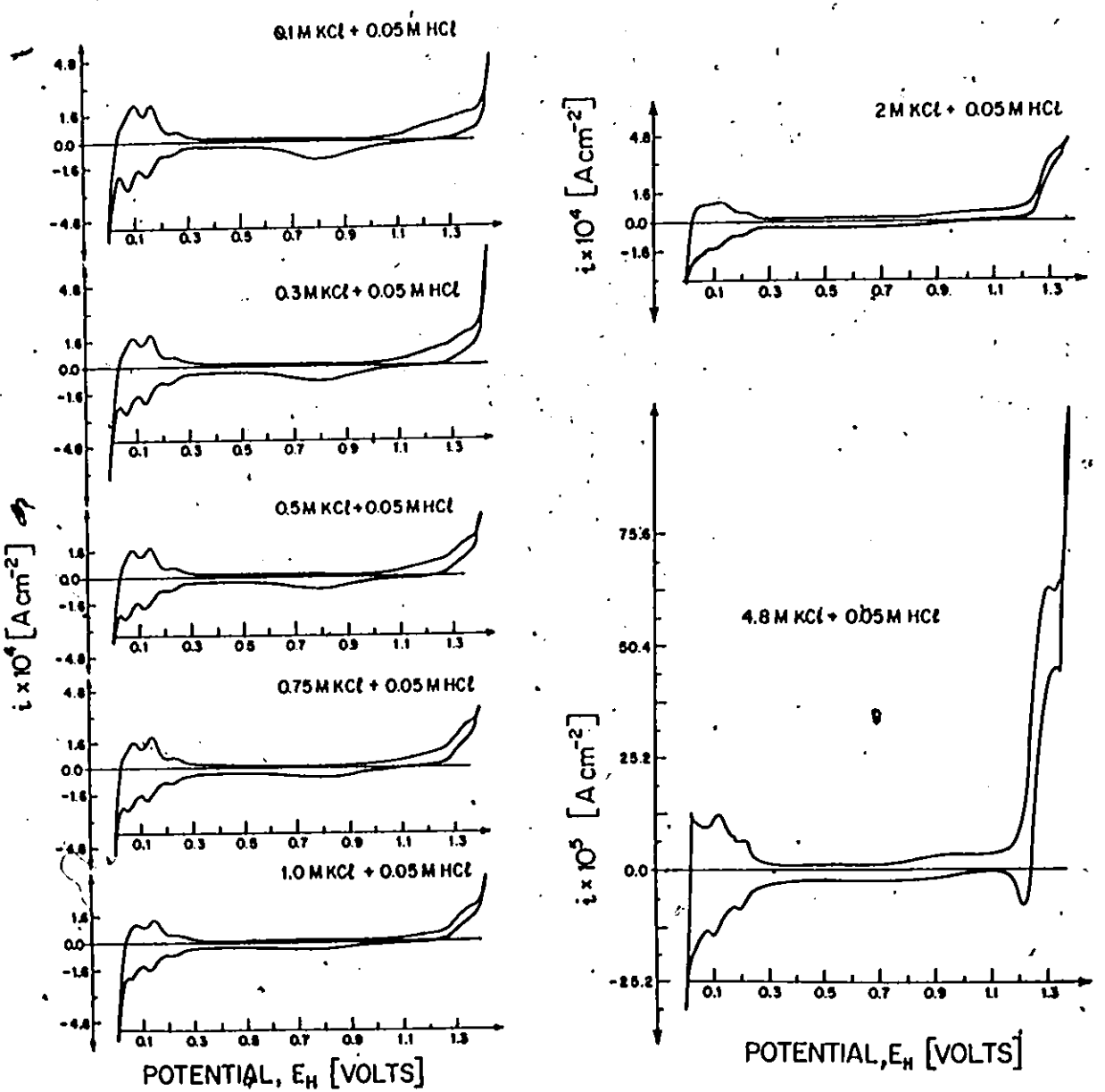

Fig. 18 Family of cyclic voltammetry curves for Pt in various aq. solutions of HCl + KCl at 298 K showing blocking of surface oxidation of the Pt anode.

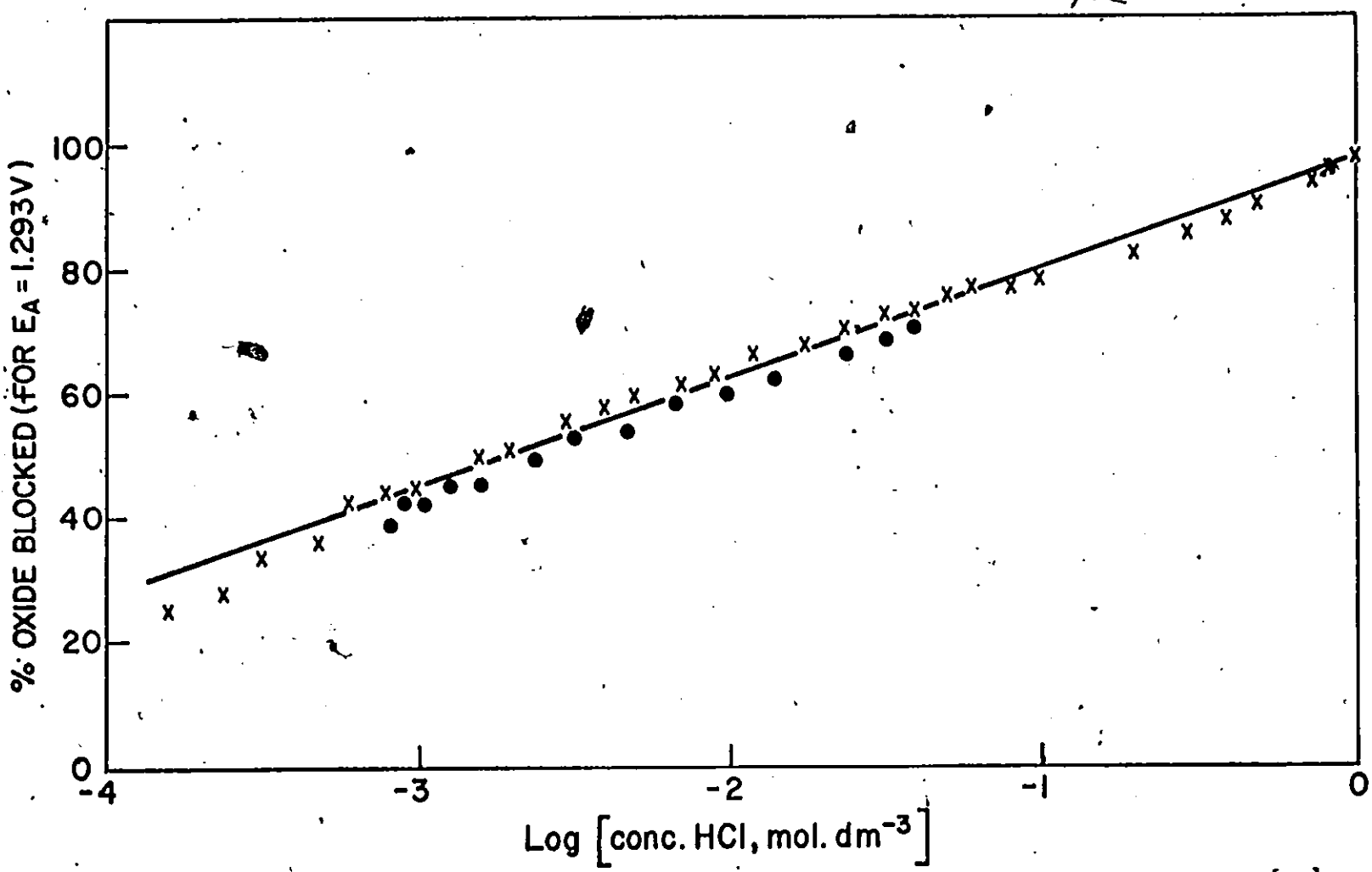

Fig. 19 Linear relation (Temkin behaviour) between % oxide blocked at Pt by Cl^- ion and log $[Cl^-]$. Data for two runs (● and ×) are shown. End potential of anodic sweep = 1.293 V E_H, T = 298 K .

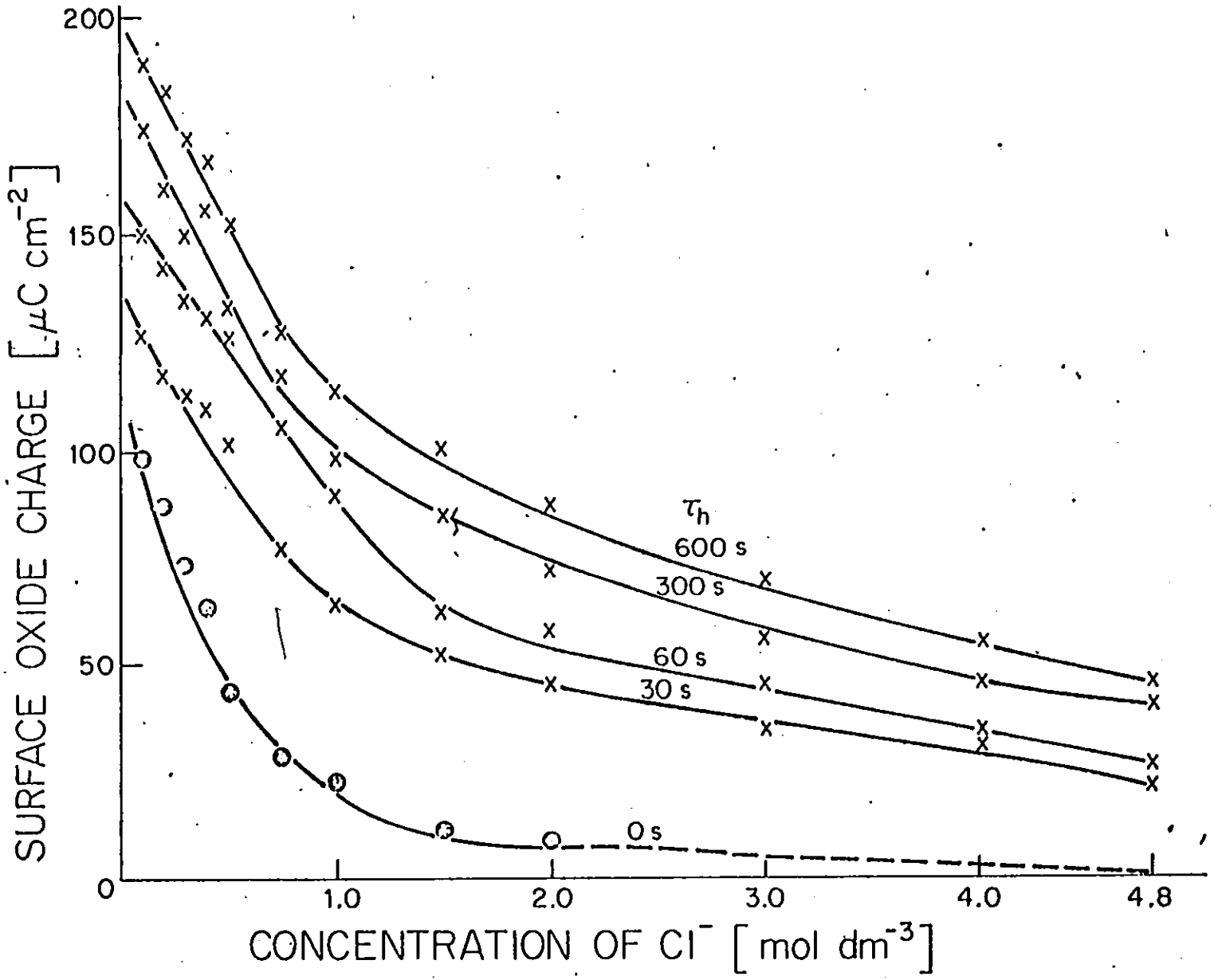

Fig. 20 Plots of surface oxide reduction charge at Pt as a function of [Cl^-] for surface oxide generated in a potential sweep taken to 1.4V E_H with various times τ_h of holding at 1.4V. Sweep-rate = 0.15 V s^{-1} .

appreciable rotation speeds (6400 r.p.m.) in order to avoid currents for reduction of evolved Cl_2 obscuring the cathodic currents for oxide film reduction. As seen in Fig. 20, this procedure works quite satisfactorily, although the oxide film reduction charge cannot be determined quite as accurately as at potentials below those for significant rates of Cl_2 evolution or as accurately as in aq. H_2SO_4 below the potential for O_2 evolution[73,61]. It is found (Fig. 21) that in the presence of Cl^- ion, limiting oxide coverages are attained which are dependent on the anode potentials and are logarithmically dependent on [Cl^-] (Fig. 22). This implies that the coverage by specifically adsorbed Cl^- itself depends on log [Cl^-] as may be expected for general thermodynamic reasons when a Temkin-type adsorption isotherm applies.

(iii) Reaction Order: For electrochemical reactions, reaction orders, R, of various kinds may be defined[206], depending on what condition of constant potential (e.g. overpotential, η , or electrode potential, V) is specified or whether diffuse-layer effects have been rendered almost invariant by use of a supporting electrolyte which maintains constant ionic strength. Other complications due to adsorption also enter into the significance of R. It will be useful therefore first to discuss a little the significance and interpretation of reaction orders,

For ordinary homogeneous reactions, the reaction order R with respect to a species i is simply defined as

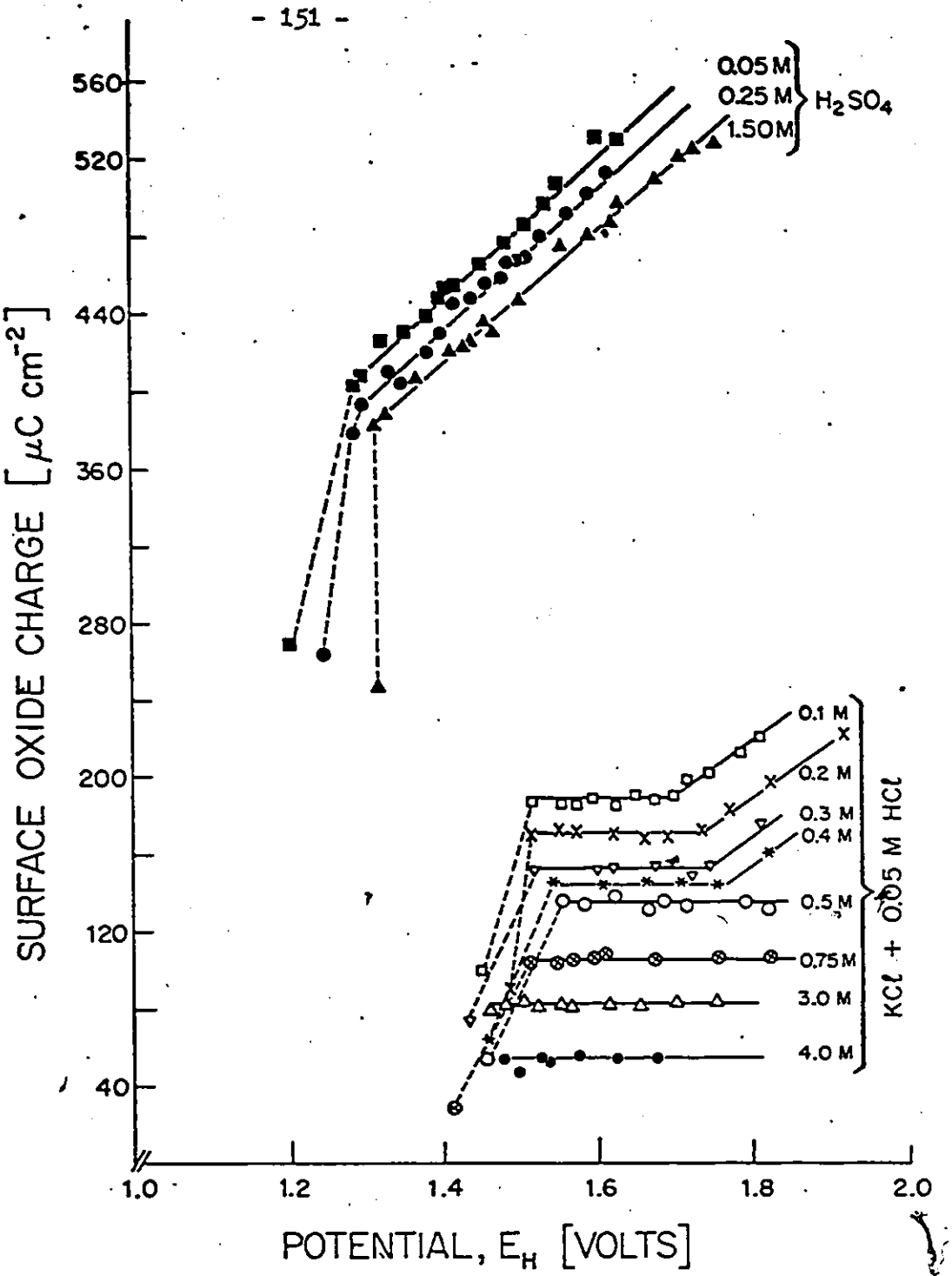

Fig. 21 Plots of surface oxide reduction charge at Pt as a function of potential held for τ_h = 60 s at positive end of potential sweep in Cl_2 evolution region, for various Cl^- ion concentrations. Also shown for comparison is the potential-dependence of surface oxide reduction charge measured in Cl^--free aq. H_2SO_4 solutions. Electrode rotation rate = 1600 r.p.m. Initial points marked are for τ_h = 0 in multi-sweep at the lowest potential.

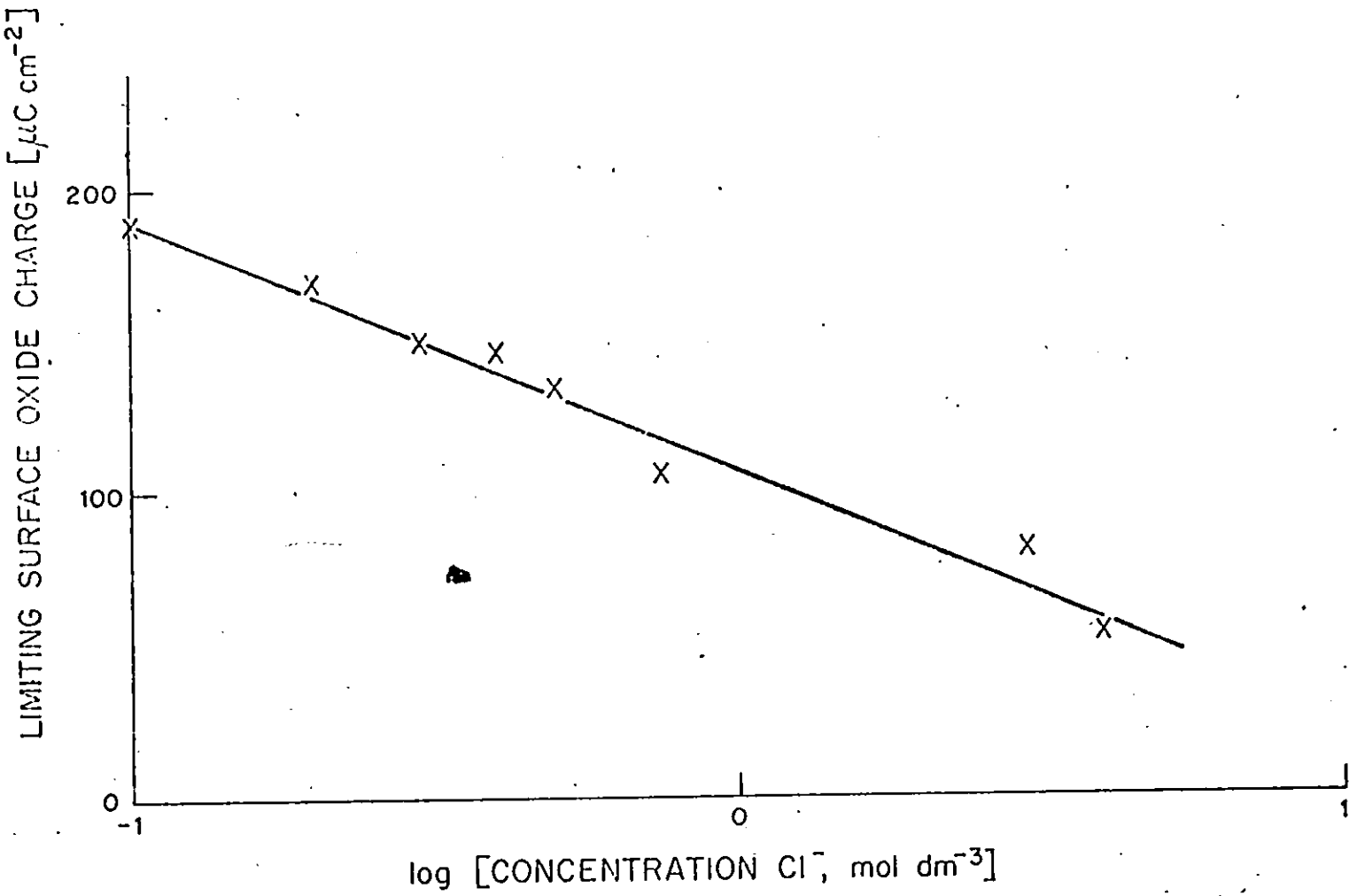

Fig. 22 Values of limiting surface oxide reduction charge at Pt in Cl^- solutions as a function of log [Cl^-].

$$R = \left(\partial \ln v / \partial \ln c_i \right)_{j,k...} \qquad (30)$$

for a reaction rate v dependent on concentration of a reactant species i, when concentrations of any other kinetically involved species j,k... are kept constant.

In heterogeneous reactions, the significance of reaction orders is more complex owing to the adsorption of reactants which usually takes place. Then a surface reaction order, R_s, in terms of coverage θ_i of species i can first be defined as

$$R_s = \left(\partial \ln v / \partial \ln \theta_i \right)_{j,k...} \qquad (31)$$

However, this is usually not the reaction order experimentally measured with respect to bulk concentrations or partial pressures since θ_i is related to c_i by an adsorption isotherm $\theta_i = f(c_i)$ where $f(c_i)$ is also dependent on temperature. Then the observable reaction order, R, is also related to R_s by an equation of the form:

$$R_s = \left(\frac{\partial \ln v}{\partial \ln c_i} \right)_{j,k} \left(\frac{\partial \ln c_i}{\partial \ln \theta_i} \right)_{j,k} = R \left(\frac{\partial \ln \theta_i}{\partial \ln c_i} \right)_{j,k} \qquad (32)$$

so that R can be expressed as

$$R = R_s \left(\frac{\partial \ln \theta_i}{\partial \ln c_i} \right)_{j,k} \qquad (33)$$

where the term multiplying R_s is seen to be the differential coefficient of the adsorption isotherm, plotted logarithmically.

In electrode reactions, further complications arise depending on how R is measured: at constant " electrode potential " or constant overpotential, or in the case where the double-layer potential profile may vary with ionic strength, at constant ionic strength or not. Because the reversible potential of all electrode/ion/molecule reactions depends on the ln of the ionic concentration and /or molecule concentration (Nernst equation), the definition of R for constant overpotential ($\eta = V - V_{rev}$) implies an extra concentration-dependent term in the measurement of R at constant η which does not arise in non-electrochemical reactions. The interpretation of reaction orders of electrochemical reactions must take this into account (cf. refs. 206,209). For example, the reaction order of the Cl_2 evolution reaction at constant η in the absence of added inactive supporting electrolyte would be <u>zero</u> in sufficiently dilute Cl^- solutions due to cancellation of various $[Cl^-]$ - dependent terms - an unhelpful result in mechanism identifications!

In the case of the anodic Cl_2 evolution of interest in the present work, where the kinetics may be controlled by the non-electrochemical Cl·-recombination step, so that the prior Cl^- ion discharge process may be regarded as almost at equilibrium (cf.refs. 168 and Chapter II), the diffuse-layer effects related to the double-layer "ψ" potential[236] cancel out. Then the kinetics are independent of the ionic strength of

the reactant electrolyte[237], as far as electrostatic effects are concerned. However, as will be shown later, effects due to the specific adsorption of the Cl^- ion can lead to a dependence of the limiting chemical recombination rate, i_{lim}, on Cl^- ion concentration or, more explicitly, on its surface concentration at the electrode interface.

From the experimental curves of Fig. 16 , the dependence of log (i) on log[Cl^-]can be plotted, as shown in Fig. 23 , for various overpotentials giving

$$(R)_\eta = \left(\frac{\partial \log i}{\partial \log [Cl^-]} \right)_\eta \qquad (34)$$

Data for the ascending and descending η vs. log i curves are shown in Fig. 23 and give $R_\eta = 0.81 \sim 0.91$ over the Cl^- concentration range 10^{-1} to 10^0 M . Beyond this concentration, $(R)_\eta \to 0$ corresponding to saturation coverage by the specifically adsorbed Cl^- ion. This is also indicated by the trend towards independence of i_{lim} on concentration of Cl^- ion at high concentrations shown in Fig. 17 . The $(R)_\eta$ values for the descending curves are a little higher , near 1.0 . The significance of these $(R)_\eta$ values from Fig. 23 will be discussed later.

4. DISCUSSION

(i) Test of the Recombination Mechanism : The form of the experimental results seems characteristic of a rate kinetically limited by a recombination step involving discharged $Cl^\bullet$ species on the Pt surface according to a reaction scheme of the type (cf. refs. 143,144,146,148,149,160,168,173-175) suggested previously by various workers and treated in Chapter II:

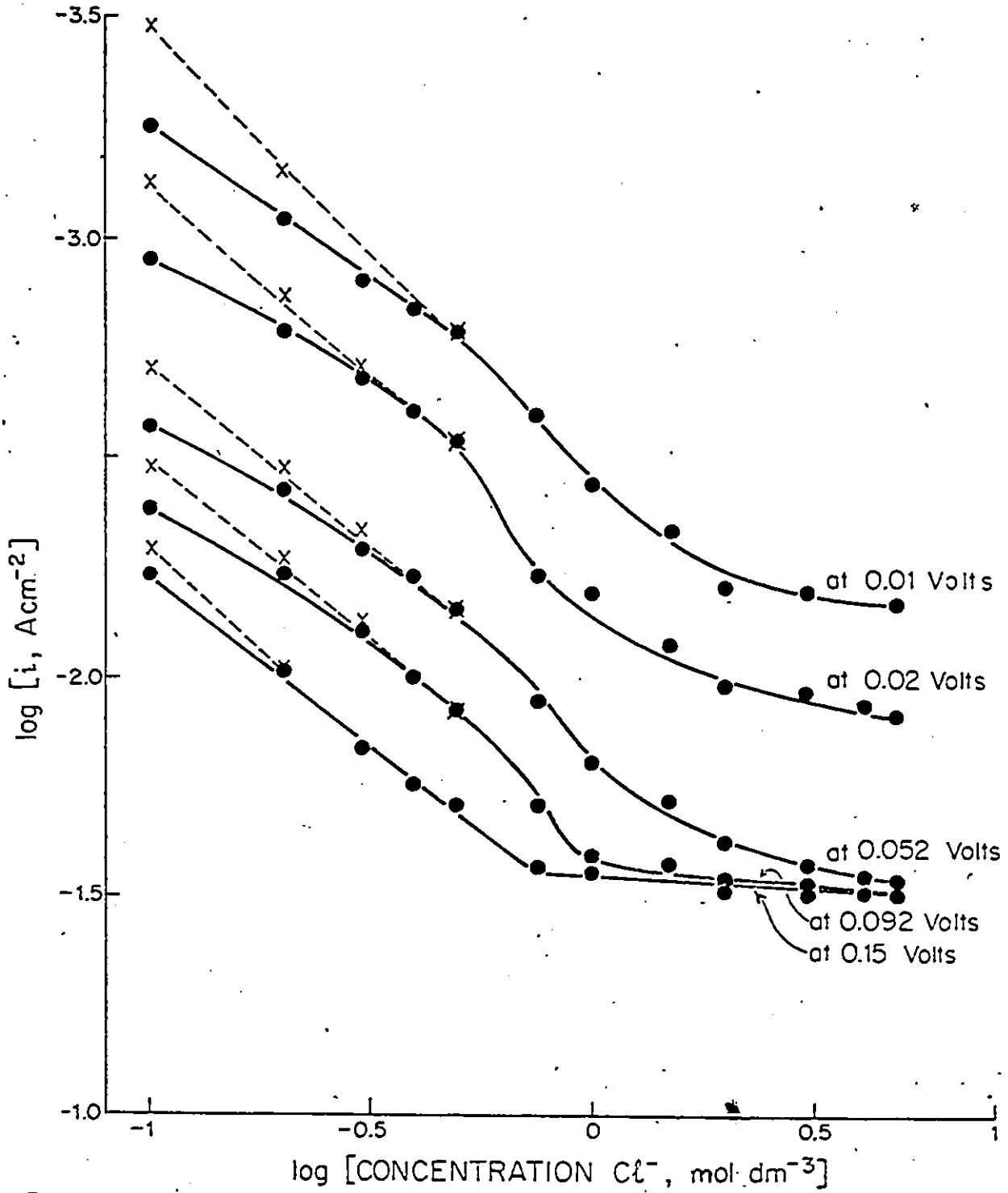

Fig. 23 Experimental reaction order plots for Cl_2 evolution at Pt at 298 K. Log [i] , i.e. current-densities at various constant η values are plotted against log [Cl^-] (——→ ascending and —•---- descending η values).

$$Cl^-_{aq} + Pt(Ox) \rightleftharpoons Pt(Ox)Cl^{\bullet}_{ads} + e^- \qquad \text{I}$$

$$2Pt(Ox)Cl^{\bullet}_{ads} \longrightarrow 2Pt(Ox) + Cl_2 \qquad \text{II}$$

where II is the rate-controlling step and i_{lim} for II arises as $\theta_{Cl^{\bullet}} \rightarrow 1$. Pt(Ox) represents the oxidized (or partially oxidized) Pt electrode surface.

Although the form of the log i vs. η profiles of Fig. 16 appears characteristic of an approach to a kinètically limited rate, it is necessary to examine the form of the i-V profiles quantitatively in a way in which such a mechanism I , II can be more exactly tested. This is also required: (a) because the experimental log i vs. η curves do not show an initial linear region of slope $RT/2F \sim RT/F$ which would normally* characterize a recombination-controlled mechanism at sufficiently low $\theta_{Cl^{\bullet}}$ ($\theta_{Cl^{\bullet}} \leq 0.15$)(as discussed in Chapter II) and (b) because in the work reviewied in Chapter II it has not uniformly been concluded (e.g. see refs. 168,174,175) that recombination-controlled kinetics apply for Cl_2 evolution from aq. Cl^- at Pt, although some authors[143] have reached this conclusion.

In order that such a special test of the mechanism could be

*It is the participation of the back reaction near the reversible potential that causes the observed log[current] vs. potential relations to approach the reversible potential in continuous curves (Fig. 16) without an intermediate linear Tafel region of slope RT/2F or RT/F[197]. The latter will only be observed for $\theta_{Cl^{\bullet}} <$ ca. 0.15 and thus only if the $Cl^{\bullet}$ coverage at the reversible potential is appreciably smaller than this figure, as shown in Chapter II. A linear Tafel section of the log[current] vs. potential relation can, however, be observed in a N_2-bubbled solution in which the Cl_2/Cl^- reversible potential is less positive but unfortunately not well defined due to the uncertainty of local Cl_2 partial pressure.

reliably pursued, the log i vs.η curves were defined by as many experimental points (Fig. 16) as possible, as in the experiments described in Chapter II.

The method proposed in Chapter II enables the kinetic behaviour associated with steps I, II (see p. 82 Chapter II) to be represented over the whole range of θ_{Cl}. and corresponding currents up to i_{lim}, i.e. without restriction to special conditions (cf. refs. 197,238) corresponding to Tafel slopes of RT/2F, RT/F or ∞ (limiting current). If the recombination step II, with I in quasi-equilibrium, determines the rate over a wide range of overpotentials and corresponding coverages, this will be indicated by the two kinds of diagnostic plots described in Chapter II. Thus, in the first procedure, a plot of $\exp[\eta F/RT] / i_2^{\frac{1}{2}}$ vs. $\exp[\eta F/RT]$ [eqn. (9)] should give a straight line of slope $(2Fk_2)^{-\frac{1}{2}}$ and an intercept $(2Fk_2)^{-\frac{1}{2}}/K_1 C_{Cl^-}$, as shown in Fig. 24a . The alternative way of plotting the results, which is based on eqn. (10)[see Chapter II, Discussion section (ii), p. 87] gives a similar test plot but provides a more sensitive basis for analyzing the kinetic behaviour at high θ_{Cl}. .

Both k_2 and $\bar{K}_1$ can be evaluated from the slope and intercept of the plot of $i_2^{-\frac{1}{2}}$ vs. $\exp -[\eta F/RT]$, as shown in Fig. 24b. Were the log[current-density] vs. potential relations simply Tafel lines having constant slopes, the results would not plot out according to eqns. (9) or (10) with intercepts related simply to $\bar{K}_1$ and k_2.

Since the plots in Figs. 24a,b are satisfactorily linear over most of their ranges (the hook at the lower ends of the lines in Fig. 24a can be shown [p. 95 , Chapter II] quantitatively to be due to participation of the back reaction* of step I near the Cl_2/Cl^- reversible potential), recombination-control in the scheme I,II seems to apply for all Cl^- concen-

*See Appendix I. concerning this point.

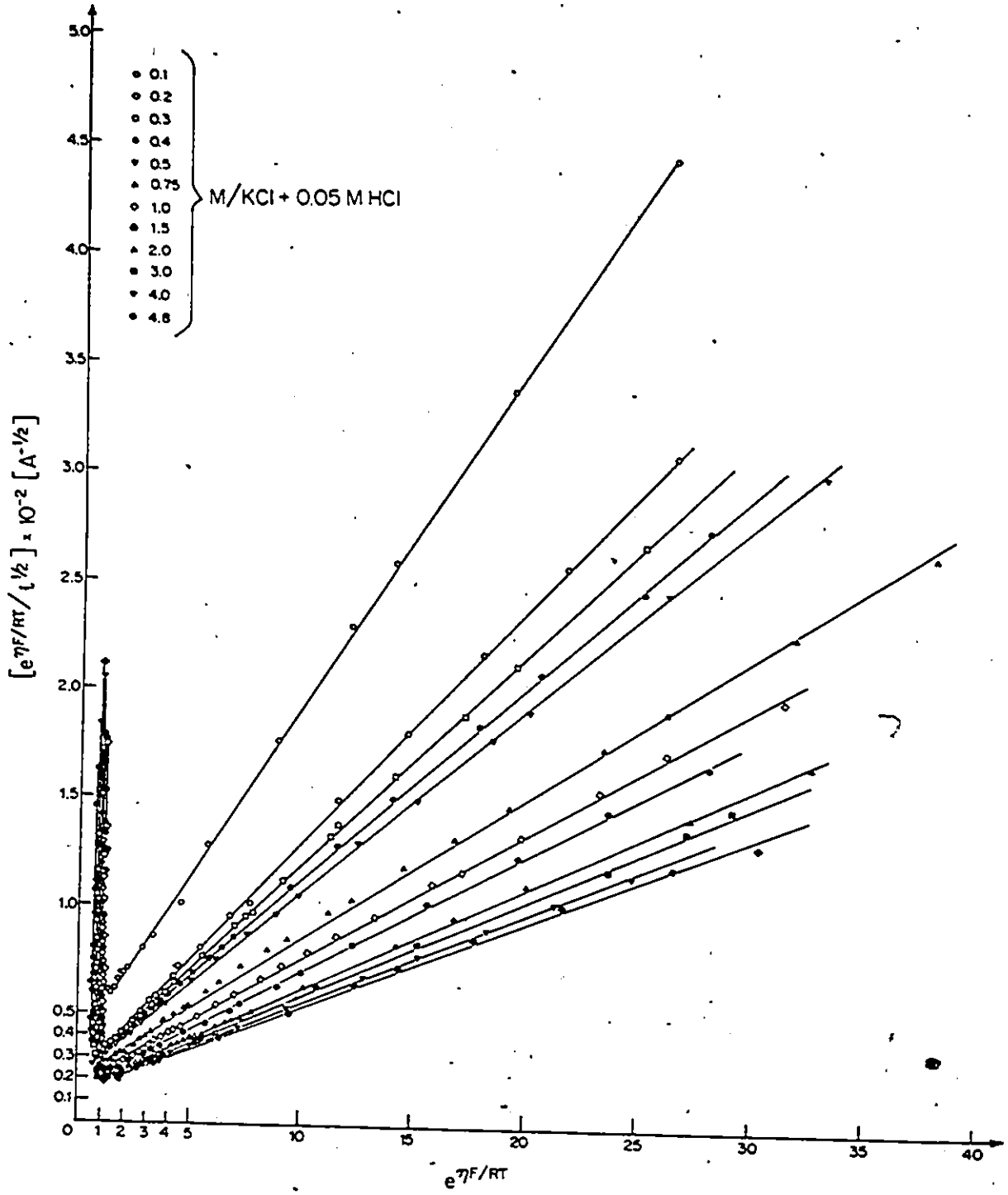

Fig. 24 Theoretically based plots for testing a recombination-controlled mechanism for anodic Cl_2 evolution for various Cl^--ion concentrations: a) $(\exp \eta F/RT)/ i^{\frac{1}{2}}$ against $\exp \eta F/RT$ (Hook at low η end of lines is due to participation of the back reaction.)

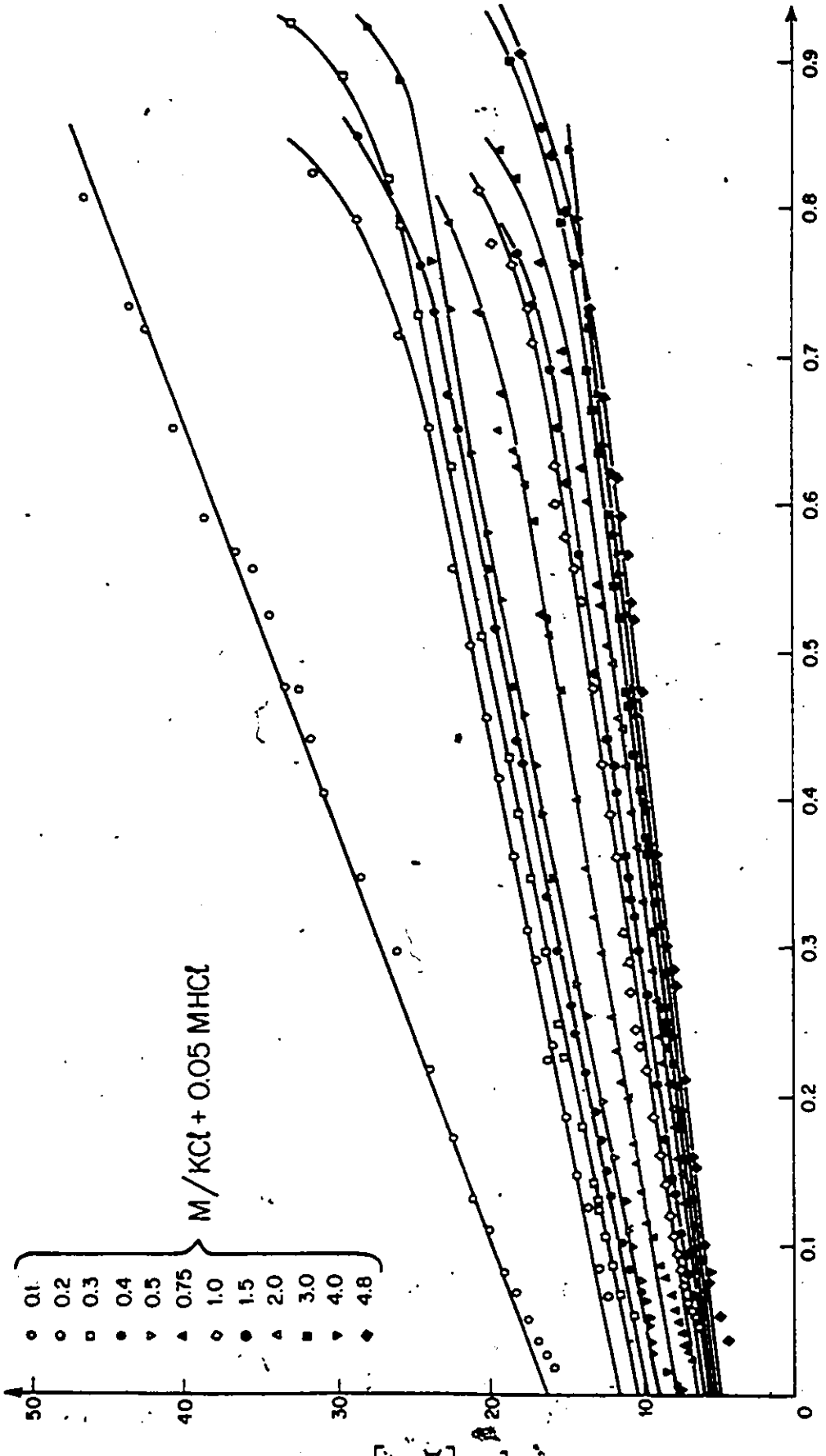

Fig. 24 Theoretically based plots for testing a recombination-controlled mechanism for anodic Cl_2 evolution for various Cl^- ion concentrations:

b) $i^{-\frac{1}{2}}$ against exp $-\eta F/RT$.

trations. Also, values of $\bar{K}_1$ and k_2 can be evaluated for each Cl^- concentration, as shown in Fig. 25 . The relation between log k_2 and log $\bar{K}_1$ over the Cl^- concentration range 0.1 to 4.8 M (+ 0.05 M HCl) is shown in Fig. 26 .

Although the plots based on eqn. (10) (Chapter II) are agreeably linear over most of their range, there is some tendency for downward curvature at the high θ_{Cl}. end (low exp $-\eta F/RT$ values in Fig. 24b). As discussed in Chapter II for the behaviour in TFA as solvent, this is probably due to repulsive lateral interaction effects between electrodeposited $Cl^{\cdot}$ species and between $Cl^{\cdot}$ and OH or O , or adsorbed Cl^- ions. If interaction effects are significant, i.e. if $g > 0$ in eqns. (11) and (12), the kinetic behaviour must be tested by numerical computation methods using eqns. (11) and (13) . Eqn. (13) accounts for the curvature at the high θ_{Cl}. end of the plot in Fig. 24b for 0.5M KCl + 0.05M HCl, taking a value of $g = 2 \sim 3$ RT mol^{-1}, as was also shown in Chapter II for the results in TFA. A similar value of g is required to simulate the shape of the approach of the anodic current-density towards its limiting value for 0.5M KCl + 0.05M HCl solution (Fig. 15). Increasing values of g cause the approach to i_{lim} to be progressively less steep than for $g = 0$ (Langmuir conditions).

(ii) Effects of Chloride Ion Adsorption on Extent of Surface Oxidation at Platinum Anodes: It is seen from Figs. 20 and 21 that Cl^- ion has a substantial competitive effect with respect to anodic oxide film formation at Pt, as was found similarly by Bagotskii et al.[201] for Br^- ion adsorption. The results of Fig. 21 show how the degree of surface oxidation in the presence of Cl^- ion depends on potential for the various

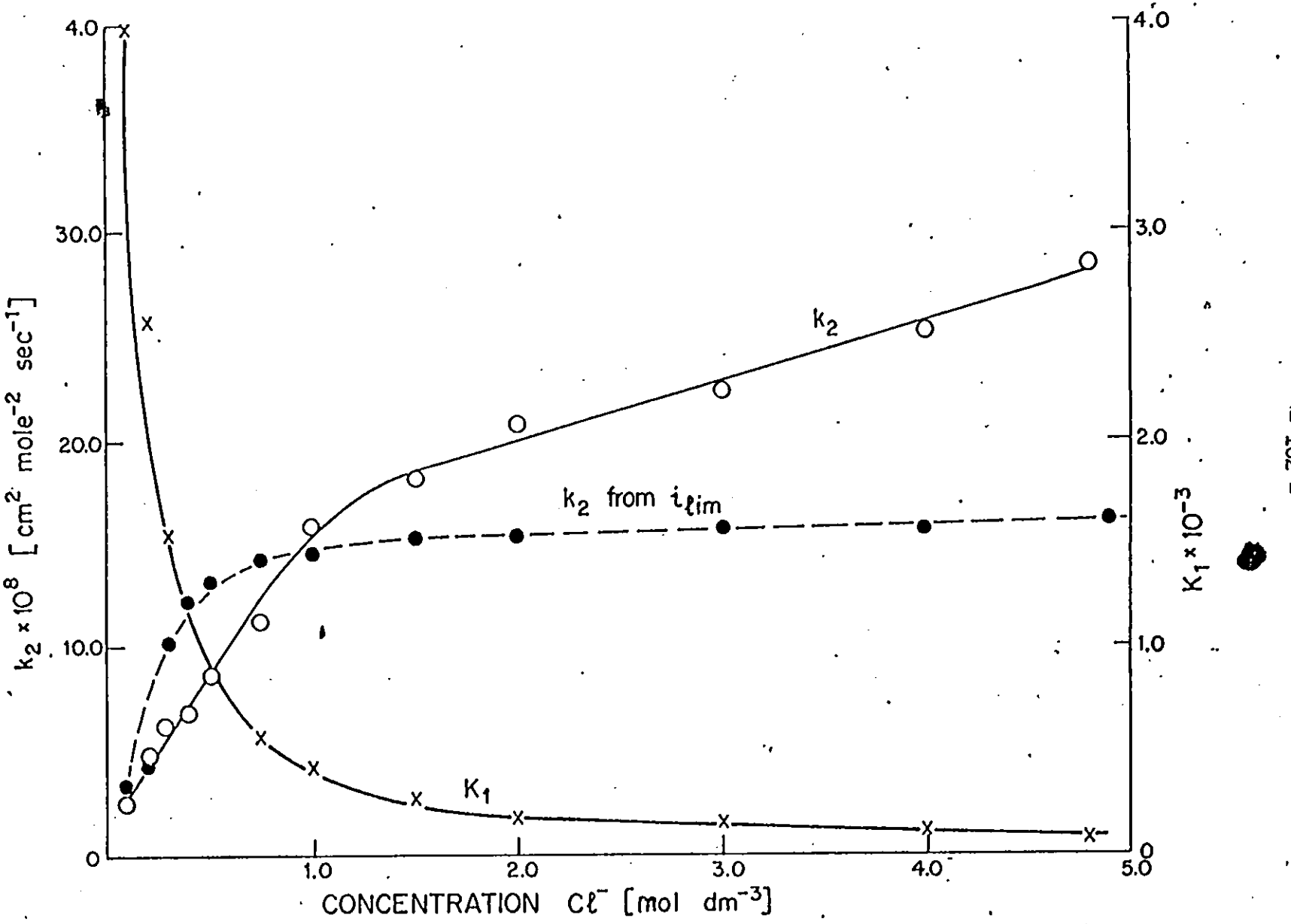

Fig. 25 Values of $\bar{K}_1$ and k_2 for the Cl_2 evolution mechanism I,II as a function of Cl^- ion concentration. k_2 from i_{lim} is also shown as f [Cl^-] .

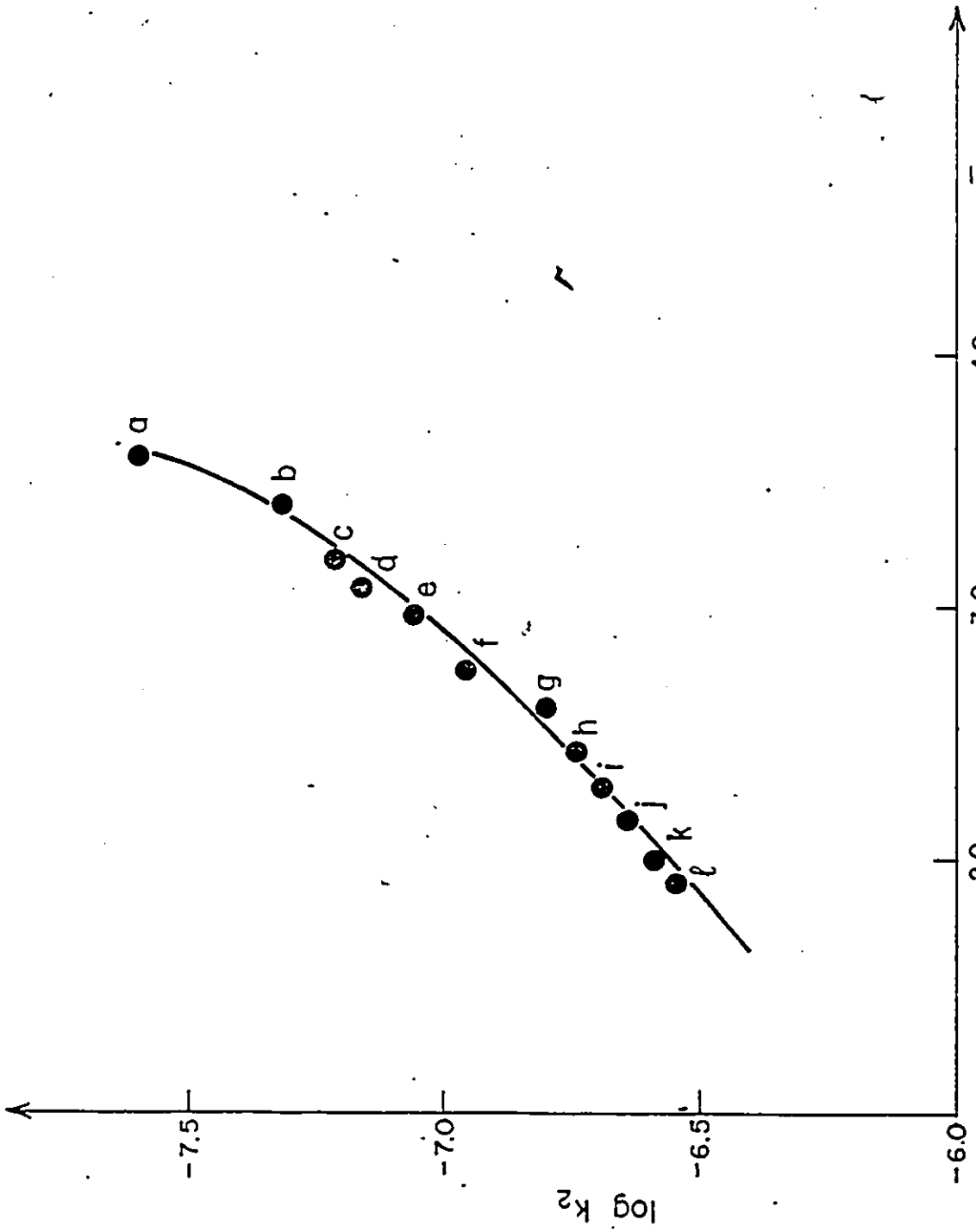

Fig. 26 Relation between log $\bar{K}_1$ and log k_2' for the concentrations indicated by: a) 0.1; b) 0.2; c) 0.3; d) 0.4; e) 0.5; f) 0.75; g) 1.0; h) 1.5; i) 2.0; j) 3.0; k) 4.0 and l) 4.8 mol dm^{-3}.

Cl^- concentrations employed in the kinetic experiments. It is interesting that for a given $[Cl^-]$, the surface coverage of oxide species (as e/Pt atom) tends to remain constant with increasing electrode potential, whereas, in aq. H_2SO_4, it tends to increase in the well known way[61;62,96,239] as shown for comparison in Fig. 21 . The data in Fig. 21 cover ranges of potential into the region where appreciable Cl_2 evolution currents arise (see Fig. 16).

The attainment of limiting extents of surface oxidation with increasing potential in the presence of varying concentrations of Cl^- ion suggests that the exponential electrode potential term $\exp[VF/RT]$, which determines (together with the coverage factor[72], $\exp[-g\theta]$) the potential dependence of the degree of surface oxidation of noble metal electrodes, is cancelled by a similar electrode potential term for the competitive specific adsorption of Cl^- ion. The limiting coverages by surface oxygen species are readily accounted for in terms of competitive adsorption of OH/O species and Cl^- ion. For the Langmuir case, the equations for competitive adsorption take the well known form

$$\frac{\theta_{OH/O}}{1-\theta_{OH/O}-\theta_{Cl^-}} = K_{OH/O}C_{H_2O}\exp[VF/RT] \qquad (35a)$$

and, for an assumed potential-dependence of Cl^- adsorption,

$$\frac{\theta_{Cl^-}}{1-\theta_{OH/O}-\theta_{Cl^-}} = K_{Cl^-}C_{Cl^-}\exp[VF/RT] \qquad (35b)$$

where the K's are the respective electrosorption equilibrium constants and θ's the coverages by the indicated species. For any electrode potential,

V , these relations obviously lead to a ratio

$$\theta_{OH/O}/\theta_{Cl^-} = \frac{K_{OH/O}}{K_{Cl^-}} \cdot \frac{C_{H_2O}}{C_{Cl^-}} \qquad (36)$$

which is constant for a given composition of solution and thus independent of V. Then, since in the monolayer $\theta_{OH/O} + \theta_{Cl^-} \doteq 1$, $\theta_{OH/O}$ tends to a constant, potential-independent value.

The experimental results shown in Figs. 19 and 22 indicate that a logarithmic rather than a linear relation in $[Cl^-]$ applies to the competitive adsorption of surface oxide and Cl^- species, so that a Temkin, rather than a Langmuir, form of the above isotherm should be used which would lead to a logarithmic dependence of the limiting extents of surface oxidation on Cl^- concentration, as observed (Fig. 26).

The above explanation for the attainment of limiting surface oxide coverages is consistent with the observation that in most of the kinetic experiments the current vs. potential relations (Fig. 15) for " descending " changes of potential are almost identical with those for " ascending " changes. This is not , however the case, e.g., in O_2 evolution from aq. H_2SO_4 where there is appreciable hysteresis[62] between ascending and descending current vs. potential relations due to irreversible and potential-dependent surface oxide film formation.

The results of Fig. 21 also show that the extent of surface oxidation attained in the presence of Cl^- ion at potentials where Cl_2 is evolved decreases with increasing $[Cl^-]$. This implies a corresponding increase in the surface coverage by adsorbed Cl^- ion with increasing $[Cl^-]$.The percentage of the surface blocked by oxide species

in the presence of Cl^- ions for the concentrations 0.1 - 4.8M was estimated to be in the range from 80 - 100%, depending on the concentration of Cl^- ions, as shown in Fig. 19.

(iii) Significance of Lateral Interaction Effects at the Pt Surface and the Influence of Adsorbed Cl^- Ion: The linear relations in Figs. 24a and 24b demonstrate that Cl· recombination control characterizes the kinetics of Cl_2 evolution. However, the i_{lim} is not a constant value but varies with Cl^- concentration (Fig. 17). This is an apparantly contradictory situation since, according to eqn. (6), $i_{lim} = 2Fk_2$ = constant, as $\theta_{Cl\cdot} \to 1$. This dilemma is resolved if allowance is made for interaction effects of adsorbed Cl· with adsorbed Cl^- ion and the consequently changed surface oxide and H_2O molecule coverage.

Thus, it is well-known[162,202,203] that Cl^- ion is specifically adsorbed at the Pt electrode and (a) displaces the H underpotential deposition peaks to less positive (vs. H_2/H^+) electrode potentials and (b) displaces the surface oxide formation process to more positive potentials, depending on Cl^- concentration.

If the current for step II is influenced by interaction effects according to eqn. (7) but with the " $g\theta$ " term characterizing interactions not only between Cl· and Cl· but also between Cl· and adsorbed Cl^-, then it is seen how i_{lim} can depend on Cl^- rather than being constant. If $g > 0$ (repulsive interactions), the apparent bond energy of chemisorbed Cl· to the Pt electrode surface decreases with increasing $\theta_{Cl\cdot}$ and/or θ_{Cl^-} so that recombination of chemisorbed Cl· is facilitated according to eqn. (11). The effective rate constant will, in fact, be $k_2 \exp 2g$ at $\theta = 1$ instead of k_2, and thus be dependent on g. The magnitude of the g factor

will be determined by (a) interaction between Cl· and Cl·; (b) interaction between Cl· and specifically adsorbed Cl^- ions; and (c) interaction between Cl· and electrodeposited surface OH or O species (the effect demonstrated in the previous Chapter). Then if g increases with coverage by adsorbed Cl^-, i_{lim} will depend on bulk Cl^- ion concentration. As seen from Fig. 17, i_{lim} appears to reach a saturation value with increasing $[Cl^-]$ which is consistent with saturation specific-adsorption of Cl^- being reached as its bulk concentration increases.

This interaction effect accounts for (a) the dependence of i_{lim} on Cl^- concentration through concentration-dependent specific adsorption of Cl^- ion and (b) the difference in the values of k_2 evaluated from i_{lim} (where $\theta_{Cl\cdot} \rightarrow 1$) and from the slopes and intercepts of the linear parts of the plots shown in Figs. 23 and 24 for which $\theta_{Cl\cdot}$ is appreciably less than unity.

(iv) Significance of Reaction Orders in Relation to Mechanisms: When the reactant is an anion whose surface concentration depends on bulk concentration and electrode potential, and in the present case on the state of oxidation of the electrode surface, the interpretation of reaction orders, R , becomes difficult and, in general[206], must take into account (a) the concentration-dependence of the ψ_1-potential and (b) the distribution of reactant ions at the interface relative to the bulk, through the factor $\exp -[ze\psi_1/kT]$ and a corresponding factor in the specific adsorption energy. However, for a recombination-controlled reaction with the prior ion discharge step at quasi-equilibrium, the " double-layer " effects cancel in the expression for the coverage $\theta_{Cl\cdot}$ of the intermediate for any value of the symmetry factor β.

For the recombination process [rate equation (6)] , the reaction order, R_s , of the surface process itself is given by

$$R_s = (\partial \ln i_2 / \partial \ln \theta_{Cl\cdot}) = 2 \qquad (37)$$

For a process involving an adsorbed intermediate, the coverage of which is a function of reactant concentration and potential, the interpretation of the observed reaction order must take into account this dependence. The relation between the experimentally accessible reaction order, R , (at a given electrode potential V or overpotential η) and the isotherm for adsorption of the intermediate is then, for $[Cl_2]$ = constant,

$$R = \left(\frac{\partial \ln i_2}{\partial \ln C_{Cl^-}} \right) = \left(\frac{\partial \ln i_2}{\partial \ln \theta_{Cl\cdot}} \right) \left(\frac{\partial \ln \theta_{Cl\cdot}}{\partial \ln C_{Cl^-}} \right) \qquad (38)$$

where (a) the second term in brackets must be specified as either at constant electrode potential, V , or constant overpotential η defined by $V - V_{rev} = \eta$ and (b) ($\partial \ln \theta_{Cl\cdot} / \partial \ln C_{Cl^-}$) is derived from the differential coefficient of the adsorption isotherm, eqn. (7) or eqn. (12). By making the differentiation, it is easily found for the Langmuir case ($g = 0$) that

$$\left(\frac{\partial \ln \theta_{Cl\cdot}}{\partial \ln C_{Cl^-}} \right)_V = \frac{1}{1 + K_1 C_{Cl^-} \exp VF/RT} = 1 - \theta_{Cl\cdot} \qquad (39)$$

Hence

$$R = R_s (1-\theta_{Cl\cdot}) = 2(1-\theta_{Cl\cdot}) \qquad (40)$$

which gives the expected reaction order of 2 for $\theta_{Cl\cdot} << 1$ (i.e., when the Tafel slope is RT/2F) and of 0 as $\theta_{Cl\cdot} \to 1$ (limiting current).

If the reaction order is derived for constant η (Fig. 23), as is most conveniently obtained from the experimental results (Fig. 16), then from an equation similar to (7), written as

$$\theta_{Cl\cdot}/(1-\theta_{Cl\cdot}) = K_1 C_{Cl^-} \exp VF/RT = K_1 C_{Cl^-} \exp (V_{rev} + \eta)F/RT \quad (41)$$

and noting that $V_{rev} = V^o_{rev} - \frac{RT}{F} \ln C_{Cl^-}$ for Cl^- ion, it is seen that $\theta_{Cl\cdot}/(1-\theta_{Cl\cdot})$ will be independent of C_{Cl^-} , i.e., $(\partial \ln \theta_{Cl\cdot}/\partial \ln C_{Cl^-}) = 0$. Hence $R_\eta = (\partial \ln i_2 / \partial \ln C_{Cl^-})_\eta = 0$ for all conditions.

The observed reaction orders at various η values are found experimentally (Fig. 23) to be > 0, and near unity except at high Cl^- concentration. Since Figs. 24a and 24b are consistent with recombination-controlled kinetics, it must be concluded that the experimental values of R_η are determined by effects of specifically adsorbed Cl^- ion. This seems to be consistent with (a) the observation of approaches to limiting currents which are, however, concentration-dependent (Fig. 16); and (b) the ultimate trend of R_η towards zero (Fig. 23) at sufficiently high Cl^- concentration where presumably the adsorption of this ion reaches saturation (see Fig. 19).

The adsorption of the Cl^- ion will itself be complicated by potential-dependent competition from electrodeposition of OH and O species at the surface. Correspondingly, Cl^- ion affects the state of the oxidized Pt surface through competitive adsorption, so that the dependence of catalytic properties of the surface on Cl^- adsorption enters into the significance of the reaction order. Hence, with changing state of the electrode surface, reaction orders cannot simply be interpreted in terms of ψ -potential effects

in the double-layer and of molecularities of the various steps in the reaction w.r.t. Cl^- participation as in Yokoyama and Enyo's work[168,193]. These authors were led to conclude, from reaction order measurements, that the Cl_2 evolution mechanism was $\frac{1}{2}\ Cl_2 + Pt \rightleftharpoons Pt\text{-}Cl^{\bullet}_{ads}$; $Pt\text{-}Cl^{\bullet}_{ads} + Cl^- \rightarrow \frac{1}{2}\ Cl_2 + e^-$, with the latter step rate-controlling. They did not, however, quantitatively examine the characteristics of the current-potential relations for the reaction, although their curves are similar in form to ones obtained in the present work (see Fig. 4 of ref. 168). It is, in fact, difficult to see how their mechanism* can lead to an approach to a limiting current except if the first step (Cl_2 dissociation) were to become rate-controlling, which was not their conclusion. As long as the Cl_2 dissociative adsorption step (in their mechanism) remains almost at equilibrium, a linear Tafel relation of slope ca. 2.3 2RT/F should arise in the usual way, and not the observed curved one.

(v) Inhibition Effects: A general feature of the cyclic-voltammetry curves for relatively high $[Cl^-]$, as exemplified in Fig. 27 , is that an inflection is observed both in the anodic and cathodic sweeps at almost the same potential. This inflection cannot therefore be due to surface oxidation since the oxide reduction does not occur until less positive potentials are reached in the descending than in the ascending curves, as is seen in Fig. 27, . Also, as shown in Chapter II, an auto-inhibition effect due to the adsorbed $Cl^{\bullet}$ intermediate itself does not arise unless the g factor in eqns. (11) and (12) is negative. This is not consistent with the observed rates of approach of i towards i_{lim} with increasing

*viz. $\frac{1}{2}Cl_2 \rightleftharpoons Cl^{\bullet}$; $Cl^{\bullet} + Cl^- \rightarrow Cl_2 + e$. Such a mechanism is not consistent with the mechanism test plots shown in Figs. 24a,b .

according to eqn. (13) , as was shown in Chapter II.

Fast-sweep experiments show that the inhibition inflection decreases rather than increases with sweep-rate (Fig. 27a oscilloscope photo), so is not an artifact due to co-deposition of a chemisorbed species such as OH or O. Also, the inflection bump remains in the anodic direction with increasing anodic and cathodic sweep-rates. With electrode rotation, the inflection moves to higher currents (Fig. 27b oscilloscope photo) but this is only an indirect effect due to the spinning away of evolved Cl_2 which lowers the local reversible potential for Cl_2/Cl^- so that significant Cl_2 evolution currents can arise at lower potentials on the instrument potential scale than in an unstirred solution: thus, the inflection itself remains at almost the same measured potential (Fig. 27b).

It is difficult to identify the origin of the observed inhibition effect, since it cannot be due to surface oxide formation and reduction, nor to auto-inhibition by $Cl^\bullet$. Since the effect is evidently " reversible " with respect to the direction of changing potential, it may be due to solvent reorientation in the Cl^-/oxide film which could change Cl^- adsorption, or to adsorption/desorption of Cl_3^- ions which are in equilibrium with Cl^- and evolved Cl_2. Perhaps a more probable explanation is that there is an effect of reversibly electrosorbed $Cl^\bullet$ [cf. eqn. (7)] on an initially observable Pt-dissolution partial-current which depends on $[Cl^-]$, since the effect increases (see Fig. 18) with increasing $[Cl^-]$.

(vi) Conclusions: The kinetics of anodic Cl_2 evolution are shown to be dependent on Cl^- ion concentration through a discharged $Cl^\bullet$ recombination mechanism for which the rate constant is dependent on specific adsorption of Cl^- ion and the state of oxidation of the Pt surface. A new method for

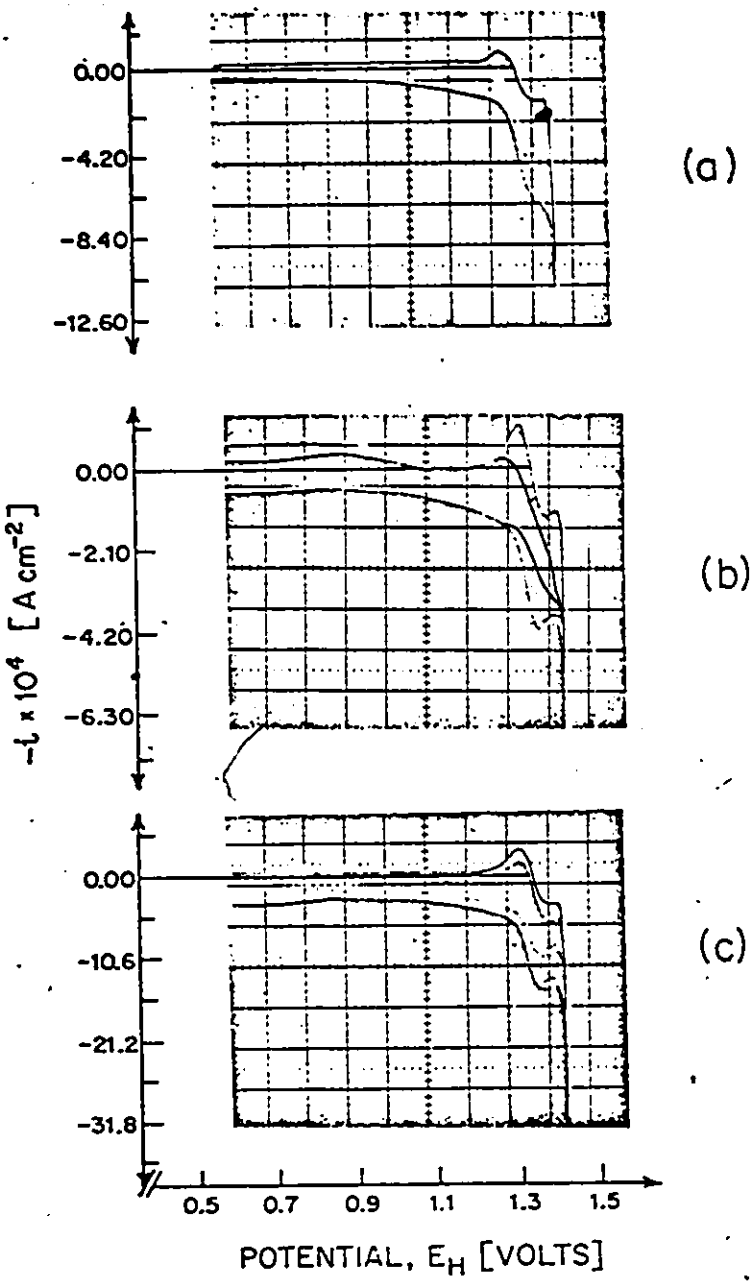

Fig. 27 Oscilloscope photos of the inhibition effect in the initial Cl_2 evolution current-potential behaviour in a cyclic-voltammetry experiment at Pt. (a) Behaviour at sweep-rate of 0.142 Vs^{-1}; (b) Behaviour with and without electrode rotation at 1600 r.p.m. (sweep-rate 0.142 V s^{-1}); (c) Behaviour with and without electrode rotation at 1600 r.p.m. (sweep-rate = 1.42 V s^{-1}).

testing the applicability of the ion discharge/recombination pathway shows that this mechanism applies over a wide coverage range and for a range of concentrations of Cl^- ion. The procedure enables both the rate constant, k_2, for the recombination step and the quasi-equilibrium constant, $\bar{K}_1$, for the prior discharge step to be quantitatively evaluated. Both k_2 and the formal $\bar{K}_1$ are shown to be dependent on Cl^- ion concentration. The reaction-order behaviour is consistent with Cl^- specific adsorption effects in the recombination kinetics. The adsorption of Cl^- ion also causes important changes in the coverage of OH and O species at the Pt electrode at potentials for which Cl_2 is evolved at appreciable rates.

CHAPTER IV

SURFACE OXIDATION IN THE OSCILLATORY KINETICS OF H_2 OXIDATION AT Pt IN AN ALMOST ANHYDROUS SOLVENT

In this Chapter, new work on oscillatory kinetics of H_2 oxidation at Pt will be discussed. The role of the Pt oxide film and anion adsorption in this type of process is investigated in trifluoroacetic acid with traces of water present. This gives a controllable, small degree of oxidation of the metal surface over a wide potential range, as was described in Chapter II for the study of Cl_2 evolution under similar conditions.

First, an introduction on some background aspects of oscillatory reactions and a brief review of previous work will be given.

1. INTRODUCTION

While many chemical processes can take place under steady-state conditions, provided that a uniform supply of reactants is maintained, it is very interesting that a number of chemical[240-243], electrochemical[244-246] and enzyme catalysed reactions[247-249] behave kinetically in a periodic manner. Renewed interest in oscillatory phenomena in chemical reactions has arisen recently both in physical and biochemistry[247-251].

Oscillatory processes can be of two types: (i) a damped oscillatory approach towards a steady-state (in kinetics) or towards an equilibrium (in thermodynamics of a reversible process); (ii) a sustained oscillation associated with consumption of a continuously supplied reactant and/or provision of free energy from some exo-energetic process or continuous energy source. In electrochemical sustained oscillations, charge and energy

are provided from the external power source or from the electrochemical free energy of a cell reaction. In this Chapter, an oscillatory process of type (ii) will be discussed, where reaction is driven at a net (but periodic) rate away from the equilibrium condition by application of a non-equilibrium potential difference.

In periodic reactions no stable steady-state can exist and the process oscillates in rate between velocities corresponding limitingly to two unstable steady-states. In terms of the thermodynamics of irreversible processes, these states are characterized by negative rates of entropy production (hence instability) in contrast to positive dS/dt for a stable steady-state situation. In homogeneous reactions, oscillatory kinetics are rare[241-243] but in heterogeneous, especially electrochemical, reactions they are well known but the conditions under which they can arise are not well understood; probably a variety of factors are involved.

Thus, in a number of electrochemical and chemical reactions, a situation can arise where evidently no steady-state of the reaction can be established. The system then exhibits sustained oscillations around an unstable steady-state. Such processes often involve diffusion of the reactant(s) coupled with an electrochemical surface reaction which can suffer inhibition, leading to a current-potential relation for the process which shows an inversion corresponding to negative resistance or positive feedback.

It has been found that oscillations in electrochemical systems can originate in two ways: (a) by coupling with appropriate impedance components of an external circuit to make an " electrochemical oscillator " device[252] and (b) intrinsically, as a property of the kinetics and mechanism of the reaction [240,253]. The latter type of oscillatory

phenomenon is of more fundamental interest in the kinetics of coupled electrochemical reactions, and is the type which has been studied in the present work.

In most of the work on electrochemical oscillations, attempts have been made to explain the phenomena in a qualitative way through a cycle of several steps which occur in a repetitive and regular manner. Few attempts have been made to develop a full mathematical treatment of the oscillatory kinetics which arise in certain electrochemical reactions, but in one or two cases the factors which can lead to steady-state kinetic equations which have no real solutions were formulated mathematically, e.g. by Wojtowicz, Marinčić and Conway[246], and in more detail by Wojtowicz[253] and Wojtowicz and Conway[254].

In some cases, periodicity has been simulated by means of analogue-computer circuits[249,254]. In these approaches, the periodic nature of the kinetics follows as a natural consequence of the time-dependent components of the rate equation, e.g. diffusional fluxes, changes of concentration or coverage by intermediates, etc. It is because of the difficulty of formulating and, even more, of solving the appropriate differential equations for the rates of complex processes which exhibit oscillatory kinetics, that the discussion of most oscillatory chemical reactions has been of a qualitative kind. This applies to the present section of the work on periodicity in H_2 oxidation kinetics.

Oscillatory processes are described as " linear " or " non-linear " depending on the index of the power, or the form, of the " restoring force " as a function of some displacement, " Δ ", from an equilibrium or initially static situation. Linear oscillations are well known in simple harmonic processes and lead to a periodicity which is sinusoidal in time,

e.g. the motion of a pendulum or vibrations of a diatomic molecule in a low quantum state. More extensive displacements usually give rise to higher order terms in the relation between Δ and restoring force, and lead to non-linear oscillations (non-sinusoidal).

In electrochemical processes, the constraint leading to a displacement from any equilibrium is an easily definable quantity and corresponds to the factor $\exp \pm \alpha\eta F/RT$, where η is an overpotential. Such a constraint is highly non-linear and is probably the reason for most of the " spikey " oscillations that are observed in such reactions. However, for small η , the exp constraint always becomes a linear one ($\exp \pm[\alpha\eta F/RT] \doteq 1 \pm [\alpha\eta F/RT]$) so that near the reversible potential of a process oscillations, if they occur at all, can become sinusoidal.

The formulation of analytical functions which have periodic solutions for the kinetics is usually extremely difficult. However, for non-electrochemical reactions and some physical processes, a number of special cases have been identified[249,256,257] for which differential equations having periodic solutions have been formulated[258-260]. Advanced mathematical treatments of non-linear oscillations are to be found in the monographs of Minorsky[256], Hayashi[257], Andronov and Chaikin[258] and in papers by Prigogine[259]; however, these approaches are beyond the scope of the present Chapter.

(i) Brief Review on the Existence of Periodic Reactions, Especially in Electrode Processes

(a) General Requirements and Conditions for Oscillatory Behaviour:

The conditions under which periodic processes arise are essentially of two kinds: (1) those involving diffusion[261,262] and (2) those involving activation control of the kinetics of the reaction[261],

However, oscillatory reactions in which diffusion plays an important role are usually coupled with adsorption-electrochemical processes such as surface oxide formation and consequent passivation. When periodicity in reactions arises in activation-controlled kinetics, it is necessary to take into account competitive adsorption together with chemical " positive feedback " which can be identified with autocatalytic effects. The autocatalytic step is considered necessary to initiate and sustain periodic behaviour[263] and provides the positive feedback characteristics such as are required in many known mechanical and electrical oscillators.

The general requirements for oscillations to arise in an electrode reaction seem to be:

(1) existence of an S-shaped current-potential curve[252,264-266] (Fig. 28) such as arises when passivation, e.g. by an oxide film[264, 267,268], occurs. This gives the possibility for two values of the potential to correspond to a given current. Also, such a relation has a " negative-resistance" characteristic along part of the curve which is known to lead to instability in electrical circuits, e.g. periodic firing of neon tubes.

The importance of the type of i-V relation is emphasized by the observation of periodicity in a cathodic process, the reduction of $S_2O_8^{2-}$ at Hg[269], where no passivating film can arise but the i-V curve is still S - shaped. In this case, this is due to double-layer " ψ-potential " effects near the potential of zero charge.

The negative resistance characteristic provides the positive feedback function commonly required for self-sustaining oscillations, e.g. as in an electric oscillator with inductive coupling. The impedance characteristics of this type of situation at electrodes have been considered by

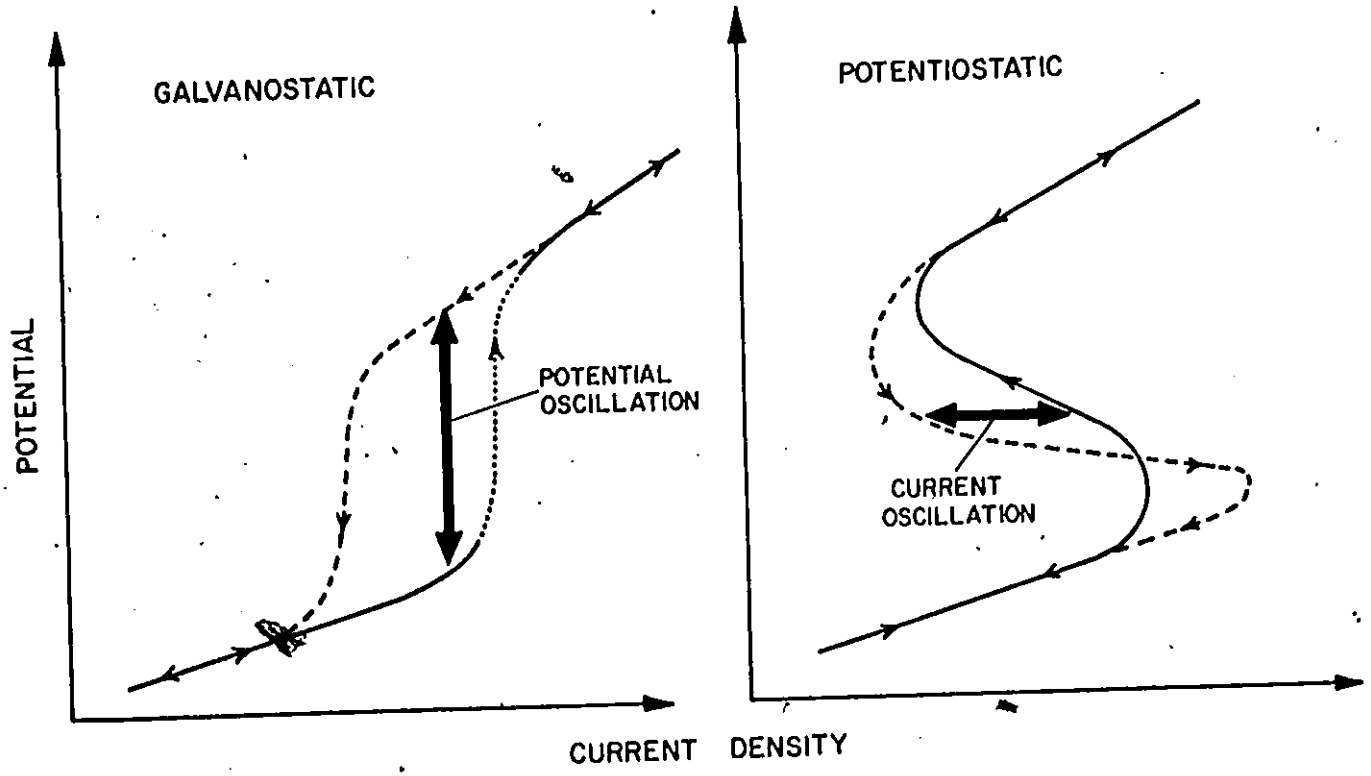

Fig. 28 Types of current-potential curves arising due to a passivation effect.

Epelboin[270].

(2) a coupling of the electrode surface process with a partially diffusion-limited step associated with transport of the reactant to the electrode surface[253,254]. This condition is commonly, but not exclusively required.

In the case of electrochemical reactions, oscillatory behaviour has usually been observed upon anodic polarization of various metals, as in the case of Ni[261], Cu[245] ; Ag[267] or Fe[245] anodes.

Upon anodization under special conditions, the surfaces of such metals tend to become covered with a passivating oxide film. Oscillatory oxidation currents are then often observed and have been ascribed to heterogeneity of the electrode surface, with periodic formation and dissolution of the oxide film occurring at the metal surface. Coupled diffusion of dissolving ions and of H^+ or OH^- determining the local pH, is often involved.

Periodic kinetics often arise also in anodic oxidation of organic substances, e.g. HCHO[268], HCOOH[246,268], C_2H_4[246] at noble metals where the formation of a monolayer oxide film can passivate the organic oxidation reaction . Similar behaviour was also observed with H_2 oxidation at Pt anodes, first by Armstrong and Butler[271].

(b) Some Examples of Oscillatory Behaviour in Previous Work:

(1) Metal Oxidation Processes: As was mentioned earlier, oscillatory phenomena are often formed under conditions where metals passivate upon anodic oxidation. These conditions lead to S-shaped i-V curves of the kind referred to above. Periodic " active "- " passive " - " active " transitions occur as an oxide film is deposited and removed. Some of the first detailed studies of this kind of electrochemical periodicity were made at Fe and Cu by Bonhoeffer and Gerischer[245]. The conditions leading

to such behaviour were also treated by Franck[250] in terms of instabilities in the current-potential relation.

Oscillatory behaviour in passivation of metals was observed by a number of other workers, e.g. Hoare and Mowat[261] (Ni in 50% H_2SO_4), Dmitriev and Rzhevskaya[262] and Pointu[263] (Cu in H_3PO_4), Frances and Colmer[272] and Lal, Thirsk and Wynne-Jones[267] (electropolishing of Ag where films of Ag_2O, AgCl or AgCN can be formed, depending on the electropolishing solution), and Piggott, Leckie and Schreir[273] (Ti in formic acid). Oscillatory behaviour is also observed during corrosion[273,274] for the same reasons as those associated with anodic oxidation - the formation and breakdown of passive films, but in this case coupled with diffusion of H_2 and/or O_2 produced or consumed, respectively, in the corrosion reaction. Specific influences of anions (SO_4^{2-} or Cl^-) which can be adsorbed were noted[274] as well.

(2) Organic Oxidation Processes: Oscillatory currents have often been observed in the electrochemical oxidation of simple organic substances, e.g. MeOH[275], HCHO[252], HCOOH[246,252], C_2H_4[246] at Pt or Pd. In these cases no corrosion of the metal can be involved but passivation of the electrocatalytic sites at the free metal surface by very thin (monolayer) oxide films can arise at Pt and Pd and also the initially deposited OH or O species at these metals can react chemically with such organic molecules and lead to a stripping of the film. The well known hysteresis in the ranges of potential for electrochemical formation and for reduction of the oxide films at these metals is probably an important factor in oscillatory behaviour.

Various studies with organic oxidation processes that are oscillatory have been made: Pavela[275] examined the origin of oscillations of potential which develop at sufficiently high current-densities during

oxidation of MeOH at Pt anodes. It was pointed out that at 0.69 V E_H there is a small coverage by MeOH at the electrode surface which can be easily oxidized. As the potential rises to 0.87 V E_H, the initial oxide formation at the Pt surface commences and the deposited OH species react with adsorbed MeOH, forming formaldehyde and formic acid. It was stated that oxidation of these substances provided time for MeOH diffusion to the electrode, leading to a periodic process. Pavela[275] showed that only a fraction of the electrode surface takes part in the reaction since only ca. 1% of the charge corresponding to full occupation of the electrode surface by MeOH is used during each cycle.

Buck and Griffith[268] investigated the oscillations associated with oxidation of MeOH, formaldehyde and formic acid. They concluded that the surface of Pt plays an important role and raised the question why, independently of whether the reaction of the organic radical with the surface oxide is slower than diffusion of the organic reactant to the surface, the process should not reach a steady-state at some intermediate potential. This is always the problem question with qualitative discussions of oscillatory reactions.

Similar conclusions about the role of the surface oxide were reached by Shropshire[264] in his work on periodic oxidation of HCHO. Periodic formation of the oxide and its reaction with blocking adsorbed species derived from HCHO was proposed.

Hunger[252] studied potential oscillations observed in the anodic oxidation of HCHO in 3.5 M H_2SO_4 at smooth and platinized Pt anodes under galvanostatic conditions. Oscillations were observed at both types of electrodes showing that the real/apparent area ratio was not a significant factor. Periodic chemisorption of an intermediate and its oxidative desorption were proposed. The charge associated with each oscillation

(428 $\mu C\ cm^{-2}$) was compared with that required to oxidize a saturated layer of " HCHO " radicals (182 $\mu C\ cm^{-2}$). This led to the conclusion that electrodeposited surface oxide is also involved, accounting for extra charge (428 - 182 $\mu C\ cm^{-2}$), as was concluded in some other papers[246,264,268].

Since the oscillatory behaviour on Pt surfaces appeared to be connected with the formation and reduction of the oxide film, Wojtowicz, Marinčić and Conway[246] studied the role of surface oxidation in the periodic oxidation of formate and ethylene at Pt and Pd anodes. The periodicity of formate oxidation is sufficiently slow (20 ~ 30 s) that direct observations could be made by means of cathodic galvanostatic transients taken <u>during</u> a given oscillation cycle from several values of potential attained during the various phases of the periodic variation of potential occurring under constant current anodic polarization. This type of experiment provided evidence that periodic growth and removal of the oxide film at Pt was directly connected with the oscillations.

Oscillatory behaviour observed in the electrochemical oxidation of formate and ethylene was found to be different with regard to the mechanisms involved. In the case of formate, the oxide film on the Pt anode was found to play an important role. Thus, the galvanostatic discharge experiments indicated that the oxide film first reaches a critical coverage (~ 180 $\mu C\ cm^{-2}$) upon which formate radicals can be discharged with increasing rate as the potential approaches the critical value just before a sudden (periodic) descent of potential sets in. On the other hand, oscillations in ethylene oxidation on Pt or Pd anodes are diffusion-controlled and the oxide species are co-deposited amongst C_2H_4 residues on the available free sites and their coverage was found to be constant at a given potential and coverage by ethylene.

(3) Oxidation of H_2: One of the first observations of oscillatory kinetics of an electrochemical reaction was made under galvanostatic conditions by Armstrong and Butler[271] who observed oscillatory behaviour in H_2 oxidation at bright Pt in dilute H_2SO_4. The potential was found to oscillate between the reversible value 0.0 and an alternative value of 0.4 V E_H. The phenomenon was qualitatively interpreted in terms of diffusion of H_2 to the electrode surface, causing re-establishment of the reversible potential, and deactivation of the electrode so that the reversible potential could no longer be maintained, eventually moving towards a more positive value where O species could be deposited. In some cases, the electrode could be re-activated at ~ 0.8 V E_H and the oscillations would then occur between 0.0 and 0.8 V E_H.

Sawyer and Seo[276] observed oscillations due to anodic oxidation of H_2 at Pt in 1M HCl solutions. Since they found (surprisingly) that stirring had no effect on the oscillatory behaviour, they proposed a different interpretation: that at potentials above 0.8 V E_H, an oxide film was formed on the Pt surface (Chapter I), but the activity of the surface can be then regenerated through oxidation of dissolved H_2, which is formed at the reversible potential, $E_{H,rev}$. As continued exposure to H_2 takes place, the electrode becomes deactivated and the potential rises again towards that for surface oxidation in a repetitive manner. The deactivation in this work may be due to well known impurity effects at Pt and the reactivation to their removal by the reactive oxide film.

Potential oscillations have also been observed with H_2/CO mixtures at platinized Pt electrodes in 3M H_2SO_4 solutions in work by Szpak[277].

(3) Oscillations in Other Types of Systems: Oscillatory phenomena in various other types of electrochemical processes have been observed,

e. g. at Pt in organic solvents with a coupled redox-system, Ce^{3+}/Ce^{4+}(266,278), Fe^{2+}/Fe^{3+}(279) or Mn^{2+}/Mn^{3+}(279). Also periodic changes in adsorption of Cl^- ions were found by Horanyi and Inzelt(265) in studies on the oscillatory oxidation of various organic compounds.

(ii) Kinetics of H_2 Oxidation at Pt in Aqueous Solutions: In several papers in the literature, the kinetics of oxidation of dissolved H_2 have been studied at Pt electrodes(117,282-284). In these cases, non-oscillatory currents were observed but the behaviour and mechanism of the reaction is obviously relevant to the periodic kinetics which arise under other conditions, as in the work to be described here and in ref. 271.

The rate of H_2 oxidation on Pt anodes is found to increase up to a potential 0.8 V E_H at which the rate decreases with increasing potential. This is the potential for onset of Pt surface oxidation, so the decrease of H_2 oxidation rate is due to a passivation effect. In aq. solutions, prior to passivation, H_2 oxidation at Pt is an almost completely diffusion-controlled reaction. The term " passivation " is used in a general sense as the inhibition of electrochemical reactions by oxide layers. The phemenon was also studied on various other metals e.g. Ir(22b,280), Rh(22b,280-281), Pd(281) and Au(280). In the case of the Pt matals, it is clear that passivation sets in at the potential at which anodic formation of the oxide film commences. However, the decrease in the rate of oxidation of H_2 at Pt, due to passivation of the electrode surface, was also found to depend on pretreatment of the electrodes as well as on the method used for the measurements(117). Breiter(117) used the potentiostatic method(22a) in order to obtain reproducible i-V curves and to measure oxide coverage under the same conditions but by switching to a galvanostatic circuit and obtaining

a cathodic charging curve. He observed that the rate of H_2 oxidation decreases rapidly between 0.8 V E_H and 1.1 V E_H, where the oxide coverage (in the presence of H_2) increases from zero to ca. 21%. This is sufficient to cause substantial inhibition by blocking the active sites for H_2 dissociation/oxidation. Beyond 1.1 V E_H where the surface is virtually completely covered by OH species, little further increase in the inhibition effect arises. Thus, Breiter[117] concluded that oxidation of H_2 occurs at a large rate only on certain active sites which constitute only < 10% of the surface area. When these sites are covered with oxide, then H_2 oxidation has to proceed on less active sites, although the inhibiting effect is smaller on those sites. The decrease of rate of H_2 oxidation with increasing oxide coverage could be practically compensated by increasing the rate of H_2 oxidation by an increase in potential on the less active sites.

Schuldiner et al.[116,282] conducted further studies on the H_2 oxidation (and on H_2 evolution and O_2 evolution) reactions on polycrystalline Pt and on Pt single-crystal orientations by employing steady-state measurements. They showed that the limiting H_2 oxidation current is essentially independent of crystal orientation*, although ~ 10% lower current-densities were observed for the (100) orientation of the Pt surface. More significant differences between the kinetics at the three principal planes of orientation are observed in the passivation region, since the potential at which passivity commences increases in the order (100), (110) and (111). It should be mentioned here that the three principal index planes of Pt electrode surface had been characterized in 1965 by Will[285] for H adsorption/desorption and appreciable differences had been observed, e.g.

*Over ranges of potential where H_2 oxidation is diffusion-controlled the measured rate of the reaction per cm^2 will, of course, be independent of the orientation of the crystal face of the electrode.

the electrochemical adsorption isotherms for H were easily distinguishable.

Schuldiner et al.[282] concluded that during the H_2 oxidation reaction H_2 reacts with the surface oxide species which would lead to a decrease in the coverage by OH or O species at a given potential. At the same time it was suggested[116] that anion adsorption would tend to increase, initiating passivation, and be a major cause of the rapid decrease in the rate of H_2 oxidation up to at least 1.2 V E_H.

Schuldiner and Warner[50] supposed that the increase in the rate of H_2 oxidation below 1.1 V E_H at Pt was connected with migration of oxygen on the electrode surface, while Mayell[286] attributed this effect to a change in the state of the oxide film during the reaction. Burke and Moynahan[287] proposed more recently that the increase in the rate of H_2 oxidation with decreasing potential is connected with the rate of removal of PtO since the oxide film presumably inhibits the reaction. A similar view was treated more quantitatively (see below) by Shibata[283]. Hoare[288] concluded that the H_2 oxidation reaction at potentials<1.1 V E_H would produce some uncovered Pt sites. H_2 oxidation on covered Pt sites proceeds only slowly and is more difficult than on uncovered sites.

The kinetics of H_2 oxidation were further studied in some detail in an interesting paper by Shibata and Sumino[283] who based their discussion of the kinetics on the existence of two kinds of sites on the Pt surface: oxide-covered and oxide-reduced (free) sites. The experiments were carried out under open-circuit conditions with a smooth Pt electrode in 1M H_2SO_4 solution with dissolved H_2. It was found that the reaction proceeds at first as a pure chemical reaction in which Pt-O is reduced at a slow rate which was found to be second-order in the surface concentration,

θ , of chemisorbed oxygen in the range $1 \geq \theta \geq 0.65$, with the rate constant determined as $0.49\ s^{-1}$. This type of reaction must produce some Pt (oxide-free) sites so that further reaction could therefore become more rapid for coverages $0.6 \geq \theta > 0$. As the potential falls, ionization of dissociatively adsorbed hydrogen on oxide-free Pt sites occurs in parallel with electrochemical reduction of adjacent PtO sites, e.g.

$$PtO + 2e^- + 2H^+ \longrightarrow Pt + H_2O \quad (\text{see below}).$$

Two principal mechanisms for the reaction of H_2 at oxidized Pt electrodes were proposed: (i) the direct chemical reaction of H_2 with PtO (formed at a potential 1.5 V) which was found to be second order in [PtO] so that the reaction was written as

$$\begin{matrix} Pt\text{-}O \\ | \\ Pt\text{-}O \end{matrix} + H_2 \longrightarrow \begin{matrix} Pt\text{-}OH \\ | \\ Pt\text{-}OH \end{matrix}$$

where the line between Pt atoms indicates that they are adjacent sites. A mechanism of reaction of H_2 with PtO, fully covering the surface, was not offered. The above step was assumed to be followed by the elimination of H_2O:

$$\begin{matrix} Pt\text{-}OH \\ | \\ Pt\text{-}OH \end{matrix} \longrightarrow \begin{matrix} Pt \\ | \\ Pt\text{-}O \end{matrix} + H_2O$$

Alternatively, a further reaction of H_2 with " Pt-OH " could have been written for the formation of oxide-free Pt sites.

(ii) The alternative reaction of H_2 with the oxide film at lower potentials is a <u>coupled</u> dissociative adsorption and electrochemical reaction applying to conditions where free Pt sites are, or become, available:

$$\begin{matrix} Pt \\ | \\ Pt \end{matrix} + H_2 \longrightarrow \begin{matrix} Pt\text{-}H \\ | \\ Pt\text{-}H \end{matrix} \longrightarrow \begin{matrix} Pt \\ | \\ Pt \end{matrix} + \boxed{2H^+ + 2e^-}$$

coupling

with $PtO + \boxed{2e^- + 2H^+} \longrightarrow Pt + H_2O$

It is to be noted that the appearance of free Pt sites from reaction by either pathway should provide an autocatalytic effect since the greater is the extent of reduction of PtO producing free Pt sites, the more rapid (per cm^2 surface of the electrode) will be the coupled dissociative adsorption of H_2 providing a greater flux of electrons for the coupled electrochemical step. This aspect of the reaction mechanism was not mentioned by Shibata but it is the kind of factor required to account for the possibility of onset of oscillations which were observed in the aq. solution case by Armstrong and Butler[271].

In a later paper[289], Shibata applied his idea on H_2 reduction of Pt-oxide films to the behaviour of the multilayer α and β type oxides he described earlier (see review in Chapter I).

In Shibata's work, the experimental evaluation of the H_2 oxidation kinetics was made by measuring the reaction time for removal of various fractional coverages of oxide at a number of H_2 -partial pressures. These experiments showed that the rate constant for H_2 oxidation fell from 1.72 to 1.19 s^{-1} for an increase in degree of oxidation, Q_0, from 90 to 110 $\mu C\ cm^{-2}$. This was attributed to a change in the nature of the oxide layer on the Pt surface as the degree of oxidation changes. It was suggested that the electronic state of Pt atoms on the surface may be changed by chemisorption of oxygen atoms and the adsorbed O-atom which has higher electronegativity than Pt can affect the electronic state of neighbouring Pt atoms. Since the H adsorption reaction proceeds rather slowly (if at all) on PtO sites and much faster on oxide-free Pt sites, it was necessary to assume that some inhibition of the electrochemical reaction occurred on oxide-free Pt sites, caused by a deactivating effect arising from neighbouring PtO sites.

If the coverage by oxide species is high compared with the surface fraction of free Pt sites, the H_2 oxidation reaction proceeds very slowly since the oxide-free sites tend to loose almost completely their activity for the electrochemical reaction due to the " extended deactivation " effects from surrounding PtO sites. A much faster reduction was found for a pre-oxidized Pt electrode surface having 6.8% of its surface unoxidized. In this case, although the fraction of Pt-oxide-free sites is small, the free-site area was considered to be completely active for the electrochemical reaction, because all of the available Pt sites on the surface were assumed to be neighbours to each other so that their activity would not be affected by Pt-O sites. Therefore almost all Pt-O species on the anodized surface would be removed in the beginning by the fast electrochemical reduction initiated at the unoxidized Pt sites.

However, it must be mentioned that Shibata and Sumino restricted their experiment to the potential range 0.03 - 1.5V E_H and assumed that only a monolayer PtO is formed on the Pt surface, thus eliminating further oxidation of PtO to " PtO_2 " (see Chapter I) which begins to occur at potentials higher than 1.5V E_H .

A theoretical reexamination of the kinetics of Pt oxide reduction by H_2 (studied by Shibata and Sumino[283]) was given by Rader and Tilak[284] who made an attempt to provide a unified theory of the mechanism of Pt oxide reduction applicable over the entire range of Q_0 . Agreement between the theorethical predictions[284] and Shibata and Sumino's[283] results was found, leading to the conclusion that the most reasonable mechanism at high oxide coverages is the chemical reaction of H_2 with two adjacent PtO sites, which is the rate-determining step. Further reduction proceeds

via a coupled chemical-electrochemical mechanism as proposed by Shibata and Sumino[283]. The theoretical calculations for high oxide coverages had to account for molecular interactions between the adsorbed OH/O species, while good agreement at lower oxide coverages was obtained by taking into account the dissociative adsorption of H_2 to form H on Pt.

2. OBJECTIVES OF THE WORK

In two previous papers[246,254] the origin of electrochemical oscillatory phenomena was examined and demonstrated the role of reactive oxide films and diffusion effects at the Pt electrode in relation to the periodic kinetics of formic acid and ethylene oxidation[246]. In an earlier paper[290], large oscillations in the oxidation of anhydrous formic acid were reported. The electrochemical reactions which formic acid and ethylene undergo at electrodes are known to be complex[291-293], so the study of a simpler system which exhibits oscillations was desirable.

Oscillatory kinetics were observed in the electrochemical oxidation of H_2 at Pt. This is a simple reaction in which dissociative adsorption of H_2 followed by electrochemical oxidation of chemisorbed H ("PtH") can occur in potential ranges below and near those for Pt surface oxidation, according to the reaction steps:

$$Pt + \tfrac{1}{2} H_2 \longrightarrow PtH \qquad \text{III}$$

or

$$Pt + H_2 + H_2O \longrightarrow PtH + H_3O^+ + e^- \qquad \text{IIIa}$$

coupled with

$$PtH \longrightarrow Pt + H^+ + e^- \qquad \text{IV}$$

The region of significant H coverage (θ_H) at Pt is 0 to +0.35V E_H[2,294]; above this potential, $\theta_H \rightarrow 0$. Beyond the potential (ca. +0.8V E_H) of significant oxidation of the Pt surface, it is well known[282] that H_2 oxidation is inhibited but residual oxidation of H_2 on the oxidized Pt

surface can, in principle, occur according to the following formal reactions (cf. refs. 283,284):

$$PtOH + \tfrac{1}{2} H_2 \longrightarrow Pt + H_2O \qquad V$$

$$Pt + H_2O \longrightarrow PtOH + H^+ + e^-, \text{ rapid} \qquad VI$$

Since Pt-oxide formation can play an important role in the H_2 oxidation reaction, it was of interest to determine the reactivity of oxidized Pt electrode surfaces for this reaction by controlling the extent of oxide film formation by varying the H_2O content, as had been done in the work on Cl_2 evolution described in Chapter II.

By conducting the oxidation of H_2 in an almost anhydrous solvent medium, trifluoroacetic acid (TFA), it was found that sustained H_2 oxidation current oscillations can be observed under controlled-potential conditions and limited oscillations under linear potential-sweep[246] conditions. An attempt to explain the nature of this oscillatory behaviour was made by relating the phenomenon to the extent of surface oxidation of the Pt in almost anhydrous TFA, to the mass-transfer of dissolved H_2 by diffusion and to the co-adsorption of CF_3COO^- anions.

3. EXPERIMENTAL

(i) Choice of Solvent System: Trifluoroacetic acid (TFA) was chosen as solvent because (a) it can be made initially almost anhydrous (cf. ref. 189b), pure by normal solvent purification and drying procedures, and very anhydrous by " gettering " remaining traces of water by addition of a trace of trifluoroacetic anhydride through the reaction $CF_3CO\ O\ COCF_3 + H_2O$ traces $\longrightarrow 2\ CF_3COOH$; (b) it is a good ionizing

solvent for a number of salts including potassium trifluoroacetate (KTFA); (c) it is itself, with KTFA as electrolyte, not oxidizable until above + 2.2 V E_H when it undergoes the Kolbe reaction[189a]. Hence there exists a large anodic potential range over which the solvent is electrochemically inactive: for example, no H atoms dissociatively active at Pt exist in the molecule as they do with some other non-aqueous solvents such as CH_3OH, C_2H_5OH or CH_3COOH . TFA is thus an ideal electrochemically inactive solvent, anodically*, and since it does not have actively available the " elements of oxygen " there is also no possibility of oxidation of the Pt electrode surface over a wide range until the carboxylate function is discharged. Hence, effects of controlled trace additions of water which lead to limited surface oxidation of the Pt and to oscillatory behaviour in H_2 oxidation, can conveniently be examined.

(ii) Chemicals and Purification Procedures: All chemicals used were of analytical reagent purity. Further purification procedures were performed as described below:

(a) TFA (Eastman Kodak Co.,) was first gently refluxed over $KMnO_4$ (Fisher Co., Ltd.) for at least 24 hours. The mixture was then slowly distilled, three successive distillations being performed. Prior to the third distillation, 0.05% of trifluoroacetic anhydride was added to reduce to virtually zero the water content in the acid to be used immediately after the distillation in the experimental run.

(b) Trifluoroacetic anhydride (Eastman Kodak Co.,) was used to remove any residual water in the TFA, as mentioned above. It was purified by performing a slow distillation at 312.5 K, prior to use in a run. Later,

*There is evidence[189a] that, in aq. media, cathodic reduction of TFA can occur. However, in the present work, the effects were mostly at potentials well positive to those where reduction of the molecule could occur.

the anhydride was also distilled from $KMnO_4$.

(c) KTFA, used as electrolyte, was prepared by neutralization of previously purified TFA with 5M K_2CO_3 (Fisher ACS analytical grade). The mixture was heated gently until saturation was achieved. The solution was then left to crystallize slowly. The crystals were washed with the mother liquor and dried under vacuum at 110° C.

(d) Water used for water additions in the runs was obtained by the pyrocatalytic distillation procedure previously described[73] in which water is distilled through a silica column containing Pt/Rh gauze at 750° C with O_2 to ensure removal of traces of organic impurities.

(e) H_2 and N_2 gases used for bubbling in the cell were purified as described previously[62,296] with special provision of drying stages (charcoal traps in liquid N_2) in the gas line. The gases were pre-saturated with TFA by bubbling through small traps just prior to entry into the cell.

(iii) Solutions: The solutions used consisted of 0.5M KTFA dissolved in the pure 100% TFA liquid. The dryness or wetness of each solution was controlled with successive additions of trifluoroacetic anhydride or of the pyrodistilled water, respectively.

(iv) Glassware and Cleaning Procedures: A small cell having a volume of 40 cm^3 was employed. The cell was first cleaned with concentrated H_2SO_4, rinsed repetitively first with hot and later with cold pyrodistilled water. Prior to use in a run, the cell was dried for 12 hours in an oven maintained at 200° C. After cooling it for a few minutes just before the run, the inside of the cell was rinsed with trifluoroacetic anhydride to ensure complete dryness.

All glassware used for preparation of the solutions was always treated in the same way.

(v) Apparatus: Potentiodynamic sweep experiments (cf.ref. 22a) were carried out using a Wenking potentiostat driven by a Servomex LF 141 function generator. The current-potential curves were recorded on an Hewlett-Packard XY-recorder through an high-impedance cathode follower. Oscillations generated at constant potential, in time, were recorded on a Y-time recorder.

(vi) Electrodes and Their Purity: Spectroscopically pure Pt wire and gauzes were used. Special attention was given to the procedure for cleaning the electrodes. The following treatment was used: the electrodes were stored in pure B.D.H. Aristar H_2SO_4, then rinsed with the pyrodistilled water and stored in it for a day. They were rinsed with trifluoroacetic acid just prior to being inserted in the cell. A small Pd/H bead electrode was used as a reference element as this electrode could be immersed directly in the electrolyte within the Luggin capilary of the cell thus diminishing the resistance that otherwise arises through a bridge to a separate hydrogen compartment[62,295].

(vii) Experimental Procedure: The solution was first deoxygenated by bubbling purified dry N_2 through the cell for about 20 minutes. Then the current-potential profiles generated by a repetitive linear sweep were recorded. The amount of water present in the solution could easily be characterized (cf. ref. 296) by the quantity of charge associated with the oxide reduction peak[22a,69] at Pt.

Under conditions when only traces of water were present, holding the potential at the anodic end of the sweep for a few minutes enabled an

increase in the oxide reduction peak to be recorded, corresponding to diffusion of H_2O and growth of the oxide film. The same procedure was performed as a test for ultra-dryness of the solution; thus, with holding at the anodic end of the sweep there would be no change in the flat current-potential profile over the oxide reduction region if no water was present. This was found to be the case for five min. holding in solutions " gettered " with trifluoroacetic anhydride.

In order to record oscillations in H_2-oxidation current, the solution under study was bubbled with H_2 for at least 20 minutes. Then the current-potential profile was obtained, showing anodic current-oscillations at about + 1.3 V vs. PdH. To obtain repetition of the oscillatory behaviour for the same solution, H_2 gas was re-bubbled before each recording of the i-V profile.

To obtain current oscillations in time due to H_2 oxidation at constant potential, the Servomex function generator was specially set to terminate a sweep at a predetermined controlled potential (in the cathodic direction) at the value where oscillations were found to commence. They were then recorded on a fast Y-time recorder at chart speeds up to 200 mm s^{-1}.

In all experiments, a reference i-V profile for the Pt electrode in the solution in the absence of H_2 was taken before and after the H_2 oxidation current behaviour was observed. For the profile taken after the H_2 oxidation current experiment, the solution had, of course, to be bubbled out again with dry N_2.

In some experiments, simultaneous relative reflectance $(\Delta R/R)_{\parallel}$ experiments (cf. ref. 297) were performed* while the electrode was giving a periodic H_2-oxidation current. This experiment was conducted in order to indicate if periodic formation and reduction of an oxide film

*These experiments were carried out in collaboration with Dr. F.C. Ho in our Laboratory.

was involved.

4. RESULTS AND PRELIMINARY DISCUSSION

In the presence of H_2 in TFA solution, current oscillations at the Pt electrode were observed under both potentiostatic and potentiodynamic conditions. The oscillatory behaviour was found to depend (a) on degree of dryness of the solution, i.e. on the extent to which the Pt electrode surface was oxidized at appropriate positive potentials, and (b) on stirring.

It was first necessary to define the state of the Pt electrode surface in anhydrous TFA solutions and those containing traces of water by establishing the H adsorption characteristics at Pt in this solution and the extent of surface oxidation that arises in the presence of various trace concentrations of water. In these initial experiments, no molecular H_2 which gives rise to the oscillatory behaviour was present.

(i) The Current-Potential Profiles for Pt in Anhydrous TFA and with Added Traces of Water

(1) Effects of Added Water: The potentiodynamic i-V profile at Pt for the most anhydrous TFA solutions was shown in Fig. 3a and comparatively in Figs. 3b, 3c (see Chapter II, Experimental Section (i), page 73) those for the same solution with controlled additions of water. Holding effects at the positive limit E_a of the anodic sweep are also shown. These results demonstrate (Fig. 3a) the initial dryness of the solution where no detectable (< 1% coverage) surface oxidation of Pt occurs (cf. ref. 296) and how a small and controllable degree of surface oxidation arises (Figs 3b, 3c) when traces of water are present. If the initial dried preparation of distilled

TFA contains, as it usually does, a trace of water, this is indicated by small but significant oxide film formation currents at potentials more positive than ca. 0.95 V E_H and a small oxide reduction peak in the cathodic sweep. An ultra-dry solution can then be obtained by controlled trace additions of trifluoroacetic anhydride until the i-V profile takes the form of Fig. 3a with zero surface oxidation current and no oxide reduction peak in the cathodic sweep. Confirmation of ultra-dryness is given by holding the potential at the positive end of the sweep for 1 - 5 min. (cf. Experimental, Section (vii), page 73) and demonstrating (Fig 3a, curves 2, 3) no development of any Pt-surface oxide reduction peak in a following cathodic sweep: such a Pt-surface oxide reduction peak is found to arise only if traces of water are present when a non-diffusion-controlled oxidation of Pt occurs from traces of water adsorbed at the Pt (perhaps surprisingly there is no effect of bubbling N_2 on the degree of surface oxidation of Pt attained in the presence of H_2O).

The extents of surface oxidation of Pt in Figs. 3a-c are found, as expected, to be substantially below a monolayer (this is obvious in comparison with the H atom charge for the same electrode) when only traces of water are present.

(2) H Adsorption in Anhydrous and Almost Anhydrous TFA: It is interesting that even in the driest solution, current peaks for adsorbed H atom deposition and ionization[22a] are observed (Fig. 3a) indicating that underpotential deposition[298] of chemisorbed H in at least two states (there are 4 or 5 observable in water [297,298]) on the Pt surface is possible in a solvent other than water. By comparative experiments in 0.1M aq. $HClO_4$ on the same electrodes, it was shown that the H-accommodation at Pt in anhydrous TFA up to the H_2-reversible potential is about 40% of

that in water. The charge for H deposition and ionization on the same electrode studied in 0.1M aq. $HClO_4$ was therefore used as a standard of reference[298] for evaluation of extents of surface oxidation of Pt in the TFA solutions. The appearance of adsorbed H starts at + 0.2V to the H_2-evolution potential in TFA (instead of + 0.35V in aqueous $HClO_4$). This is almost certainly due to competitive adsorption of the TFA anion in this solution, as e.g. is found for halide adsorption in aqueous solutions (see Chapter III). The remainder of coverage by H up to a monolayer presumably occurs by deposition at potentials negative to the reversible H_2 potential in TFA as solvent. However, this H is inacessible to direct measurement.

It is to be noted that when the solution has been " gettered " with trifluoroacteic anhydride, there is a significant (10%) diminution of H accommodation at the Pt surface due presumably to adsorption of residual anhydride. However, upon addition of traces of water (Fig. 3b), the full extent (± 2%) of H adsorption for the TFA solvent is attained again after about 0.74 mol% of water has been added.

That the coverage by adsorbed H in excess TFA as solvent does attain a well-defined value up to the H_2 reversible potential was demonstrated by " holding " experiments (Figs. 3b, 3c) in which progressively increased quantities of surface oxide were generated in the presence of traces of water by keeping the potential at the positive end (+ 2.15V E_H) of a potential sweep for periods τ_h of 30, 60 and 120 s. These experiments show that the i-V profile for H deposition and ionization on the electrode remains almost constant (Figs. 2b, 3c), thus indicating that the below-monolayer coverage attained was not due to adsorption of impurities which are normally oxidatively displaced by this procedure. The H deposition/

ionization charge in Fig. 3c is 109 ± 10 $\mu C\ cm^{-2}$ compared with 270 μ C per apparent cm^{-2} observed for the same electrode in aq. 0.1M $HClO_4$.

(3) Surface Oxidation of Pt in Almost Anhydrous TFA in Relation to that in Water: The effects of added water on the i-V profiles for Pt in TFA were shown in Figs. 3a-c. The behaviour of the oxide film formed at Pt from traces of water in TFA, i.e. when the oxide film is present only at low coverages, is seen to be surprizingly similar to that of fuller films on Pt in water (Figs. 29 and 30). Despite the low coverage ($\theta_{OH} \simeq 0.1$ can easily be achieved in a " fairly dry " solution); the surface oxide begins to be formed in TFA at ca. 1.05 V E_H (Fig. 3b) but is reduced only at appreciably less positive potentials, commencing at 0.95 V E_H, as is the oxide formed in the fully aqueous solution. This suggests that the small coverage by oxide may be present as islands on the Pt surface.

If the potential sweep at Pt in TFA in the presence of ~~≈9~~ mol% water is progressively cut from 2.090 to 1.560 V E_H, the extent of surface oxidation (and the corresponding charge for reduction of the surface oxide) diminishes as in fully aqueous solutions[69]. Thus the oxide reduction charge Q decreases linearly with diminishing end potential E_a in the previous anodic sweep (Fig. 29) and the reduction peak potential V_p is linear in the oxidation charge Q (Fig. 30). These two figures also show comparatively the behaviour in aq. $HClO_4$ solutions. However, the slope $-dV_p/dQ$ in Fig. 30 is much larger in TFA than it is in aq. solution while dQ/dE_a (Fig. 29) is much smaller. This suggests that there is a relatively greater stabilization due to place exchange of the oxide film grown in TFA from traces of water than that grown from fully aqueous

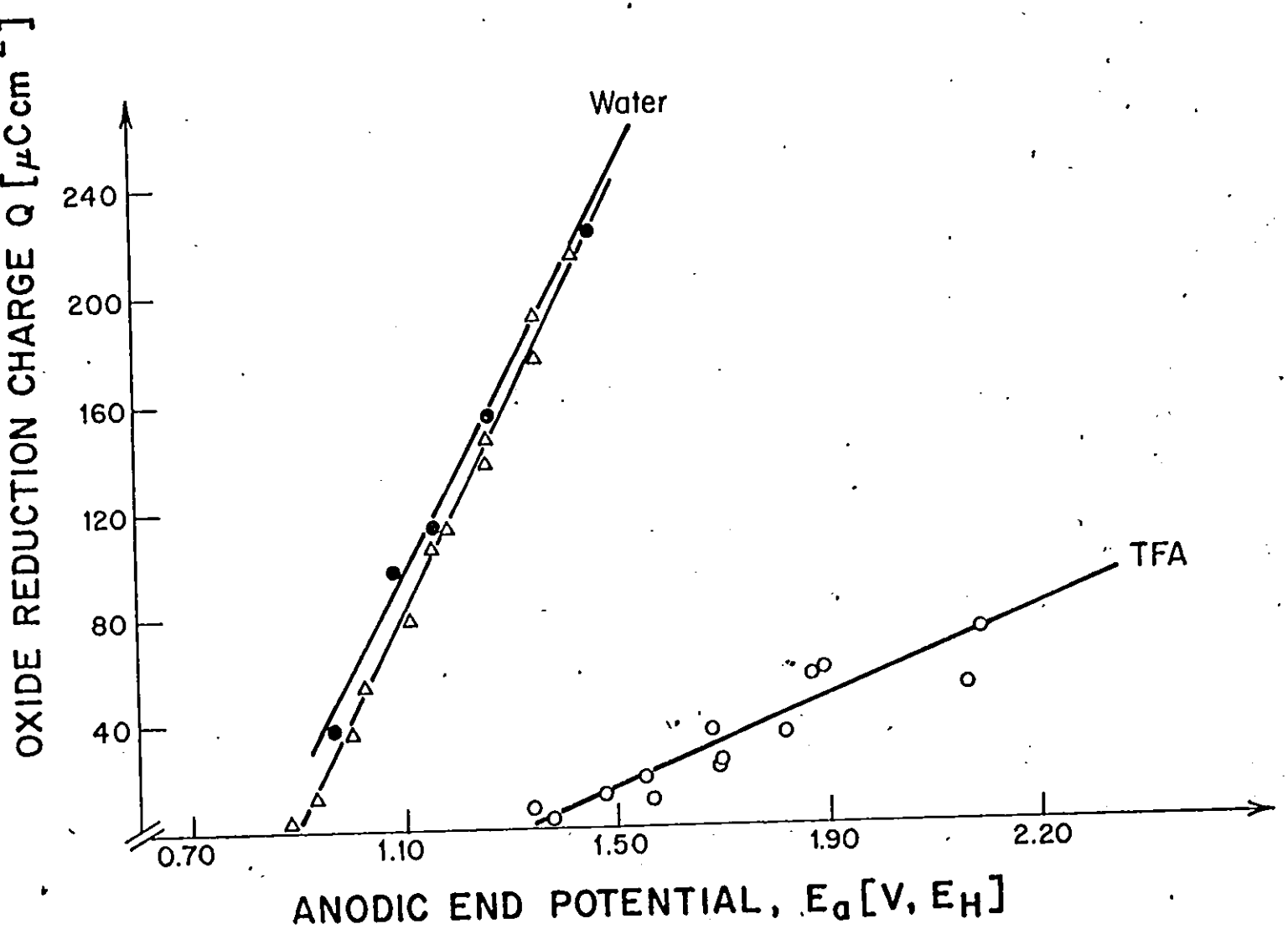

Fig. 29 Effect of diminishing positive end potential E_a in the anodic sweep at Pt in TFA containing 0.42 mol% H_2O (and in 0.1 and 1.0 M aqueous $HClO_4$ for comparison) on the charge for surface oxide formation and reduction ; (△) 1M aqueous $HClO_4$; (●) 0.1M aqueous $HClO_4$; (○) 0.5 M KTFA in TFA.

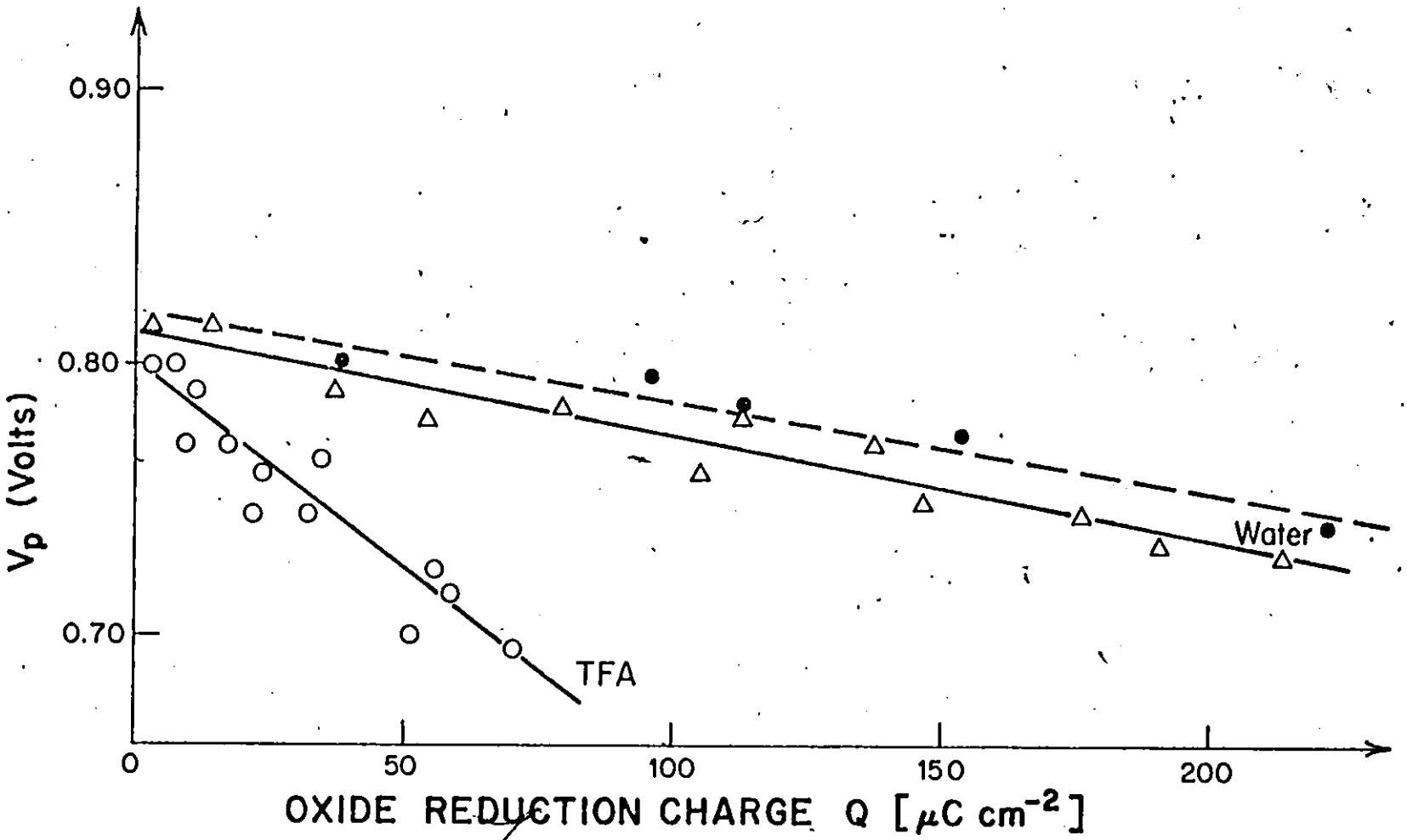

Fig. 30. Plot of cathodic peak potential V_p for reduction of surface oxide at Pt as a function of the charge for reduction in TFA and aqueous 0.1 and 1.0 M $HClO_4$; (△) 1.0M aqueous $HClO_4$; (●) 0.1 M aqueous $HClO_4$; (○) 0.5 M KTFA in TFA with 0.42 mol% H_2O. Scale for V_p: H_2/H^+ potential in the same (aqueous or TFA) solution.

solution. Presumably this arises from the different strengths of adsorption of the two solvents (cf. refs. 299,300 for H_2O adsorption) at the oxidized Pt surface and the greater metal/solution field that can exist in the double-layer due to the lower dielectric constant of TFA than that of water.

(ii) Oscillations in H_2-Oxidation under Potentiostatic Conditions:

From potential-sweep experiments [see Section (iii) below] it was found that oscillations in the molecular H_2-oxidation current arise at a critical potential, V_c , corresponding to the commencement of reduction of surface oxide at Pt. The potential V_c depends on the surface coverage of the oxygen film as can be seen from Fig. 29 and is, of course, dependent on water concentration since the latter determines the extent of surface oxidation at a given potential. That the oscillations are not due to participation of the external circuit (cf. ref 252) was shown by varying the resistance from which the current measurement is made or by varying a series resistance in the reference-electrode circuit. They are thus intrinsic kinetic oscillations of the type that has been previously observed in other systems[244,245,246].

Sustained oscillations could be demonstrated by adjusting the potential potentiostatically at the value V_c and following the oscillating current on an high input-impedance potential-time recorder system. Examples of this kind of oscillating current behaviour for H_2-oxidation are shown in Figs 31a, b, c, d.

In contrast to the oscillatory behaviour of HCOOH or C_2H_4 oxidation[246], the H_2-current periodicity is initially (Fig. 31a and to some extent as in 31b) almost sinusoidal corresponding to " linear-oscillation "[256] behaviour. This may be connected with the simpler

Fig. 31 - see following page

Fig. 31 Four examples (a, b, c, d) of potentiostatic (+ 1.24 V) oscillations of H_2 oxidation current at the Pt electrode in TFA: (a) is the almost sinusoidal oscillation occurring initially; (b) is the nonsinusoidal, but still simple, oscillation which develops later; (c) and (d) are compound oscillations which develop subsequently (the relative amplitudes of the two components also vary slowly with time). The time base was 4 cm s^{-1}. (e) Record of an apparent simple type oscillation on a faster time base (20 cm s^{-1}) showing " nonsinusoidal " behaviour (the very low amplitude oscillations superimposed on this record are due to writing noise in the recorder).

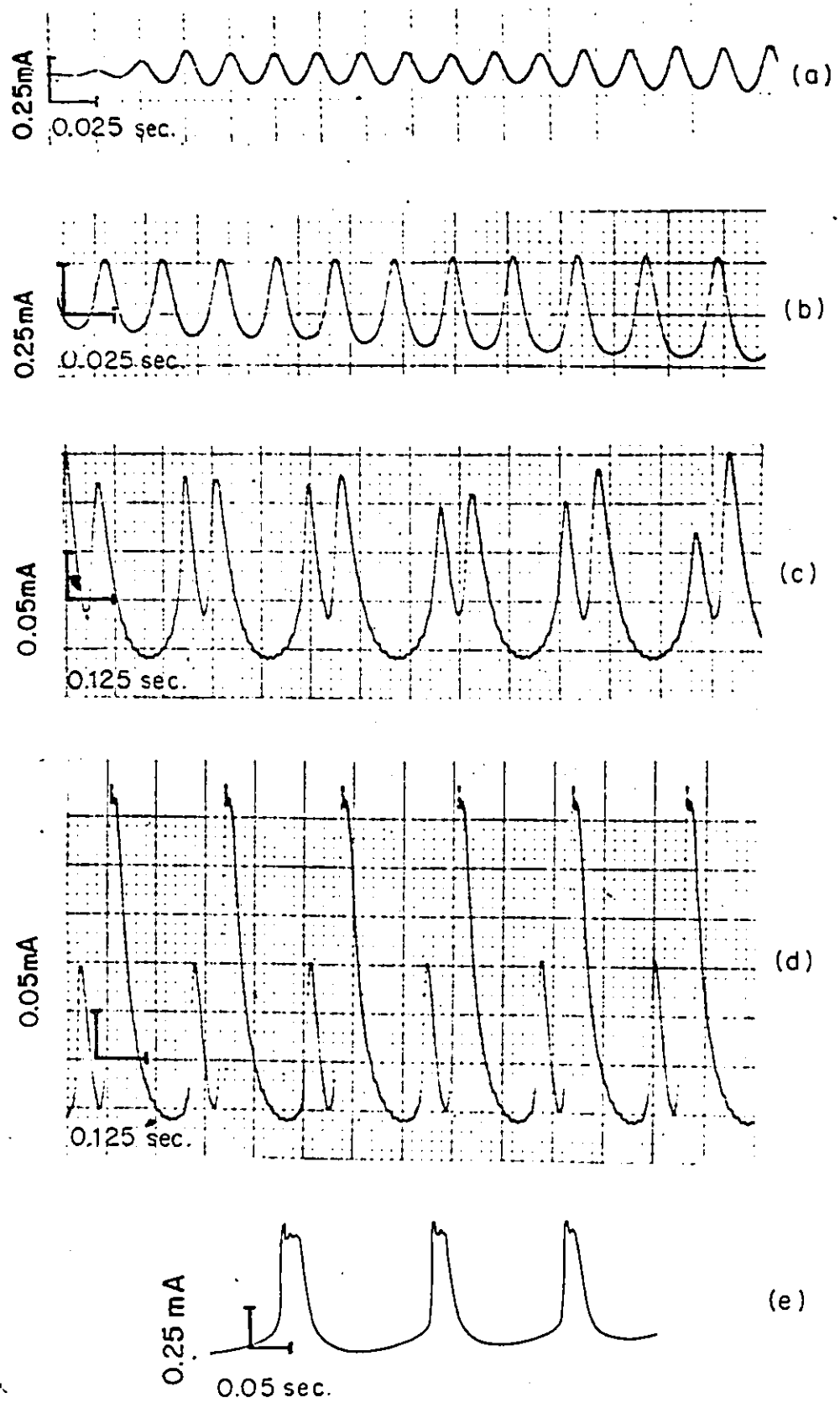
0.25mA
0.025 sec.
(a)
0.25mA
0.025 sec.
(b)
0.05mA
0.125 sec.
(c)
0.05mA
0.125 sec.
(d)
0.25 mA
0.05 sec.
(e)

reaction involved with H_2 than with HCOOH or C_2H_4. However, it is evident from Figs. 31c,d for example, that there is some compound oscillation also involved as there are two components in the " sinusoidal " oscillations which develop in Figs. 31c,d and show a superimposed longer-period change of amplitude. No oscillations arise if the solution is " absolutely anhydrous " nor if excess water is present [see Section (iii) below]. An enlarged record of a single-peaked oscillation on a faster time-base is shown in Fig 31e from which it is clear that once the oscillations have become established, they deviate substantially from the almost regular sinusoidal form of Fig. 31a.

The charges q in each oscillation can be evaluated from $\int_0^\tau i\,dt$ over a single oscillation. Two questions arise with regard to these charges q : do they correspond to the charges for reduction (by H_2) of a small area of Pt surface oxide periodically generated from the traces of water or do they correspond to charges for oxidative depletion of H_2 in the diffusion-layer? It is therefore of interest to evaluate the Faradaic charges q involved in selected samples of the current oscillations (see Figs. 31a-d). This can be easily done by calculating $\int_0^\tau i\,dt$ over the period τ of the oscillation which can be accurately measured from the calibrated recorder traces (e.g., Figs. 31a-d). Values are shown in Table 2 for the sample oscillations in Figs. 31a-d. Two samples were taken of each oscillatory mode and gave reasonable reproducibility of the respective q values.

At the beginning of the potentiostatic oscillation, q is small (ca. 6 $\mu C\ cm^{-2}$, Fig. 31a) while later, when the oscillations have developed in amplitude, q attains values in double peaks (Fig. 31c) up to 296 $\mu C\ cm^{-2}$. The latter values are much larger than would correspond to periodic reduction and re-formation of the oxide film in almost dry

TABLE 2

CHARGES ASSOCIATED WITH OSCILLATIONS IN CURRENT AT CONSTANT POTENTIAL

Oscillation	Charge per unit area of electrode ($\mu C\ cm^{-2}$) ± 2%	
Fig. 31a initial oscillation	7.7	
initial oscillation	8.9	
initial oscillation	6.4	mean 6.1
initial oscillation	3.1	
initial oscillation	4.5	
Fig. 31b sample 1, double peak	128.5	
larger component	100.5	
smaller component	28.0	
sample 2, double peak	130.0	
larger component	100.0	
smaller component	30.0	
Fig. 31c sample 1, double peak	286.0	
larger component	136.0	
smaller component	150.0	
sample 2, double peak	296.5	
larger component	145.5	
smaller component	151.0	
Fig. 31d sample 1, double peak	284.5	
larger component	175.5	
smaller component	109.0	
sample 2, double peak	256.5	
larger component	152.0	
smaller component	104.5	

solutions (viz. 20 - 40 $\mu C\ cm^{-2}$) and must therefore correspond to oxidation of H_2 from the diffusion layer.

The quantity of H_2 in the diffusion-layer in a static solution, based on an estimate of the solubility of H_2 in TFA + 0.5 M KTFA, is approximately 4.4×10^{-8} mol cm^{-2} in a lamina of thickness of 0.02 cm. This corresponds to a charge of ca. 8800 μ C cm^{-2}, i.e. very much larger than the charge in a single oscillation at constant potential, but only partial depletion of the diffusion-layer may, of course, occur. This suggests that although oscillations are connected with diffusion, since they no longer occur in a stirred solution [see Section (iii) below] , the charge in the oscillation could, in part, be connected with the periodic reduction of an oxide film. It is to be noted, however, that in the potentiodynamic experiments (see following section), the current spikes in a static solution (e.g. in Figs. 38, 40 see below) almost reach the diffusion-limited current measured in a well-stirred solution.

In solutions containing controlled additions of water, the oscillations always commence or occur in the cathodic i-V profile just where reduction of the incomplete oxide film commences, that is where, on the anodic sweep, oxide film formation is also just commencing. It is known[69] that the commencement of surface oxide formation at Pt (up to $\theta_{OH} = 0.15$ in aq. solution) is an almost reversible process. Hence, at this potential, some small fractional coverage of surface oxide can periodically be formed and reduced. It is clear, however, that a large coverage of OH or O species cannot behave in this way because of the well-known hysteresis[22a,61,69] between formation and reduction of appreciable coverages of OH and O species on Pt. Thus, coverage in excess of a monolayer of OH is only achieved in water beyond 1.1 V E_H but reduc-

tion of this quantity of material only commences at ca. 0.75 V E_H. Hence, only a small reversible component (cf.ref. 69) of such an oxide film could sustain oscillations associated with periodic formation and reduction of the film over a narrow potential range.

(iii) Oscillations in H_2-Oxidation Current under Potentiodynamic Conditions

(1) Behaviour in almost Dry Solutions: In an extremely dry solution, gettered by the anhydride, the i-V profile of Fig. 32 is observed and no oscillations arise. Under these conditions, inhibition of H_2 oxidation which normally occurs at ca. 0.9 - 1.0 V E_H (see Fig. 35,36) does not arise; H_2 oxidation then continues with substantial currents up to high positive potentials (+ 1.86 V E_H in Fig. 32). Then both the anodic and cathodic i-V profiles are almost identical and no oxide inhibition effect occurs. This is consistent with the background i-V profile for the Pt electrode in anhydrous TFA in the absence of H_2 (curve b of Fig. 32) which shows no sign of surface oxidation, even after holding the potential for up to 5 min at 1.86 V E_H. Stirring increases the current substantially (Fig. 32), depending on stirring rate, so that H_2 oxidation is diffusion controlled.

If a very small trace of water is, however, still present or is added, the system exhibits oscillation on the cathodic sweep right from the most positive end of the sweep as shown in Fig. 33 . The oscillations, it seems, are not dependent, in this case, on the reduction of a significant fractional oxide film on the Pt surface as they are when more water is present (see Figs. 35, 37, 38 below). These oscillations

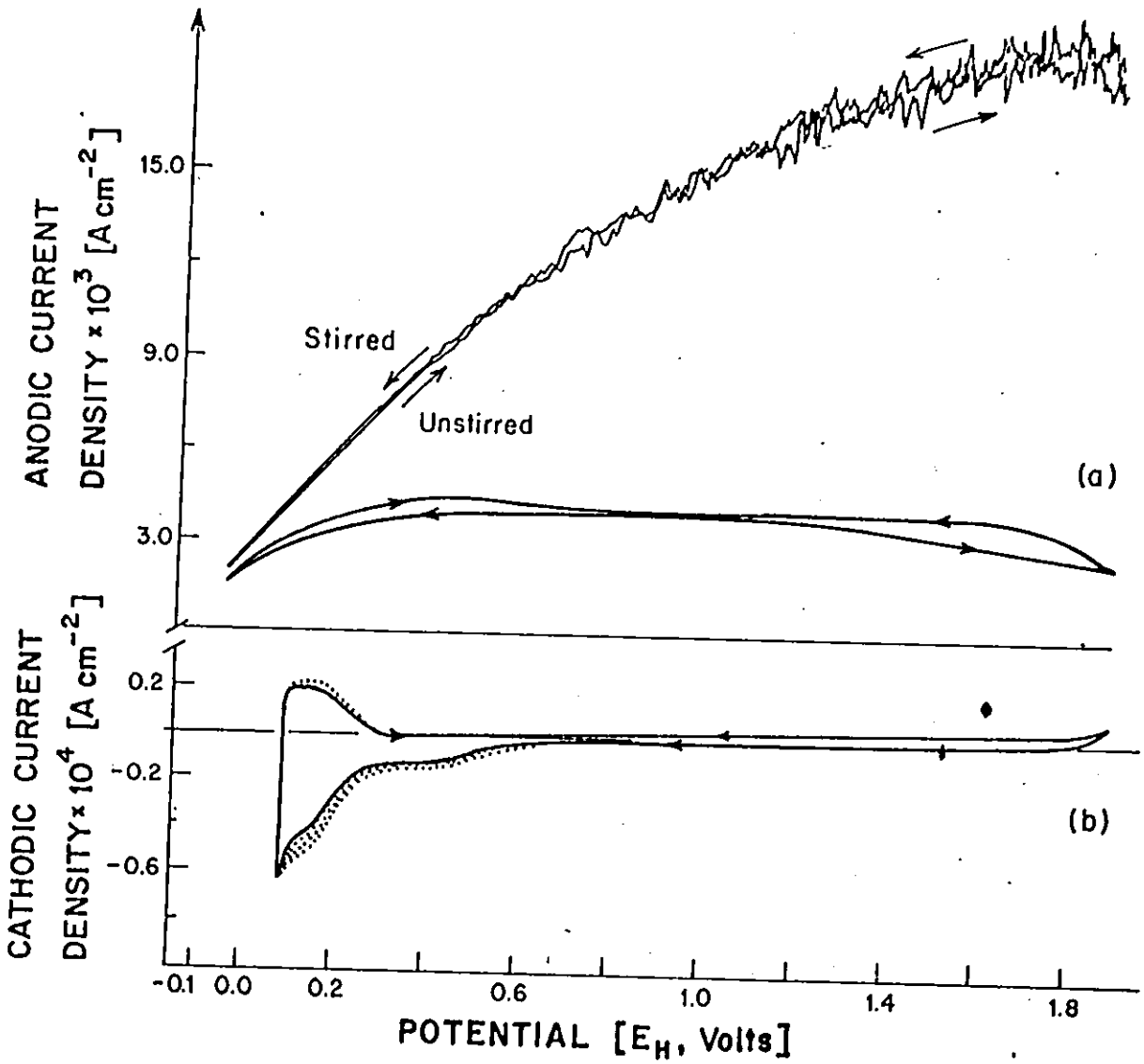

Fig. 32 (a) Current-potential profiles for H_2 oxidation in very dry TFA + 0.5M KTFA solution (stirred and unstirred) ; $s = 7.7 \times 10^{-2}$ V s^{-1}, T = 298 K. (b) Background i-V profile for Pt in the TFA solution in absence of H_2. In (a), irregular curve is due to stirring " noise ".

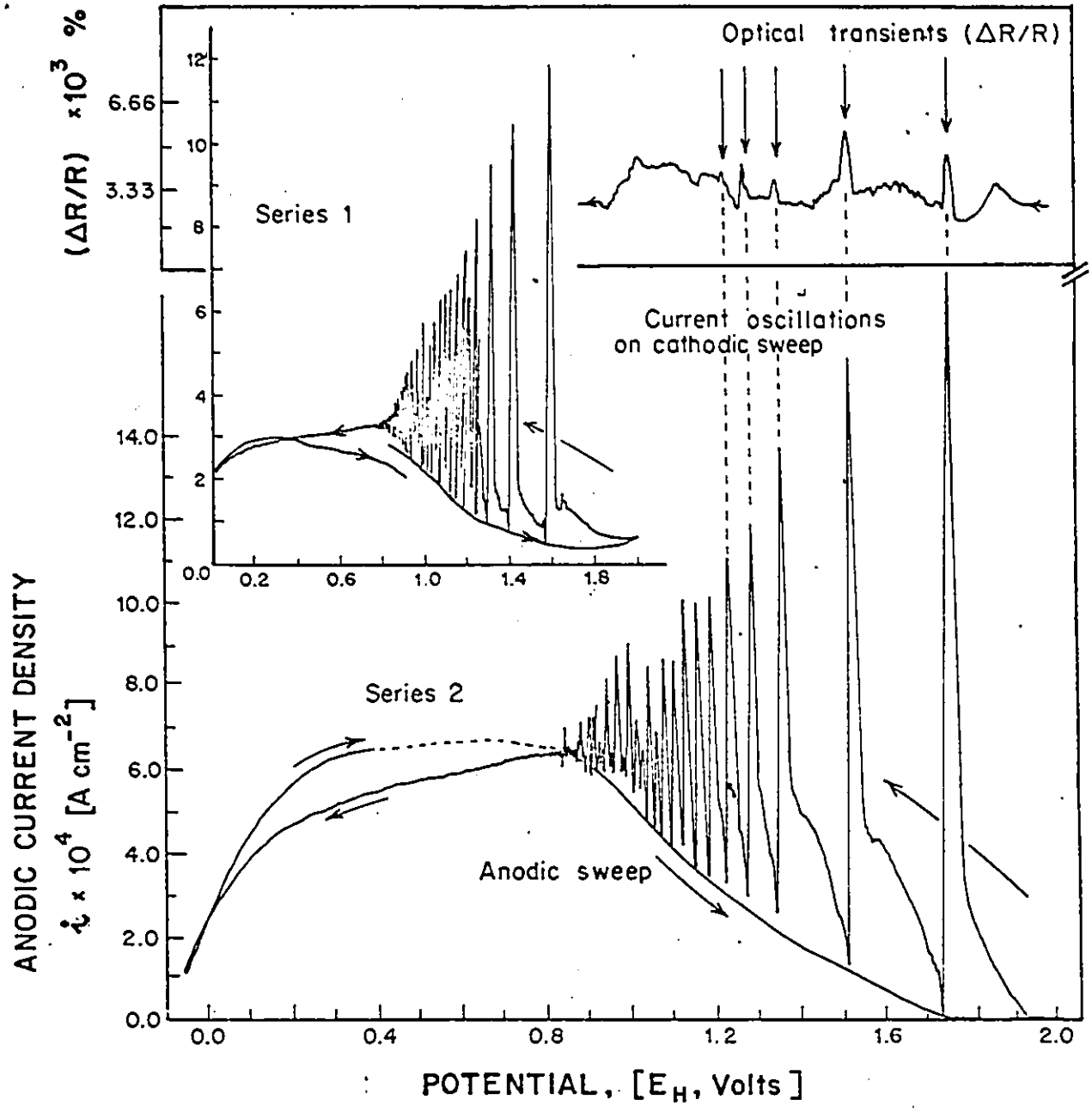

Fig. 33 Current oscillations in H_2 oxidation on the cathodic sweep in two potentiodynamic experiments on H_2 oxidation at Pt in almost dry TFA + 0.5 M KTFA ($s = 8 \times 10^{-2} V\ s^{-1}$, T = 298 K). Note: potential scale of series 1 is half sensitivity of that for series 2 to accomodate the results on a single graph. Upper curve, relative reflectance changes ($\Delta R/R$) measured simultaneously with the oscillations.

have an amplitude which almost reaches the current profile attained in a well-stirred solution (Fig. 32) and their lower limits are seen (Fig. 33) to coincide with the locus of currents generated on the previous anodic sweep. This situation is again different from that arising when sufficient water is present to produce a significant oxide film (see Figs. 35, 37, 38 and 40).

Inspection of the series of oscillations in Fig. 33 shows that their interval diminishes as their amplitude decreases during the progress of the cathodic sweep. This suggests that each current pulse occurs after an interval of time, Δt , from the previous spontaneous pulse (Fig. 33) determined by the period required for the H_2 concentration at the electrode to recover, by diffusion, almost to its bulk value in the diffusion-layer. When this situation is established, the electrode is reactivated for H_2-oxidation and a new current pulse is generated. This mechanism leads to the expectation, based on well-known principles of diffusional transport and the concept of " transition time "[301], that the magnitude of successive current pulses in the sweep should decrease with the square-root of the time interval, Δt , between the successive oscillations of Fig. 33.

This is elegantly proved by the plots in Fig. 34 which show that the amplitude of successive oscillations is a good linear function of $(\Delta t)^{\frac{1}{2}}$ for two separate examples of oscillatory behaviour. As required for this mechanism, the i vs. $(\Delta t)^{\frac{1}{2}}$ plots extrapolate through the origin. The key role of diffusion coupled with the electrode reaction at the Pt surface is thus established by the plots in Fig. 34.

The " on-off " nature of the periodicity of current under poten-

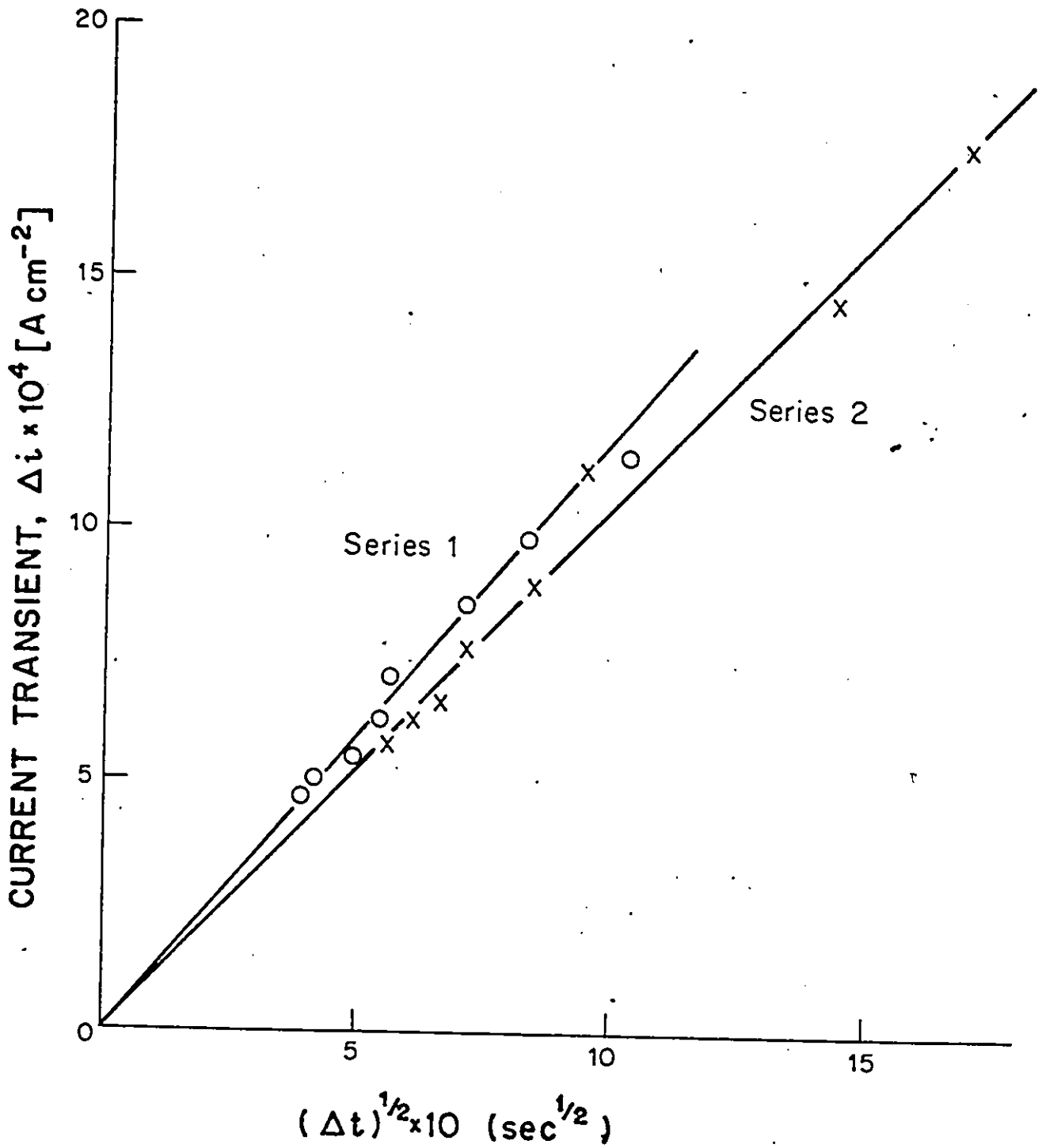

Fig. 34 Test of relation between current oscillation amplitudes Δi in Fig. 33 and the square-root of the time interval, Δt, between successive oscillations for the two series of oscillations shown in Fig. 33 for separate experiments.

tiodynamic conditions (Fig. 33), where the oscillations are virtually well separated pulses, suggests that the integrated equation for diffusion of H_2 at an electrode at which the H_2 is oxidized at a current density i, viz.

$$c_b - c_e = \frac{2i}{zF}\left(\frac{\Delta t}{D}\right)^{\frac{1}{2}} \qquad (42)$$

can be applied to each pulse as though it were a current transient with an associated transition time, Δt , for c_e to approach zero. In eq. (42), c_b is the bulk concentration of H_2 in mol cm^{-3}, c_e that at the electrode, D is the diffusion constant of H_2, t the time and z the number of Faradays per mol for the oxidation reaction. From the maximum (initial) current pulse in Fig. 33 and the corresponding time interval Δt (see relations in Fig. 34), an estimate of $c_b - c_e$ can be made. It is found to be almost equal to c_b the saturation solubility of H_2. Thus the current oscillation consumes almost all the H_2 built up previously in the diffusion layer while H_2 oxidation was inhibited.

The upper curve of Fig. 33 shows that the oscillations are accompanied by significant periodic relative reflectivity (cf. ref. 297) changes of the surface, indicating that the current periodicity is not just due to periodic diffusion effects but also to changes of state of the surface of the electrode. In this experiment, the TFA was almost, but not completely, dry as indicated by the anodic current profile for H_2 oxidation and a separate background experiment in the absence of H_2. In these circumstances, it seems that the periodic transients in $\Delta R/R$ should be related to anion desorption/readsorption rather than to oxidation and reduction of the surface involving the traces of water [see Discussion, Section (iii)] , although some oxide film effect is almost certainly present.

(2) Relation to Surface Oxidation of Pt in TFA with Controlled Additions of Water: Under potentiodynamic conditions where a range of potentials is scanned, it was always easy to generate temporary oscillations as the potential in the sweep passed through a range near V_c [see Results, section (iii)] provided that (a) the solution was not too dry or (b) a substantial concentration of water (> 5%) was not present (see below). The behaviour observed was reproduced on many occasions at various electrodes and from different solutions over a period of two years.

If the quantity of water present is small, so that only a fraction of the Pt surface is covered by an oxide film, then oscillations occur on the cathodic sweep (three or four, or more, are observed depending on extent of prior oxidation of the electrode) once the potential for commencement of oxide reduction has been reached at V_c. The charges associated with the oscillations vary from ca. 6 to 40 $\mu C\ cm^{-2}$, i.e., comparable with the charge required for depletion of H_2 in the diffusion layer. Fig. 35 shows an example of the potentiodynamic i-V profile for H_2 oxidation at Pt in TFA + 0.2 mol% H_2O. Contrast Fig. 32 for very dry TFA.

In order to understand this behaviour, it is useful first to relate it to the i-V profiles for H_2-oxidation which arise (without oscillations) in aqueous solutions.[117] Under such conditions, molecular H_2 is oxidized continuously at Pt in a diffusion-controlled reaction over the potential range 0.0 to 0.75 V E_H and in the H atom adsorption region at Pt (0.0 to 0.35V E_H) the H_2 molecule oxidation current simply adds to that of chemisorbed H (Fig. 36). Around + 0.75V E_H, however, (Fig. 37) inhibition of the H_2-oxidation commences, until by 1.1V E_H where the Pt

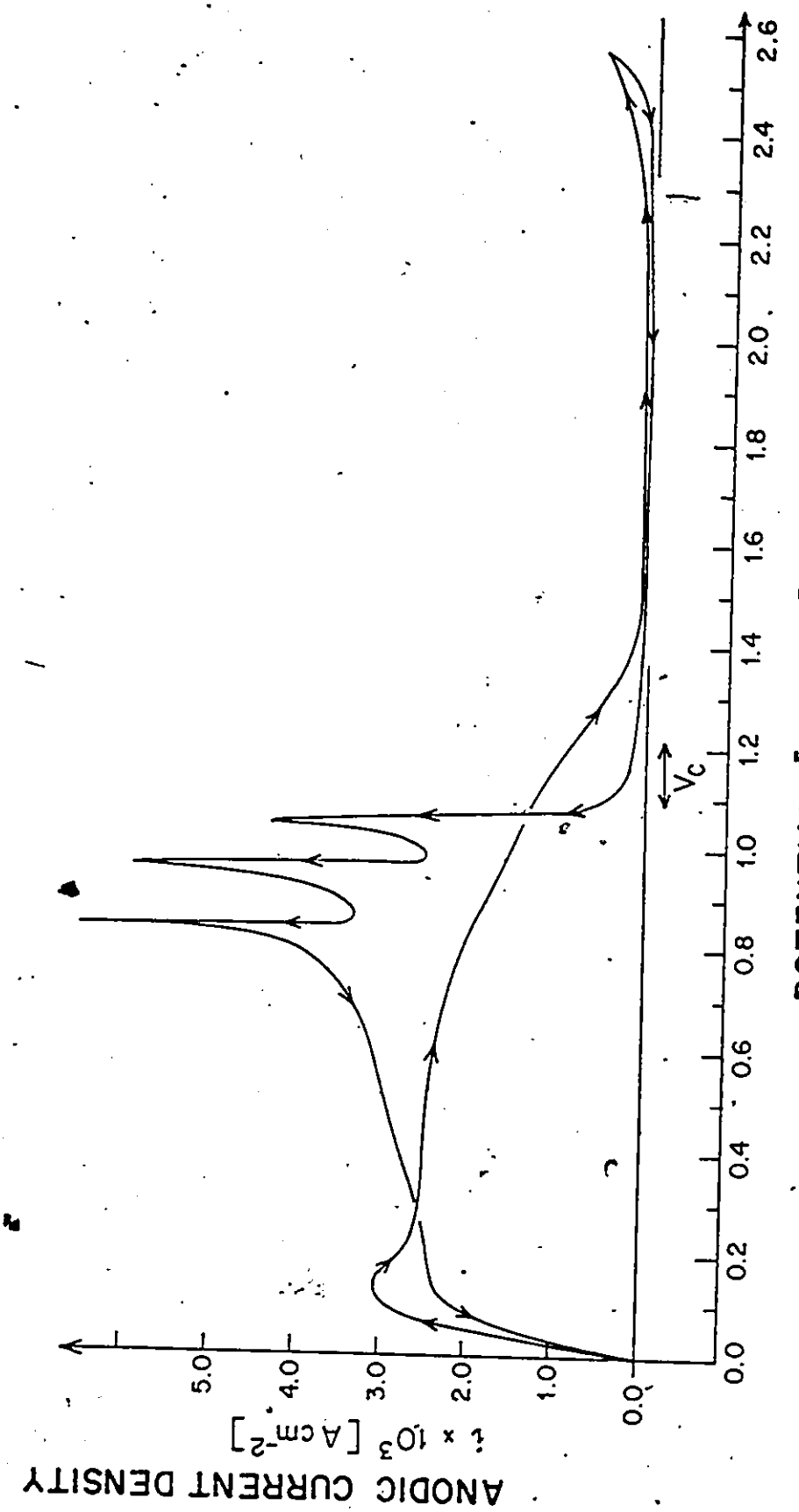

Fig. 35 Current oscillations in H_2 oxidation on the cathodic sweep in a potentiodynamic experiment at Pt in TFA + 0.2 mol% added water.

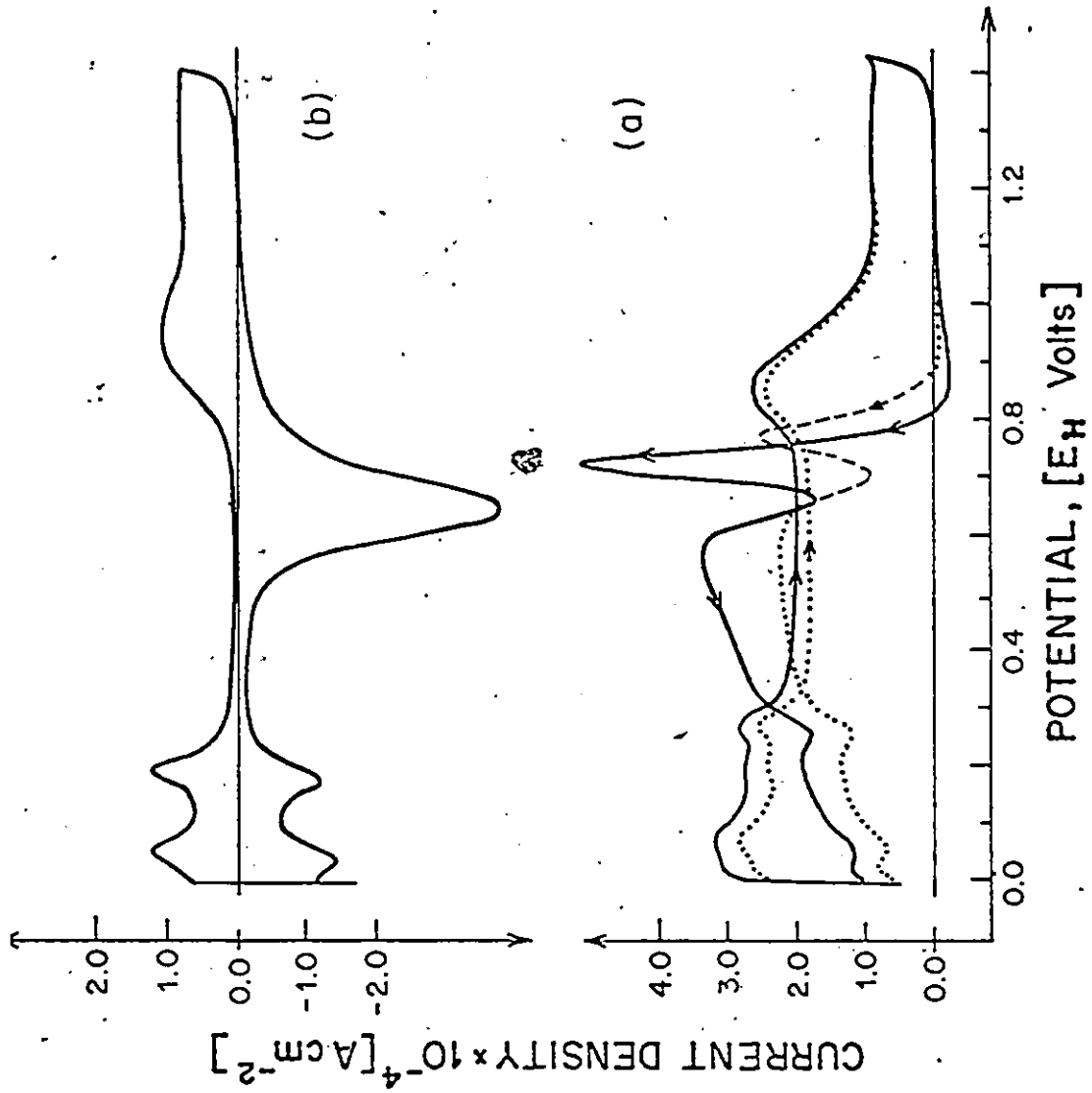

Fig. 36 Potentiodynamic i-V profiles for H_2 oxidation at Pt in 0.1 M aqueous $HClO_4$ without (broken line) and with (solid line) holding at 1.453 V E_H for 2 min; (a) Background curve (without H_2 present) for Pt surface oxidation and reduction over the same potential range at the same sweep rate shown above for comparison in (b). Sweep rate = 1.15×10^{-1} V s^{-1}.

electrode is fully covered by OH species[69], the H_2-oxidation current has become negligible. The behaviour is illustrated in Fig. 36 where the i-V profile for H_2 oxidation at Pt is compared with that for formation and reduction of the surface oxide in the absence of H_2. The H_2-oxidation current is, to a close approximation (cf. refs. 283,284), the difference between these two curves as shown in Fig. 37. The two current contributions (from H_2 oxidation and that of the surface) may not be entirely independent since in the potential regions where OH is just appearing on the surface or the oxide film is just being reduced (in the cathodic sweep) some direct chemical reaction of H_2 with the OH or O species could arise (cf. refs. 283,284). However, on the anodic sweep, this effect is not significant.

The main point of similarity to Fig. 35 is that as soon as oxide film reduction begins, a sharp increase in the anodic current component for H_2-oxidation arises but subsequently the cathodic current for oxide film reduction becomes temporarily appreciable and reverses the direction of change of the current giving a maximum in the net anodic current (since the oxide film reduction current increases in proportion to sweep rate, this component appears more important at higher sweep rates). This effect is seen more clearly in Fig. 37 , curve (b) where the electrode has been held for 2 min. at the positive end of the anodic sweep allowing more oxide to be formed[22a,69] than in the case of curve (a) for a repetitive sweep; then, on the cathodic sweep, the H_2-current increase is sharper when oxide film reduction commences but the oxide film reduction current is also larger due to the greater quantity of oxide formed because of potential holding. The sharp increase of H_2-oxidation current in the cathodic sweep is seen to be

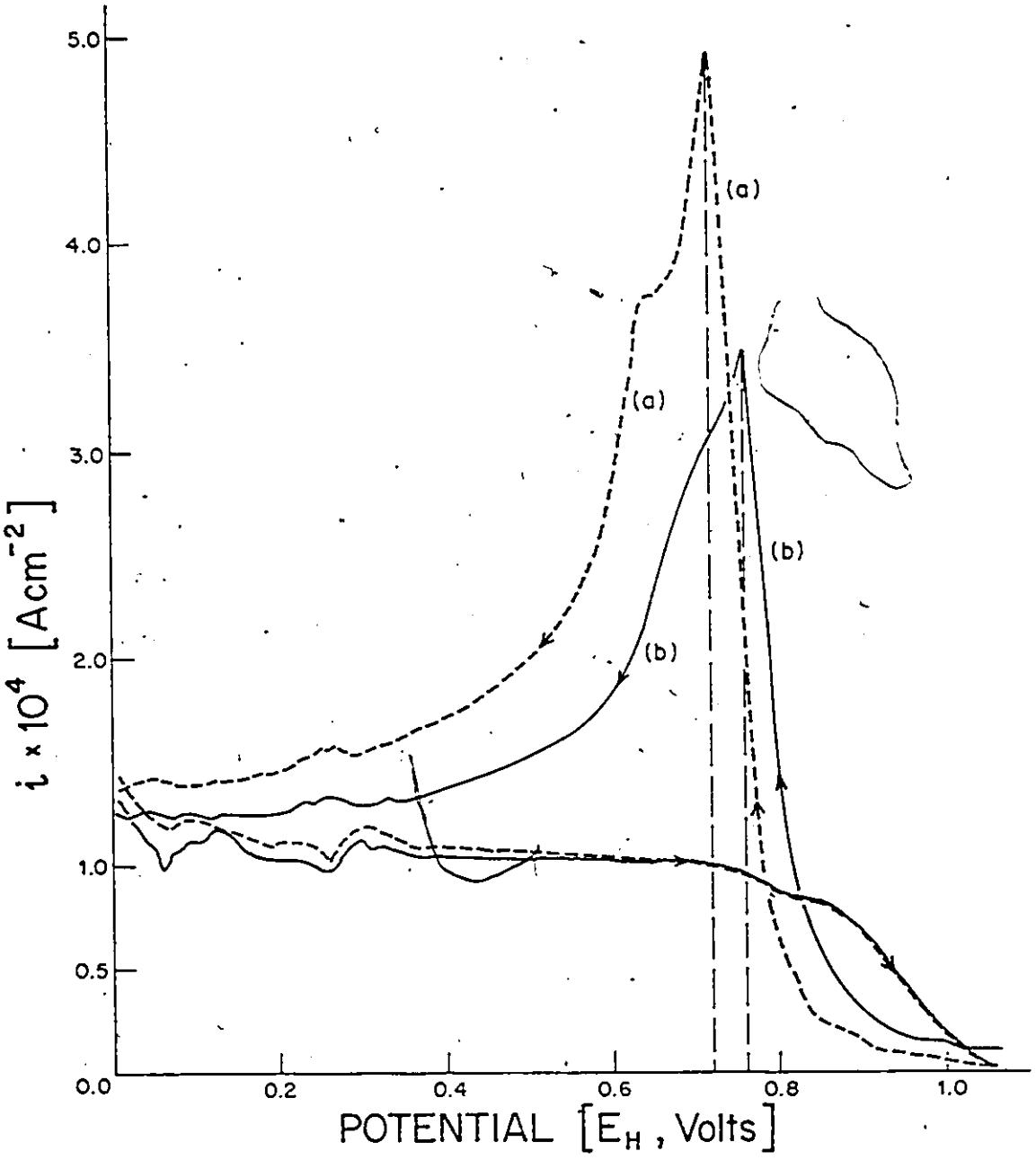

Fig. 37 Current difference curves for H_2 oxidation at Pt in 0.1 M aqueous $HClO_4$ with holding for 2 min (a) and without holding (b) (as in Fig. 36), i.e., after subtraction of background i-V profile for Pt in absence of H_2.

analogous to that in Fig. 35 at the potential where oscillations commence in TFA but no oscillations are generated in the aq. medium case (Figs. 36 and 37).

In the " nonaqueous " solution case with TFA, it is significant that the derivative di/dV at the point where oxide film reduction just commences (Fig.35) is larger than for the case of aqueous solutions and approaches " infinity " where the oscillations commence, i.e., no stable steady state is realized. This behaviour is similar to that associated with a bifurcation set in the cusp-catastrophe theory of discontinuos processes[302].

An important part of the sudden increase of H_2-oxidation currents in Figs. 36 and 38 at the commencement of oxide film reduction, especially after anodic holding, must be due to the accumulation of H_2 in the diffusion layer (cf. page 211) during the time in the sweep when H_2-oxidation was inhibited. When inhibition is relieved by surface oxide reduction in the cathodic sweep, a sudden increase of current to values larger than on the anodic sweep arises because (a) the free catalytic surface of Pt is generated having high activity (as also observed in oxidation of organic substances at Pt) and (b) the H_2 concentration at the interface in the diffusion layer has become increased towards the bulk value. The same will apply to the behaviour in the almost anhydrous TFA solutions in the oxide inhibition region but the quantity of oxide generated as a film in Figs. 36 and 37 (ca. 600 μ C cm^{-2}) when water is in excess is, of course, much greater than that in Fig. 35 where only a small coverage of OH and O species is generated from the trace of water present in the TFA solution.

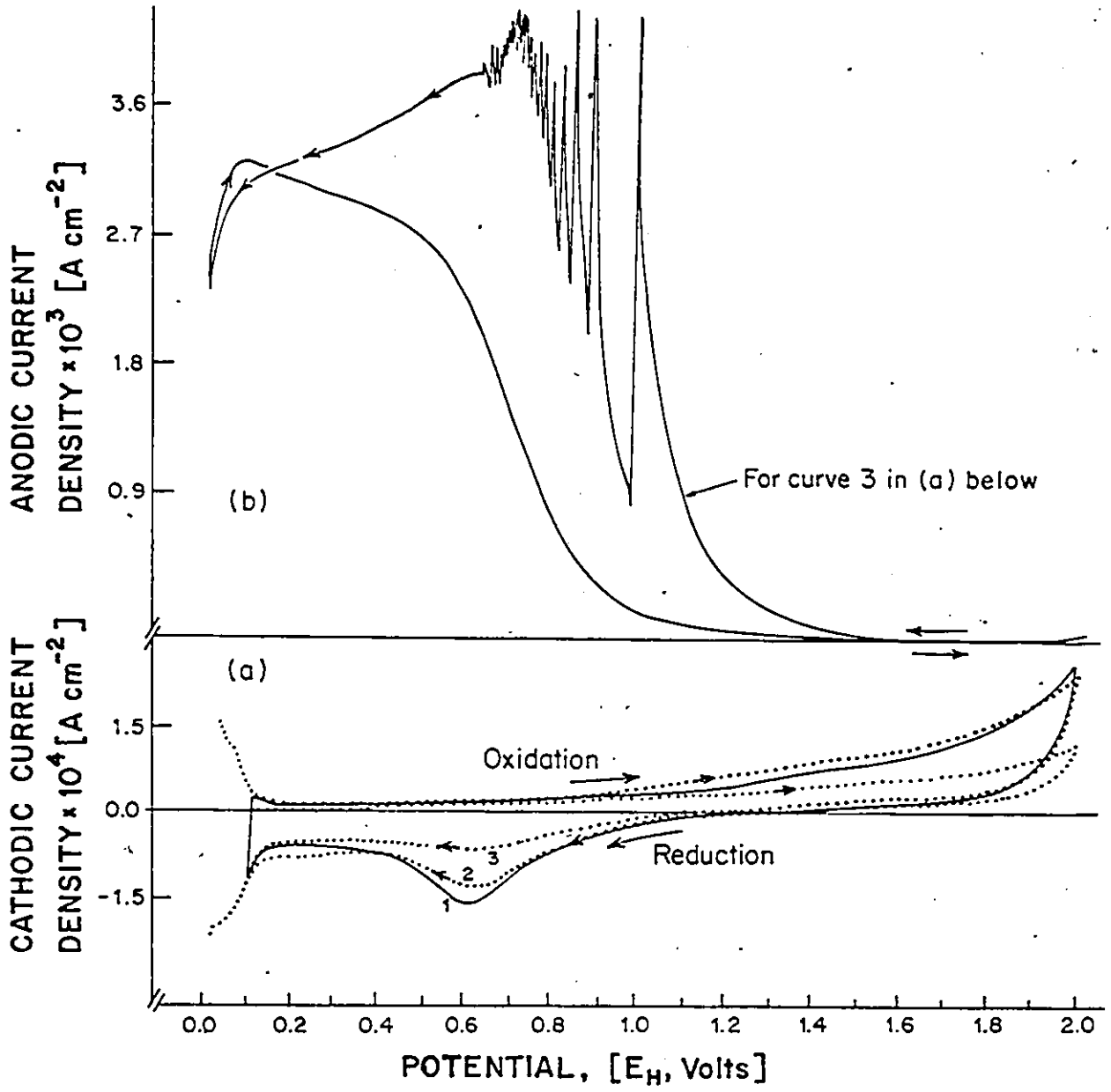

Fig. 38 Transitional case between oscillatory behaviour in Fig. 33 and that in Fig. 35 . A small quantity of water is present and corresponding small surface oxide coverage is generated: (a) background i-V profile for Pt for two additions of trifluoroacetic anhydride (curves 2,3) in relation to initial curve (1) for wetter solution; (b) oscillatory behaviour of H_2 current.

The importance of diffusion and oxidation following periodic H_2 accumulation is substantiated by the observation that stirring eliminates the periodic current behaviour (cf. the case of C_2H_4, ref. 246) and increases all currents up to a new mass-transfer-controlled limit. Then, apart from some inhibition effects when the oxide film is formed and relief of inhibition when the oxide film reduction commences (Figs. 35, 39 and 41), the anodic and cathodic i-V profiles are almost the same (Figs. 39 and 41). Although effects of stirring indicate the role of diffusion, it is clear from the existence of the oscillations that the reaction conditions must change in a periodic way between partial and virtually complete diffusion control. Thus, if the reaction was at all times completely diffusion controlled, no periodic increases in its rate would be observed in unstirred solutions.

Transitional behaviour between that in Fig. 33 for almost completely dry TFA and that in Fig. 35 for a less dry solution is shown in Fig. 38. Here oscillations again commence when the oxide film begins to be reduced but a sequence of many current pulses is generated on the cathodic sweep as in Fig. 33. The lower series of curves (a) show the i-V profiles for Pt in the absence of H_2 for two successive additions of trifluoroacetic anhydride to a TFA solution that was initially slightly wet. The quantity of oxide measured by the charge under the reduction peak, becomes progressively smaller with the additions of anhydride. The oscillations in Fig. 38 b correspond to a condition of surface oxidation characterized by curve 3 in Fig. 38a.

Considering Fig. 32 in relation to Fig. 35, it is clear that if the solution is ultra-dry, inhibition of H_2-oxidation which normally

occurs at ca. 0.9 - 1.0 V E_H does not arise.

In the presence of traces of water, the anodic current curve exhibits (Fig. 35) inhibition at ca. 1.2 V E_H but reactivation of the electrode surface occurs in the cathodic sweep as soon as potentials are reached (1.1 - 1.3 V E_H) where surface oxide reduction commences. The potentials for the latter process depend (Fig. 29), as found in aq. solution work[61,69] (see also Fig. 29), on the extent of oxide formation attained in the anodic sweep, i.e. on the potential and time spent in the anodic oxide formation region.

Figs. 35 and 39 show that in TFA with traces of water, H_2 oxidation is almost completely inhibited beyond potentials of ca. 1.2 V E_H despite the fact that only about 10% of the surface is covered by an oxide film under the conditions of experiments giving Figs. 35 and 39 . Only in the driest solutions, " gettered " with the trifluoroacetic anhydride (Fig 32), are appreciable H_2-oxidation currents maintained up to ca. + 1.86 V E_H without inhibition effects setting in.

These somewhat surprising results suggest that the H_2-oxidation reaction takes place normally on only a small fraction of the Pt surface (cf. ref. 117) where active centers, or suitable adges or steps, are available. The behaviour is not inconsistent with Somorjai's recent findings[303] on the catalytic activity of Pt single-crystal surfaces cut at high index planes.

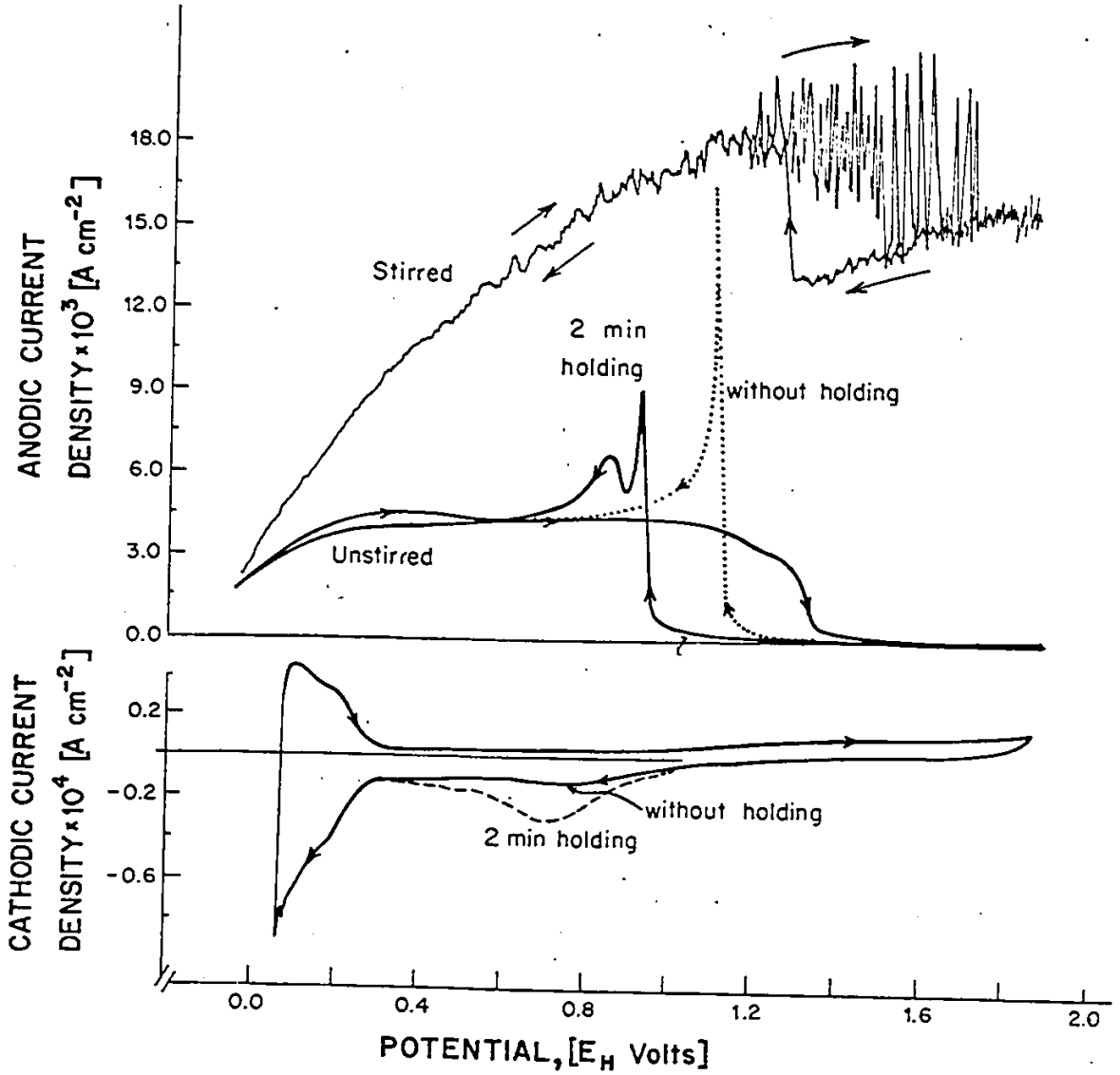

Fig. 39 Current oscillations in H_2 oxidation at Pt in TFA as in Fig. 35 but with an increased quantity of added water. Lower curve shows background i-V profile for Pt in the TFA solution in absence of H_2.

The charges associated with the oscillations in potentiodynamic sweeps (similar to that in Fig. 35) are given in Table 3.

TABLE 3

CHARGES ASSOCIATED WITH SUCCESSIVE PERIODIC H_2 OXIDATION CURRENT PEAKS IN POTENTIODYNAMIC EXPERIMENTS (AS IN FIG. 35)

Run 1.	Charge $\mu C\ cm^{-2}$	Run 2.	Charge $\mu C\ cm^{-2}$	Run 3.	Charge $\mu C\ cm^{-3}$
peak 1	180	peak 1	130	peak 1	22
peak 2	200	peak 2	390	peak 2	59
peak 3	140	peak 3	380	peak 3	179
				peak 4*	135

* Four peaks are sometimes observed.

If the sweep is taken anodically just into the region where surface oxidation of Pt commences in TFA to which traces of water have been added, and is then reversed, multiple oscillations arise as shown in Fig. 40 . These occur as the very small quantity of surface oxide generated in the restricted range of anodic sweep is reduced.

Further additions of water allow the electrode to become more extensively oxidized in the sweep, or on holding the potential at the

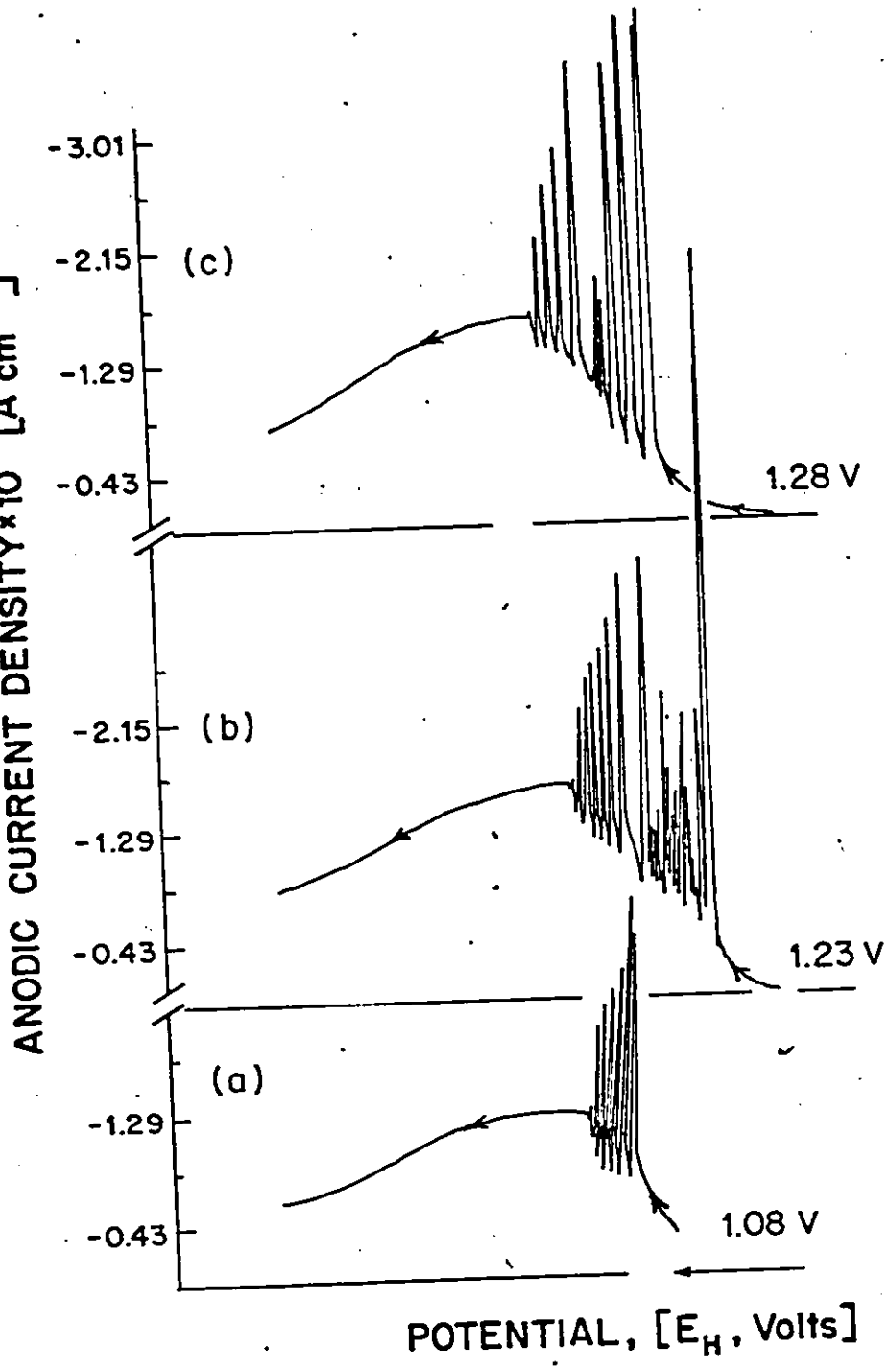

Fig. 40 Oscillations in H_2 oxidation at Pt in TFA containing traces of water on a cathodic sweep initiated just at the potential where surface oxidation commences.

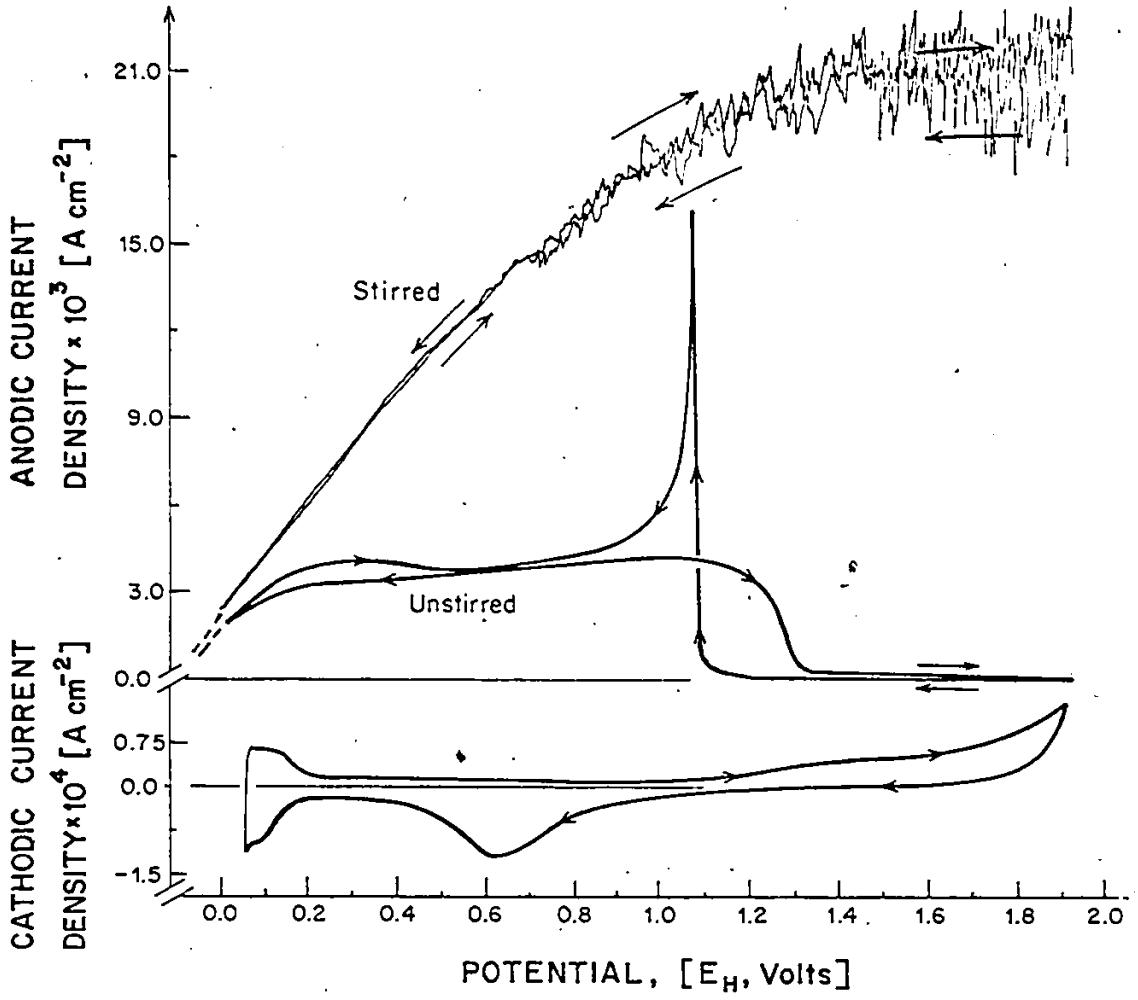

Fig. 41 As in Fig. 38 but with further addition of traces of water. Lower curve shows background i-V profile for Pt in the TFA solution in absence of H_2 . Note larger surface oxide reduction peak than in Fig. 38, curve 3.

positive end of the sweep. Then, in the cathodic sweep, only a single current spike is initiated at the commencement of surface oxide reduction but no oscillations occur (Fig.41). In fully aqueous medium (0.1 M aq. $HClO_4$), the behaviour is similar as was shown in Figs. 36 and 37; again no oscillations occur. The single current spike in Fig. 41 and the multiple ones shown in earlier diagrams is suggestive of an autocatalytic oxide stripping process of the kind suggested previously[246] in related work from this Laboratory, connected with nucleation and spreading of holes in the oxide film by reduction by H_2 coupled with transport from the diffusion layer.

It is interesting that when the spike current is initiated (Fig. 41) its maximum value approaches the (steady) current which can be generated in a strongly stirred solution where diffusion effects are diminished. Of course, at the moment the spike current is established, as mentioned earlier with regard to Figs. 33, 36 and 38, there is almost no concentration gradient of H_2 at the electrode surface since the H_2-oxidation current has previously remained inhibited at more positive potentials in the cathodic sweep, as explained earlier.

5. GENERAL DISCUSSION

(i) Origins of Oscillatory Behaviour: It was mentioned earlier how oscillating kinetic behaviour in a reaction arises under special conditions when no stable steady-state exists[62,246-248]. This corresponds to a situation where the differential equation representing the kinetics of the reaction has a periodic solution in time rather than a unique

steady-state solution.

It has been shown previously[95,246] that oscillatory behaviour can often arise when an electrode surface reaction is coupled with a reactant diffusion process[254], especially when the surface process is one of passivation which exhibits a negative-resistance characteristic corresponding to positive feedback. This is the situation with the present case of H_2 oxidation: (a) the i-V curves show an inhibition or reactivation region with negative dV/di; and (b) a diffusion process exists which provides a kind of capacitance for the reaction (in a Warburg impedance element), so that coupling of these two conditions can, in principle, give rise to periodic kinetic behaviour analogous to that in an inductively coupled oscillator. The positive feedback component is usually an autocatalytic step or one that behaves in a kinetically equivalent manner, i.e., the negative resistance characteristic of the S-shaped passivation i-V profile.

It is to be noted that the observed oscillations in H_2 oxidation occur only on the cathodic sweep. This arises presumably because, in the anodic-going sweep, a situation of increasing kinetic stability obtains, with oxide film coverage tending to increase and anion adsorption becoming stronger. In the cathodic sweep, the contrary situation arises, and tends to cause increasing rates of H_2 oxidation as the potential decreases, i.e., a positive feedback situation is established leading to instability with oscillatory behaviour in the kinetics.

(ii) Kinetic Equations: In order to illustrate the complexity of the problem of oscillations at an electrode, it will be useful to enumerate the factors which control the kinetics and write the appropriate

rate equations. Six factors must be taken into account in formulating a system of kinetic equations that represent the behaviour of the H_2-oxidation reaction: (a) the role of diffusion[254] of H_2 indicated by stirring effects and by Fig. 33; (b) the reactivity of an incomplete oxide film at Pt[283,284]; (c) the electrode potential; (d) the free surface area, "(1-θ)", available for direct electrocatalytic reaction of H_2 and electrochemical coupling with oxide reduction; (e) inhibition of catalytic activity of surface sites by anion adsorption; and (f) reversibility ond irreversibility (hysteresis[69]) in the formation and reduction of the oxide film on Pt.

The concentration of H_2 at the electrode will be denoted by C_e and that in the bulk by C_b, and the distance variable over which a concentration gradient can be set up as x. The diffusion process is

$$\underset{C_b}{H_2(\text{bulk})} \longrightarrow \underset{C_e}{H_2(\text{electrode})} \qquad \text{VII}$$

for which

$$\frac{dq_{H_2}}{dt} = -\frac{Dd\,C}{dx} = i/2F \qquad (43a)$$

per unit area where i is the current density and D the diffusion coefficient of H_2. Also Fick's second law gives

$$D\left(\frac{\partial^2 C}{\partial x^2}\right)_t = \left(\frac{\partial C}{\partial t}\right)_x \qquad (43b)$$

and the condition of interest is $C = C_e$ when $x = 0$, i.e. at the electrode surface.

The reactions of H_2 which can occur at the surface are

$$H_2 + 2Pt \longrightarrow 2\ PtH \qquad \text{III}$$

$$PtH \longrightarrow H^+ + e^- + Pt \qquad \text{IV}$$

and (cf. ref. 284,285)

$$H_2 + 2PtOH \longrightarrow 2H_2O + 2Pt \qquad \text{V}$$

Anion adsorption at coverage θ_A is represented by

$$A^- + Pt \longrightarrow Pt(A^-) \qquad \text{VIII}$$

The surface oxidation reactions of Pt are

$$Pt + H_2O\ (\text{traces}) \longrightarrow PtOH + H^+ + e^- \longrightarrow PtO + H^+ + e^-$$

at higher potentials IX

$$PtOH \longrightarrow \text{" OHPt "}\ (\text{place-exchanged state of deposited OH}) \qquad \text{X}$$

Both H_2 and adsorbed H generated in step III could react with the surface oxide species but the ionization reaction IV is very rapid at Pt at potentials > 0.4 V E_H, so the coverage by H at potentials where the Pt surface is oxidized will be negligible. Then the following kinetic equations can be written noting that the subscript numbers on rate constants, k , refer to the respective reaction steps enumerated above with corresponding Roman numerals:

$$\frac{d\theta_H}{dt} = k_4(1-\theta_H-\theta_{PtOH})^2\ C_e - k_5\ \theta_H \exp V/b \qquad (44)$$

where b is a Tafel slope factor $RT/\beta F$;

$$\frac{d\theta_{OH}}{dt} = k_7(1-\theta_{PtOH}-\theta_{OHPt}) \exp V/b - k_6\theta_{PtOH} C_e \qquad (45)$$

The overall velocity of H_2 oxidation in terms of current-density i can be written

$$\frac{i}{2F} = v_{III} + v_V \qquad (46)$$

where III is coupled with VII through diffusion involving C_e (eqns. 43a and 43b), i.e.

$$\frac{i}{2F} = \frac{-dC_e}{dt} = k_4 (1-\theta_H-\theta_{PtOH})C_e - k_6\theta^2_{PtOH} C_e \qquad (47)$$

The concentration would normally be obtained, as in other diffusion problems, through eq. (43b) by integration with suitable boundary conditions. However, in the case of oscillatory i, C_e will be periodic. If the periodicity is treated as a series of pulses (cf. the form of Fig. 33), the boundary conditions are a little easier to define, at least for the maximum current pulses: when $i \to i_{max}$, eq. (42) indicates $C_e \to 0$; when $i \to i_{min}$ or 0 (i.e., when inhibition prevails), $C_e \to C_b$.

Szpak and Rice[304] treated a related problem by assuming a periodic boundary condition of a sinusoidal form. This does not seem an acceptable procedure since the form of the oscillatory behaviour has then virtually been assumed in advance. The periodic " boundary condition " is really generated by the kinetics of the oscillatory process itself which makes the solution of the coupled kinetic and diffusion equations singularly difficult.

Inhibition effects arise in eq. (47) through the "(1-θ)" terms and probably additionally (see below) through the coverage θ_A- by

adsorbed TF anions, and reactivation (in a cathodic sweep) as this term becomes smaller. Autocatalytic effects can arise[246] in the oxide film stripping step V . Potential-dependence of i arises indirectly through the dependence of θ_{H}, θ_{OH}, θ_{A^-} , and the corresponding "(1-θ)" terms on VIII. Neither steady-state nor quasi-equilibrium expressions can be assumed for these coverage terms, viz., $1-\theta_{H} - \theta_{OH}$ and θ_{PtOH} in eqns. (44) and (45).

(iii) Role of Inhibition by Anion Adsorption and H_2 Accumulation and Transport in the Diffusion Layer: The oscillatory behaviour appears to arise from periodic inhibition and reactivation of the surface, coupled with diffusion (indicated by the results of Fig. 34) and H_2 accumulation in the diffusion layer, as discussed in relation to the results of Fig. 33 . The behaviour in this figure also indicates that the oscillations are unlikely to arise directly from periodic formation and reduction of the oxide film at low coverages since they commence already at 1.8 V E_H and persist down to ca. 1.0 V E_H under conditions where only a very small coverage by " oxide species " can exist. Thus the behaviour of the oxide film itself in the absence of H_2 shows (Fig. 37) that, even for the small coverages generated by traces of water, there is a large hysteresis between the formation and reduction processes with respect to the potential range involved so that oxide existing at 1.8 V E_H could hardly be reduced and re-formed in a periodic manner over a short potential range. The oscillatory behaviour is, however, also accompanied by " in-phase " periodic changes of state of the electrode surface as indicated by the $\Delta R/R$ results of Fig. 33 . The combination of these results indicates that the inhibition/reactivation involved in the oscillatory behaviour is more likely to be associated with anion adsorption since the oxide coverage

in many experiments is insufficient to provide inhibition of H_2 oxidation on more than ca. 10% of the apparent surface.

If oxidation of H_2 is initiated by a fluctuation , the pH will be locally decreased (note, the solvent is ca. 100% TFA) due to production of H^+ from H_2 in the diffusion layer which could decrease inhibiting anion adsorption by protonation of adsorbed trifluoroacetate anions giving increased H_2 oxidation in a positive feedback (autocatalytic) process and a consequent current pulse. As the H_2 in the diffusion layer is consumed, its rate of oxidation at the electrode becomes diminished ($C_e < C_b$) and anion readsorption with inhibition is restored as the pH recovers its initial value at the electrode surface.

Figs. 35, 38 and 39 show that in the presence of larger traces of water the oscillations are initiated at the potential where reduction of the oxide film commences. At first it was thought (cf. refs. 246 and 254) that the oscillations were directly associated with periodic formation and reduction of the oxide film at ca. 1.0 V E_H through its reversible component (cf. ref. 69). The results of Fig. 33 and the transitional case, Fig. 37 , suggest, however, that the oscillations which arise at the potential of commencement of reduction of the film are also associated with anion desorption/adsorption effects. The presence of traces of water causes complete inhibition of H_2 oxidation in the anodic sweep despite the fact that only 10 - 20% of the surface is covered by oxide film - this oxide presumably is preferentially formed on high energy (least noble) catalytically active sites which are thereby blocked. Inhibition remains effective on the cathodic sweep until the (island ?) regions of surface oxide are just reduced; then new free surface sites are generated at which a large H_2-oxidation current-density can be temporarily

sustained. The behaviour in Fig. 33 for an almost dry solution gives a clue to the origin of the oscillatory behaviour in the wetter solutions: the trifluoroacetate anion can cause inhibition at the newly regenerated free Pt sites but as the reduction of the limited oxide film continues, reactivation of H_2 oxidation can occur several times depending on the water content, i.e., oxide film coverage (Figs. 37 and 40), and the potential range in the cathodic sweep over which it is reduced. No H_2 oxidation can occur until new active sites are generated in the wetter solutions by reduction of the small coverage by oxide which blocks the active regions of the surface in that case.

(iv) Cycle of Processes in Periodic H_2 Oxidation: It will be useful to summarize the effects associated with the reactions given above by means of the cycle of activity of the electrode as shown in Scheme II (see following page).

SCHEME II

CYCLE OF PROCESSES IN PERIODIC H_2 OXIDATION

H_2 concentration in diffusion layer approaches bulk value (inhibited state; H_2-flux minimized; current minimum)

Reactivation due to increase of H_2 concentration at electrode surface - positive feedback step

Reactivated surface due to oxide reduction by H_2 and/or desorption of adsorbed anions by reaction $H^+ + A^-_{ads} \rightarrow HA$ from H^+ produced by H_2 oxidation at surface

H_2 consumption facilitated

Diffusion layer depleted in H_2; flux of H_2 maximized (active state, H_2-oxidation current maximized)

$+ A^- + H_2O$

Surface inactivated due to anion readsorption and/or surface oxidation (hysteresis with respect to desorption directions of these processes)

Inactivated surface; H_2 concentration in diffusion layer recovers to larger values

H_2 flux diminishes

APPENDIX I (Chapter II)

The method (p. 83) for analysis of recombination-controlled kinetics necessarily applies to the anodic component, i_a , of the net current-density, i . Near the reversible potential, i_a differs from the measured net current i according to $i_a = i + i_c$ [see Chapter II , Section (iii), p. 95] , where i_c is the back reaction component of i. For a general case, i is expressed as

$$i = i_a - i_c = 2Fk_2\theta^2 - 2Fk_{-2}(1-\theta)^2 \qquad (48)$$

At $\eta = 0$, $i = 0$ and $i_c = i_a = i_o$ and $\theta = \theta_r$, the value of θ at the reversible potential. Then i can be written in terms of θ and θ_r, with i_a and i_c as

$$i = i_o\theta^2/\theta_r^2 - i_o(1-\theta)^2/(1-\theta_r)^2 \qquad (49)$$

where i_o is defined by comparing the last equation with eqn. (48) . i_a is obtained from eqn. (48), after elementary rearrangements, as

$$i_a = i \Big/ \left[1 - \frac{(1-\theta)^2}{\theta^2} \quad \frac{\theta_r^2}{(1-\theta_r)^2}\right] \qquad (50)$$

Quasi-equilibrium in step I enables θ and θ_r to be related to the reversible potential V_r and η as follows:

$$\frac{\theta_r}{(1-\theta_r)} = K_1 C \exp\left[\frac{V_r F}{RT}\right] \; ; \quad \frac{\theta}{1-\theta} = K_1 C \exp\left[\frac{V_r + \eta}{RT}\right]$$

.....(51)

so that

$$\frac{\theta}{1-\theta} = \frac{\theta_r}{1-\theta_r} \exp\left[\frac{\eta F}{RT}\right] \qquad (52)$$

Hence

$$i_a = i \Big/ \left\{1 - \exp\left[\frac{2\eta F}{RT}\right]\right\} \qquad (53)$$

Thus, near the reversible potential, the measured net current-densities, have to be corrected by the factor $\left\{1 - \exp\left[-\frac{2\eta F}{RT}\right]\right\}^{-1}$ in order to obtain the relevant anodic current-densities controlled by the kinetics of the recombination step.

Application of this correction causes the points in the hook of the lines of Figs. 6a and 6b, as well as Fig. 24, at their lower ends to be reduced in magnitude so that they all fall more or less on the line after correction. The hook is therefore due to participation of the back reaction at low η values.

CONTRIBUTIONS TO ORIGINAL RESEARCH

1. A new approach to the study of the kinetics of anodic Cl_2 evolution and molecular H_2 oxidation at Pt is made by using an unreactive non-aqueous solvent, trifluoroacetic acid (TFA), to which controlled additions of H_2O are made enabling the extent of surface oxidation to be controlled independently of the range of potentials employed, and thus its role in these two reactions to be investigated.

2. An appreciable, 15 - 45 fold electrocatalytic effect of the surface oxide formation on Pt electrodes on the rate constant of the recombination-controlled process of anodic Cl_2 evolution at Pt has been demonstrated by comparing the rate of the reaction in TFA where no surface oxide film is shown to be present, and in water where it is present.

3. The kinetics have been studied over the whole composition range 0 - 100% H_2O in TFA/H_2O mixtures.

4. A new method has been developed for the kinetic analysis of current-potential relations for an electrochemical process that may be controlled by the rate of recombination of electrochemisorbed atoms, e.g. $Cl^{\cdot}$, produced in a prior ion-discharge step, e.g. from Cl^-. It can be applied over the whole range of currents i and corresponding potentials V when the i-V relation is a curved one.

5. The method clearly shows that the anodic Cl_2 evolution reaction is

kinetically controlled by a recombination step under all conditions examined: in 100% TFA, in TFA/H_2O mixtures and in 100% aq. medium over a range of Cl^- concentrations. Two methods of plotting the results enable the curved relation of current and potential data to be tested by linear plots, the extrapolations of which lead to a quantitative evaluation of the rate-constant, k_2 , for the rate-controlling recombination step and the quasi-equilibrium constant, $\bar{K}_1$, for the prior step of electrosorption of $Cl^\cdot$ at Pt from Cl^-. The k_2 and $\bar{K}_1$ values thus derived are related to solvent composition in TFA/H_2O mixtures, and to surface oxide coverage and Cl^- specific adsorption at various $[Cl^-]$ values.

6. A method for allowing for the back reaction current component in the kinetic analysis is proposed and demonstrated.

7. In TFA/H_2O and in 100% H_2O , it is shown that not only the oxide film but the specific adsorption of Cl^- ions is important in leading to better electrocatalysis for the Cl_2 evolution reaction at Pt.

8. In relation to 7. , competitive effects of adsorbed Cl^- ion vs. surface oxide formation are demonstrated and it is shown that the competitive adsorption isotherm (Cl^- vs. OH/O) is logarithmic in $[Cl^-]$, giving a good example of Temkin type behaviour. A precise micro-titration procedure was developed for determination of these competitive adsorption effects down to very low concentrations of halide ions.

9. By using TFA solutions with traces of H_2O present, so that very small degrees of surface oxidation could be controllably generated over a wide potential range at a Pt anode, it was shown that H_2 oxidation kinetics are oscillatory. Current oscillations under both potentiostatic and potentiodynamic conditions were established and analysed quantitatively in terms of passage of charge and diffusion effects.

10. The role of diffusion control in the periodicity of H_2 oxidation current was clearly demonstrated by showing that a square-root relation exists between spontaneously generated periodic current pulses and the time intervals, Δt , in this oscillatory behaviour. This was supported by the observation that all oscillatory behaviour is eliminated by stirring. The oscillatory currents were also shown to be in-phase with periodic reflectivity changes at the electrode surface associated with anion adsorption/desorption and/or formation and reduction of small coverages of surface oxide.

11. The oscillatory kinetics of H_2 oxidation were found to be critically dependent on water content of the mainly anhydrous medium, i.e. on the extent to which surface oxidation of the electrode occurred. A reaction cycle involving periodic surface oxidation, anion (TF^-) adsorption and desorption, and depletion of H_2 from the diffusion layer was proposed as a basis for the oscillatory behaviour of H_2 oxidation under the experimental conditions used.

REFERENCES

1. F.P. Bowden and E.K. Rideal, Proc. Roy. Soc., A120(1928)59;80.
2. A. Slygin and A.N. Frumkin, Acta Physicochim., U.R.S.S., 3(1935)791.
3. W. Böld and M. Breiter, Z. Elektrochem., 64(1960)897.
4. B.E. Conway and M.A.Sattar, J.Electroanal.Chem., 19(1968)351.
5. J.O'M. Bockris, A. Damjanović and W.E. O'Grady, J.Colloid and Interface Sci., 34(1970)387.
6. J.S. Hammond and N. Winograd, J. Electroanal. Chem., 78(1977)55.
7. G.C. Allen, P.M. Tucker, A. Capon and R. Parsons, J. Electroanal. Chem., 50(1974)335.
8. S. Shibata, Electrochim.Acta, 22(1977)175.
9. S. Schuldiner and R.N. Roe, J.Electrochem.Soc., 110(1963)332.
10. M. Breiter, H. Kammermeir and C.A. Knorr, Z.Elektrochem., 60(1956)37.
11. S.W. Feldberg, C.C. Enke and C.E. Bricker, J.Electrochem.Soc., 110 (1963)826.
12. J.N. Sarmousakis and M.J. Prager, J.Electrochem.Soc., 104(1957)454.
13. J.P. Hoare, Nature,London, 204(1964)71.
14. S. Gilman,Electrochim.Acta, 9(1964)1025.
15. H.A. Laitinen and C.G. Enke, J.Electrochem.Soc., 107(1960)773.
16. M. Breiter, J.Electroanal.Chem., 7(1964)38.
17. C. Formaro and S. Trasatti, Electrochim.Acta, 12(1967)1457.
18. L. Young, Anodic Oxide Films, Academic Press, London, New York, 1961.
19. J.P. Hoare, The Electrochemistry of Oxygen, Interscience, New York, 1968.

20.a A.K. Vijh, Electrochemistry of Metals and Semiconductors, Marcel Dekker Inc.,New York,1973.

b J.W. Schultze and K.J. Vetter, Electrochim. Acta,18(1973)889.

21. J.W. Diggle, T.C. Downie and C.W. Goulding, Chem.Rev.,69(1969)365.

22.a F.G. Will and C.A. Knorr, Z. Elektrochem.,64(1960)258.

b F.G. Will and C.A. Knorr, Z. Elektrochem.,64(1960)270.

23. S. Gilman, Electroanal. Chemistry,(A.J. Bard ed.) Vol.2, Marcel Dekker Inc.,New York,1967.

24. S. Barnartt,J.Electrochem.Soc.,106(1959)722.

25. J.W. Schultze and K.J. Vetter, J. Electroanal. Chem.,44(1973)63.

26. A.N. Frumkin, B. Damaskin and O. Petrii, J.Electroanal.Chem.,53(1974)57.
see also K.J. Vetter and J.W. Schultze,ibid.,53(1974)67.

27. B.E. Conway, L.H. Laliberté, S. Gottesfeld and H. Angerstein-Kozlowka, Proc.Symposium on Oxide-Electrolyte Interfaces,1971,p.181.

28. T. Biegler, D.A.J. Rand and R. Woods, J.Electroanal.Chem.,29(1971)269.

29. W. Visscher and M.Blijlevens, Electrochim.Acta,19(1974)387.
see also W. Visscher and M. Blijlevens, J.Electroanal.Chem.,47(1973)363.

30. J.A.V. Butler and G. Drever, Trans Faraday Soc.,32(1936)427.

31. E.I. Khrushcheva, N.A. Shumilova and M.R. Tarasevich, Elektrokhimiya, 2(1966)277.

32. J. Llopis and M. Vazques, Electrochim. Acta,9(1964)1655.

33. J.M. Otten and W. Visscher,J.Electroanal.Chem.,55(1974)1,13.

34. J.O. Zerbino, N.R. deTacconi and A.J. Arvia, J.Electrochem.Soc.,125 (1978)1266.

35. F.P. Bowden, Proc.Roy.Soc.,A125(1929)446.

36. A. Slygin, A.N. Frumkin and V.I. Medvedovskii, Acta Physicochim.,4 (1936)911.

see also: ibid.,5(1936)819.

37. J.A.V. Butler and G. Armstrong, Proc.Roy.Soc.,A137(1932)604.

38. G. Armstrong and J.A.V. Butler, J.Chem.Soc.,(1934)743.

39. J. Pearson and J.A.V. Butler, Trans.Faraday Soac.,34(1938)1163.

40. G. Armstrong, F.R. Himsworth and J.A.V. Butler, Proc.Roy.Soc.,A143 (1933)89.

41. M.W. Breiter, Electrochim.Acta,11(1966)905.
see also D.A.J. Rand and R. Woods, J.Electroanal.Chem.,35(1972)209.

42. A. Hickling, Trans.Faraday Soc.,41(1945)333.

43. B.V. Ershler, Disc.Faraday Soc.,1(1947)269.

44. B.V. Ershler and M.W. Proskurnin, Acta Physicochim.,U.R.S.S.,6(1937)195.

45. B.V. Ershler, Acta Physicochim.,U.R.S.S.,7(1937)327.

46. B.V. Ershler, B.G. Deborin and A.N. Frumkin, Acta Physicochim., U.R.S.S., 8(1938)365.

47. B.V. Ershler and A.N. Frumkin, Trans.Faraday Soc.,35(1939)1.

48. S.E.S. El Wakkad and S.H. Emara, J.Chem.Soc.,(1952)461.

49. S. Schuldiner and T.B. Warner, J.Phys.Chem.,68(1964)1223.

50. S. Schuldiner and T.B. Warner, J.Electrochem.Soc.,112(1965)212.

51. J.P. Hoare, J.Electrochem.Soc.,112(1965)602,849.

52. J.P. Hoare, J.Electrochem.Soc.,110(1963)1019.

53. J.P. Hoare, J.Electrochem.Soc.,113(1966)846.

54. M. Breiter, C.A. Knorr and W. Volkl, Z.Elektrochem.,59(1955)881.

55. M. Breiter, K. Francke and A.C. Knorr, Z.Elektrochem.,63(1959)226.

56. W. Böld and M. Breiter, Electrochim.Acta,5(1961)145.

57. K.J. Vetter and D. Berndt,Z.Elektrochem.,62(1958)378.

58. F. Anson and J.J. Lingane, J.Am.Chem.Soc.,79(1957)4901.

59. M. Breiter and J. Weininger, J.Electrochem.Soc.,109(1962)1135.

60. K.S. Kim, G.K. Winograd and R.E. Davis, J.Am.Chem.Soc.,93(1971)6296.

61. P. Stonehart, H.A. Kozlowska and B.E. Conway, Proc.Roy.Soc.,London, A310(1969)541.

62. D. Gilroy and B.E.Conway, Can.J.Chem.,46(1968)875.

63. V.I. Tikhomirova, A.I. Oshe and V.S. Bagotskii, Dolk.Akad.Nauk S.S.S.R., 159(1965)644.

64. B.E. Conway and S. Gottesfeld, J.Chem.Soc.,Faraday Trans.I,69(1973)1090.

65. B.E. Conway, H. Angerstein-Kozlowska and W.B.A. Sharp, J.Chem.Soc., Faraday Trans.I,74(1978) 1373.

66. S.B. Brummer, J. Ford and M.J. Turner, J.Phys.Chem.,69(1965)562,3424.

67. T. Biegler and R. Woods, J.Electroanal.Chem.,20(1969)73.

68. J.P. Hoare, R. Thacker and C.R. Wiese, J.Electroanal.Chem.,30(1971)15.

69. H. Angerstein-Kozlowska, B.E. Conway and W.B.A. Sharp, J.Electroanal. Chem.,43(1973)9.

70. A. Damjanović, A.T. Ward, B. Ulrick and M. O'Jea, J.Electrochem.Soc., 122(1975)471.

71. A. Ward, A. Damjanović, E. Gray and M. O'Jea, J.Electrochem.Soc., 123(1976)1599.

72. B.V. Tilak, B.E. Conway and H. Angerstein-Kozlowska, J.Electroanal. Chem.,48(1973)1.

73. B.E. Conway, W.B.A. Sharp, H. Angerstein-Kozlowska and E.E. Criddle, Anal.Chem.,45(1973)1331.

74. S. Shibata and P.M. Sumino, Electrochim. Acta, 17(1972)2215.

75. S. Shibata, Electrochim.Acta, 17(1972)395.

76. N. Sato and M. Cohen, J.Electrochem.Soc.,111(1964)512.

77. B.M.W. Trapnell and D.O. Hayward, Chemisorption, (ed. W.E. Garner), Butterworth,Lomdon and Washington,D.C.,1964,p.210.

78. T. Dickinson, A.F. Povey and P.M.A. Sherwood, J.Chem.Soc.,Faraday Trans.I,71(1975)298.

79. A.K.N. Reddy, M. Genshaw and J.O'M. Bockris, J.Electroanal.Chem., 8(1964)406.

80. A.K.N. Reddy, M. Genshaw and J.O'M. Bockris, Chem.Phys.,148(1968)671.

81. T.B.Warner and S.Schuldiner, J.Electrochem.Soc.,112(1965)853.

82. S. Schuldiner, T.B. Warner and B.J. Piersma, J.Electrochem.Soc.,114 (1967)343.

83. R. Thacker and J.P. Hoare, J.Electroanal.Chem.,30(1971)1.

84. S. Schuldiner and R.M. Roe, J.Electrochem.Soc.,110(1963)1142.

85. R. Greef, J.Chem.Phys.,51(1969)3148.

86. B.E. Conway, Symp.Faraday Soc.,41(1970)94.

87. R. Parsons and W.H.M. Visscher, J.Electroanal.Chem.,36(1972)329.

88. A. Damjanović, A.T. Ward and M. O'Jea, J.Electrochem.Soc.,121(1974)1186.

89. S.H. Kim, W. Paik and J.O'M. Bockris, Surface Sci.,33(1972)617.

90. J. Ord and F.C. Ho, J.Electrochem.Soc.,118(1971)46.

91. W.J. Moore and L. Pauling, J.Am.Chem.Soc.,63(1941)1392.

92. V.E. Kazarinov and N.A. Balashova, Dokl.Akad.Nauk U.S.S.R.,157(1964)1174. see also Dokl.Fiz.Khim.,157(1964)795.

93. I.I. Labkovskaya, V.I. Lukyanycheva and V.S. Bagotskii, Elektrokhimiya, 5(1969)580.

94. G. Horányi and G. Inzelt, J.Electroanal.Chem.,86(1978)215.

95. D. Gilroy and B.E. Conway, J.Phys.Chem.,69(1965)1259.

96. D. Gilroy, J.Electroanal.Chem.,71(1976)257.

97. D. Gilroy, J.Electroanal.Chem.,83(1977)329.

98. A. Damjanović and B. Jovanović, J.Electrochem.Soc.,123(1976)374.

99. A. Damjanović and A.T. Ward,MTP, International Review of Science, Physical Chemistry, Series II, Butterworth, London,1976.,p.103.

100. K.J. Vetter and J.W. Schultze, J.Electroanal.Chem.,34(1972)131.

101. K.J. Vetter and J.W. Schultze, J.Electroanal.Chem. 34(1972)141.

102. J.L. Ord and D.J. DeSmet, J.Electrochem.Soc.,113(1966)1258.

103. N. Cabrera and N.F. Mott, Rept.Prog.Phys.,12(1948-49)163.

104. N. Cabrera,The Oxidation of Metals, in Semiconductor Surface Physics, University of Pennsylvania Press, Philadelphia,1957.,p.372.

105. R.E. Meyer, J.Electrochem.Soc.,107(1960)847.

106. J.O'M. Bockris, A.K.N. Reddy and B. Rao, J.Electrochem.Soc.,113(1966)1133.

107. K. Hauffe and M. Ilschner, Z.Elektrochem.,58(1954)382.

108. A.T. Fromhold and E.L. Cook, J.Chem.Phys.,44(1966)4564.

109. A. Damjanović and A.T. Ward, Electrochemistry: The Past Thirty and the Next Thirty Years,(ed. H. Bloom and F.G. Gutmann),1977., Chapter 6,p.107.

110. S. Shibata and M.P. Sumino, Electrochim.Acta,16(1971)1089.

111. M. Fleischman, I.R. Mansfield and W.F.K. Wynne-Jones, J.Electroanal. Chem.,10(1965)511.

112. A.K. Vijh and B.E. Conway, Z.Anal.Chem.,224(1967)160.

113. S. Shibata, Bull.Chem.Soc.,Japan,36(1963)526.

114. A. Damjanović, A. Dey and J.O'M. Bockris, Electrochim.Acta,11(1966)791.

115. A. Damjanović and V. Brusić, Electrochim.Acta,12(1967)615.

116. S. Schuldiner, J.Electrochem.Soc.,115(1968)363.

117. M.W. Breiter, Electrochim.Acta,7(1962)601.

118. A. Damjanović, A. Dey and J.O'M. Bockris, J.Electrochem.Soc.,113(1966) 739.

119. T. Arikado, C. Iwakura and H. Tamura, Electrochim.Acta,23(1978)9.

120. A.T. Kuhn and P.M. Wright, J.Electroanal.Chem.,38(1972)291.

121. M. Breiter, Electrochim.Acta,8(1963)457.

122. D.A.J. Rand and R. Woods, J.Electroanal.Chem.,70(1976)73.

123. J.O'M. Bockris and H. Wroblowa, J.Electroanal.Chem.,7(1964)428.

124. J.O'M. Bockris and A.K.M.S. Huq, Proc.Roy.Soc.,A237(1956)271.

125. A. Damjanović and V. Brusić, Electrochim.Acta,12(1967)1171.

126. A.C. Makrides, J.Electrochem.Soc.,113(1966)1158.

127. A. Damjanović and J.O'M. Bockris, Electrochim.Acta,11(1966)376.

128. P.W.T. Lu and S. Srinivasan, J.Electrochem.Soc.,125(1978)265.

129. A.K. Vijh, Electrochim.Acta,17(1972)91.

130. A.K. Vijh, J.Electrochem.Soc.,116(1969)972.

131. L. Pauling, The Nature of the Chemical Bond, Cornell University Press, 1960,,p.79.

132. H. Wroblowa, B.J. Piersma and J.O'M. Bockris, J.Electroanal.Chem., 6(1963)401.

133. S. Gilman and M.W. Breiter, J.Electroanal.Chem.,109(1962)1099.

134. M.W. Breiter, Electrochim.Acta.,8(1963)973.

135. O.A. Petrii, R.I. Podlovchenko, A.N. Frumkin and K. Lal, J.Electroanal.Chem.,10(1965)253.

136. P. Kohl and J.W. Schultze, Ber.Bunsenges Phys.Chem.,77(1973)953.

137. A.C. Makrides, J.Electrochem.Soc.,111(1964)392.
see also, ibid,111(1964)400.

138. A.K. Vijh, Electrochim.Acta,14(1969)921.

139. A.K. Vijh, J.Electrochem.Soc.,116(1969)353.

140. A.C. Makrides, J.Electrochem.Soc.,113(1966)1158.

141. M.W. Breiter, Electrochim.Acta,8(1963)447.

142. G. Bianchi, J.Appl.Electrochem.,1(1971)231.

143. G. Faite, G. Fiori and N. Nidola, J.Electrochem.Soc.,117(1970)1333. see also, ibid.,120(1973)1702.

144. G. Faita and G. Fiori, J.Appl.Electrochem.,2(1972)31.

145. S. Trasatti and G. Buzzanca, J.Electroanal.Chem.,29(1971)1.

146. D. Galizzioli, F. Tantardini and S. Trasatti, J.Appl.Electrochem., 4(1974)57., see also, ibid.,5(1975)203.

147. C. Iwakura, H. Tada and H. Tamura, Electrochim.Acta,22(1977)217.

148. A.T. Kuhn and C.J. Mortimer, J.Appl.Electrochem.,2(1972)283.

149. T. Arikado, C. Iwakura and H. Tamura, Electrochim.Acta,23(1978)9.

150. B.E. Conway, Electrochemical Data, Elsevier Publ. Co.,Amsterdam,1952.

151. T. Dickinson, R. Greef and Lord Wynne-Jones,Electrochim.Acta,14(1969)467.

152. F.T. Chang and H. Wick, Z.Phys.Chem.,33(1935)129.

153. S. Glasstone and A. Hickling, J.Chem.Soc.,(1934)10.

154. J.S. Mayell and S.H. Langer, Electrochim.Acta,9(1964)1411.

155. G.A. Tedoradze, Zh.Fiz.Khim.,33(1959)129.

156. A. Hickling, Trans.Faraday Soc.,41(1945)333.

157. A.N. Frumkin and G. Tedoradze, Z.Elektrochem.,62(1958)251.

158. J. Llopis and A. Sancho, J.Electrochem.Soc.,108(1961)720.

159. B.V. Ershler, Zh.Fiz.Khim.,14(1940)351.,see also ibid, 18(1944)131.

160. E.L. Littauer and L.L. Shreir, Electrochim.Acta,11(1966)527.

161. N.A. Balashova, Electrochim.Acta,7(1962)559.

162. M.W. Breiter, Electrochim.Acta,8(1962)925.

163. S. Gilman, J.Phys.Chem.,68(1964)2112.

164. V.S. Bagotzky and Y.B. Vasil'ev, Electrochim.Acta,9(1964)869.

165. J. Llopis and M. Vazquez, Electrochim.Acta,6(1962)167;177.

166. G. Faita, G. Fiori and J.W. Augustinsky, J.Electrochem.Soc.,116(1969)928.

167. M.W. Breiter, Electrochim.Acta,5(1961)145.

168. T. Yokoyama and M. Enyo, Electrochim.Acta,15(1970)1921.

169. A.T. Kuhn and P.M. Wright, J.Electroanal.Chem.,41(1973)329.

170. J. Llopis and L. Jorge, J.Electrochem.Soc.,110(1963)947.

171. J. Llopis and L. Jorge, Electrochim.Acta,9(1964)103.

172. S. Hadži-Jordanov,H.A.Kozlowska,M.Vuković and B.E.Conway,J.Electrochem. Soc.,125(1978)1471.

173. T. Arikado, C. Iwakura and H. Tamura, Electrochim.Acta,22(1977)513.

174. R.G. Erenburg, L.I. Krishtalik and V.I.Bystrov, Elektrokhimiya,8(1972)1740.

175. R.G. Erenburg, L.I. Krishtalik and I.P. Yaroshevskaya, Elektrokhimiya, 11(1975)1068,1072.

176. L.J.J. Janssen, L.M.C. Starmans, J.G. Vissher and E. Barendrecht, Electrochim.Acta,22(1977)1093.

177. R.U. Bondar, A.A. Borisova and E.A. Kalinovskii, Soviet Electrochem., 10(1974)37.

178. T. Arikado, C. Iwakura and H. Tamura, Electrochim.Acta,22(1977)229.

179. J. Augustinsky, L. Balsenc and J. Hinden, J.Electrochem.Soc., 125 (1978) 1093.

180. W.E. Triaca, C. Solomons and J.O'M. Bockris, Electrochim.Acta,13(1968) 1949.

181. R.G. Erenburg and L.I. Krishtalik, Elektrokhimiya,4(1968)923.

182. L.I. Krishtalik and Z.A. Rotenberg, Zh.Fiz.Khim.,39(1965)328;907.

183. L.J.J. Janssen and J.G. Hoogland, Electrochim.Acta,14(1969)1097.

184. L.J.J. Janssen and J.G. Hoogland, Electrochim.Acta,15(1970)339;941;1667.

185. L.I. Krishtalik, Elektrokhimiya,2(1966)624.

186. F. Hine, M. Yasuda and M. Iwata, J.Electrochem.Soc.,121(1974)749.

187. F. Hine and M. Yasuda, J.Electrochem.Soc.,121(1974)1289.

188. J.A. Harrison and Z.A. Khan, J.Electroanal.Chem.,30(1971)87.

189.a R. Woods, Electrochim.Acta,15(1970)815.

b B.E. Conway and A.K. Vijh, J.Phys.Chem.,71(1977)3637.

190. B.E. Conway and D.M. Novak, J.Phys.Chem.,81(1977)1459.

191. M. Mastragostino, G. Casalbore and S. Valcher, J.Electroanal.Chem.,44 (1973)37.

192.a M. Mastragostino, G. Casalbore and S. Valcher, J.Electroanal.Chem.,48 (1973)419.

b L. Sereno, V.A. Macagno and M.C. Giordano, Electrochim.Acta,17(1972)561.

193. T. Yokoyama and M. Enyo, Electrochim.Acta,13(1968)1631.

194. D. Britz, J.Electroanal.Chem.,88(1978)309.

195. Reference Electrodes,(eds. D.J.G. Ives and G.J. Jantz), Academic Press, New York,1961.,Chapter II,p.111.

196. J.O'M. Bockris and A.M. Azzam, Trans.Faraday Soc.,48(1952)145.

197. J.G.N. Thomas, Trans.Faraday Soc.,57(1961)1603.

198. B.E. Conway and E. Gileadi, Trans.Faraday Soc.,58(1962)2493.

199. B.E. Conway and R.G. Barradas, Electrochim.Acta,5(1961)319.

200. R. Parsons, Trans. Faraday Soc.,54(1958)1053.

201. V.S. Bagotskii, Y.B. Vasil'ev, J. Weber and J.N. Pirtskhalava, J. Electroanal.Chem.,27(1970)31.

202. N.A. Balashova and V.E. Kazarinov, Elektrokhimiya,1(1965)514.

203. G. Horanyi and G. Inzelt, J.Electroanal.Chem.,86(1978)215.

204. G. Horanyi and E.M. Mayer, J.Electroanal.Chem.,83(1977)367.

205. K.J. Vetter, Trans.Sympos.Electrode Processes,(ed. E. Yeager) John Wiley, New York, 1961,p.47.

206. B.E. Conway and M. Salomon, Electrochim.Acta,9(1964)1959.

207. A.N. Frumkin, Dokl.Akad.Nauk,S.S.S.R.,152(1963)156.

208. R. Parsons, Trans.Faraday Soc.,47(1951)1332.

209. M. Enyo and T. Yokoyama, Electrochim.Acta,16(1971)223.

210. A. Wold, B. Post and E. Banks, J.Am.Chem.Soc.,79(1957)4911.

211. J.T. Kim and J. Jorne, J. Electrochem.Soc.,124(1977)1473.

212. A.N. Frumkin and A. Slygin, Acta Physicochim.,S.S.S.R.,6(1936)819.

213. P. Dolin and B. Ershler, Acta Physicochim.,S.S.S.R.,13(1940)747.

214. S. Gilman, J.Phys.Chem.,68(1964)2098.

215. V.E. Kazarinov and N.A. Balashova, Dokl.Akad.Nauk,S.S.S.R.,139(1961)641.

216. M.W. Breiter, Electrochim.Acta,7(1962)25.

217. N.A. Balashova,Z.Physik.Chem.,207(1957)340.

218. J.N. Sarmousakis and J.M. Prager, J.Electrochem.Soc.,104(1957)454.

219. Ya. Weber, Dzh. Pirtskhalava, Yu.B. Vasil'ev and V.S. Bagotskii, Elektrokhimiya,5(1969)1037.

220. J. Sobkowski and A. Wieckowski, J.Electroanal.Chem.,41(1973)373.

221. R.F. Lane and A.T. Hubbard, J.Phys.Chem.,79(1975)808.

222. R.F. Lane and A.T. Hubbard, J.Phys.Chem.,77(1973)1401,1411.

223. A.L.Y. Lau and A.T. Hubbard, J.Electroanal.Chem.,33(1971)77.

224. C.N. Lai and A.T. Hubbard, Inorg.Chem.,11(1972)2081.

225. B.D. Kurnikov, A.I. Zhurin, Yu.B. Vasil'ev and V.S. Bagotskii, Elektrokhimiya,8(1972)1646.

226. B.I. Podlovchenko, N.A. Epstein and A.N. Frumkin, J.Electroanal.Chem., 53(1974)95.

227. B.I. Podlovchenko, V.F. Stenin and A.N. Frumkin, Elektrokhimiya,8 (1972)129.

228. A.N. Frumkin, O.A. Petry and R. Marvet, J.Electroanal.Chem.,12(1966)504.

229. T. Takamura, K. Takamura and E. Yeager, J.Electroanal.Chem., 29(1971)279.

230. Y.C. Chiu and M.A. Genshaw, J.Phys.Chem., 73(1969)3571.

231. A.M. Barrett and R. Parsons, Symp.Faraday Soc.,4(1970)72.

232. S. Gottesfeld and B.E. Conway, J.Chem.Soc.Faraday Trans. I,11(1974)1793.

233. S. Gottesfeld and B. Reichman, J.Electroanal.Chem.,67(1976)1793.

234. R. Adžić, E. Yeager and B.D. Cahan, J.Electroanal.Chem.,85(1977)267.

235. W.J. Anderson and W.H. Hansen, J.Electroanal.Chem.,47(1973)229.
see also:ibid,43(1973) 329.

236. D.C. Grahame, Chem.Rev.,41(1947)441.

237. A.N. Frumkin, Zeit.Phys.Chem.,A164(1933)121.
see also: O.Stern, Z.Elektrochem.,30(1924)508.

238. J.O'M. Bockris, J.Chem.Phys.,24(1956)817.

239. L.B. Harris and A. Damjanović, J.Electrochem.Soc.,122(1975)593.

240. E.S. Hedges and J.E. Myers,"The Problem of Physicochemical Periodicity ", Longmans Green and Co., 1926.

241. J. Bray, J.Am.Chem.Soc.,43(1921)1262.

242. M.G. Peard and C.F.Cullis,Trans.Faraday Soc.,47(1951)616.

243. R.J. Field, E. Kövös and R.M. Noyes, J.A.Chem.Soc.,94(1972)8649.

244. K.F. Bonhoeffer and G. Langhammer, Z.Elektrochem.,52(1948)60,67.

245. K.F. Bonhoeffer and H. Gerischer, Z. Electrochem.,52(1948)149.
see also: K.F. Bonhoeffer, ibid.,52(1948)24.

246. J. Wojtowicz, N. Marinčić and B.E. Conway, J.Chem.Phys.,48(1968)4333.

247. J. Higgins, Proc.Natl.Acad.Sci.,U.S.A.,51(1964)989.

248. R.A. Spangler and F.M. Snell, J.Theor.Biol.,16(1967)381.

249. J. Higgins, J.Ind.Eng.Chem.,59(1967)18.

250. U.F. Franck, Symp. Faraday Soc.,9(1974)137.

251. G. Viniegra-González,"Biological and Biochemical Oscillators", Academic Press, New York,N.Y.,1972.,p.71.

252. H.F. Hunger, J.Electrochem.Soc.,115(1968)492.

253. J. Wojtowicz, Modern Aspects of Electrochemistry,(eds. B.E. Conway and J.O'M. Bockris), Plenum Publ.Co.,New York, Vol.8,1972.,Chapter 4.

254. J. Wojtowicz and B.E. Conway, J.Chem.Phys.,52(1970)1407.

255. U.F. Franck and R. Fitzhugh, Z.Elektrochem.,65(1961)156.

256. N. Minorsky,"Nonlinear Oscillations",D.Van Nostrand Co.,Princeton, N.Y.,1962.

257. C. Hayashi,"Nonlinear Oscillations in Physical Systems", McGraw-Hill, New York,N.Y.,1964.

258. A.A. Andronov and C.E. Chaikin,"Theory of Oscillations", Princeton University Press, Princeton, N.Y., 1949.

260. Faraday Symposium of Chem.Soc.,London, No.9 , Physical Chemistry of Oscillatory Phenomena,(1974).

261. J.P. Hoare and J.A.S. Mowat, Nature,London,165(1950)64.

262. A. Dmitriev and E.V. Rzhevskaya, Zh.Fiz.Khim.,35(1961)871.

263. B. Pointu, Electrochim.Acta ,14(1969)1207,1213.

264. J.A. Shropshire, Electrochim.Acta ,12(1967)253.

265. G. Horanyi, G. Inzelt and E. Szetey, J. Electroanal.Chem, ,81(1977)395.

266. R.J. Field, E. Koros and R.M. Noyes, J.Am.Chem.Soc.,94(1972)8649.

267. H. Lal, H.R. Thirsk and W.F.K. Wynne-Jones, Trans.Faraday Soc.,47(1951)999.

268. R.P. Buck and L.R. Griffith, J.Electrochem.Soc.,109(1962)1005.

269. A.N. Frumkin, O.A. Petrii and N.W. Nikolaeva-Fedorovich, Dokl.Akad. Nauk.,U.R.S.S.,133(1961)1158.

270. I. Epelboin, M. Ksouri and R. Wiart, J.Electroanal.Chem.,65(1975)373.

271. G. Armstrong and J.A.V. Butler, Disc.Faraday Soc.,1(1947)122.

272. M.T. Frances and W.H. Colmer, J.Electrochem.Soc.,97(1950)237.

273. A.R. Piggott, H. Leckie and L.L.Schreir, Corrosion Sci.,5(1965)165.

274. J.L. Rosenfeld and I.P. Danilov, Corrosion Sci.,7(1967)129.

275. T.O. Pavela, Suomen Kemistilekti, 30(1957)138.

276. D. Sawyer and E.T. Seo, J.Electroanal.Chem., 5(1963)23.

277. S. Szpak, J. Electrochem.Soc., 117(1970)1056.

278. J.S. Babu, M.M. Bokadia and K. Srinivasulu, Bull.Chem.Soc., Japan, 49 (1976)2875.

279. A.M. Zhabotinskii, Dokl.Akad.Nauk., S.S.S.R., 157(1964)392.

280. M. Breiter, C.A. Knorr and R. Meggle, Z. Elektrochem., 59(1955)153.

281. M.W. Breiter and F.G. Will, Z. Elektrochem., 61(1957)1177.

282. S. Schuldiner, M.Rosen and D.R. Flinn, J.Electrochem.Soc., 117(1970)1251.

283. S. Shibata and M.P. Sumino, Electrochim.Acta., 20(1975)739.

284. C.G. Rader and B.V. Tilak, J.Electrochem.Soc., 123(1976)1708.

285. F.G. Will, J.Electrochem.Soc., 112(1965)451.

286. J.S. Mayell, J.Electrochem.Soc., 113(1966)385.

287. L.D. Burke and A. Moynihan, Electrochim.Acta., 15(1970)1434.

288. J.P. Hoare, Electrochim.Acta., 17(1952)593.

289. S. Shibata, J. Electroanal.Chem., 89(1978)37.

290. B.E. Conway and M. Dzieciuch, Nature, London, 189(1961)914.

291. M. Breiter, J.Electroanal.Chem., 15(1967)221.

292. A.N. Frumkin, B.I. Podlovschenko and H. Lal, J.Electroanal.Chem., 11(1966)12.

293. R. Parsons and A. Capon, J.electroanal.Chem., 44(1973)239.

294. A.N. Frumkin and B. Slygin, Acta Physicochim., U.R.S.S., 4(1936)991.
see also: ibid., 5(1936)819.

295. J. MacDonald and B.E. Conway, Proc.Roy.Soc., London, A169(1962)419.

296. B.E. Conway and A.K. Vijh, J.Org.Chem., 31(1966)4283.

297. B.E. Conway, H. Angerstein-Kozlowska and F.C. Ho, J.Vac.Sci.Technol., 14(1977)351.

298. B.E. Conway, H. Angerstein-Kozlowska and W.B.A. Sharp, Symposium on Electrocatalysis, The Electrochemical Society, San Francisco, 1974., p.94.

299. W. Schultze, Ber.Bunsenges.Phys.Chem.,73(1969)483.

300. S. Trasatti, J.Electroanal.Chem.,54(1974)437.,

see also: ibid.,64(1975)128., 65(1975)815.

301. M. Roseburgh and J. Lash-Miller, J.Phys.Chem.,14(1910)816.

302. E.C. Zeeman, Sci.Am.,234(1976)65.

303. G.A. Somorjai and D.W. Blakeley, Nature,London,258(1975)580.

304. S. Szpak and R.E. Rice,J.Chem.Phys.,52(1970)6336.